ESKO KEMPPAINEN

Genetic and Metabolic Suppression of Mitochondrial Disease Phenotype in *Drosophila*

■

ACADEMIC DISSERTATION
To be presented, with the permission of
the Board of the BioMediTech of the University of Tampere,
for public discussion in the Auditorium of Finn-Medi 5,
Biokatu 12, Tampere, on May 30th, 2015, at 12 o'clock.

UNIVERSITY OF TAMPERE

ESKO KEMPPAINEN

Genetic and Metabolic Suppression of Mitochondrial Disease Phenotype in *Drosophila*

Acta Universitatis Tamperensis 2062
Tampere University Press
Tampere 2015

UNIVERSITY
OF TAMPERE

ACADEMIC DISSERTATION
University of Tampere, BioMediTech
Finland

Supervised by
Professor Howard Jacobs
University of Tampere
Finland

Reviewed by
M.D., Ph.D. Orian Shirihai
Boston University
USA
Dr. Aurelio Teleman
German Cancer Research Center (DKFZ)
Germany

Cover design by
Mikko Reinikka

Distributor:
verkkokauppa@juvenesprint.fi
https://verkkokauppa.juvenes.fi

Acta Universitatis Tamperensis 2062
ISBN 978-951-44-9819-0 (print)
ISSN-L 1455-1616
ISSN 1455-1616

Acta Electronica Universitatis Tamperensis 1554
ISBN 978-951-44-9820-6 (pdf)
ISSN 1456-954X
http://tampub.uta.fi

Suomen Yliopistopaino Oy – Juvenes Print
Tampere 2015

To my family

Abstract

Mutations in genes encoding the components of the mitochondrial translational apparatus give rise to various human mitochondrial disorders with a range of clinical phenotypes. We have used a *Drosophila* mutant harbouring a missense mutation in the gene *technical knockout* (*tko*), which encodes the highly conserved mitoribosomal protein *S12*, to elucidate the pathophysiology and metabolic adaptation to such defects in multicellular organisms. The tko^{25t} mutant flies suffer from a severe oxidative phosphorylation and ATP deficiency, and exhibit a phenotype of developmental delay occurring during larval stages, sensitivity to paralytic and epileptic seizures and hearing impairment, features analogous with common clinical manifestations of mitochondrial disease in humans.

Based on my studies, this phenotype is exacerbated when mutant flies are reared on high-sugar diet. Although the exact mechanism of this sugar toxicity remains unknown, rearing the mutant flies on low-sugar diet results in significant phenotypic recovery which is associated with partial rescue of severe ATP and NADPH deficiencies as well as decreased pyruvate and lactate burden. The tko^{25t} phenotype is also rescued by overexpression of the endogenous allele in suppressor lines carrying duplications of the *tko* gene. Yet, the mutant larvae do not respond to mitochondrial dysfunction by inducing mitochondrial biogenesis or by over-expressing components of the mitochondrial translational apparatus. In turn, the mutant larvae exhibit transcriptionally a large-scale metabolic reprogramming highlighted by down-regulation of sugar metabolism and increased catabolism of lipids - changes indicating shift in fuel-preference from carbohydrates to fats and fatty acids. The results also suggest that the primary cause underlying the pathophysiology of the disease-like phenotype might be severe metabolic crisis rather than isolated ATP or NADPH deficiency.

Altogether, this study highlights the importance of understanding the molecular basis of disease and the therapeutic potential of dietary intervention in the treatment of mitochondrial disorders.

Contents

List of original communications

This thesis is based on the following original communications, which are referred to in the text by their roman numerals I-III.

I) Kemppainen E, Fernández-Ayala DJ, Galbraith LC, O'Dell KM, Jacobs HT. Phenotypic suppression of the Drosophila mitochondrial disease-like mutant tko(25t) by duplication of the mutant gene in its natural chromosomal context. Mitochondrion. 2009 Sep;9(5):353-63. doi: 10.1016/j.mito.2009.07.002.

II) Kemppainen KK*, Kemppainen E*, Jacobs HT. The alternative oxidase AOX does not rescue the phenotype of tko25t mutant flies. G3 (Bethesda). 2014 Aug 21;4(10):2013-21. doi: 10.1534/g3.114.013946.

III) Kemppainen E, George J, Garipler G, Soga T, Dunn C, Tuomela T, Kiviranta E, Jacobs HT. Mitochondrial dysfunction plus high-sugar diet provokes a metabolic crisis that inhibits growth. 2015.

*Equal contribution.

II) Publication will be included in the doctoral dissertation “Complementation of Cytochrome *c* Oxidase Deficiency by Transgenic Expression of the Alternative Oxidase in Drosophila” by Kia Kemppainen, University of Tampere.

III) Manuscript submitted to Cell Metabolism.

Abbreviations

6GPDH	6-phosphogluconate dehydrogenase
ADP	Adenosine diphosphate
adPEO	Autosomal dominant Progressive External Ophthalmoplegia
AIF	Apoptosis inducing factor
AMP	Adenosine monophosphate
ANT	Adenine nucleotide translocator
AOX	Alternative oxidase
ATP	Adenosine triphosphate
BSA	Bovine serum albumin
cAMP	Cyclic adenosine monophosphate
cDNA	Complementary DNA
cI-V	Respiratory chain complexes I-V
CNS	Central nervous system
CO_2	Carbon dioxide
CoQ	Coenzyme Q
COX	Cytochrome *c* oxidase
CPTx	Carnitine palmitoyltransferase
cyt *c*	Cytochrome *c*
DNA	Deoxyribonucleic acid
dNTP	Deoxyribonucleotide triphosphate
DTT	Dithiothreitol
EGTA	Ethylene glycol tetra-acetic acid
ER	Endoplasmic reticulum
ERMES	Endoplasmic reticulum–mitochondria encounter structure
ETC	Electron transport chain
FA	Fatty acid
FAD	Flavin adenine dinucleotide (oxidised)
FADH2	Flavin adenine dinucleotide (reduced)
FMN	Flavin mononucleotide
G3P	Glycerol-3-phosphate
GAPDH	Glyceraldehyde 3-phosphate dehydrogenase

G6PDH	Glucose 6-phosphate dehydrogenase
GFP	Green fluorsescent protein
GMP	Guanosine monophosphate
GS	GeneSwitch
GSH	Glutathione
GSSG	Glutathione disulfide
H_2O_2	Hydrogen peroxide
HRP	Horseradish peroxidase
Hsp	Heat shock protein
HSP	Heavy strand promoter
HTRA2	High Temperature Requirement Protein A2
IDH	Isocitrate dehydrogenase
IMM	Mitochondrial inner membrane
IMS	Intermembrane space
kdn	*knockdown*
KSS	Kearns–Sayre syndrome
L1-3	*Drosophila* larval instars 1-3
LCFA	Long-chain fatty acids
LDH	Lactate dehydrogenase
LHON	Leber's hereditary optic neuropathy
LRPPRC	Leucine-rich pentatricopeptide repeat containing
LSP	Light strand promoter
MAMS	Mitochondrial Associated ER Membranes
MCFA	Medium-chain fatty acids
MELAS	Mitochondrial encephalopathy with lactic acidosis and stroke-like episodes
MERRF	Myoclonus epilepsy with ragged red fibers
MFRTA	Mitochondrial free radical theory of ageing
MIRAS	Mitochondrial recessive ataxia syndrome
MNGIE	Mitochondrial Neurogastrointestinal Encephalopathy
MnSOD	Manganese superoxide dismutase
MOMP	Mitochondrial outer membrane permeabilization
MRG	mitochondrial RNA granules
MRP	Mitoribosomal protein

mRpS12	Mitoribosomal protein S12
mtDNA	Mitochondrial DNA
MTERF	Mitochondrial transcription termination factor
MTPAP	Mitochondrial Poly(A) Polymerase
mtSSB	Mitochondrial single-stranded DNA-binding protein
NAD^+	Nicotinamide adenine dinucleotide (oxidised)
NADH	Nicotinamide adenine dinucleotide (reduced)
$NADP^+$	Nicotinamide adenine dinucleotide phosphate (oxidised)
NADPH	Nicotinamide adenine dinucleotide phosphate (reduced)
NARP	Neuropathy, ataxia, and retinitis pigmentosa
Ndi, Nde	NADH dehydrogenases (alternative)
nDNA	Nuclear DNA
NO	Nitric oxide
O2•−	Superoxide anion
OH•	Hydroxyl radical
OMM	Mitochondrial outer membrane
OXA1	Mitochondrial oxidase assembly protein 1
OXPHOS	Oxidative phosphorylation
PAGE	Polyacrylamide gel electrophoresis
PCR	Polymerase chain reaction
PDH	Pyruvate dehydrogenase complex
PEO	Progressive external ophthalmoplegia
PGC-1α	Peroxisome proliferator activated receptor γ co-activator-1α
P_i	Inorganic phophate
POLG	Polymerase γ
POLRMT	Mitochondrial RNA polymerase
PPP	Pentose phosphate pathway
RNA	Ribonucleic acid
ROS	Reactive oxygen species
rRNA	Ribosomal RNA
SCFA	Short chain fatty acid
TEFM	Mitochondrial transcription elongation factor
TIM	Translocator of innermembrane
TORC1/2	Target of Rapamycin complex ½

TOM	Translocator of outer membrane
tRNA	Transfer-RNA
VDAC	Voltage-dependent anion channel
VLCFA	Very long chain fatty acid

1. Introduction

Pathogenic mutations in mitochondrial DNA (mtDNA) and nuclear encoded mitochondrial proteins give rise to a large and heterogeneous group of mitochondrial disorders, usually characterized by defective oxidative phosphorylation. Mitochondrial diseases are often multi-syndromic but manifest predominantly in the muscle and nervous system due to the high energy expenditure of these tissues (Schon, DiMauro, & Hirano, 2012; Wallace, Fan, & Procaccio, 2010). Mitochondrial disorders have classically had an orphan disease status but recent epidemiological studies have shown that collectively these disorders affect more than 1 in 10000 people in the western countries (Greaves et al., 2012).

The majority of these pathological mutations affect the machinery of mitochondrial translational machinery. Two of the most common pathogenic mitochondrial DNA mutations, 3243A>G (Goto et al. 1990) and 8344A>G (Shoffner et al. 1990), both affect mitochondrial transfer-RNAs and manifest as progressive multi-syndromic disorders characterized by epileptic seizures and lactic acidosis (Douglas C Wallace et al., 2010). A third highly prevalent mutation 1555A>G (Prezant et al., 1993), affects the 12S mitoribosomal RNA (rRNA), conferring aminoglycoside sensitivity and predisposing to sensorineural deafness. While these mitochondrial tRNA and rRNA mutations have relatively high incidence, mutations in nuclear genes encoding polypeptide components of the translation machinery are extremely rare, but equally deleterious (Boczonadi & Horvath, 2014).

A point mutation in the *Drosophila tko* (*technical knockout*) gene, encoding the conserved mitochondrial ribosomal protein S12 (mRpS12), results in a phenotype highly analogous with the clinical manifestations of human mitochondrial protein synthesis disorders. The tko^{25t} mutant phenotype is characterized by developmental delay, hearing impairment and malfunction of the central nervous system, manifesting as susceptibility to epileptic and paralytic seizures (Toivonen et al., 2001; Toivonen et al., 2003). The underlying molecular defect involves instability of the small subunit of the mitoribosome which impairs the synthesis of mitochondrially encoded subunits of the OXPHOS complexes, and ultimately

results in respiratory chain deficiency. Yet, how this gives rise to the organismal phenotype, remains largely unknown (Toivonen et al., 2001; Toivonen, Boocock, & Jacobs, 1999; Toivonen et al., 2003). Because of the similarity between the *tko*^{25t} and clinical disease phenotypes, and the numerous benefits *Drosophila* offers as a model organism, the mutant flies provide a convenient tool for studying the pathogenic mechanisms of human mitochondrial disorders, and a platform for evaluating potential therapeutic strategies.

The vast majority of mitochondrial disorders currently have no effective cures. The forms of treatment currently under investigation or already in clinical practice can be roughly divided into four distinct functional categories: antioxidant treatments to protect cells from increased oxidative damage caused by mitochondrial dysfunction, endurance exercise and small molecule compounds aimed at improving cellular energy metabolism or enhancing it by inducing mitochondrial biogenesis, gene therapy designed to compensate for a loss of gene activity or to modulate mtDNA heteroplasmy, and nutritional therapy (Kerr, 2010; Peralta et al., 2015; Pfeffer et al., 2013). In this work, we've focused on evaluating the amenability and effects of different nutritional interventions and OXPHOS bypass gene therapy using the *tko*^{25t} model.

One of the possible gene therapeutic strategies is based on nuclear expression of mitochondrially targeted single subunit respiratory chain complex alternatives, such as the alternative oxidase (AOX), which is found mostly in plants. AOX can provide a functional by-bass for the entire cytochrome segment of the respiratory chain and prevent the formation of superoxide radicals when the ubiquinone pool is over-reduced while relieving the blockage of mitochondrial substrate oxidation due to impaired cytochrome bc_1 (Complex III) or cytochrome *c* oxidase (Complex IV) complex activities (El-Khoury et al., 2013; Fernandez-Ayala et al., 2009). In addition to providing a therapeutic tool, bypassing segments of defective respiratory chain can help in identifying disease-relevant metabolic phenomena, such as ATP deficiency, elevated reactive oxygen species (ROS) production and impaired substrate oxidation, and their relative contribution to the disease pathogenesis.

A compelling alternative for gene and drug therapy is nutritional intervention. Dietary supplements, such as carnitine and coenzyme Q_{10} have already been used to treat human mitochondrial disorders with some degree of success (Horvath, 2012; Valero, 2014), and dietary intervention has shown significant promise, particularly

in murine disease models (Ahola-Erkkilä et al., 2010; Tischner et al., 2014). The *tko*^{25t} model can be easily exploited to address how modulating the balance of principal dietary components, carbohydrates, fats and proteins would affect the mutant phenotype, due to the ease of manipulating *Drosophila* diet.

Finally, one of the clear advantages *Drosophila* offers over many other multi-cellular model organisms is its genetic tractability. In earlier studies, the *tko*^{25t} phenotype has been shown to be attenuated by maintaining the mutant flies as an inbred stock (Toivonen et al., 2001). This provides a unique opportunity to discover novel genetic factors which can act to suppress phenotypes resulting from mitochondrial protein synthesis defects.

2. Review of literature

2.1 Mitochondria - Structure, functions and organization

Mitochondria are organelles harboured by virtually all eukaryotic cells and organisms. The few exceptions include certain cell types, such as mature erythrocytes, which lose their mitochondria during cell differentiation. The few amitochondriate eukaryote species existing today, such as microsporidia, have likely evolved from mitochondria-bearing ancestors (Palmer, 1997). Mitochondria have originated and evolved through a symbiotic relationship between a once free-living prokaryotic ancestor, engulfed by a host cell, the ancestral eukaryote (McInerney et al., 2014). While considerable disagreement still exists concerning the phylogenetic and evolutionary details of this endosymbiotic process, comparative genomic studies of eukaryotic mitochondrial DNA have shown that mitochondria are of bacterial ancestry, originating from the phylum α-proteobacteria (Gray, 2012).

During eukaryotic evolution, mitochondria have lost a considerable degree of their genetic independence and physiological functions. Yet, their widespread presence implies that mitochondria still participate in several vital physiological processes in eukaryotic cells. Perhaps the best appreciated of these is the ATP synthesis-coupled oxidation of nutrients, a process known as oxidative phosphorylation (OXPHOS), which provides cells with energy. The catabolism of virtually all dietary fats, proteins and carbohydrates ends in, or at least impinges on mitochondria, culminating in the flux of carbon into the tricarboxylic acid cycle (TCA cycle), in the form of acetyl-CoA and TCA cycle intermediates (Lehninger, Nelson & Cox, 2005) (**Fig. 2**). In addition to their central role in energy metabolism, mitochondria participate in several other key metabolic processes such as heme biosynthesis from succinyl-CoA (TCA cycle intermediate), which is catalyzed primarily by mitochondrial enzymes (Ponka, 1997). Mitochondria also host both, part of the mevalonate pathway and the urea cycle, enzymes catalyzing the initial steps of steroid hormone biosynthesis from cholesterol, as well as two enzymes which participate in the first steps of gluconeogenesis: pyruvate carboxylase which

converts pyruvate into oxaloacetate and the mitochondrial isoform of phosphoenolpyruvate carboxykinase which catalyzes the conversion of oxaloacetate into phosphoenolpyruvate. (Lehninger, Nelson & Cox, 2005). Mitochondria and the TCA cycle also have a crucial role in amino acid catabolism and biosynthesis. The generation of Fe/S clusters is catalyzed by mitochondrial scaffold proteins and enzymes (Rouault & Tong, 2005). Likewise, ketogenesis, *i.e.* the production of ketone bodies acetoacetate, acetone and β-hydroxybutyrate, occurs exclusively in liver cell mitochondria. Finally, mitochondria together with the endoplasmic reticulum (ER), constitute a Ca^{2+} storage and buffering compartment and thus participate in the regulation of intra-cellular calcium fluxes (Williams et al., 2013).

Mitochondria are enclosed by two membranes. The outer mitochondrial membrane (OMM) is rich in voltage-dependent anion channels (VDACs), formed by rings of porin proteins. These channels facilitate the passage of small hydrophilic molecules through the outer membrane. The inner mitochondrial membrane (IMM) is largely impermeable to solutes and import through the IMM thus relies on dedicated channel and transport proteins. The inner membrane forms highly dynamic structures, called cristae, which protrude from the IMM into the lumen of mitochondria, known as the mitochondrial matrix. The inner membrane and cristae house the numerous mitochondrial solute transporters, protein complexes of the electron transport chain (ETC), the ATP synthase and protein translocases of the inner membrane (TIMs), making it one of the most protein rich membranes known (60-70% protein by weight) (Becker et al., 2009). The inner mitochondrial membrane is also characterized by the presence of cardiolipin, a phospholipid exclusive to bacteria and the IMM. The outer and inner membranes encapsulate a compartment called the intermembrane space (IMS).

The mitochondrial matrix houses the remainder of the mitochondrial proteome consisting of *e.g.* the pyruvate dehydrogenase complex (PDH) and the enzymes of the TCA cycle, urea cycle, β-oxidation and anaplerotic pathways. Most of these processes feed electrons to the electron transport chain (ETC) via the electron carriers, NADH and $FADH_2$.

Mitochondria vary greatly in size, morphology and number between different cell types and tissues. Classically, mitochondria were described and perceived as spherical or oval, thread- and granule-like organelles with a static structure and an ascertainable copy number within the cell. The term mitochondrion originates from

the Greek words *mitos* (thread) and *chondron* (grain), and was coined by the microbiologist Carl Benda, who was among the first to discover and make observations on the shape these organelles (Benda, 1898). With the advancement of modern microscopy, it is now appreciated that, in many cell types, mitochondria actually form dynamic reticular networks which are constantly being reshaped by fission and fusion events (Bereiter-Hahn & Vöth, 1994; Lewis & Lewis, 1914; Smith, 1931), and that these transformations are genetically regulated and linked to alterations in the bioenergetic and redox state of the cell, mitochondria or distinct compartments within the mitochondrial network (Nasrallah & Horvath, 2014; Scorrano, 2013).

The mitochondrial network interfaces with the endoplasmic reticulum (ER) in many cell types. In mammalian cells, these regions of interaction between ER and mitochondria are known as Mitochondrial Associated ER Membranes or MAMS (endoplasmic reticulum–mitochondria encounter structure, or ERMES, in yeast), and have recently been shown to have distinct biochemical properties, and to provide a physical domain for many physiological processes (Naon & Scorrano, 2014). These contact site are important for mitochondrial phospholipid biosynthesis which requires phospholipid trafficking between the two organelles (Osman, Voelker, & Langer, 2011). MAMS also provide microdomains for Ca^{2+} trafficking between the ER and mitochondria. Besides stimulating TCA cycle enzymes and OXPHOS, mitochondrial Ca^{2+} fluxes are also associated with the regulation of apoptosis, creating a link between MAMS and programmed cell death (Gunter et al., 2004; Naon & Scorrano, 2014).

2.1.1 Mitochondrial genetics and DNA metabolism

Mitochondria contain their own circular, double-stranded DNA genome, which encodes a small, but functionally very significant fraction of the approximately 1500 mitochondrial polypeptides (Calvo et al., 2006). Based on comparative genomics, mitochondrial genomes have been under heavy reductive pressure during evolution which has resulted in a substantial loss of mitochondrially encoded genes due to redundant overlap in processes carried out by both mitochondria and the ancestral host cells, and through gene transfer from mitochondrial DNA (mtDNA) to nuclear DNA (nDNA) (Bernt et al., 2013). Species within the eukaryotic domain thus now

carry a small and somewhat variable number of mtDNA-encoded genes. Plants have generally retained more mitochondrial genes than animals but, in both kingdoms, the complement of mtDNA encoded genes appears to have become fixed (Bullerwell & Gray, 2004).

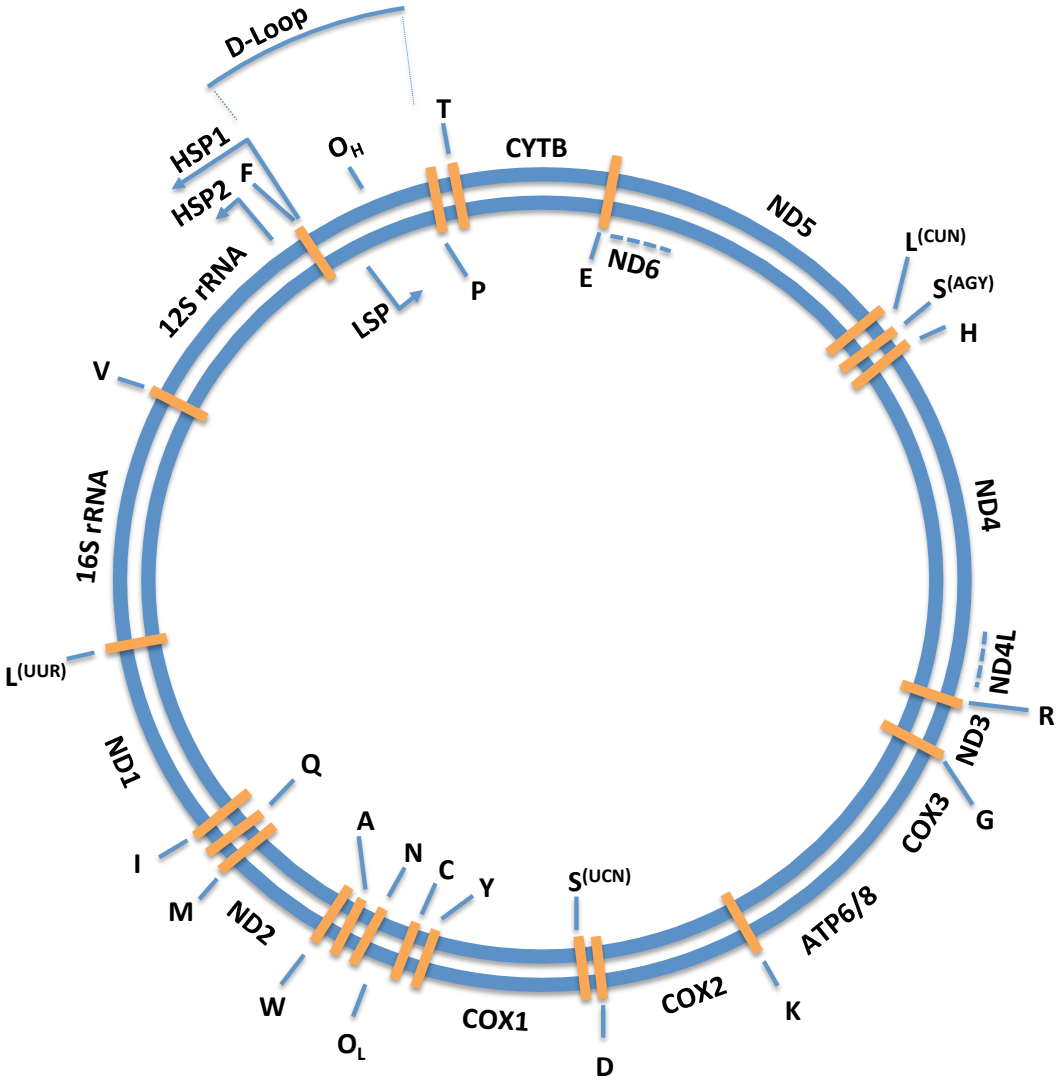

Figure 1. The organization of the human mitochondrial DNA. Abbreviations: ATPx – ATP synthase, COXx – cytochromome *c* oxidase, CYTB – cytochrome b, D-loop – displacement loop, HSPx – heavy strand promoter, LSP – light strand promoter, NDx – NADH dehydrogenase, O_H – origin of replication (heavy strand), OL – origin of replication (light strand). The single letter abbreviations designate transfer-RNA genes of the corresponding amino acid, according to standard IUPAC nomenclature.

The mammalian mtDNA encodes only 13 polypeptides, all components of the five inner membrane OXPHOS complexes (**Fig. 1**). These include 7 subunits of complex I (ND1-4, -4L, -5 and -6), one subunit of complex III (cytochrome *b*, encoded by the CYTB gene), three subunits of complex IV (COX I-III) and two subunits of complex V (subunits 6 or a, and A6L, encoded, respectively, by the ATP6 and ATP8 genes). In addition to the polypeptide encoding genes, mtDNA encodes 2 ribosomal RNAs (12S and 16S) and 22 transfer-RNAs, all of which are components of the mitochondrial translation machinery. The human mitochondrial genome is 16,569 bp long and contains only a single significant non-coding region (Anderson et al., 1981). The human mitochondrial coding sequences are intronless, and organized on the two strands in a contiguous and partially overlapping manner. The mtDNAs of other mammals and most metazoans are similar in these respects. The two strands of human mtDNA are denoted the heavy and the light strand, based on their guanine content and differential buoyant density. Mitochondrial genes are spread on both strands with a significant bias; the human light strand only carries a single protein-coding gene (ND6) (**Fig. 1**).

Mitochondrial DNA is maternally inherited and does not undergo germline recombination (Hällberg & Larsson, 2014). It also exists in multiple copies per cell, implying that several mtDNA genotypes can co-exist in a single cell. This condition is known as heteroplasmy, whereas the existence of only a single mtDNA genotype is called homoplasmy. Since mitochondrial DNA has a high mutation rate, an order of magnitude higher than that of nuclear DNA (Pakendorf & Stoneking, 2005), and is uniparently transmitted, this could potentially give rise to a phenomenon known as the Muller's ratchet, or the irreversible accumulation of deleterious mutations in an asexual population (Muller, 1964), leading to loss of fitness and eventual extinction. Several poorly understood processes are thought to exist to counter this threat. One of these is the so-called mitochondrial bottleneck, a phenomenon resulting from the fact that primordial germ cells are apportioned only a small fraction of the mitochondria of the developing embryo, and thus only a subset of the mother's mtDNA molecules are transmitted to the offspring (Shoubridge & Wai, 2007). Since this could also result in the rapid segregation of novel and potentially pathogenic mtDNA genotypes, a mechanism of purifying selection which would remove potentially deleterious mtDNA molecules, has been inferred to exist in the germ line (Stewart et al., 2008). Transmission of mtDNA mutations through the germline is also suppressed by the early embryonic lethality of *e.g.* pathogenic

tRNA mutations (Freyer et al., 2012) and the general decline in fertility caused by high levels of female germline mtDNA mutations (Ross et al., 2013).

Mitochondrial DNA copy number can vary by orders of magnitude between different cell types and tissues, ranging from the few thousands in human fibroblasts, cardiac and skeletal muscles (Kukat et al., 2011; Miller, 2003) to tens of thousands in oocytes (Chen et al., 1995). mtDNA molecules are arranged and compacted into nucleoids, nucleoprotein complexes with a mean diameter of approximately 100 nm (Brown et al., 2011; Kukat et al., 2011). Mitochondrial nucleoids have been reported to consist of 1-10 copies of mitochondrial DNA molecules (Bogenhagen, 2009; Kukat et al., 2011) and a varying complement of proteins (Bogenhagen et al., 2003; Garrido et al., 2003; Holt et al., 2007). The primary mtDNA packaging factor is the high mobility group (HMG)-box protein TFAM which binds and bends mtDNA in a histone-like manner (Ngo, Kaiser, & Chan, 2011; Rubio-Cosials et al., 2011)

Mitochondrial DNA replicates independently of nDNA and using a somewhat different mechanism. mtDNA is replicated on nucleoid-like DNA/protein complexes called replisomes, at the core of which are the two subunits of the mitochondrial DNA polymerase gamma (pol γ). This trimeric protein complex is composed of the 140 kDa pol γ catalytic subunit, encoded by POLG gene and two 55 kDa accessory subunits, encoded by the POLG2 gene (Chinnery & Hudson, 2013). In addition to synthesizing DNA, the catalytic subunit possesses a 3′-5′ exonuclease activity required for proofreading, and a deoxyribose-5-phosphate (5′dRP) lyase activity necessary for enzymatic DNA repair (Copeland, 2012). Because of the exonucleolytic proofreading activity and its high nucleotide selectivity, pol γ has extremely high fidelity, such that misinsertions during replication occur only at a rate of 1 in every 500,000 nucleotides (Copeland & Longley, 2014). The replisome also includes the 5′-3′ DNA helicase Twinkle which unwinds the double-stranded DNA. These minimal replisome components are sufficient for template directed DNA synthesis *in vitro*, but the rate of replication is greatly enhanced by the addition of the mitochondrial single stranded binding protein (mtSSB), which stabilizes the transiently single-stranded DNA template at replication forks (Korhonen et al., 2004).

2.1.2 Mitochondrial transcription

Mammalian mitochondrial RNA synthesis yields long polycistronic RNAs (Montoya et al., 1982). The basal machinery required for transcription initiation consists of the mitochondrial RNA polymerase (POLRMT), the mitochondrial transcription factor TF2BM and the dual role protein, TFAM. Transcription of the light strand, which in mammals only encodes the ND6 subunit of CI and eight tRNAs, initiates from a single light-strand promoter (LSP), located just outside of the D-loop region (**Fig. 1**). According to a long-standing hypothesis, heavy strand transcription is assumed to initiate at two sites adjacent to the D-loop, approximately 100 bp apart (Martin et al., 2005). Transcription from heavy-strand promoter 1 (HSP1) is posited to abruptly terminate immediately after the rRNA genes, where the transcription machinery encounters the mitochondrial transcription termination factor 1 (MTERF1), which is bound to its target site within the $tRNA^{L(UUR)}$ gene (Kruse et al. 1989; Martin et al. 2005). Thus, transcription initiated from the second heavy strand promoter (HSP2) would cover the entire strand with 2 rRNAs, 12 mRNAs and 14 tRNAs. This model has been implicitly challenged by data provided by a recent knockout of the mouse Mterf1 gene pair. The Mterf1 knockout in these mice does not affect rRNA gene expression, but rather the corresponding anti-sense transcripts, suggesting that MTERF1 has a role in blocking the light strand transcription unit prior to it reaching the rRNA gene region (Terzioglu et al., 2013).

Like TFAM, the transcription factors TFB2M and its homolog B1 (TFB1M) carry dual functionality. Both of them can activate transcription but also additionally act as methyltransferases for rRNAs (Cotney & Shadel, 2006; Metodiev et al., 2009; Seidel-Rogol, McCulloch, & Shadel, 2003). *In vitro*, though, TFB2M has been reported to possess a several fold higher capacity to stimulate transcription (Falkenberg et al., 2002) whereas TFB1M has a more potent methyltransferase based on *in vivo* assays performed in bacteria (Metodiev et al., 2009). In addition, three other transcription regulatory factors have been characterized in mammals: the transcription initiation regulator MTERF2 (Wenz et al., 2009) and the negative regulator MTERF3 (Park et al. 2007), both belonging to the same MTERF-family together with MTERF1. The third factor, c17orf42, is also the first putative mitochondrial transcription elongation factor (TEFM) to be identified (Minczuk et al., 2011). Elongation factors are common elements in other transcription systems (Sims, Belotserkovskaya, & Reinberg, 2004), and since mitochondrial transcription

produces long, polycistronic RNAs, their existence in mitochondria would seem plausible.

The fact that mitochondrial transcription yields polycistronic RNAs implies, that the transcripts require further processing to yield the fully mature mRNAs, tRNAs and rRNAs. The first step in this process is the cleavage of the individual RNA species. The mitochondrial precursor RNAs contain pre-mRNAs punctuated by mitochondrial pre-tRNAs. The 5' and 3' ends of these tRNAs serve as cleavage sites for two different enzymes. The mitochondrial RNase P complex, comprising the MRPP1, MRPP2 and MRPP3 subunits (Holzmann et al., 2008), cleaves the polycistronic RNAs at the 5' end of tRNAs, while the nuclease ELAC2 catalyzes the 3' cleavage (Brzezniak et al., 2011). Two gene pairs, ATP8/ATP6-COIII and ND5-CYTB, present an exception to this rule since these genes are not flanked by tRNAs on both sides. The post-transcriptional processing of these pre-mRNAs is still somewhat unclear, although the pentatricopeptide repeat domain protein (PTCD2) has been reported to be involved in the cleavage of the ND5 and CYTB transcripts (Xu et al., 2008).

The mt-mRNAs undergo polyadenylation catalyzed by the mitochondrial RNA poly-A polymerase (MTPAP) (Nagaike et al., 2005; Piechota et al., 2006). Polyadenylation is a required to inhibit mitochondrial mRNA decay (Piechota et al., 2006) but also to generate UAA stop codons, which in some cases are not encoded by the mtDNA (Anderson et al., 1981). rRNAs are also heavily modified post-transcriptionally. These modifications include methylation, 2'-O-ribose methylation and pseudouridinylation at specific positions (reviewed by Hällsberg & Larsson, 2014). Similarly, tRNAs must undergo nucleoside modifications in order to assume stability and proper folding and function (Suzuki et al. 2011; Hällberg & Larsson 2014). One of the most significant universal mt-tRNA modifications is the addition of a CCA-sequence into the acceptor stem in the 3' end of each tRNA, in a reaction catalyzed by the mitochondrial CCA-adding enzyme (TRNT1) (Nagaike et al., 2001).

Recent studies suggest that at least some of the early steps of mitochondrial transcript processing occurs co-transcriptionally in distinct foci named mitochondrial RNA granules (MRGs) (Antonicka et al., 2013; Jourdain et al., 2013), and in the close vicinity of mtDNA nucleoids (Lee et al. 2013). Furthermore, the initial steps in mitoribosome assembly and rRNA processing have been shown to

occur at, or in the close proximity of nucleoids (Bogenhagen, Martin, & Koller, 2014; Lee et al., 2013), suggesting that many key aspects of mitochondrial DNA metabolism and gene expression could be intimately linked and coordinated through physical interactions.

2.1.3 Mitochondria and cellular energy metabolism

Mitochondria and the oxidative phosphorylation system release and convert the chemical energy stored in organic compounds into the high-energy bonds linking the phosphate groups of adenosine triphosphate (ATP) molecules. This process is arguably one of the most important responsibilities of mitochondria in most eukaryotes. Numerous metabolic pathways supply mitochondria and the TCA cycle with carbon. Virtually all amino acid, carbohydrate and lipid catabolic pathways end or at least impinge on mitochondria (**Fig. 2**).

The breakdown of dietary carbohydrates in most cases proceeds through at least some of the steps of the glycolytic pathway, resulting in the production of pyruvate. While glycolysis provides rapid means of producing ATP from carbohydrates, the energy efficiency, *i.e.* the ATP yield per unit of carbohydrate, of this process is insufficient to satisfy the energy requirements of many cell types and tissues. Thus, a proportion of the pyruvate produced in the cytosol is transported into mitochondrial matrix, where it is decarboxylated to acetyl-CoA by the enormous 9.5 MDa (Gray, Tompkins, & Taylor, 2014) pyruvate dehydrogenase complex. Acetyl-CoA is then combined with the TCA-cycle intermediate oxaloacetate in a condensation reaction catalyzed by the mitochondrial citrate synthase, to supply the cycle with carbon. Acetyl-CoA is also generated by mitochondrial β-oxidation, a stepwise oxidation of fatty acids. The oxidation of short (SCFA, 4-8 carbon atoms) and medium chain (MCFA, 6-12) fatty acids is generally mitochondrial, whereas the oxidation of long chain fatty acids (LCFA, 10-16) occurs both in mitochondria and peroxisomes, and that of very long chain fatty acids (VLCFA, 17-26) is exclusively peroxisomal (Panini, 2013). Short and medium chain fatty acids can diffuse into mitochondria relatively freely but LCFA require a special import process. Prior to import into mitochondria, LCFAs are “activated” in the cytoplasm through a ligation with CoA. This reaction is ATP-dependent and catalyzed by acyl-CoA synthetases (or acyl-CoA ligases) (Nelson & Cox, 2005). The fatty acyl-CoAs then enter the intermembrane space where carnitine palmitoyltransferase 1 (CPT-I)

transfers the fatty acyl-groups to carnitine. The resulting fatty acyl-carnitine intermediates are then transported into the mitochondrial matrix by the carnitine-acylcarnitine translocase (CACT). Finally, in the matrix, the fatty acyl carnitines are acted on by a second carnitine palmitoyl transferase (CPT-II), which regenerates fatty acyl-CoA, substrate for β-oxidation. The mitochondrial β-oxidation is a four-reaction process with each full round of oxidation resulting in a sequential removal of two-carbon units (acetyl-CoA) at the β-position of fatty acyl-CoA molecule. This process can fully degrade only even-chain fatty acids, though, as the final step in the breakdown of odd-chain fatty acids results in the production of acetyl-CoA and propionyl-CoA, rather than two molecules of acetyl-CoA. In this case, the propionyl-CoA is converted into the TCA-cycle intermediate succinyl-CoA through a methylmalonyl-CoA intermediate. These intermediate steps are also required for the full degradation of methionine and the branched chain amino acids valine, leucine and isoleucine. The deamination and breakdown of each of these amino acids yields propionyl-CoA and can thus supply carbon to the TCA-cycle in the form of succinyl-CoA. Other amino acids can also be catabolized to provide energy. While the contribution of amino acids to total energy production in humans on a well-balanced diet is quite low, some 10-15% (Pasquale, 2007), this figure can be substantially higher *e.g.* for those on a low-carbohydrate diet. Amino acids are divided into two sub-classes based on the end-products of their catabolism: glucogenic and ketogenic. The deaminated carbon skeletons of glucogenic amino acids can provide carbon to the TCA cycle, in addition to succinyl-CoA, in the form of pyruvate (alanine, cysteine, glycine, serine, threonine and tryptophan), oxaloacetate (asparagine and aspartate), fumarate (aspartate, phenylalanine and tyrosine) and α-ketoglutarate (arginine, glutamate, glutamine, histidine and proline). Ketogenic amino acids (isoleucine, leucine, lysine, tryptophan and tyrosine) in turn, are degraded to acetyl-CoA. The dehydrogenases of the TCA cycle (isocitrate dehydrogenase, α-ketoglutarate dehydrogenase, succinate dehydrogenase and malate dehydrogenase) oxidize their respective substrates while reducing the electron acceptors NAD+ and FAD+ to NADH and $FADH_2$. These high-energy electron carriers, in turn, supply electrons to the electron transport chain.

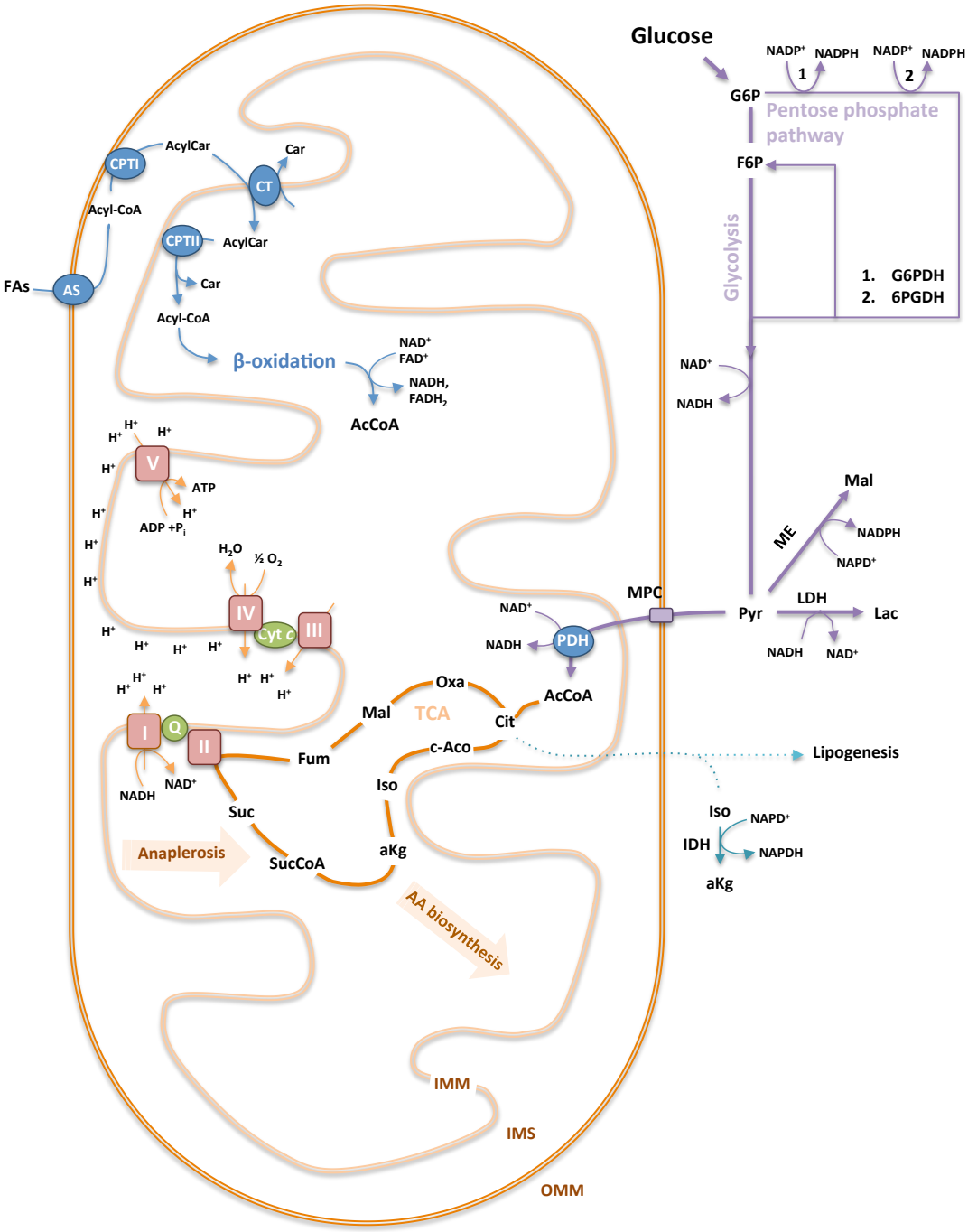
Glucose
NADP+
NADPH
1
2
G6P
Pentose phosphate pathway
F6P
Glycolysis
1. G6PDH
2. 6PGDH
NAD+
NADH
Mal
ME
NADPH
NAPD+
MPC
Pyr
LDH
Lac
NADH
NAD+
NAD+
NADH
PDH
AcCoA
Oxa
Mal
TCA
Cit
c-Aco
Lipogenesis
Iso
NAPD+
IDH
NAPDH
aKg
Fum
Iso
Suc
aKg
SucCoA
Anaplerosis
AA biosynthesis
IMM
IMS
OMM
CPTI
AcylCar
Car
CT
Acyl-CoA
CPTII
AcylCar
Car
Acyl-CoA
FAs
AS
β-oxidation
NAD+
FAD+
NADH,
FADH2
AcCoA
V
ATP
ADP +Pi
H+
H2O
½ O2
IV
Cyt c
III
I
Q
II
NADH
NAD+

Figure 2. Mitochondria participate in several of the core processes of cellular nutrient metabolism. Abbreviations: 6PGDH – 6-phosphogluconate dehydrogenase, AA – amino acid, AcCoA – acetyl-coenzyme A, AcylCar – acyl-carnitine, c-Aco – *cis*-aconitate, AS – acyl-CoA synthetase, aKG – alpha-ketoglutarate, Car – carnitine, Cit – citrate, CPTx – carnitine palmitoyl transferase, CT - carnitine acyltransferase, Cyt *c* – cytochrome *c*, F6P – fructose-6-phosphate, Fum – fumarate, G6P – glucose-6-phosphate, G6PDH – glucose-6-phosphate dehydrogenase, IDH – isocitrate dehydrogenase, IMM – inner mitochondrial membrane, IMS – intermembrane space, Iso – isocitrate, Lac – lactate, LDH – lactate dehydrogenase, Mal – malate, ME – malic enzyme, MPC – mitochondrial pyruvate carrier, OMM – outer mitochondrial membrane, Oxa – oxaloacetate, PDH – pyruvate dehydrogenase complex, Q – ubiquinone/ubiquinol, Suc – succinate, SucCoA – succinyl CoA, TCA – tricarboxylic acid cycle

2.1.4 Mitochondrial OXPHOS system

The production of ATP from ADP and organic phosphate is energetically unfavorable. The required energy is provided by the oxidation of the two electron carriers, NADH and $FADH_2$, in a chain of oxidation/reduction reactions catalyzed by four multisubunit protein complexes (complexes I-IV, CI-IV) of the inner mitochondrial membrane, known as the electron transport chain (ETC). Three of these complexes couple the transport of electrons to translocation of protons across the inner mitochondrial membrane. This proton motive force (Δp) is then used to drive ATP synthesis, catalyzed by another multimeric protein complex (complex V, CV). These two, coupled processes are collectively called the oxidative phosphorylation (OXPHOS) or cellular respiration system.

Structurally, the five OXPHOS or respiratory chain complexes consist of 92 polypeptides, 13 of which are mitochondrially encoded (Chinnery & Hudson, 2013). In addition, numerous proteins are transiently associated with the complexes during their assembly (assembly factors), or participate in their regulation and coordination. The largest of these OXPHOS complexes, complex I (NADH:ubiquinone oxidoreductase), comprises 44 subunits: 7 nDNA- and 7 mtDNA-encoded polypeptides form the functional core of CI while a further 30 nDNA encoded subunits are required for its stability and regulation (Hirst, 2011; Kmita & Zickermann, 2013). The small, four-subunit complex II (succinate: ubiquinone oxidoreductase, succinate dehydrogenase) is the only respiratory chain complex which contains no mitochondrially encoded polypeptides. It is also an enzyme of the TCA cycle. Complex III (ubiquinol:cytochrome *c* oxidoreductase) contains a single mtDNA- and 10 nDNA-encoded subunits. Complex IV (cytochrome c oxidase, COX) consists of three mitochondrially encoded core subunits, and an additional 11 encoded by the nDNA. Finally, complex V (F_0F_1-ATP synthase) comprises of 17 nDNA encoded and 2 mtDNA encoded subunits.

The core function of complexes I and II is to receive electrons from the freely diffusible NADH and the protein bound $FADH_2$, respectively, and transfer them to ubiquinone [coenzyme Q10 (CoQ)], reducing it first to ubisemiquinone and then to ubiquinol ($CoQH_2$). CoQ transports electrons to CIII, which relays them further to another diffusible electron carrier, cytochrome *c*. In the final electron transport step, cytochrome c donates electrons to CIV, which uses them to reduce molecular oxygen, the terminal electron acceptor in mammalian mitochondria, into water.

Pyruvate dehydrogenase (NAD+ to NADH), the TCA cycle (NAD+ to NADH and FAD to FADH2) and β-oxidation (NAD+ to NADH and FAD to $FADH_2$) are generally considered the primary source of reducing equivalents. However, other metabolic pathways also contribute to the mitochondrial redox-balance to a varying degree, depending on the cell and tissue type. For instance, enzymes participating in the glycine cleavage system and other reactions of mitochondrial amino-acid catabolism, such as proline oxidase and the branched-chain α-ketoacid dehydrogenase complex, can also reduce NAD+ and FAD+. In addition, the mitochondrial glycerol-3-phosphate dehydrogenase, which participates in the α-glycerophosphate shuttle, transfers electrons from the cytosol into the ubiquinone pool.

The energy released by the flow of electrons down the electron transport chain is used by complexes I, III and IV to pump protons from the matrix, across the inner membrane, into the inner membrane space. This generates an electrochemical gradient across the IMM. The potential energy of the proton gradient is used for multiple purposes: to produce ATP, to import proteins and other ions, and to generate heat by dissipating the Δp through a process called uncoupling (Ledesma, de Lacoba, & Rial, 2002). The flow of protons from the inner membrane space into the matrix through the membrane.spanning part (Fo) of complex V powers the conversion of ADP + P_i to ATP (Boyer, 1997). The inner membrane adenine nucleotide translocators (ANTs) are used to transport the mitochondrially synthesized ATP into the cytosol in exchange for ADP.

Respiratory chain complexes of intact mitochondria are arranged in larger assemblies, called supercomplexes or respirasomes. The supercomplexes of mammalian cells mainly comprise complexes I, III and IV in different stoichiometric combinations (Acín-Perez et al., 2008; Dudkina et al., 2011). Functionally, supercomplex formation stabilizes the individual complexes and provides a means for substrate channeling (Acín-Pérez et al., 2004; Schägger et al., 2004), which significantly improves the efficiency of electron flow through them (Bianchi et al., 2004). The individual complexes may also produce and release less reactive oxygen species (ROS) when bundled into supercomplexes (Maranzana et al., 2013).

2.1.4.1 Alternative respiratory chain enzymes

The OXPHOS system with its five multisubunit complexes is generally considered to provide the most energy efficient means for the terminal oxidation steps in nutrient catabolism and ATP synthesis. However, lower eukaryotes present exceptions to the generally highly conserved organization of the OXPHOS system. Baker's yeast, *Saccharomyces cerevisiae*, for example, is completely devoid of complex I, but instead uses two rotenone-insensitive, single-subunit NADH dehydrogenases, Nde1p and Ndi1p, to transfer electrons to ubiquinone, either from the cytosol (Nde1p), or from the mitochondrial matrix (Ndi1p) (Yagi et al., 2001). As opposed to complex I, neither enzyme is capable of translocating protons between mitochondrial or cellular compartments. In addition to *S. cerevisiae*, plants also carry several alternative NAD(P)H dehydrogenases, but unlike the case of yeast, these complement a standard electron transport chain (reviewed by Rasmusson, Soole, & Elthon, 2004).

Plants, in particular, utilize a second alternative enzyme which by-passes the cytochrome segment (CIII and CIV) of the respiratory chain (Siedow & Umbach, 2000). This alternative oxidase (AOX) receives electrons from ubiquinol and passes them directly to molecular oxygen. The AOX of plants is integral to the inner mitochondrial membrane and is believed to operate as a homodimer, with no proton translocation activity (Juszczuk & Rychter, 2003). Although the exact physiological function of AOX in plants is unknown, biochemical evidence suggests that AOX can facilitate the maintenance of mitochondrial substrate oxidation and TCA-cycle activity when high levels of ATP are being produced concomitantly by photosynthesis (Noguchi & Yoshida, 2008; Rustin & Lance, 1986). AOX is enzymatically inactive *in vivo* under normal physiological conditions, since it has a very low affinity for ubiquinol and is only activated by a significant over-reduction of the quinone pool (Yoshida et al., 2010).

In recent years, the alternative respiratory chain enzymes have been extensively studied in the context of respiratory chain dysfunction, and its compensation using the molecular bypass of dysfunctional complexes provided by these enzymes. AOX has been successfully used to rescue cytochrome *c* oxidase deficiency in human cells (Dassa et al., 2009; Hakkaart et al., 2006), flies (Kemppainen et al., 2014) and, most recently, in rodents (El-Khoury et al., 2013). Likewise, the yeast Ndi1p has been shown to ameliorate the pathological outcomes of complex I deficiency in all

three species (Bai et al. 2001; Burman et al. 2014; Cho et al. 2012; Marella et al. 2010; Park et al. 2007; Sanz et al. 2010). Furthermore, both enzymes can be used to dissect the pathological mechanisms underlying complex OXPHOS disorders by providing a bypass for isolated segments of the respiratory chain, decreasing ROS production and alleviating the metabolic block in substrate oxidation imposed by dysfunctional electron transport.

2.1.4.2 Mitochondrial reactive oxygen species

Mitochondria and the electron transport chain are often considered the primary source of ROS in the cell. While the evidence to support this notion is inconclusive or insufficient, mitochondria are certainly one of the major sources of ROS, even under normal physiological conditions (reviewed by Brown & Borutaite, 2012). Mitochondrial ROS production occurs primarily via electron leakage from the redox active prosthetic groups of complexes I and III, although many mitochondrial enzymes, such as α-ketoglutarate dehydrogenase, monoamine oxidase and mitochondrial glycerol-3-phosphate dehydrogenase can contribute to total ROS production (Balaban, Nemoto, & Finkel, 2005; Starkov, 2008). Reactive oxygen species include a number of oxygen-derived, highly reactive molecules. Most of them are derivatives of either the superoxide anion ($O_2^{\cdot -}$) or hydrogen peroxide (H_2O_2) (Brown & Borutaite, 2012). The superoxide anion is produced when escaping electrons react with, and reduce O_2. Superoxide is detoxified by converting it to hydrogen peroxide, in a reaction catalyzed by the mitochondrial manganese superoxide dismutase (MnSOD or SOD2). The freely diffusible H_2O_2 itself is detoxified by decomposition to water, catalyzed by catalases or glutathione peroxidases. Alternatively, in the presence transition metals, such as Fe^{2+}, hydrogen peroxide may react to produce the hydroxyl radical ($OH^{\cdot -}$) in the so-called Fenton reaction (Winterbourn, 2013). H_2O_2 is the least reactive and most stable of the three reactive oxygen species, while $OH^{\cdot -}$ has the shortest half-life time but also the highest reductive potential (Holmström & Finkel, 2014).

Cells process endogenous ROS by a variety of antioxidant mechanisms, including the aforementioned detoxifying enzymes, and the glutathione system, which decomposes H_2O_2 to water. This reaction is catalyzed by glutathione peroxidases, and results in the oxidation of glutathione (GSH) to glutathione disulfide (GSSG).

Glutathione is regenerated by glutathione reductase which reduces the oxidized glutathione back to GSH, in an NADPH-dependent manner (Wu et al., 2004). These antioxidant defenses may become insufficient when ROS-production is elevated for prolonged periods of time, such as in the case of high Δp, $NADH/NAD^+$ and $CoQH_2/CoQ$ ratios, resulting from respiratory chain dysfunction (reviewed by Murphy, 2009). The close proximity of the mtDNA molecule to the site of production of the highly reactive ROS, $O_2^{\cdot -}$ and $OH^{\cdot -}$, makes it exceptionally prone to oxidative lesions.

To counter the DNA lesions inflicted by ROS and other environmental stressors, mitochondria have several repair mechanisms. Such mechanisms have been shown to include at least mismatch repair, base excision repair and degradation and regeneration of damaged mtDNA molecules (Alexeyev et al., 2013; Copeland & Longley, 2014; Kazak, Reyes, & Holt, 2012).

2.1.5 Mitochondrial protein homeostasis

2.1.5.1 Mitochondrial protein synthesis

The existence of mitochondrial translation machinery was postulated in the early 1960's. The first mitochondrial ribonucleoprotein complexes were isolated from rat liver a few years later. Due to the endosymbiotic origin of mitochondria, prokaryotic and mitochondrial proteins synthesis systems have some fundamental similarities, yet considerable structural divergence has occurred between mitoribosomes and the ancestral system of bacteria. The mammalian 55S mitoribosome consists of two subunits, the 28S small subunit and the 39S large subunit. The backbones of the small and large subunits are formed by the 12S and 16S rRNAs, respectively. The rest of the mitoribosome comprises approximately 80 nuclear-coded polypeptides, of which 15 SSU and 20 LSU polypeptides display no significant homology to bacterial proteins, suggesting that these are newly acquired ribosomal proteins (Koc et al. 2000, 2001; Suzuki et al. 2001; Cavdar et al. 2001). The prokaryotic (70S) ribosomes likewise consist of small (30S) and large (50S) subunits, and are generally smaller than mitoribosomes despite having higher sedimentation coefficients. This disparity in metrics is explained by the higher protein content, and thus more porous structure of the mitoribosome. Mammalian mitoribosomes have a

protein to RNA ratio of 2 to 1, whereas the opposite is true for prokaryotic ribosomes (Sharma et al., 2003).

The rRNA stem-loops of the small subunit coordinate codon-anticodon pairing, making the SSU largely responsible for the decoding process and fidelity of translation. The large subunit in turn interacts with the acceptor arms of tRNAs and covalently links amino acids to the nascent polypeptide chain, thus carrying out the peptidyl transferase reaction.

Mitochondrial protein synthesis proceeds in four discernible steps, but many aspects of the process remain poorly understood, largely due to the lack of an in vitro mitochondrial translation system (Rorbach et al., 2007). One of the most enigmatic questions in mitochondrial protein synthesis remains how translation is initiated *i.e.* how ribosomes are directed to the initiation codon. Mitochondrial mRNAs lack 7-methylguanylate cap structures in their 5'-ends and upstream leader sequences which facilitate initiation in the eukaryotic cytoplasm, and also lack the Shine-Dalgarno sequences of the prokaryotic mRNAs (Montoya, Ojala, & Attardi, 1981). Two initiation factors, $IF2_{mt}$ and $IF3_{mt}$, have been identified in mammalian mitochondria (Koc & Spremulli, 2002; Liao & Spremulli, 1991). The absence of the prokaryotic IF1 in mammalian systems could simply be explained by functional redundancy: the *Escherichia coli* IF1 fails to stimulate translation initiation of the 55S ribosomes, while $IF2_{mt}$ alone can catalyze translation initiation of the 70S ribosomes, in the absence of IF1 (Spremulli et al., 2004). $IF2_{mt}$, like its bacterial orthologue, is believed to promote tRNA-SSU interaction (Spencer & Spremulli, 2004).

In bacteria, translation commences with the formation of an initiation complex, consisting of 30S SSU, mRNA, N-formylmethionylated tRNA ($tRNA^{fMet}$), the three IFs and GTP (Boelens & Gualerzi, 2002). Initiation factors assist the first methionyl-tRNA to access the ribosomal P-site. All the subsequent aminoacylated-tRNAs will enter the ribosome at the A-site. IF3, which interacts with the small subunit at the vicinity of the P-site, is required to block the premature association of the two ribosomal subunits (Brock, Szkaradkiewicz, & Sprinzl, 1998) and to proofread the correct selection of tRNA during initiation (Meinnel et al., 1999). The GTP-bound form of IF2 forms a ternary complex with $tRNA^{fMet}$ resulting in the release of IF3. The dissociation of IF3 primes subunit adhesion, which in turn triggers IF2 to hydrolyze GTP to GDP and the subsequent release of all initiation

factors. This concludes the initiation phase and the ribosome proceeds to the elongation cycle. The translation initiation phase of eukaryotic mitoribosome is somewhat less well characterized, but believed to occur through highly analogous steps.

Translation elongation requires three accessory proteins, EF-Ts, EF-Tu and EF-G, in bacteria and mitochondria alike, with the exception of yeast, which lacks EF-Ts. Although mitochondrial polypeptide chain elongation has not been extensively studied, the substantial homology between the mitochondrial elongation factors and their bacterial counterparts suggests that the process proceeds in a similar fashion in both systems (Rorbach et al., 2007). Elongation begins with the aminoacylated-tRNA entering the ribosomal A-site in a ternary complex with EF-Tu and GTP. The anticodon site of the tRNA interacts with the mRNA, causing GTP hydrolysis and the release of EF-Tu-GDP, while the ribosomal peptidyl transferase center catalyzes the formation of a new polypeptide bond. The nascent polypeptide chain then translocates together with the peptidyl-carrier tRNA to the P-site exposing the A-site for a new aminoacyl-tRNA. This translocation is promoted by ribosome bound EF-G-GTP and GTP-hydrolysis. Simultaneously, the ribosome advances a single codon length along the mRNA. The inactive EF-Tu-GDP is activated to EF-Tu-GTP by EF-Ts. Once the tRNA has translocated through the A and P-sites, it exits the ribosome at an E-site. The existence of a bacteria-like E-site in mitoribosomes is unclear since the contact sites between the ribosome and tRNA are poorly conserved (Mears et al., 2002; Mears et al., 2006). This elongation cycle continues until the ribosome encounters a stop codon.

Translation termination is the least well-studied phase of mitochondrial protein synthesis. The translation termination and release factor family consists of four members, identified based on sequence homology: mtRF1 (Nozaki et al., 2008), mtRF1a (Soleimanpour-Lichaei et al., 2007), ICT1 (Richter et al., 2010) and C12orf65 (Antonicka et al., 2010). Termination in mitochondria is signaled by one of the four stop codons: the non-conventional AGA and AGG, and the canonical UAA and UAG, found in 11 of the 13 mitochondrial open reading frames. The latter two stop codons are decoded by the mitochondrial release factor RF1a (mtRF1a). Two competing theories exist on how the remaining two, non-canonical stop codons AGA and AGG are decoded. The first possibility is that the mitoribosome undergoes a -1 frameshift upon the entry of either of these triplets on to the A-site, thus effectively placing a standard UAG in to the A-site (Temperley et al., 2010).

The second possibility is that AGA and AGG are truly stop codons but translation termination is catalyzed by ICT1 instead of mtRF1a (Akabane et al., 2014; Lind, Sund, & Aqvist, 2013).

After translation termination, one more crucial step is required before the mitoribosome is ready for a new round of protein synthesis. This process of ribosome recycling involves dissociation of the ribosome-mRNA-tRNA complex and the two mitoribosomal subunits from each other, assisted by special recycling factors (RFs). Two mitochondrial RFs, RRF_{mt} and EF-G2 (also referred to as $RRF2_{mt}$), have been characterized in mammalian mitochondria so far (Tsuboi et al., 2009; Zhang & Spremulli, 1998) but the exact mechanistic details of the recycling process are still under investigation.

2.1.5.2 Mitochondrial protein import

The mitochondrial genome encodes only 13 polypeptides while proteomics studies have estimated the mitochondrial proteome to comprise approximately 1500 polypeptides in mammals and 1000 in yeast (Pagliarini et al., 2008; Reinders et al., 2006; Sickmann et al., 2003). This implies that the vast majority of mitochondrial proteins are synthesized on cytosolic ribosomes and imported through the mitochondrial double membrane in a controlled fashion (reviewed by Dudek et al., 2013). Synthesis of mitochondrially targeted proteins occurs in the proximity of the mitochondrial outer membrane, but protein import is considered to take place post-translationally, with SOD2 and fumarase amongst the few known exceptions (reviewed by Dudek et al., 2013).

Protein targeting into mitochondria requires a specific targeting sequence, which is usually an N-terminal, 15 to 55 amino acid-long presequence containing amphipathic α-helices and a net positive charge (Vögtle et al., 2009).

Transport across the outer membrane is performed by the Translocase of the Outer Membrane (TOM complex). Transported proteins are initially docked to Tom20 and Tom70 proteins, which proofread the existence of a correct import signal. Hydrophobic proteins are escorted to the docking site with the assistance of chaperone proteins, which prevent premature and misfolding. Upon entry to the intermembrane space, proteins destined to the outer membrane are bound by small

Tim chaperones and transported into the Sorting and Assembly Machinery (SAM), which integrates them into the OMM. The various inner membrane metabolite carriers are inserted into the IMM by the Translocase of the Inner Membrane 22 (TIM22 complex), with the help of membrane potential. Protein translocation to the matrix continues directly from the TOM complex to the presequence translocase, or the Translocase of the Inner Membrane 23 (TIM23 complex). In addition to the matrix, the TIM23 complex can also sort proteins laterally to the inner membrane. IMM sorting and integration is driven by membrane potential alone, while protein translocation into the matrix requires additionally the Presequence translocase-Associated import Motor (PAM) and ATP.

The mitochondrial import presequence is removed in the IMS, IMM or the matrix by either one of the classical presequence peptidases, MPP (the mitochondrial presequence peptidase), IMP (the inner membrane peptidase) and Oct1, or other mitochondrial proteases (Mossmann et al. 2012).

2.1.6 Mitochondrial quality control

The term mitochondrial quality control (QC) comprises of all of the various cellular pathways responsible for the controlled turnover of mitochondrial proteins and lipids, even entire organelles, and the processes involving the regulation of mitochondria dynamics and morphology. The goal of the QC machinery is to maintain and restore the integrity of mitochondrial function and to protect the cell from the deleterious consequences of organelle failure. Defective quality control has been most prominently linked to neurodegenerative disorders, such as mitochondrial forms of Parkinson's disease.

QC at the macromolecular level inside mitochondria involves highly conserved proteases and chaperone proteins which monitor the folding and assembly of mitochondrial proteins, and remove damaged and misfolded polypeptides (reviewed by Tatsuta & Langer, 2008). On the organellar level, functionality may be restored via fusion between damaged and intact mitochondria, or alternatively, segments of the mitochondrial network may be removed by fission. Both of these processes are regulated by the factors governing mitochondrial dynamics (Detmer & Chan, 2007). Finally, if mitochondria are damaged beyond repair, individual organelles can be

recycled through an autophagy-like process, termed mitophagy (Kim et al. 2007). This protects the cells from the inadvertent release of pro-apoptotic proteins from dysfunctional mitochondria (reviewed by Maiuri et al, 2007).

2.1.6.1 Mitochondrial protein degradation and unfolded protein response

The mitochondrial proteolytic QC machinery recognizes and degrades misfolded and damaged proteins in the intermembrane space and in the matrix. This process is catalyzed by ATP-dependent proteases which cleave their substrate proteins into short peptides, which are then further acted on by various oligopeptidases. Since many mitochondrial proteins are components of multi-protein assemblies, their degradation requires the help of mitochondrial chaperone proteins.

Two proteases of the AAA+ superfamily, Lon and ClpXP, chaperone and degrade mitochondrial proteins in the matrix, while a third family member, m-AAA is an inner membrane protease which cleaves membrane proteins on the matrix side (Goard & Schimmer, 2014). The Lon protease, in particular, has been shown to be assisted by the Hsp70 and Hsp100 family chaperone proteins, which prevent or dissolve protein aggregates and thus enable proteolysis (Tatsuta & Langer, 2008). The m-AAA cleaves membrane protein domains protruding into the matrix, whereas the i-AAA protease catalyzes analogous proteolysis in the inter-membrane space (Leonhard et al., 2000). The mitochondrial proteases are also involved in a number of processes in a regulatory capacity. For example, in mice and yeast, the m-AAA protease is required to process the preprotein form of the mitoribosomal protein L32, and failure to do so results in protein synthesis deficiency (Bonn et al., 2011; Nolden et al., 2005). The Lon protease in turn, has been demonstrated to regulate mitochondrial gene expression and mtDNA copy number through its target, TFAM, at least in *Drosophila* (Matsushima, Goto & Kaguni, 2010).

Under some circumstances, the processing capacity of the mitochondrial proteases and chaperones may be exceeded, resulting in a mitochondrial proteotoxic stress. This may trigger the mitochondrial unfolded protein response UPR_{mt}, a response distinct from the much better studied ER-specific UPR. UPR^{mt} may be induced, for instance, when mitochondrial gene expression is inhibited, creating a disequilibrium between cytosolically and mitochondrially synthesized polypeptides inside

mitochondria (Martinus et al., 1996; Zhao et al., 2002). Induction of the mitochondrial UPR results in the up-regulation of mitochondrial chaperones and proteases, namely Hsp60, Hsp70^{mt}, Hsp10 and ClpXp (Haynes & Ron, 2010). The retrograde signaling which induces the UPR^{mt} is still somewhat poorly characterized. In mammals, the transcription factor CHOP regulates at least some of the unfolded protein responsive genes while in *C. elegans*, a shift in the localization of a transcription factor ATFS-1 from cytosol/mitochondria to nucleus has been shown to activate UPR^{mt} (Haynes & Ron, 2010; Nargund et al., 2012; Pellegrino, Nargund, & Haynes, 2013).

2.1.6.2 Mitochondrial dynamics and quality control

Mitochondrial QC is also exerted through the regulation of mitochondrial network dynamics. Four dynamin-related GTPases have been identified as the central mediators of mitochondrial fission and fusion: the cytosolic DRP1 is recruited to the outer membrane to catalyze mitochondrial fission, while the mitofusins MFN1 and MFN2 in the outer membrane, and OPA1 in the inner membrane, control membrane fusion (Cerveny et al., 2007; Hoppins & Nunnari, 2009).

Mitochondrial fission creates smaller mitochondria, which can *e.g.* facilitate mitophagy. Upon its activation and translocation to the outer membrane, DRP1 multimerizes and forms a ring-like structure, which constricts and separates a fraction of the larger mitochondrion (Lee et al., 2004; Zhu et al., 2004).

Mitochondrial fusion allows content mixing between mitochondria. This process can potentially dilute damaged mitochondrial content such as, mutated DNA, by replenishing it with healthy macromolecules. Fusion is mediated by the outer membrane mitofusins, which form homodimeric or heterodimeric coiled-coil linkages between adjacent mitochondria. Mitofusins are degraded in mitophagy through PINK1/PARKIN-mediated ubiquitination and proteolysis (Tanaka et al. 2010).

2.1.6.3 Mitophagy

Once mitochondria become damaged beyond rescue by fusion, parts of the mitochondrial network may be sequestered. These mitochondrial fragments are removed by mitophagy. A cascade of events resulting in mitophagy can be triggered by the loss of membrane potential, which causes OPA1 inactivation and inhibits mitochondrial fusion. Two genes, PINK1 and PARKIN, are intimately linked to the regulation of mitophagy of depolarized mitochondria (Clark et al., 2006; Greene et al., 2003). PINK1 is a serine/threonine kinase which accumulates on mitochondria upon loss of membrane potential and recruits PARKIN from the cytosol (Matsuda et al., 2010; Narendra et al., 2008). The E3 ubiquitin ligase PARKIN, polyubiquitinates its substrates, which include mitofusins and VDACs, and thus induces the engulfment and subsequent degradation of mitochondria by the autophagosome-lysosome pathway (Narendra et al. 2008; Geisler et al. 2010; Tanaka et al. 2010). Mutations in both PINK1 and PARKIN have been linked to the pathogenesis of neurodegenerative disorders, most notably Parkinson's disease.

Recently, an alternative PINK1 and PARKIN-mediated pathway for recycling mitochondrial content via mitochondrially derived vesicles (MDVs) was discovered (McLelland et al., 2014). This pathway operates independently of DRP1 and canonical mitophagy, and is triggered by oxidative stress, rather than membrane depolarization. Furthermore, the MDVs only appear to transport a selected subset of proteins to degradation at lysosomes.

2.1.6.4 Mitochondria and programmed cell death

Severe mitochondrial dysfunction may ultimately result in necrotic or apoptotic cell death (Lemasters et al., 1999). Mitochondria were first linked to apoptosis through the discovery that a core component of the apoptotic machinery, Bcl-2, was anchored to the outer mitochondrial membrane in *C. elegans* (Hengartner & Horvitz, 1994). For a while, mitochondria were thought to act merely as a signaling scaffold for the apoptotic machinery, but it is now well understood, that mitochondria can actively regulate programmed cell death (Galluzzi et al., 2012). The exact mechanistic details of the early steps after the induction of apoptosis are still not fully resolved, and may vary between taxa. The dissipation of the

mitochondrial membrane potential is known to be one of the inducing signals for the tightly regulated multi-step process resulting eventually in cell death. The loss of membrane potential induces outer membrane permeabilization, which in apoptosis is mediated by two Bcl-2 family members, BAX and BAK (Breckenridge and Xue, 2004; Green and Kroemer, 2004). The permeabilization also releases a number of mitochondrial proteins, including cytochrome *c*, SMAC/Diablo and HtrA2/Omi, which initiate the apoptotic caspase cascade (Galluzzi et al., 2012).

2.1.7 Mitochondrial disorders

Mitochondrial disorders form a large and heterogeneous group of individually rare syndromes with a highly variable age of onset, severity and tissue specificity, and which generally arise as a result of respiratory chain dysfunction caused by mutations in mtDNA or genes nuclear-coded mitochondrial proteins (Nunnari & Suomalainen, 2012; Schon et al., 2012; Wallace et al., 2010). Respiratory chain dysfunction can occur as an isolated deficiency of a single OXPHOS complex, often caused by a mutation in a gene for a structural subunit or assembly factor, such as in the case of Leigh syndrome with COX deficiency, which results from mutations in the cIV assembly factor SURF1. More often though, most of the respiratory chain is affected, *e.g.* as a result of point mutations in the mtDNA-encoded mitochondrial tRNAs or rRNAs, or substantial mtDNA depletion. In such cases, the individual's and tissue-specific heteroplasmy levels play a major role in determining the disease outcome. Due to the involvement of both genomes, mitochondrial disorders resulting from non-sporadic mutations can be transmitted either maternally or in Mendelian fashion. Largely due to reasons of mtDNA heteroplasmy and stochastic segregation in post-mitotic tissues, mitochondrial disorders may not manifest in every generation or affected individual, or the same mutation may result in a different disease outcome in even closely related individuals.

The first case of a patient suffering from a mitochondrial disorder was reported already over half a century ago (Luft et al. 1962), but the era of mitochondrial disease research genuinely started in the late 80's after the discovery of the first pathogenic mtDNA mutations (Holt, Harding, & Morgan-Hughes, 1988; Wallace et al., 1988). Since then, 150 distinct mitochondrial disorders have been characterized and more than 300 mtDNA lesions have been associated with clinical

manifestations. Altogether, the different respiratory chain disorders are currently predicted to affect at least 1 in 5000 individuals (Skladal, Halliday, & Thorburn, 2003; Vafai & Mootha, 2012).

Mitochondrial disorders can manifest essentially in only a single organ, such as in the eye, in the case of Leber's hereditary optic neuropathy (LHON), or can affect multiple organs and tissues, with at least the muscle and central nervous system usually being affected. Mitochondrial DNA mutations, in particular, can manifest with extreme phenotypic variability. Syndromes which involve multiple deletions or loss of mitochondrial DNA, such as progressive external ophthalmoplegia (PEO), MIRAS (mitochondrial-associated recessive ataxia syndrome), SANDO (Sensory ataxia, neuropathy, dysarthria, ophthalmoparesis), IOSCA (infantile onset spinocerebellar ataxia), the Alpers-Huttenlocher syndrome or MDS (mitochondrial DNA depletion syndrome) can display either autosomal dominant or recessive inheritance (Rötig & Poulton, 2009). These disorders result from mutations in nuclear encoded genes involved in mtDNA maintenance, such as POLG, Twinkle, or in deoxyguanosine kinase (dGK) and thymidine kinase 2, two enzymes of the mitochondrial nucleoside salvage pathway (El-Hattab & Scaglia, 2013; Rötig & Poulton, 2009). Mitochondrial DNA point mutations in tRNA and rRNA genes are the cause of some of the most prevalent mitochondrial disorders, such as MELAS (mitochondrial encephalomyopathy with lactic acidosis and stroke-like episodes), MERRF (myoclonus epilepsy with ragged red fibers) (Rötig 2011; Vafai & Mootha 2012). In addition to point mutations and deletions, mtDNA duplications are associated with mitochondrial diseases. Although generally rare, duplications are often detected in patients suffering from Kearns-Sayre syndrome (KSS) (Poulton et al., 1995).

Occasionally, mitochondrial disorders involving respiratory chain dysfunction arise from mutations not affecting the respiratory chain or mtDNA maintenance and expression machinery directly. Examples of this include impaired mitochondrial Fe-S cluster assembly which may result in Friedreich's ataxia, and Coenzyme Q10 deficiency which is associated with familial mitochondrial cytopathies (González-Cabo & Palau, 2013; Ogasahara et al., 1989). Defective mitochondrial quality control, in turn, has been linked to neurodegenerative disorders such as Parkinson's disease (Nunnari & Suomalainen, 2012).

Finally, diseases which are not necessarily characterized by features of classical mitochondrial disorders, may be of mitochondrial origin. Alterations in mitochondrial metabolism, for example, are being increasingly associated with many pathological conditions such as obesity, type 2 diabetes and cancer (Arruda et al., 2014; Chandel, 2014; Montgomery & Turner, 2014).

2.1.8 Disorders of mitochondrial protein synthesis

The mitochondrial protein synthesis machinery is responsible for translating only 13 mtDNA encoded polypeptides, but altogether approximately 100 nuclear genes are required to encode the translation machinery itself. Pathogenic mutations could theoretically affect any of these genes, which include those encoding mitoribosomal proteins, tRNA-modifying enzymes and aminoacyl-tRNA synthetases, translation initiation and elongation factors, and translational activators. Likewise, mtDNA-encoded tRNAs and rRNAs are common targets of pathogenic, protein synthesis impairing mutations.

The first mtDNA mutations affecting mitochondrial protein synthesis were described over 20 years ago. One of the most prevalent, the A3243G mutation in the $tRNA^{L(UUR)}$ gene, results in the childhood onset MELAS syndrome, a mitochondrial cytopathy characterized by lactate buildup and stroke-like episodes (Goto et al. 1990). A second highly prevalent mitochondrial tRNA mutation is the A8344G in the $tRNA^{Lys}$ gene. This mutation accounts for approximately 80% of MERRF cases (Shoffner et al., 1990b). A third mitochondrial tRNA gene often found mutated is that encoding $tRNA^{Ile}$. Mutations in $tRNA^{Ile}$ are usually heteroplasmic and present as cardiomyopathy and PEO (Rötig, 2011). More than 150 tRNA mutations with different clinical manifestations (*e.g.* myopathy, encephalomyopathy, Leigh syndrome, chronic progressive external ophthalmoplegia) have been characterized, but mutations in these three tRNA genes comprise over half of them (Rötig, 2011). tRNA mutations can affect translation in multiple ways: by causing defective tRNA folding, preventing nucleotide modifications, affecting tRNA stability or by causing amino acid misincorporation and thus decreasing the stability of mtDNA-encoded proteins (Börner et al., 2000; Sasarman, Antonicka, & Shoubridge, 2008). The mitochondrial tRNAs are frequently pseudouridylated, which stabilizes their secondary and tertiary structure. Mutations in the mitochondrially targeted isoform of pseudouridine synthase (PUS1), which converts uridine to pseudouridine, have

been found in patients suffering from mitochondrial myopathy, lactic acidosis and sideroblastic anemia (MLASA) (Bykhovskaya, Casas, Mengesha, Inbal, & Fischel-Ghodsian, 2004).

Mitoribosomal rRNA mutations have been associated with aminoglycoside-induced sensorineural hearing loss. The A1555G mutation in the 12S rRNA is one of the best-characterized mtDNA mutations. The mutation is usually homoplasmic and has a very high incidence in clinical populations, particularly in Asia (Rötig, 2011).

Pathogenic mutations in mitoribosomal protein genes themselves are very rare, possibly due to their early lethality. Two proteins of the small subunit, MRPS16 and MRPS22, have been found to be mutated in patients suffering from muscle hypotonia and lactic acidemia (Miller et al., 2004; Saada et al., 2007). In both cases, the patients had decreased levels of 12S rRNA and significantly decreased activities of complexes I, III and IV. Likewise, mutations in two large subunit genes, MRPL3 and MRPL44 have been recently discovered using exome-sequencing (Carroll et al., 2013; Galmiche et al., 2011). In the case of the MRPL3, MRPL44 and MRPS22 mutations, all patients exhibited cardiomyopathy.

Finally, an increasing number of pathological mutations in mitochondrial translation elongation and terminations factors, as well as aminoacyl-tRNA synthetases, are being identified. The manifestations of these mutations generally involve respiratory chain deficiency and clinical features commonly seen in other mitochondrial disorders.

2.2 *Drosophila* - a genetically tractable model organism

Research on the genetic and molecular basis of the pathophysiology of complex human disorders has traditionally relied heavily on vertebrate model organisms, such as the mouse and the rat. Physically small, and genetically and physiologically simple invertebrates such as the nematode *Caenorhabditis elegans* and the fruit fly *Drosophila melanogaster* are, however, well suited for studying many aspects of human disorders. *Drosophila melanogaster*, in particular, has been the model system of choice in genetics and developmental biology over the last century. *Drosophila* was used extensively *e.g.* by the evolutionary biologist, geneticist Thomas Hunt Morgan and his students, in their work with the chromosome theory of heredity in the early 20th century. This pioneering work laid foundations for modern-day genetics and contributed greatly to the transformation of biology into a more of an experimental science.

The small fruit flies are easy and cheap to rear, and have a short life cycle (10 days) and lifespan (60-100 days). Thus, establishing genetic crosses or inbred lines is much faster compared to rodents. Adult males reach sexual maturity within hours after eclosing and females are capable of laying hundreds of eggs during their reproductive life cycle. Many *Drosophila* tissues and organs are functionally analogous to their mammalian counterparts, but often slightly down-scaled in terms of number of cells/cell types and functional complexity. These include the gut, the central nervous system, heart and skeletal muscle, the Malpighian tubules (analogous to the kidney) and the fat body, the fly equivalent of the liver and white adipose tissue.

Fly genetics have many unique features which can be exploited for research purposes. The fly genome is compact, only approximately 5% of the size of the human genome, but still carries over 13,000 predicted protein-coding genes (Celniker & Rubin, 2003; Rubin, 2000), and approximately 75% of known human disease genes have orthologues in *Drosophila* (Bier, 2005). The genome is distributed on five chromosomes (X, Y, 2L/R, 3L/R and 4) which can be paired experimentally with balancer chromosomes, *i.e.* artificially generated chromosomes containing multiple inversions that suppress meiotic recombination with the corresponding endogenous chromosome. Balancer chromosomes also carry point mutations resulting in visible phenotypic traits, such as curly wings or stubble bristles. Balancers are especially useful in maintaining recessive, often lethal

mutations, and tracking their segregation with the help of the phenotypic markers they carry. Likewise, transgenes are usually linked with an eye colour marker, allowing their tracking in genetic backgrounds lacking eye colour.

Transgene expression in *Drosophila* is easily achieved using the bipartite GAL4-upstream activating sequence (UAS) derived from yeast. The GAL4/UAS-system (Elliott & Brand, 2008) allows for the transgenic expression of any UAS-controlled construct, *e.g.* short hairpin RNAs (shRNA), to be induced ubiquitously or in a tissue specific manner. The expression may also be temperature or drug induced, as in the case of the progesterone analogue (RU486, mifepristone) activated GeneSwitch-GAL4 system (Roman et al., 2001).

The *Drosophila* genome is highly accessible for manipulation using chemical/irradiation mutagenesis, P element-mediated mutagenesis or methods for producing defined genomic deficiencies and mutations. One of Morgan's students, Herman J. Muller, was the first to demonstrate the mutagenicity of X-rays, a discovery which has since been vastly exploited alongside the use of the mutagenic agent EMS, in impairing and deducing functions of previously uncharacterized genes in *Drosophila*. P element-mediated mutagenesis strategies take advantage of transposable elements unique to *Drosophila*, which can be mobilized to generate imprecise excisions in the genome (Rio, Laski, & Rubin, 1986). Large libraries of predefined P element insertions (gene disruptions) and excisions generated using other transposable elements, are commercially available. Targeted mutagenesis in *Drosophila* is currently possible using either the CRISPR/Cas9 (Bassett & Liu, 2014) system or homologous recombination (Maggert, Gong, & Golic, 2008).

This palette of tools and characteristics has made *Drosophila* a widely used model organism in a diverse field of research ranging from neurodegeneration, obesity, aggression, and alcoholism, to learning and memory.

2.2.1 The development and life cycle of *Drosophila*

Drosophila development proceeds through four discrete stages: embryogenesis, the larval (juvenile) stage, pupal development which also includes sexual maturation, and reproductive adulthood (reviewed by Tennessen and Thummel, 2013). These developmental stages are also distinctive morphologically. The transparent embryos

develop for a day when reared at 25 °C and hatch from the eggs as worm-like larvae. This is followed by the first two larval stages (L1 and L2), both of which last for one day. After the third and final larval stage (L3), and the 4th day of larval development, growth is terminated and a puparium forms. Metamorphosis proceeds to produce a pharate adult, which ecloses after 4-5 days of pupal development. Progression through these stages is under neuroendocrine regulation. Pulses of the insect steroid molting hormone, 20-hydroxyecdysone (20E) control transitions from one developmental stage to another (Riddiford, Cherbas, & Truman, 2000; Thummel, 2001). The prehormone ecdysone is synthesized from cholesterol in the insect endocrine organ, the prothoracic gland, and released into the circulation. Ecdysone is further processed in the peripheral tissues to produce the active 20E form of the hormone (Huang, Warren, & Gilbert, 2008; Thummel, 2001), which can then exert its action through the ecdysone receptor. The 20E receptor is a heterodimer of two nuclear receptors, the ecdysone receptor (EcR) and Ultraspiracle (USP), and its activation triggers expression cascades of stage specific genes (Gilbert & Warren, 2005; Huang et al., 2008).

Under normal circumstances, growth in *Drosophila* is restricted to the larval stages, during which larvae increase in body mass up to 200 fold (Tennessen & Thummel, 2011). The correct timing of the high 20E titer at the end of the L3 stage is thus crucial, since this marks not just the end of the exponential growth phase, but also the end of the feeding stage during which the larva has had to accumulate sufficient nutrient reserves to survive through the pupal stage. This implies that the hormonal regulation must be under tight genetic control, and sensitive to the nutritional status of the animal.

Two somewhat poorly understood major transitions occur in larvae towards the end of the juvenile stage. The first one is surpassing a minimal viable weight around the L2 to L3 molt, which signifies that larvae have reached sufficient body mass to complete development in the absence of nutrients (C. Mirth, Truman, & Riddiford, 2005). Poor nutrient conditions after this point will only delay the final 20E pulse and the onset of metamorphosis, but not prevent it. Next, larvae need to reach a second checkpoint, which is the critical weight. The attainment of this milestone commits the larvae to metamorphosis within a definite period of time (C. K. Mirth & Riddiford, 2007; Tennessen & Thummel, 2011). Further feeding or starvation beyond this time point will only produce large or smaller adults, respectively, but does not affect the timing of the onset of pupariation.

Metamorphosis triggers the maturation of adult tissues. Most larval tissues, *e.g*. the larval fat body, are degraded during pupal development to provide energy and macromolecules for the biosynthesis of adult tissues. Many adult tissues, especially the appendages such as the wings, legs and antennae, develop from special tissue termed the imaginal discs. Imaginal discs consist of progenitor cells allocated largely during embryogenesis, and which remain quiescent during the larval stages. Upon metamorphosis, these cells are activated and start differentiating according to their predetermined fates.

2.2.1.1 Conserved signalling network regulates development in Drosophila

All of these aforementioned processes, and their timing in particular, are orchestrated by a conserved network of cellular growth regulators and diffusible signaling factors, which coordinate the growth of peripheral tissues based on several cues, such as nutritional status. Damage to key tissues, such as the imaginal discs, can also stall development prior to metamorphosis through systemic signaling. Two signaling pathways form the backbone of the growth and metabolic regulatory network. The first one is the Target of rapamycin complex (TOR), which in various configurations is present all through *Eukaryota*. TOR is a major regulator of processes required for cell growth, such as translation, transcription and autophagy (Kapahi et al. 2010; Albert & Hall 2014). The second, likewise highly conserved pathway is induced by eight insulin/insulin-like growth factors in *Drosophila*, known as the insulin-like peptides (ILPs). These circulating messengers are structurally and functionally related to mammalian insulins, and activate the sole fly insulin receptor (InR), and subsequently the downstream phosphatidylinositol 3-kinase (PI3K)/AKT protein kinase signaling pathway. The TOR and PI3K/AKT pathways are interlinked, but may also act independently of each other (Hietakangas & Cohen, 2009).

The TOR kinase is present in two signaling complexes: TOR complexes 1 (TORC1) and 2 (TORC2) (Loewith et al., 2002). TORC1 is the primary mediator of amino acid and energy sensing while the TORC2 modulates insulin signaling through the PI3K/AKT pathway. The major phosphorylation targets of the TORC1 include the ribosomal protein S6 kinase (S6K) and the eukaryotic initiation factor 4E binding protein (4E-BP) (Miron, Lasko, & Sonenberg, 2003). In the phosphorylated state, 4E-BP is blocked from inhibiting cytosolic translation by binding to initiation factor

eIF4E. S6K phosphorylation primes it for activation via 3-phosphoinositide-dependent protein kinase 1 (PDK1)-mediated phosphorylation. The activated S6K further phosphorylates ribosomal protein S6 and eIF4B to promote the formation of the translation preinitiation complex (Holz et al., 2005). *Drosophila* S6K mutants are severely growth retarded and have a small body size due to reduced cell size (Montagne et al., 1999), whereas 4E-BP mutations have a much milder phenotype, characterized by sensitivity to starvation and oxidative stress (Teleman, Chen, & Cohen, 2005; Tettweiler et al., 2005).

The PI3K/AKT pathway is activated in response to circulating insulins and insulin-like growth factors (IGFs). These ligands activate receptor tyrosine kinases, such as the insulin receptors (InR), on the cell surface. Actived insulin receptor recruits both the adaptor protein insulin receptor substrate (IRS, *chico* in *Drosophila*) and the catalytic subunit of the PI3K, resulting in its activation (Engelman, Luo, & Cantley, 2006). Activated PI3K then phosphorylates the plasma membrane phosphatidylinositol-4,5-diphosphate (PIP2) to yield phosphatidylinositol-triphosphate (PIP3). The phosphatidylinositol-triphosphates further recruit the PDK1 and AKT kinases to the plasma membrane, where AKT is activated by PDK1 via phosphorylation of Thr308 (Alessi et al., 1997; Yang et al., 2006). This AKT phosphorylation precedes another catalyzed by TORC2 at Ser473 (Ser505 in *Drosophila*). Two key AKT targets are the TORC1 inhibitors tuberous sclerosis 2 (TSC2) (Inoki et al., 2002; Potter, Pedraza, & Xu, 2002) and the proline-rich substrate of AKT 40 (PRAS40) (Sancak et al., 2007; Vander Haar et al., 2007). Another well-characterized AKT regulated protein in *Drosophila* is the Forkhead box class O (FoxO) transcription factor. The *Drosophila* Akt actively phosphorylates *FoxO* to retain its cytosolic localization (Brunet et al., 1999). If Akt activity is low under adverse conditions, FoxO becomes nuclearly localized and activates the transcription of its target genes, including the translation inhibitor *Thor* (encoding *Drosophila* 4E-BP) (Jünger et al., 2003).

The insulin receptor ligands in *Drosophila* comprise of 8 insulin-like peptides (ILP1-8). These peptides are considered to be functionally analogous to the mammalian insulin and insulin-like growth factors. The various ILPs are secreted from different fly organs, and most have well characterized spatiotemporal expression patterns. All ILPs share a similar domain structure and sequence homology with mammalian insulin (Grönke et al., 2010) and *e.g.* ILP5 can active the human InR (Sajid et al., 2011). In a nutrient-rich environment, ILP2, ILP3 and

ILP5 are synthesized primarily by the median neurosecretory cells of the fly brain (Brogiolo et al., 2001; Ikeya et al., 2002). ILP6 synthesis begins at the end of the 3rd larval stage and is highest in the fat body (Bai, Kang, & Tatar, 2012). The most recently discovered ILP, ILP8, is expressed predominantly in the ovaries but is also secreted from imaginal discs during the larval stages in response to tissue damage, in order to prevent progression to metamorphosis and allow for tissue regenerative processes to proceed (Colombani, Andersen, & Léopold, 2012; Garelli et al., 2012).

2.2.1.2 Nutrition and energy sensing regulate growth

As illustrated by the relationship between size, feeding behavior and developmental timing in larvae, nutrition is a key regulator of growth and growth signaling. In this context, the fat body is perhaps the most pivotal organ in sensing nutritional status *in Drosophila*.

The fat body is the primary insect nutrient store and is functionally analogous with mammalian liver and white adipose tissue. It also has the capability to regulate the growth of peripheral tissues: silencing of the exclusively fat body-specific cationic amino acid transporter *slimfast* (*slif)*, inhibits growth and produces small adults (Colombani et al., 2003). This effect is mediated by the TOR complex as demonstrated by the fact that inactivation of TOR specifically in the fat body phenocopies *slif* loss-of-function, while overexpression of a TOR downstream target, the S6 kinase (S6K), partially rescues it (Colombani et al., 2003; Oldham et al., 2000; Zhang et al., 2000). The exact nature of the fat body-derived, amino acid responsive humoral signal which regulates the growth of the entire organism remains unknown (Géminard, Rulifson, & Léopold, 2009). The fat body is known to respond to dietary sugars and lipids through a cytokine, Unpaired 2 (Upd2), which regulates *ILP* secretion (Rajan & Perrimon, 2012). The TOR-mediated response to amino-acid starvation is somewhat better understood, although it is unclear which amino acids are key to this regulation. Leucine, arginine and glutamine have all been implicated in this process, while the leucyl-tRNA synthetase has been linked functionally to TOR activation in response to leucine levels in human cells (reviewed by Jewell et al. 2013).

In addition to nutrients, cellular energy supply is a crucial determinant of growth rate. A decrease in cellular ATP levels results in an elevated AMP/ATP ratio. AMP

binds the γ subunit of the AMP-activated protein kinase (AMPK) and allows AMPK to be phosphorylated by the LKB1 kinase (Hardie, 2011). Activated AMPK inhibits growth primarily via regulating TORC1 activity through phosphorylation of two target proteins: the TORC1 inhibitor TSC2 (Inoki et al. 2003) and the TORC1 component RAPTOR (Gwinn et al., 2008).

2.2.2 *tko*^{25t}

Many proteins of eukaryotic mitochondrial ribosomes have no apparent orthologues in prokaryotes and thus represent a class of novel mitoribosomal genes, whereas some ribosomal proteins and rRNA tertiary structures have been preserved over hundreds of millions of years of evolution. The mitoribosomal small subunit protein S12 is one such highly conserved ribosomal protein and a key component of the ancient ribosome decoding centre. It has been characterized in numerous organisms including bacteria, mammals and *Drosophila* (Royden, Pirrotta, & Jan, 1987; Toivonen et al., 1999; Toivonen et al., 2001). Mutations in the bacterial S12 have been shown to result in hyperaccurate translation and a reduced rate of elongation (Bilgin et al., 1992).

The *Drosophila* mitoribosomal protein S12 (mRpS12), is encoded by the gene *technical knockout* (*tko*). The *tko* gene maps to the X-chromosome and is expressed ubiquitously at a relatively low level throughout development (www.flybase.org). The *tko* gene derives its name from the stress ("bang") sensitive behavioural phenotype exhibited by one of its few known non-lethal mutant alleles, *tko*^{25t} (Judd et al., 1972; Shannon et al., 1972; Royden et al., 1987; Shah et al., 1997). The bang sensitive mutants form a very heterogeneous group of genetic abnormalities, all of which result in a phenotypic high susceptibility to hyperactivity and paralytic and epileptic seizures, induced by mechanical or electric stimulus. Some of the other mitochondrial bang sensitivity loci include the adenine nucleotide translocase *sesB* (Zhang et al., 1999), the mitochondrial voltage-dependent anion channel *porin* (Graham et al., 2010), mitochondrial fission protein *Drp1* (Verstreken et al., 2005) and the *Drosophila* mitochondrial citrate synthase gene *knockdown* (Fergestad, Bostwick, & Ganetzky, 2006). The large number of mitochondrial mutants exhibiting stress-sensitivity is not surprising since mitochondrial function is particularly indispensable for signaling over neuromuscular junctions. In

Drosophila, mitochondrial dysfunction has been shown to specifically impair the mobilization of reserve pool vesicle during intense neurotransmission (Verstreken et al., 2005).

The hypomorphic *tko*^{25t} mutation creates one of the best-studied defects of mitochondrial protein synthesis in *Drosophila*. It results in the substitution of a conserved leucine residue with histidine at position 85 (L85H). The mutant phenotype is associated with a severe OXPHOS deficiency and a decreased steady-state level of the 12S rRNA, indicating impaired assembly or stability of the mitoribosomal small subunit (Toivonen et al. 2001, 2003). Similar observations have been made in the two reported cases of human mitoribosomal SSU mutations (Miller et al., 2004; Smits et al., 2011). The *tko*^{25t} phenotype in *Drosophila* further includes developmental delay (slow larval growth), hearing impairment and defective male courtship. However, rather surprisingly, the *tko*^{25t} mutants exhibit no gross morphological changes with the exception of small and thin sensory bristles.

3. Aims of research

The primary aim of this study was to identify genetic and nutritional factors modulating the phenotypic outcome of impaired mitochondrial protein synthesis and OXPHOS deficiency, in a multi-cellular disease model (*tko*^{25t}), which recapitulates some of the most common manifestations of human mitochondrial disorders. We also attempted to discover some of the naturally occurring adaptive metabolic responses deployed by the mutant flies during development. This work was subdivided into three independent studies, presented in the corresponding articles (I and II) and manuscript (III):

I) The goal of the first study was to exploit the naturally occurring phenotypic recovery of the *tko*^{25t} mutants, achieved by selective inbreeding, to identify phenotype-suppressing alleles.

II) The aim of the second study was to test whether the expression of the alternative respiratory enzymes could alleviate some of the major phenotypic features of the *tko*^{25t} mutants and to use the *Ciona intestinalis* alternative oxidase (AOX) to dissect the relationship between particular OXPHOS and phenotypic manifestations of mitochondrial protein synthesis defects.

III) The aim of the final study was to investigate the metabolic adaptation to mitochondrial dysfunction during development, using primarily metabolomics and transcriptomics methods. In addition, we investigated how mutant flies responded to dietary intervention.

4. Materials and methods

4.1 *Drosophila* stocks and maintenance

Unless otherwise indicated, the tko^{25t} mutant and wild-type flies and larvae used were of Oregon-R genetic background and had been maintained inbred in a controlled laboratory for hundreds of generations. Additionally, a Canton-S and Oregon-R/Canton-S hybrid background was used for some experiments. The transgenic lines A1 and A3, carrying either a single, or multiple insertions of the tko^{25t} -allele have been described in (Toivonen et al. 2003) and the UAS-AOX and UAS-Ndi1 transgenic constructs and flies in (Fernandez-Ayala et al. 2009) and (Sanz et al. 2010), respectively.

Unless otherwise stated, flies were maintained on a standard medium (high-sugar, HS) consisting of 1% agar (Oriola), 1.5 % (w/v) sucrose, 3% glucose, 3.5% Instant Dry yeast, 1.5% maize flour, 1% soy flour, 3% Lyle's black treacle (Tate & Lyle, UK), 0.5% propionic acid (Sigma-Aldrich) and 1.0% methyl 4-hydroxybenzoate (Sigma), and a 12 h light/dark cycle at 25 °C. Variations of this medium were as follows:

ZS ('zero-sugar' medium) – 3.5% dried yeast, 1% soya flour, 1.5% maize flour.

Sugar series – ZS medium but with variable sucrose content, from zero to 10%.

Isocaloric media with decreased sugar and increased protein and/or fat content: LS (low sugar) medium – 5.5% dried yeast, 2.5% maize flour, 2.5% soya flour, 3% treacle; HP (high protein) medium – 5.5% dried yeast, 1% maize flour, 1% soya flour, 3% soya protein, 3% treacle; HF (high fat) medium – 5.5% dried yeast, 1.5% maize flour, 1.5% soya flour, 0.75% olive oil, 3% treacle.

Sugar type series – HS medium but with all of the sugars as sucrose, fructose or glucose (denoted S, F and G, respectively)

Various supplements, as indicated in figures and legends, were generally added from stock solutions after medium was cooled to 50 °C, including sodium pyruvate or lactate (25 mg/ml), ornithine (5 or 20 µg/ml), cycloheximide (up to 250 µg/ml)

4.2 Developmental time

Less than 5 day-old virgin females and males were pre-mated for 2 days, tipped into fresh vials or bottles every 24 h 3-4 times in succession, and then discarded. Eclosing progeny were counted once per day. Mean eclosion time ± SD was generated for each genotype from a minimum of three independent replicates of this experimental setup.

4.3 Bang sensitivity

Flies were anesthetized using CO_2, sexed, separated into individual empty culture vials and allowed to recover from anesthesia for a minimum of 3 h. Individual flies were then vortexed at maximum speed for 10 s in order to induce temporary paralysis. The duration of the paralytic/epileptic seizures was timed and means ± SD of the time taken for recovery of normal posture and mobility were generated using a minimum of 25 flies per genotype.

4.4 Larval feeding behaviour

Larval feeding behaviour was determined based on ingestion of a die-supplemented medium. Briefly, individual larvae grown on HS or ZS medium were placed on petri dishes of the same medium containing 0.16% erioglaucine for 20 min, washed with PBS, dried, and then homogenized in 100 µl PBS. Homogenates were centrifuged at 12000 g_{max} and dye uptake was measured spectrophotometrically (absorbance at 630 nm) using the supernatant fractions.

4.5 DNA extraction

25-40 anesthetized flies or larvae were collected in a 1.5 ml microcentrifuge tube on ice. Flies or larvae were homogenized in 400 µl of lysis buffer (100 mM Tris-HCl, 100 mM EDTA, 100 mM NaCl and .5% w/v SDS). Samples were incubated at 65 °C for 30 min. 800 µl of buffer consisting of 1.43 M potassium acetate and 4.29 M lithium chloride was then added, and samples were incubated on ice for 1 h. Samples were centrifuged at 12,000 g_{max} for 15 min and the resulting supernatant was transferred to a fresh microcentrifuge tube. DNA was precipitated by adding 600 µl of isopropanol and centrifuging at 12000 g for 15 minutes. After centrifugation, the supernatant was discarded and the pellets washed twice with 70% ethanol. DNA was dissolved in TE buffer and stored at -20 °C.

4.6 Construction of *mRpL14* transgenic flies

Arguably this section should appear in Results. Transgenic lines carrying insertions of the Drosophila *mRpL14* gene with its putative promoter were generated as described in (I). Briefly: *mRpL14* was amplified from genomic DNA together with 750 bp segment upstream and 430 bp segment downstream of the transcription unit. This fragment was cloned and amplified using Zero Blunt TOPO PCR Cloning kit (Invitrogen). The insert was then introduced into a modified pGREEN-H-Pelican vector (Barolo et al. 2000, obtained through Drosophila Genomics Resource Center, USA) which carries gypsy insulator elements in order to prevent read-through transcription. The plasmid was amplified, extracted and phenol/chloroform purified using standard procedures. Transgenic flies were generated by Vanedis Drosophila Injection Service (Oslo, Norway) using germ cell micro-injection and P element mediated transgenesis, followed by several consecutive generations of crosses of the transgene-harboring progeny into the w^{1118} background. Insertion site mapping was performed as described below.

4.7 Insertion site mapping using inverse-PCR

3.5 µg of genomic DNA from transgenic flies was digested with 10 U of ScrFI (Fermentas) in manufacturer's buffer for 3 h at 37°C in a total volume of 25 µl. The

enzyme was heat-inactivated and the digested DNA was self-ligated with 4 Weiss units of T4 DNA ligase (Fermentas) in a total volume of 400 µl. Ligated DNA was ethanol precipitated and resuspended in 100 µl of 10 mM Tris-HCl (pH 8.0). 10 µl of the resuspended DNA was used as a template in a PCR-reaction with pGREEN-H-Pelican vector specific inverse-PCR primers. The resulting PCR-products were sequenced using the same primers in order to identify the genomic insertion site of the P element construct, by BLAST searching against the genomic DNA sequence.

4.8 RNA extraction

For RNA-sequencing, RNA was extracted from flash-frozen groups of 30 larvae using miRNA Easy Mini Kit (Qiagen) according to manufacturer's instructions. Three biological replicate samples were produced by pooling 4 independent preparations to produce each replicate.

For Quantitative Reverse Transcription-PCR (QRTPCR), RNA was extracted using the TRIzol-method. Briefly, 100 mg of flies or larvae (approx. 30 females, 40 males or 25 larvae) were homogenized in 1 ml of TRIzol-reagent (Life Technologies). The homogenate was incubated at room temperature for 5 min after which 200 µl of chloroform was added to the samples. Samples were then incubated at room temperature for 3 min and centrifuged at 12000 g for 10 minutes at 4 °C. 600 µl of the upper aqueous phase was transferred into a fresh microcentrifuge tube and RNA was precipitated by adding an equal volume of 2-propanol and incubating at room temperature for 10 min. RNA was then pelleted by centrifuging at 12000 gmax for 10 min at 4 °C. The pellets were washed with 75% ethanol in DEPC-dH_2O and resuspended in 200 µl of DEPC-dH_2O.

Prior to cDNA synthesis, RNA samples were DNase I treated with 0.05 U/ml of DNase I (Thermo Scientific) in DNase I buffer (100 mM Tris-HCl, 25 mM $MgCl_2$, 1 mM $CaCl_2$) at 37 °C for 1 h. RNA was then phenol:chloroform purified, ethanol precipitated and washed, and resuspended in DEPC-treated dH_2O.

4.9 Analysis of gene expression using Quantitative Reverse Transcription-PCR (QRTPCR)

One µg of RNA was used for cDNA synthesis using the High-Capacity cDNA synthesis kit (Life Technologies) according to manufacturer's instructions. Two replicate reactions of each sample were pooled and diluted 1:20 with dH_2O. 2 µl of the pooled and diluted sample was used for quantitative (real-time) PCR performed using Fast SYBR Green Master Mix (Life Technologies) and 0.5 mM final primer concentrations. Triplicate real-time PCR reactions were performed and data was acquired using a StepOne Plus instrument and software (Life Technologies). Gene expression was analyzed relative to the housekeeping gene *RpL32*.

For microarray data verification, RNA was transcribed using random hexamers (Amersham Biosciences) and M-MuLV reverse transcriptase (Fermentas). Real-time PCR was performed using QuantiTect SYBR Green PCR Master Mix (Qiagen) and Light Cycler (Roche) instrument following manufacturers' instructions. The data was acquired and analyzed using Light Cycler data collection software version 3.5 (Roche).

Gene-dosage analysis was performed as described above but using approximately 500 ng of genomic DNA and 0.5 mM primer concentration in a final reaction volume of 20 µl. Two biological and three technical replicates per genotype were used for each gene analyzed and gene dosage was measure relative to *RpL32*.

4.10 Analysis of gene expression using RNA-sequencing

RNA sequencing analysis was performed on Hiseq 2500 sequencers (Illumina) using a paired-end library and 100 bp read-legnth and otherwise standard protocols. Expression analysis was performed using the Chipster. Sequencing reads were mapped to the *Drosophila* reference genome (BDGP release 5.72) using TopHat version 2.0.9, and differential expression analysis was performed using CuffDiff.

4.11 Analysis of gene expression by Western blotting

Total protein was extracted from 20 frozen larvae per sample. Three replicate samples per condition per experiment were pooled to produce a single individual sample. Experiments were repeated independently at least three times. Larvae were homogenized in 200 µl of buffer containing 150 mM NaCl, 1 mM EDTA, 2 M urea, 1.3 % (w/v) SDS, 10 mg/ml cOmplete protease inhibitor mix (Roche) and PhosSTOP phosphatase inhibitor mix (Roche). Homogenates were centrifuged for 1 min at 12000 g_{max} at 4 °C. The supernatant was mixed with 4 x Laemmli loading buffer consisting of 40% (w/v) glycerol, 8% (w/v) SDS, 250 mM Tris-HCl (pH 6.8), 0.015% (w/v) bromophenol blue and 200 mM DTT, heated for 7 min at 95 °C and cooled on ice. Approximately 30 µg of protein was loaded on Criterion TGX AnyKD precast SDS-PAGE gels (Bio-Rad) and run in ProSieve EX Running buffer (Lonza). Protein was transferred to 0.45 µm Hybond ECL nitrocellulose membrane (Amersham, GE Heathcare Life Sciences) in ProSieve EX Transfer Buffer (Lonza) using Criterion blotters (Bio-Rad). Membranes were blocked at room temperature for 1 h in either TBS-Tween with 2.5% (w/v) milk or with PBS-Tween with 2.5% (w/v) BSA. Primary antibody incubations were carried out overnight at 4 °C in in PBS-Tween with 2.5% (w/v) BSA. Membranes were then washed 3 x 5 min in PBS-Tween and incubated with HRP-conjugated secondary antibody for 1 h at room temperature in PBS-Tween with 2.5% (w/v) milk. After this, the unbound secondary antibody was washed off 3 x 5 min in PBS-Tween and finally once in PBS. Protein was detected and visualized using SuperSignal West Femto Chemiluminescent Substrate (Pierce, Thermo Scientific) and ChemiDoc imager (Bio-Rad).

Primary antibodies used were: Anti-Akt #4691 (Cell Signaling), Anti-phospho-Akt #4054 (Cell Signaling), anti-AMPK #80039 (Abcam) and anti-phospho-AMPK #4188 (Cell Signaling). HRP-conjugated secondary antibodies were Peroxidase Horse Anti-Mouse IgG #PI-2000 (Vector Labs) and Peroxidase Goat Anti-Rabbit IgG #PI-1000 (Vector Labs). Primary and secondary antibodies were used as 1:1000 and 1:10000 dilutions, respectively. Alpha-Tubulin #52866 (Abcam) was used as loading control in a 1:10000 dilution.

4.12 Metabolic assays

4.12.1 Metabolomics

Fifteen mid-third instar larvae were harvested, washed with PBS and snap-frozen in liquid nitrogen. Frozen samples were completely homogenized by a cell disrupter (Shake Master NEO; Bio Medical Science, Tokyo, Japan) at 4°C, after adding 500 µl of methanol-containing internal standards [20 µM each of methionine sulfone, 2-(N-morpholino)-ethanesulfonic acid (MES) and D-Camphol-10-sulfonic acid(CSA)]. The homogenate was then mixed with 200 µl of Milli-Q filtered water and 500 µl of chloroform and centrifuged at 9100 g_{max} for 4 hr at 4°C. Subsequently, the aqueous solution was centrifugally filtered through a 5-kDa cut-off filter (Millipore) to remove proteins. The filtrate was centrifugally concentrated and dissolved in 50 µl of dH2O containing reference compounds (200 µM each of 3-aminopyrrolidine and trimesate). Prior to CE-TOFMS analysis, the sample solution for anion was diluted five times and that for cation was diluted 10 times with dH_2O. Note that these procedures for metabolite analysis were performed by the laboratory of Dr. Tomoyoshi Soga, Keio University, Japan, using biological materials supplied by myself.

4.12.2 Triglycerides and free glycerol

The assay was slightly modified from (Tennessen et al. 2014). 20 mid 3rd instar larvae were collected, rinsed several times with PBS in a 1.5 ml microcentrifuge tube and snap frozen in liquid nitrogen. Frozen larvae were homogenized in 100 µl of cold PBS + 0.05% Tween 20. Ten µl of the homogenate was diluted 1:10 with PBS and set aside to measure protein content using the Bradford assay. The larval lysate was incubated at 70 °C in order to inactivate endogenous lipases. One 20 µl aliquot of the heat-treated lysate was mixed with 20 µl of triglyceride reagent (Thermo Scientific, Konelab, Indiko) and another with 20 µl of PBS. Both reactions were then incubated at 37 °C for 1 h. After this, 100 µl of free glycerol reagent (Sigma) was added to each sample. Samples were mixed well, incubated at 37 °C for 5 min and finally centrifuged for 3 min at full speed. 100 µl of the supernatant was used to measure absorbance at 540 nm. Glycerol solution (0.26 mg/ml in PBS, equaling 2.5 mg/ml of triolein) was used to generate a standard curve. The

triglyceride content of each sample was determined by subtracting the glycerol content of the untreated sample from the triglyceride reagent-treated aliquot.

4.12.3 ATP, lactate and pyruvate assays

Twenty larvae or adult flies were homogenized in 100 µl of 6 M guanidine hydrochloride on ice. The homogenate was incubated at 95 °C for 5 min and centrifuged at 12000 g_{max} for 5 min at 4 °C. The supernatants were transferred to fresh microcentrifuge tubes and stored at -80 °C.

The samples were diluted 1:10 and with PBS (pH 7.4) for analysis. Steady-state ATP levels were assayed using an ATP determination kit (Molecular Probes, Life Technologies) according to the manufacturer's protocol. 90 µl of the ATP reaction mix was combined with 10 µl of the diluted sample to initiate the reactions and luminescence was measured immediately at 535 nm using a Hidex Chameleon plate reader. ATP standards were used to generate a standard curve and ATP concentrations were normalized to soluble protein in the samples, measured with the Bradford assay.

Pyruvate and lactate were measured using 1:10 diluted samples with commercially available fluorescence based determination kits (Abcam) according to manufacturer's instructions. Ten µl of sample was combined with 50 µl of either lactate or pyruvate reaction mix. Reactions were incubated at room temperature for 30 min after which fluorescence was measured (excitation at 535 nm/emission at 590 nm) using a plate reader. Lactate and pyruvate standards were used to generate a standard curves and concentrations were normalized to soluble protein as before.

4.12.4 Enzymatic assays

Enzymatic assays were adapted from (Hinman & Blass 1981), (Merritt et al. 2005) and (Merritt et al. 2009). 20 frozen larvae were homogenized on ice in 200 µl of ice-cold 100 mM Tris-HCl (pH 7.4). The reaction conditions for each enzyme were as follows (all at pH 7.4): malic enzyme activity was assayed in the presence of 100 mM Tris-HCl, 0.34 mM NADP, 50 mM $MnCl_2$, 50 mM DL-malic acid; glucose-6-phosphate dehydrogenase was assayed in the presence of 100 mM Tris-HCl, 0.34 mM NADP, 3.5 mM D-glucose-6-phosphate; 6-phosphogluconate dehydrogenase

was assayed in the presence of 100 mM Tris-HCl, 0.34 mM NADP, 3.5 mM 6-phosphogluconate; isocitrate dehydrogenase activity in the presence of 100 mM Tris-HCl, 0.34 mM NADP, 0.84 mM $MgCl_2$, 1.37 mM DL-isocitric acid,. Enzyme inhibitors sodium gluconate, sodium pyruvate and sodium lactate were used at 100 mM final concentration where indicated. Reactions were initiated by combining 10 µl of the larval homogenate with 90 µl of each reaction mixture. Increase in absorbance at 510 nM was detected in the presence of .6 mM iodonitrotetrazolium chloride and 6.5 µM phenazine methosulfate. Absorbance was measured kinetically at 1-2 min intervals for 15 min and NADPH standards were used to transform absorbance values into changes in NADPH concentration. Enzyme activity was normalized to total soluble protein, measured with the Bradford assay.

Isocitrate dehydrogenase and glutamate dehydrogenase activities were also analyzed separately using a commercially available IDH activity kit (Abcam) in order to evaluate the relative contributions of the NAD^+/NADH- and $NADP^+$/NADPH-dependent isoforms to the total enzyme activity. For this, 20 frozen larvae were homogenized as before in 200 µl of cold manufacturer's IDH assay buffer. Enzyme activities of IDH and GDH were analyzed using manufacturer's IDH substrate and 100 mM L-glutamate as substrates, respectively, and either NAD^+ or $NADP^+$ as enzyme co-factors. Reactions were initiated by combining 50 µl of the reaction mix with 10 µl of sample. Absorbance measurement (at 450 nm), enzyme activity determination and normalization were carried out as before.

4.12.5 Hemolymph glucose measurement

30-50 freshly collected larvae were rinsed with PBS, dried and transferred into a 0.2 ml vial with small holes in the bottom. Larvae were then punctured several times with a 27 gauge ¾" needle and the small vial inserted inside of a larger vial. Larvae were then centrifuged at 1500 g_{max} for 5 min at 4 °C in order to drain hemolymph. Two µl of hemolymph was transferred into a fresh vial containing 8 µl of ice-cold TBS (pH 6.6). Samples were incubated at 70 °C for 5 min and subsequently centrifuged at 12000 g_{max} for 1 min at RT. The supernatant was transferred into a fresh vial and stored frozen at -20°C until analysis. All possible steps were performed on ice.

Trehalose and free glucose were measured using Glucose (HK) reagent (Thermo Scientific). Three µl of hemolymph were incubated with 0.5 µg of porcine kidney trehalase (Sigma-Aldrich) overnight at 37 °C. This was mixed with 150 µl of the glucose reagent, after which reactions were incubated at 37 °C for 1 h and absorbance at 530 nm was measured with a Hidex Chameleon plate reader. Non-trehalase treated samples were analyzed in parallel and the values subtracted from the trehalase-treated aliquots to give an estimate of free glucose in the sample. Glucose standards were used to determine the absolute glucose levels in the samples. Glucose levels were normalized to the amount of soluble protein in the samples, as determined using the Bradford assay. A minimum of eight replicate samples per genotype and condition were used.

4.13 Mitochondrial isolation

Mitochondria were isolated from 40 freshly harvested larvae or adults. Flies or larvae were homogenized with mortar and pestle in 2 ml of isolation buffer containing 250 mM sucrose, 5 mM Tris-HCl, 2 mM EGTA and 0.1% (w/v) BSA (pH 7.4). The homogenate was filtered and transferred into a microcentrifuge and centrifuged at 150 g_{max} for 3 min. The supernatant was then decanted into a fresh microcentrifuge tube and centrifuged at 9000 g_{max} for 10 min. Finally, the supernatant was discarded and the mitochondrial pellet resuspended in 50 µl of isolation buffer without BSA. All steps were carried out at 4 °C.

4.14 ROS measurements

H_2O_2 production was measured using 0.05 mg/ml of isolated mitochondria in 100 µl of assay buffer containing 120 mM KCl, 5 mM $KH_2PO^-_4$, 3 mM HEPES, 1 mM EGTA, 1 mM $MgCl_2$ and 0.2% (w/v) (BSA pH 7.2), 0.05 U/ µl superoxidase dismutase (Sigma-Aldrich), 0.1 U/µl of horseradish peroxidase (Life Technologies) and 10 µM Amplex Red (Life Technologies). Substrates and inhibitors were used at the following concentrations: 5 µM pyruvate, 5 µM proline, 20 mM sn-glycerol-3-phosphate, 1 mM ADP, 0.5 µM rotenone and 0.5 µM antimycin A.

5. RESULTS

5.1 Phenotypic rescue of *tko*^{25t} is achieved by modulating gene dosage (I)

5.1.1 Selective inbreeding rescues the *tko*^{25t} phenotype in suppressor lines

Based on our previous observations, we knew that maintaining the *tko*^{25t} mutants inbred over several generations would result in a gradual attenuation of the mutant phenotype (Toivonen et al., 2001; Toivonen et al., 2003). We decided to exploit this phenomenon in order to discover possible genetic suppressors of the *tko*^{25t} mitochondrial disease phenotype. Thus, we first backcrossed the mutant allele from a long-maintained laboratory stock into two different wild-type strains, Oregon-R (OR) and Canton-S (CS), over 12 generations. This crossing procedure was considered sufficient to eliminate possible pre-existing phenotypic suppressor alleles. We then mated flies of these two strains to produce an F1 generation with a severe and fully penetrant mutant phenotype (CS/OR *tko*^{25t}). We picked individual mating pairs and placed these under selection for accelerated development, *i.e.* choosing the first eclosing males and females in each generation to establish the next. Over 12 generations, this resulted in all of the inbred lines exhibiting stable but characteristically different degrees of rescue of both developmental delay and bang sensitivity. Remarkably, three of these lines, denoted *Weeble1-3* (*Wb*$^{1\text{-}3}$), exhibited an especially pronounced rescue of the disease-like phenotype (**Fig. 3**). We verified by sequencing that these three lines still carried the *tko*^{25t} mutation (**Fig. 3A**) and had not acquired additional mutations within the *tko* coding region. We then characterized these suppressor lines in further detail. All three *Weeble* lines showed nearly complete rescue of developmental delay compared with *tko*^{25t} in a hybrid genetic background (**Fig. 3B**). The degree of rescue was moderate but still substantial also in the three other suppressor lines (A-C).

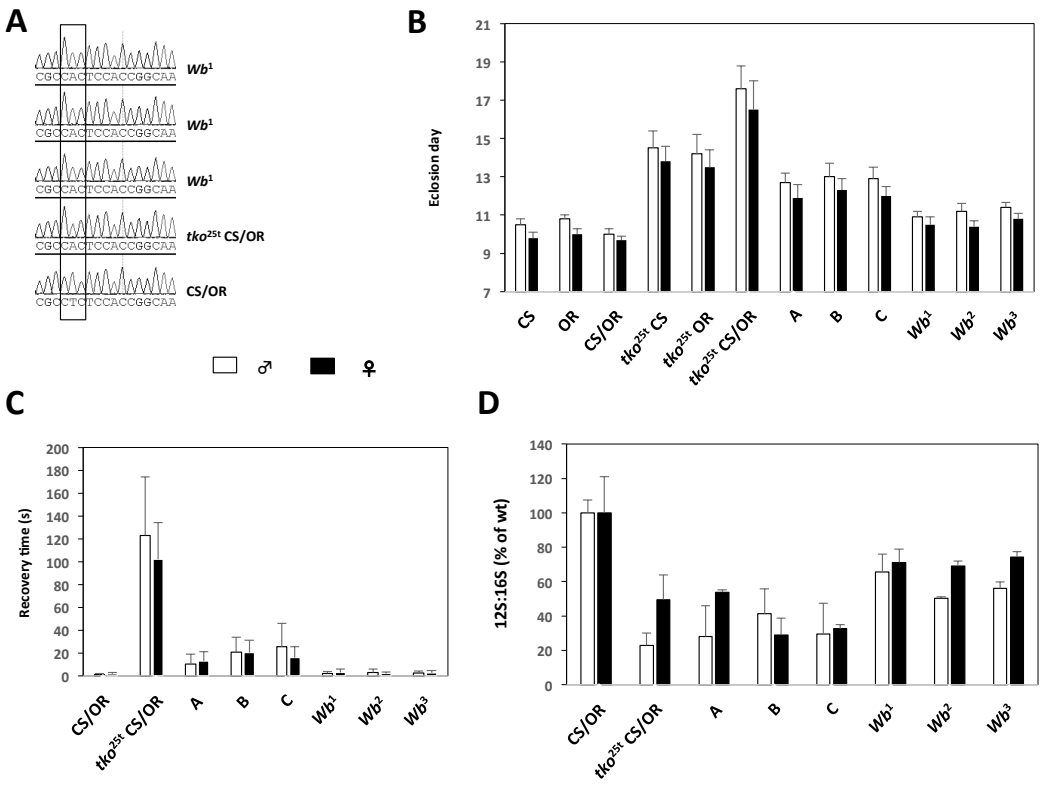

Figure 3. A) Sequencing of the suppressor and control lines at the region of the *tko*^{25t} point mutation region. **B**) Developmental time (determined as mean eclosion day + SD) at 25 °C. **C**) Bang sensitivity of <1 day old adults (mean recovery time from paralysis). **D**) Ratios of mitoribosomal 12S and 16S RNAs, determined using Q-RT-PCR. Sex, strain and phenotype as indicated. CS – Canton S, OR – Oregon R, CS/OR – F1 hybrid of Canton S females and Oregon R males, A-C – moderate suppressor lines, *Wb*$^{1-3}$ – *Weeble* suppressors.

The *Weeble* lines, likewise, no longer exhibited bang sensitivity while the mild suppressor lines still exhibited a moderate phenotype (**Fig. 3C**). Finally, we quantified the ratio of mitochondrial ribosomal RNAs (*12S*:*16S*), which is considered representative of the ratio of small and large mitoribosomal subunits, and a diagnostic marker for the *tko*^{25t} phenotype (Toivonen et al. 2001, Toivonen et al., 2003). We observed the expected decrease in the steady-state ratio (**Fig. 3D**) in the mutant background, whether outbred (CS/OR *tko*^{25t}) or inbred (A-C), attributable to the depletion of the 12S mitoribosomal RNA. The ratio was significantly recovered in the suppressor lines (*Wb*$^{1-3}$) in both sexes, consistent with the improvement in phenotype.

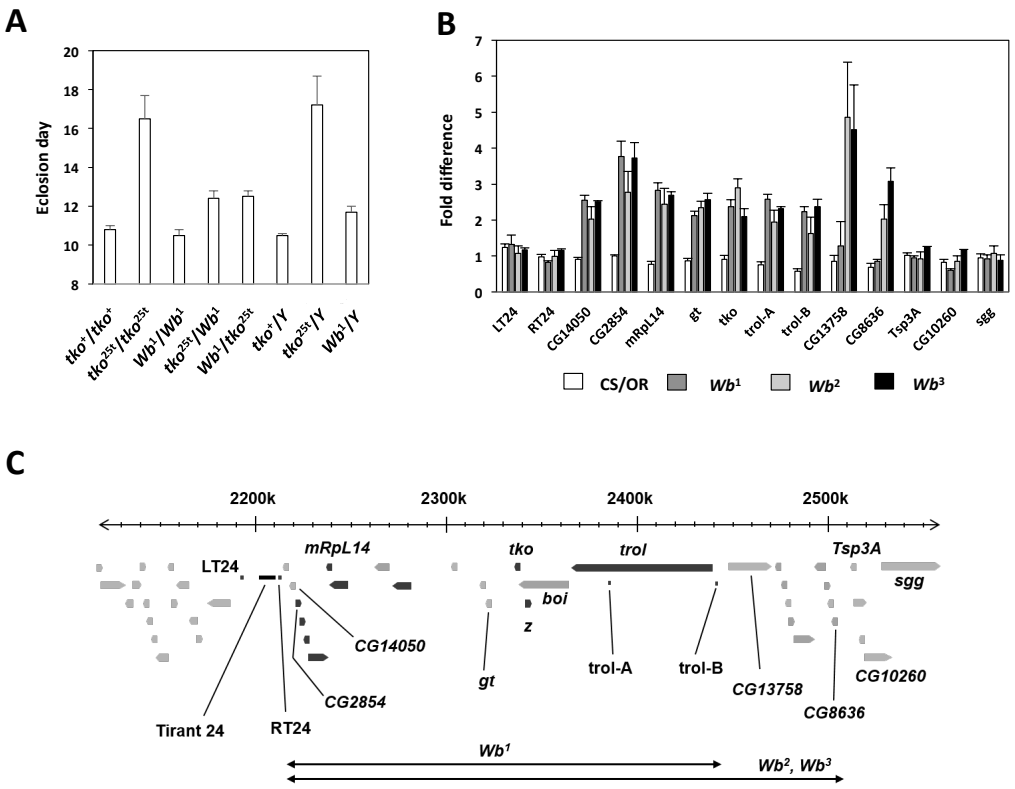

Figure 4. *tko*^{25t} phenotype is sensitive to allelic copy number. **A**) Mean eclosion time of flies carrying wild-type alleles (*tko*$^{+}$), or two (*tko*^{25t}/*tko*^{25t}, *Wb*^{1}/Y), three (*tko*^{25t}/*Wb*^{1}) or four (*Wb*^{1}/*Wb*^{1}) copies of the *tko*^{25t} allele. Numerator indicates maternal and denominator paternal inheritance of the allele. **B**) Gene copy number analysis performed using Q-RT-PCR and genomic DNA template. **C**) X-chromosomal mapping of the duplicated intervals in the suppressor lines, as suggested by the copy number analysis.

5.1.2 Suppressor lines carry X-chromosomal duplications surrounding the *tko* locus

In order to identify the *Weeble* suppressor, multiple genetic experiments were performed to discover its genomic location. Based on a series of crosses between *tko*^{25t} and *Wb*^{1}, the suppressor allele appeared to be dominant and X-linked, irrespective of the parent of origin (**Fig. 4A**). This also implied that mitochondrial genotype did not contribute to the phenotypic suppression. We then performed a transcriptomic analysis of the *Weeble* suppressor lines and outbred wild type and *tko*^{25t} flies. This revealed a contiguous set of X-chromosomal loci, including the *tko* gene, to be consistently approximately two-fold elevated in expression in both suppressor lines (**Fig. 4B**). Since this was suggestive of a corresponding

chromosomal duplication, we performed a gene dosage analysis using southern blotting, targeting *tko* and two other X-chromosomal genes *CG8636* and *CG12498* (I). The first gene chosen was located within the region exhibiting the 2-fold elevated expression in Wb^2 but not in Wb^1, and the latter was outside of this region in both. Southern blotting confirmed that the copy number of *tko* was indeed elevated in both suppressor lines, while that of *CG8636* only in Wb^2. *CG12498* and *RpL32*, which was used as a single copy control, both had uniform copy number throughout the sample set. We verified these findings using qPCR, and further extended the analysis to cover all three suppressor lines, and genes within, and just outside of the potentially amplified region. Using genomic DNA of males, we confirmed that the amplification spanned a wide region of the X-chromosome surrounding the *tko* locus in all *Weeble* lines (**Fig. 4B**). We mapped the left end of the duplication to a region between the transposable element, *Tirant 24*, and the gene *CG14050* in all suppressor lines. The right breakpoint in Wb^1 was discovered to be located within the region between *trol* and *CG13758*, whereas in Wb^2 and Wb^3 the duplication extended some 60-65 kB further downstream, with the right end mapping to a region between the genes *CG8636* and *Tsp3A*.

5.1.3 Ubiquitous ectopic expression of tko^{25t} or *mRpL14* does not suppress the tko^{25t} phenotype

Based on previous data, we knew that ectopic copies of a transgenic tko^{25t} allele in the mutant background did not confer significant phenotypic rescue, not even when the extra alleles were expressed at a level several fold higher than that of the endogenous gene (Toivonen et al. 2003). Since the duplicated region in all suppressor lines also carried a second mitoribosomal gene, *mRpL14*, we hypothesized that the amplification of both of the genes is required for a more substantial rescue of the tko^{25t} phenotype. We therefore cloned *mRpL14* together with its putative promoter region of approximately 750 bp, and established several transgenic fly lines carrying ectopic copies of the gene. We then chose two suitable transgenic lines, both of which, based on an insertion site analysis, had only a single genomic integration site on either the chromosome arm 2R (14-2R) or 3R (14-3R), did not interrupt the coding sequence of any known gene and did not reside within large heterochromatic regions. Finally, we performed a series of crosses to introduce the *mRpL14* transgenes into the tko^{25t} background, and produced *mRpL14* transgenic

mutant flies with and without additional ectopic copies of the *tko*^{25t} allele. We used the previously characterized (Toivonen et al. 2001) transgenic lines, A1 and A3, to provide the extra copies of the *tko*^{25t} -allele, under the regulation of the endogenous promoter sequence. While the *Wb*^{1} suppressor allele was sufficient to rescue male and female *tko*^{25t} mutants, both transgenes, whether alone or in combination, failed to complement the mutant phenotype (**Fig. 5A, 5B and 5**C), despite causing an increase in transcript levels comparable with that of the suppressors (**Fig. 5D**).

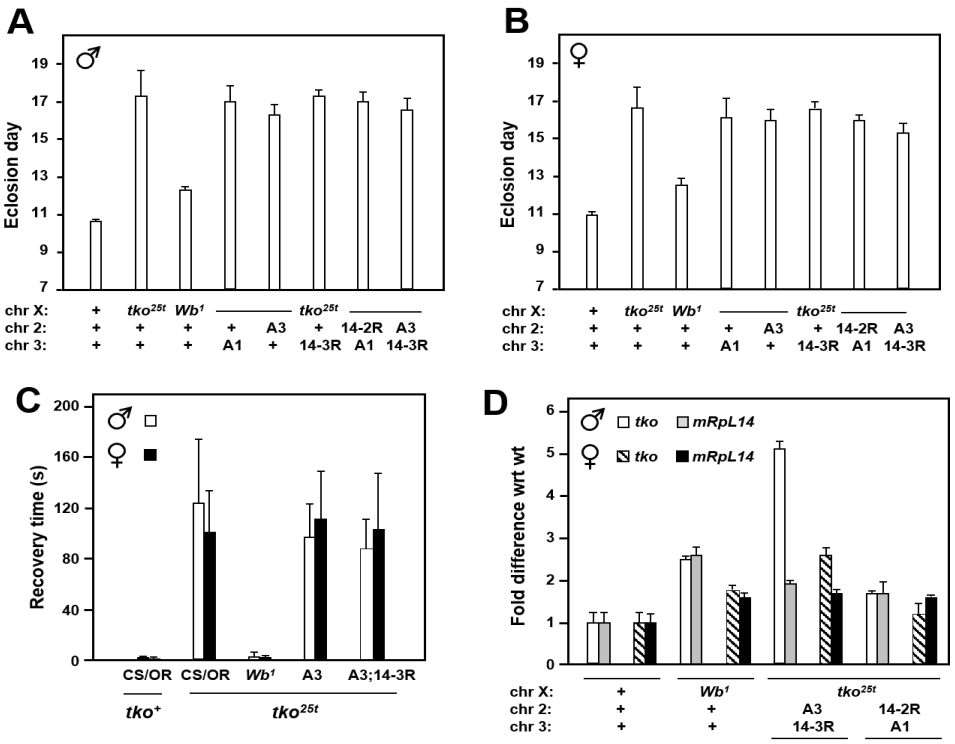

Figure 5. Ectopic expression of *tko*^{25t} and *mRpL14* does not alleviate *tko*^{25t} phenotype. **A**) and **B**) Developmental time of male and female flies expressing transgenic copies of *tko*^{25t} (A1 and A3) and *mRpL14* (14-2R and 14-3R). **C**) The effect of transgene expression on bang sensitivity. **D**) Relative (to wild-type of the same sex) expression levels of *tko*^{25t} and *mRpL14* expressing flies.

5.1.4 The phenotypic rescue in suppressor lines is dosage and chromosomal context dependent

After we failed to rescue the *tko*^{25t} mutants by introducing the extra copies of *mRpL14* and *tko*^{25t}, both of which produced approximately 2-fold elevated expression, we decided to further investigate the gene dosage effect and its dependence on chromosomal context. Hence, we combined *Weeble* suppressors X-chromosomes with a *tko* null allelle, *tko*^{3}. We also introduced the extra autosomal copies of the *tko*^{25t} allele carried by the transgenic construct A3 to the fully *tko* deficient *tko*^{3} background and characterized the resulting progeny. Females with the combination of a *Wb* allele and *tko*^{3} behaved essentially as females homozygous for *tko*^{25t}, eclosing with a considerable developmental delay and exhibiting bang sensitivity (**Fig. 6A** and **6B**). Increased gene copy number of the *Wb*/*tko*^{25t} and *Wb*/*Wb* females was sufficient to rescue both phenotypes. Consistent with our previous findings, similar or even higher *tko*^{25t} copy number, achieved by introducing the A3 transgenic alleles into the *Wb/tko*^{3} background, was insufficient

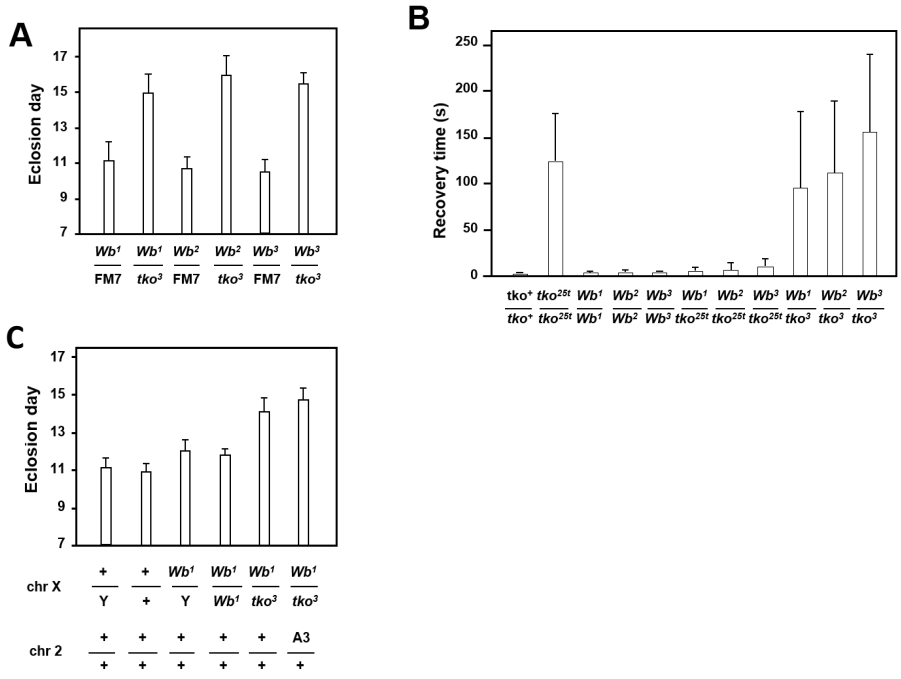

Figure 6. *Weeble* suppression is dependent on elevated *tko*^{25t} copy number. **A**) and **B**) Developmental time and bang sensitivity. **C**) Unlike *Weeble*, extra ectopic copies of *tko*^{25t} (A3) are insufficient to rescue the mutant phenotype. Genetic nomenclature as before. FM7 indicates a balancer chromosome wild-type for *tko*.

to rescue the mutant phenotype (**Fig. 6C**). This and the previous results thus strongly implied that while increase in gene dosage and transctipt levels is necessary for the phenotypic rescue of the *tko*^{25t} mutants, coordinate expression provided only by the *Weeble* amplifications is critical for the full suppressor effect.

5.2 Targeting the OXPHOS deficiency in *tko*^{25t} with alternative respiratory chain enzymes (II)

5.2.1 AOX expression does not rescue *tko*^{25t}

The sea squirt *Ciona intestinalis* alternative oxidase (AOX) has been successfully used to compensate multiple respiratory chain complex defects in flies (Fernandez-Ayala et al. 2009), particularly those affecting the cytochrome *c* oxidase (Kemppainen et al. 2014). We therefore decided to test whether bypassing the cytochrome segment of the respiratory chain would alleviate the *tko*^{25t} phenotype. AOX was expressed using the drug-inducible GeneSwitch-system (Barolo et al. 2000), a modified version of the UAS-GAL4 system (Brand & Perrimon, 1993),

combined with a ubiquitous α-tubulin promoter, and a concentration of the inducing drug RU486 that was found to produce maximal expression during development and adulthood. For further details see (II).

When expressed during development in a *tko*^{25t} background, AOX had no obvious effect on either eclosion time or bang sensitivity (data shown on II), compared to either non-induced (no drug) or driver or transgene-only controls. Likewise, when the induction was initiated upon eclosion, AOX did not mitigate bang sensitivity after reaching its maximum expression level in two-day-old adults (II). We also tested prolonged AOX expression during adulthood, but even after 30 days, we failed to detect any rescue of the phenotype. However, it is noteworthy that we did not detect any further functional deterioration in the aged mutant adults either, as determined by the recovery times in the bang sensitivity assay (II).

5.2.2 Ndi1 and its co-expression with AOX throughout development is lethal to *tko*^{25t}

After failing to rescue the *tko*^{25t} phenotype using AOX, we tested whether an equivalent bypass of complex I could do so. Complex I is quantitatively the most severely affected of the respiratory chain complexes in *tko*^{25t}, at least during development (Toivonen et al., 2003). For the CI bypass, we used the yeast NADH dehydrogenase Ndi1 (Sanz et al. 2010). Ndi1 expression was induced in the *tko*^{25t} background throughout development using the ubiquitous *daughterless*-GAL4 (*da*-GAL4) driver (detailed crossing scheme in II). When expression was induced during development at the standard experimental temperature of 25 °C, Ndi1 was almost fully lethal to both mutant male (*tko*^{25t}/Y) and female (*tko*^{25t}/*tko*^{25t}) flies (**Table 1**). Ndi1 expression also conferred partial lethality upon phenotypically wild-type heterozygous *tko*^{25t} (*tko*^{25t}/FM7) females. The lethality was equally penetrant when Ndi1 was co-expressed with AOX at 18 °C during development (**Table 2**). We thus concluded that, unlike AOX-expression, which simply failed to rescue the *tko*^{25t} phenotype, the transgenic expression of Ndi1 is selectively lethal to mutant flies.

Genotype	Sex	Number of Progeny
tko25t / FM7 ; CyO / 2 ; daGAL4 / 3	Female	152
tko25t / FM7 ; UAS-Ndi1 / 2 ; daGAL4 / 3	Female	72
tko25t / tko25t ; CyO / 2 ; daGAL4 / 3	Female	57
tko25t / tko25t ; UAS-Ndi1 / 2 ; daGAL4 / 3	Female	1
FM7 / Y ; CyO / 2 ; daGAL4 / 3	Male	65
FM7 / Y ; UAS-Ndi1 / 2 ; daGAL4 / 3	Male	25
tko25t / Y ; CyO / 2 ; daGAL4 / 3	Male	20
tko25t / Y ; UAS-Ndi1 / 2 ; daGAL4 / 3	Male	1

Table 1. The effect of Ndi1 expression on *tko*^{25t}. Total number of eclosed progeny of each genotype class, reflecting survival through development. FM7, CyO and Ser are essentially wild-type balancers for the X, 2nd and 3rd chromosomes, respectively.

Genotype	Sex	Number of Progeny
tko25t / FM7 ; CyO / 2 ; daGAL4 / Ser	Female	54
tko25t / FM7 ; CyO / 2 ; daGAL4 / UAS-AOX	Female	48
tko25t / FM7 ; UAS-Ndi1 / 2 ; daGAL4 / Ser	Female	34
tko25t / FM7 ; UAS-Ndi1 / 2 ; daGAL4 / UAS-AOX	Female	35
tko25t / tko25t ; CyO / 2 ; daGAL4 / Ser	Female	23
tko25t / tko25t ; CyO / 2 ; daGAL4 / UAS-AOX	Female	17
tko25t / tko25t ; UAS-Ndi1 / 2 ; daGAL4 / Ser	Female	5
tko25t / tko25t ; UAS-Ndi1 / 2 ; daGAL4 / UAS-AOX	Female	0
FM7 / Y ; CyO / 2 ; daGAL4 / Ser	Male	26
FM7 / Y ; CyO / 2 ; daGAL4 / UAS-AOX	Male	27
FM7 / Y ; UAS-Ndi1 / 2 ; daGAL4 / Ser	Male	8
FM7 / Y ; UAS-Ndi1 / 2 ; daGAL4 / UAS-AOX	Male	7
tko25t / Y ; CyO / 2 ; daGAL4 / Ser	Male	19
tko25t / Y ; CyO / 2 ; daGAL4 / UAS-AOX	Male	14
tko25t / Y ; UAS-Ndi1 / 2 ; daGAL4 / Ser	Male	6
tko25t / Y ; UAS-Ndi1 / 2 ; daGAL4 / UAS-AOX	Male	0

Table 2. The effect of Ndi1 and AOX co-expression on *tko*^{25t}. Total number of eclosed progeny of each genotype class, reflecting survival through development. FM7, CyO and Ser are essentially wild-type balancers for the X, 2nd and 3rd chromosomes, respectively.

5.2.3 ATP and ROS do not correlate with phenotype in Ndi1 expressing *tko*^{25t} flies

We have previously show that the *tko*^{25t} mutants exhibit elevated ROS production and decreased ATP levels (Chen et al., 2012). In order to understand how these physiological changes contribute to the phenotype in *tko*^{25t}, we repeated the measurements in the presence of the bypass enzymes, hoping that this might also elucidate why the two bypass enzymes failed to rescue *tko*^{25t}. This time the expression of both transgenes was induced independently in the mutant background using *da*-GAL4, and at a more permissive temperature of 18 °C, in order to obtain enough flies to quantify H_2O_2 production and the steady-state level of ATP in induced and non-induced *tko*^{25t} mutant flies, and phenotypically non-mutant controls.

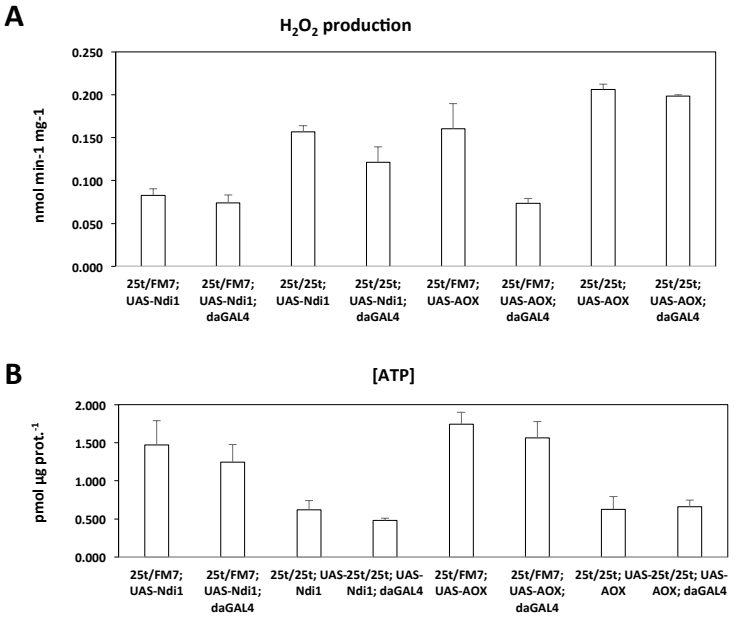

Figure 7. **A**) H_2O_2-production and **B**) steady state ATP-levels in AOX and Ndi1-expressing (daGAL4) and non-expressing, phenotypically wild-type (25t/FM7) and *tko*^{25t} mutant (25t/25t) females.

Consistent with previous findings, we again observed elevated mitochondrial ROS production and lower steady-state ATP levels in homozygous mutants compared to heterozygous controls (**Fig. 7A**). Ubiquitous expression of either AOX or Ndi1 had no significant effect on ATP, and only Ndi1 was able to slightly alleviate ROS production (**Fig. 7B**). Despite this modest positive effect, the overall effect of Ndi1 expression is deleterious to *tko*^{25t}, implying that ROS production is not a crucial determinant of the disease-like phenotype.

5.3 Phenotypic rescue of *tko*^{25t} can be achieved by modulating diet

5.3.1 *tko*^{25t} phenotype is sensitive to diet composition but not calorie content

Since rescuing the OXPHOS deficiency in *tko*^{25t} using the alternative respiratory chain enzymes had failed, we rationalized that the mutant phenotype could be due to a complex metabolic defect that was not simply the inability to produce sufficient ATP by OXPHOS, or a simple redox disturbance that AOX or Ndi1 should be able to correct. This was supported by the fact that neither ROS production nor ATP deficiency in adults appeared to correlate with the severity of the phenotype. We therefore decided to investigate how the mutant phenotype would respond to disturbances of metabolic homeostasis through dietary manipulation.

We first performed the bang sensitivity and developmental time assays on five different isocaloric diets (see Materials and Methods). These diets, denoted high sugar (HS), intermediate sugar (IS), high fat (HF), high protein (HP) and low sugar (LS), were generated by replacing some of the sugar components of the high sugar medium with equicaloric amounts of fats (olive oil), proteins (soy protein extract) or both. Wild-type flies were largely unaffected by the dietary modulation while mutant flies exhibited high correlation between the dietary sugar content and severity of the phenotype (**Fig. 8A** and **8B**): both developmental delay and bang sensitivity were substantially rescued on the three diets with least sugar, HP, HF and LS. In order to corroborate this initial result, we performed the same experiment with five diets with identical composition, with the exception of dietary sugar

(sucrose). Again, the developmental delay in *tko*^{25t}-mutants was aggravated by elevated sugar content in a dose-dependent manner while wild-type flies remained relatively unaffected by the diet composition (**Fig. 8C**). Finally, we verified that the apparent developmentally toxic effects of the high sugar diets were not specific to a certain type of source of sugar by alternating between glucose, sucrose and fructose as the primary sugar component in the diet. We observed little to no difference on developmental time between the alternative sugars (**Fig. 8D**).

Encouraged by these observations, we decided to explore the relationship between the *tko*^{25t} phenotype and dietary sugar content, and chose two diets upon which to carry out further experiments: a high-sugar diet (HS) and a zero-sugar diet (ZS), referred to as the 0% diet in the sugar concentration series. Both of these diets were

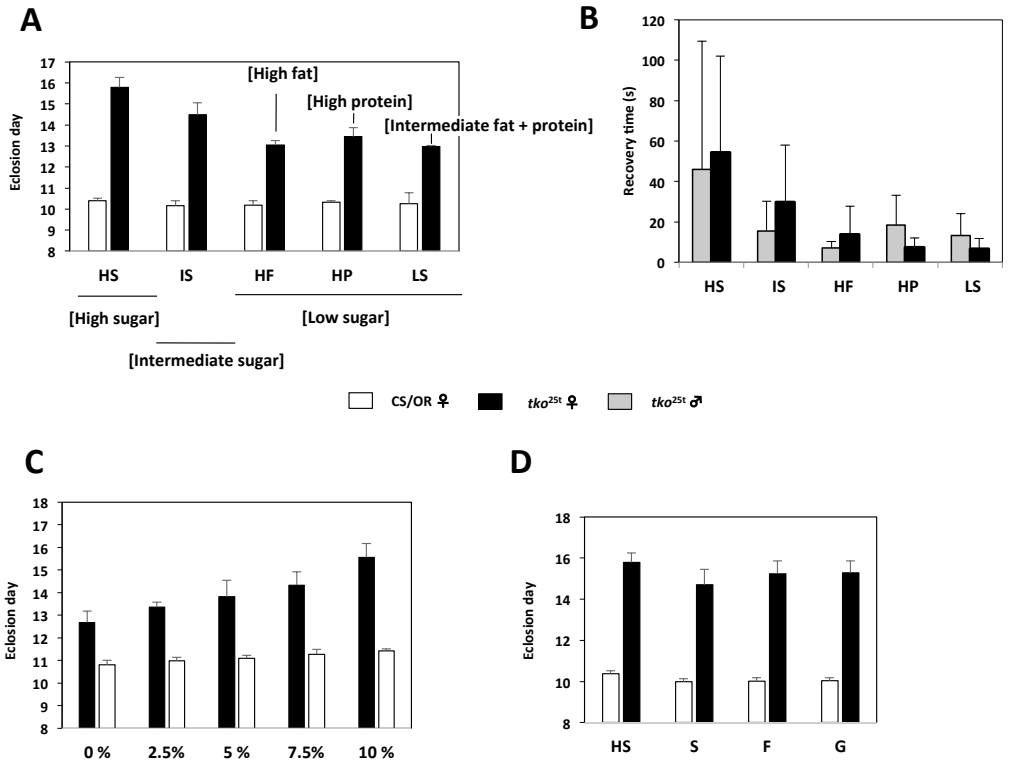

Figure 8. Dietary sugar retards growth in *tko*^{25t} irrespective of other dietary components. **A**) Mean eclosion day on isocaloric diets. **B**) Bang sensitivity of *tko*^{25t} on isocaloric diets. **C**) and **D**) Mean eclosion day on medium with different sugar concentrations and different sugar types. Genotypes as indicated. HS – High sugar, IS – intermediate sugar, HF – High fat, HP – High protein, LS – Low sugar, S – Sucrose, F – Fructose and G – Glucose.

based on the same dietary formulation, the only difference being the omission of the pure sugar components of the HS medium, with consequently decreased calorie content (**Fig. 9A**). We verified that neither wild-type nor mutant larvae exhibited compensatory feeding on the lower calorie diet by quantifying feeding behavior and food intake on both diets during a short period of time. Based on the feeding assay, all larvae fed less on the ZS diet while the *tko*^{25t} larvae generally exhibited lower food consumption than wild-type (**Fig. 9B**). We also tested how the dietary sugar load, together with feeding behaviour and genetic background were reflected in the combined circulating trehalose and glucose levels in the larvae. Trehalose is the primary circulating form of sugar in *Drosophila*, but it is rapidly interconverted with glucose inside cells. Zero-sugar diet markedly decreased sugar levels, while *tko*^{25t} larvae exhibited lower circulating sugar levels than wild-type larvae (**Fig. 9C**).

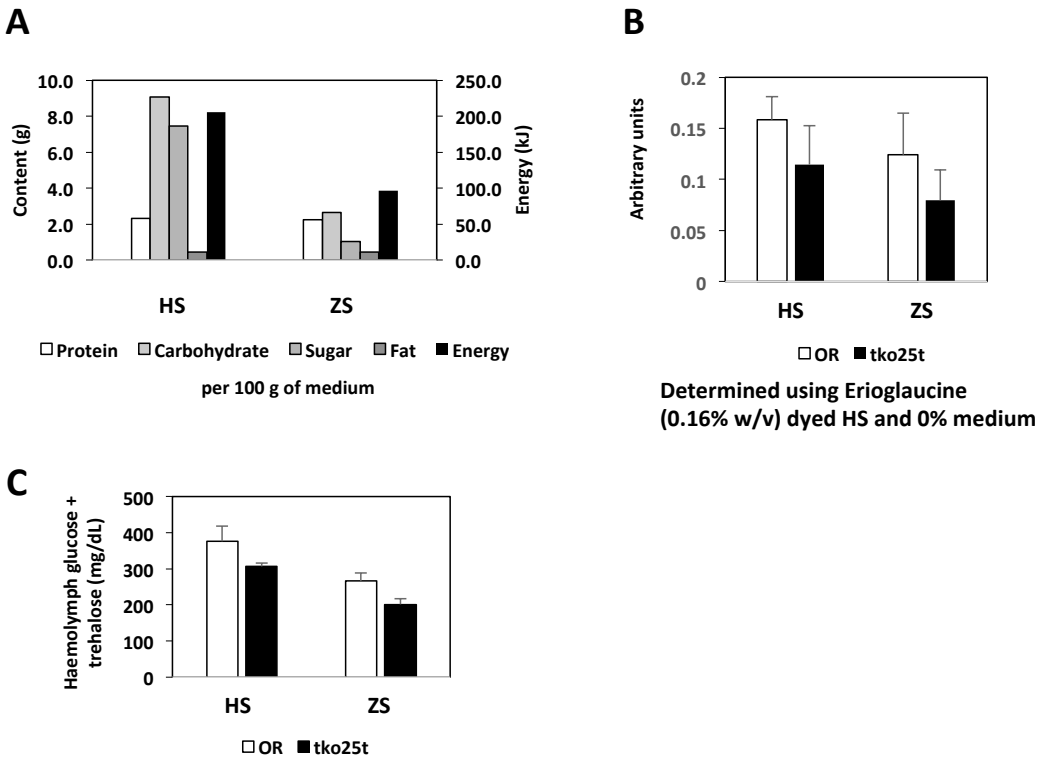

Figure 9. **A**) Dietary content of the (standard) high-sugar and zero-sugar diets. **B**) Feeding behaviour of larvae on HS and ZS diets. **C**) Circulating trehalose and glucose (combined) levels of larvae reared on HS and ZS diets.

5.3.2 Metabolic homeostasis is disturbed by mitochondrial dysfunction in *tko*^{25t}

In order to characterize how the mitochondrial dysfunction is reflected in global metabolism in the *tko*^{25t} mutants, we performed a small molecule CE/TOFMS analysis and compared the metabolic profiles of mutant and wild-type mid-third instar larvae reared on high- and zero-sugar diets. The metabolomics data was filtered for metabolites, which were not reliably detected in replicates of at least one sample type and analyzed for statistical significance between sample groups using two-tailed Student's t-test (**Appendix I**). Changes with a p-value < 0.01 were considered significant, although in the case of up- or down-regulated metabolic pathways, changes with a p-value of < 0.05 were considered due to the small sample size.

Of particular interest were metabolites, which exhibited either increased or decreased levels in *tko*^{25t} larvae reared on high-sugar in comparison with wild-type, but were present at significantly more wild-type like levels in mutants on zero-sugar diet. We considered this to be a possible indication of accumulation or depletion of an individual metabolite or products of a metabolic pathway being detrimental for growth. Quantitatively, the abundance of a much higher number of metabolites was affected by genotype than by diet. 24 metabolites exhibited decreased and 11 increased levels, in *tko*^{25t} larvae on both diets, while only 4 metabolites were up and 5 down in both genotypes on high-sugar versus zero-sugar diet.

The metabolites elevated on HS in wild-type and mutant larvae included alanine, ornithine, GABA, gluconate and 3-hydroxykyrurenine while isocitrate, glucuronate, carnitine, citrulline and N-epsilon-Acetyllysine were partially depleted on the same diet.

Metabolites which were detected at significantly lower levels in *tko*^{25t} on both diets included *e.g.* multiple amino acids and their derivatives (see below), glycolytic and pentose phosphate pathway intermediates fructose-1,6-bisphosphate (**Fig. 10E**) and sedoheptulose-7-phosphate, putrescine and β-alanine. As expected, the metabolomics analysis also confirmed the steady-state ATP deficiency in *tko*^{25t} (**Fig. 10B**). Perhaps most intriguingly, the level of NADPH, which is required by the glutathione system and many biosynthetic processes, such as fatty acid biosynthesis, was down in *tko*^{25t} on both diets (**Fig. 10G**).

The concentrations of only three compounds: alanine, methionine sulfoxide and saccharopine, were significantly elevated in HS *tko*^{25t} larvae and concomitantly markedly reduced on ZS diet. Vice versa, the steady-state levels of seven compounds: glucuronate, adenylosuccinate, UDP-N-acetylglucosamine, glutamate, arginine, dopamine and perhaps most notably ATP and NADPH, were significantly down in *tko*^{25t} on HS diet but at least partially recovered on the ZS diet.

5.3.2.1 Amino acid homeostasis

Most amino acids were relatively unaffected by either diet or the *tko*^{25t} mutation reflecting metabolic plasticity of *Drosophila* (see **Appendix I**, **Fig. 10D**). Alanine and histidine levels were elevated on the high-sugar diet whereas those of glutamate and threonine were higher on the zero-sugar diet. Again, the *tko*^{25t} mutation had a substantially greater impact on amino acid homeostasis than diet. Glycine, alanine, serine and threonine were elevated while aspartate, asparagine, lysine, glutamate, histidine and tryptophan were partially depleted in mutant larvae on both diets. This amino acid depletion in *tko*^{25t} was also reflected in metabolites which are direct downstream products of amino acid metabolism. 3-hydroxykynurenine and histamine, for example, are products of tryptophan and histidine degradation, respectively, and both were partially depleted in *tko*^{25t}. Furthermore, aspartate is a biosynthetic precursor for multiple compounds and other amino acids, such as β-alanine, adenylosuccinate, argininosuccinate and asparagine (through asparagine synthase), all of which were decreased in *tko*^{25t} larvae.

Due to the presumed absence (see Discussion) of a canonical urea cycle in insects, the pathways resulting in nitrogen removal are likely to be very different between flies and mammals. Nevertheless, metabolites putatively involved in the removal of nitrogenous waste products exhibit distinct imbalance between the two diets and genotypes. The mammalian urea cycle intermediates ornithine and citrulline (**Fig. 10D**), in particular exhibit very different patterns of abundance. Ornithine levels were generally higher on the high-sugar diet whereas citrulline exhibited the opposite trend. Citrulline levels were in turn systematically higher in mutant larvae while the lowest ornithine level was detected in *tko*^{25t} on ZS and highest on HS. The accumulation of ornithine in the HS *tko*^{25t} larvae may be indicative of increased arginase activity, since the concentration of arginine is concomitantly reduced on

HS, and rescued to a wild-type like level on ZS in *tko*^{25t}. The two common nitrogenous waste products in insects, urate and urea, were substantially and systematically increased and decreased, respectively, in *tko*^{25t} larvae on both diets.

5.3.2.2 Lipid metabolism

The methodology chosen for the global metabolomics analysis unfortunately does not detect the vast majority of the different lipid species. However, we did observe a two-fold increase in the concentration of phosphorylcholine in *tko*^{25t} on both diets. Moreover, o-acetylcarnitine, a derivative of L-carnitine and CoA, were approximately two-fold increased in *tko*^{25t} larvae. Finally, three saturated medium chain fatty acids, caprylic acid (octanoate), capric acid (decanoate) and lauric acid (dodecanoate), were detected at approximately equal levels in wild-type larvae, and in *tko*^{25t} on the ZS diet, but were either below detection level, or nearly depleted in mutant larvae on the HS diet. This suggests that the catabolism of MCFAs is particularly high in *tko*^{25t} larvae on the high-sugar diet. Yet, despite the apparent increase in fatty acid catabolism, we measured very high levels of stored triglycerides in *tko*^{25t} larvae on both diets (**Fig. 10C**).

5.3.2.3 Redox balance indicators

We have previously shown that lactate dehydrogenase (LDH) is upregulated in *tko*^{25t} adults, implying that the mutant flies are converting pyruvate to lactate in order to regenerate NAD^+ via pathway alternative to the respiratory chain (Fernández-Ayala et al., 2010). The $NADH/NAD^+$ ratio is crucial for ATP production and the equilibrium is typically shifted towards the overreduced state when the OXPHOS is inhibited. Surprisingly, this did not appear to be the case in *tko*^{25t} on either diet, despite the severe multi-complex OXPHOS deficiency (**Appendix I**, **Fig 10G**). We did observe highly elevated levels of pyruvate and lactate, though, consistent with the idea of inhibited mitochondrial substrate oxidation. This elevation was also confirmed by enzymatic assays (**Fig. 10A**). We also found the concentrations of both metabolites to be slightly but significantly lower on low-sugar diet, in both wild-type and mutant larvae. Serum lactate was likewise several fold higher in *tko*^{25t} (**Fig. 10A**), but no difference was observed

between HS and ZS, indicating that lactate clearance is likely to be operating at maximum capacity in mutant larvae under both conditions. Although the accumulation of pyruvate and lactate could merely signal increased glycolytic flux and thus reflect adaptation to both OXPHOS deficiency, we found both compounds to phenocopy the developmental retardation of tko^{25t} in wild-type larvae, when administered through diet (III). The pyruvate and lactate supplementation of zero sugar diet also aggravated the phenotype in tko^{25t} larvae and thus partially phenocopied the high sugar-effect (III).

Nicotinamide adenine dinucleotides ($NADH/NAD^+$) and nicotinamide adenine dinucleotide phosphates ($NADPH/NADP^+$) both participate in similar redox-dependent processes but in different cellular functions. The $NADPH/NADP^+$ ratio is maintained primarily through regeneration of NADPH by three subsets of enzymes: two enzymes of the pentose phosphate pathways, glucose-6-phosphate dehydrogenase (G6PD) and 6-phosphogluconate dehydrogenase (6PGD), and mitochondrial and cytosolic isoforms of the isocitrate dehydrogenase (IDH) and malic enzyme (ME). NADPH availability is vital for many biosynthetic processes, but also a crucial determinant of cellular antioxidant capacity. NADPH is required by glutathione reductase, which regenerates reduced glutathione (GSH) from the oxidized form (GSSG). In the parallel, analogous ROS detoxifying system, NADPH is used by the thioredoxin reductase (TrxR) to reduce oxidized thioredoxin molecules (Lu & Holmgren, 2014). Finally, NADPH can maintain catalase activity in the presence of high H_2O_2 by preventing its substrate-induced inactivation (Kirkman et al., 1999). On the high-sugar diet, tko^{25t} larvae exhibited a dramatic NADPH depletion in comparison to wild-type. On zero-sugar compared with high-sugar diet there was a notable increase in NADPH levels in both genotypes (**Fig. 10G**), sufficient to restore the NADPH/NADP ratio above 1. In order to investigate how the NADPH/NADP ratio is modulated in tko^{25t}, and on the two diets, we assayed the maximal activity of the primary NADPH-generating enzymes in larval homogenates (**Fig. 11A**). The activities of both pentose phosphate pathway enzymes glucose-6-phosphate dehydrogenase (G6PDH) and 6-phosphogluconate dehydrogenase (6PGDH) were down on ZS diet, but also generally slightly lower in tko^{25t} than in wild-type, implying that the maximal pentose phosphate pathway throughput is modulated by diet. Likewise, the total activity of the malic enzyme was slightly higher on the HS than on ZS diet, but significantly higher in mutant than wild-type larvae on both diets. Last, we tested the combined maximal capacity

of the various IDH isoforms. In this case, we observed only a modestly increased activity in *tko*^{25t} larvae, irrespective of the diet.

Since these measurements only reflect the *in vitro* activity of these enzymes in larval homogenates in the presence of a large excess of substrate, we also measured the enzyme activities in the presence of potential enzyme inhibitors, namely pyruvate, lactate and gluconate, all of which were elevated in *tko*^{25t}, particularly on high sugar. Gluconate, which is the product of glucose dehydrogenase-catalyzed glucose oxidation, was in fact only detected in significant quantities in wild-type and mutant larvae reared on the HS diet (**Fig. 10F**). We used the quantitative metabolomics data to determine approximately physiological substrate/inhibitor ratios. In the repeat experiments, we found all three compounds to be potent inhibitors of IDH, either each alone, or all three in combination (**Fig. 11B**). The inhibitory effect appeared not to be additive, *i.e.*, the inhibitory effect was no greater when all three compounds were applied simultaneously (in equimolar concentrations) than individually. All three inhibitors had only marginal effects on the activities of G6PDH and 6PGDH, while malic enzyme was substantially inhibited by lactate and its enzymatic product, pyruvate, but not by gluconate (**Fig. 11B**).

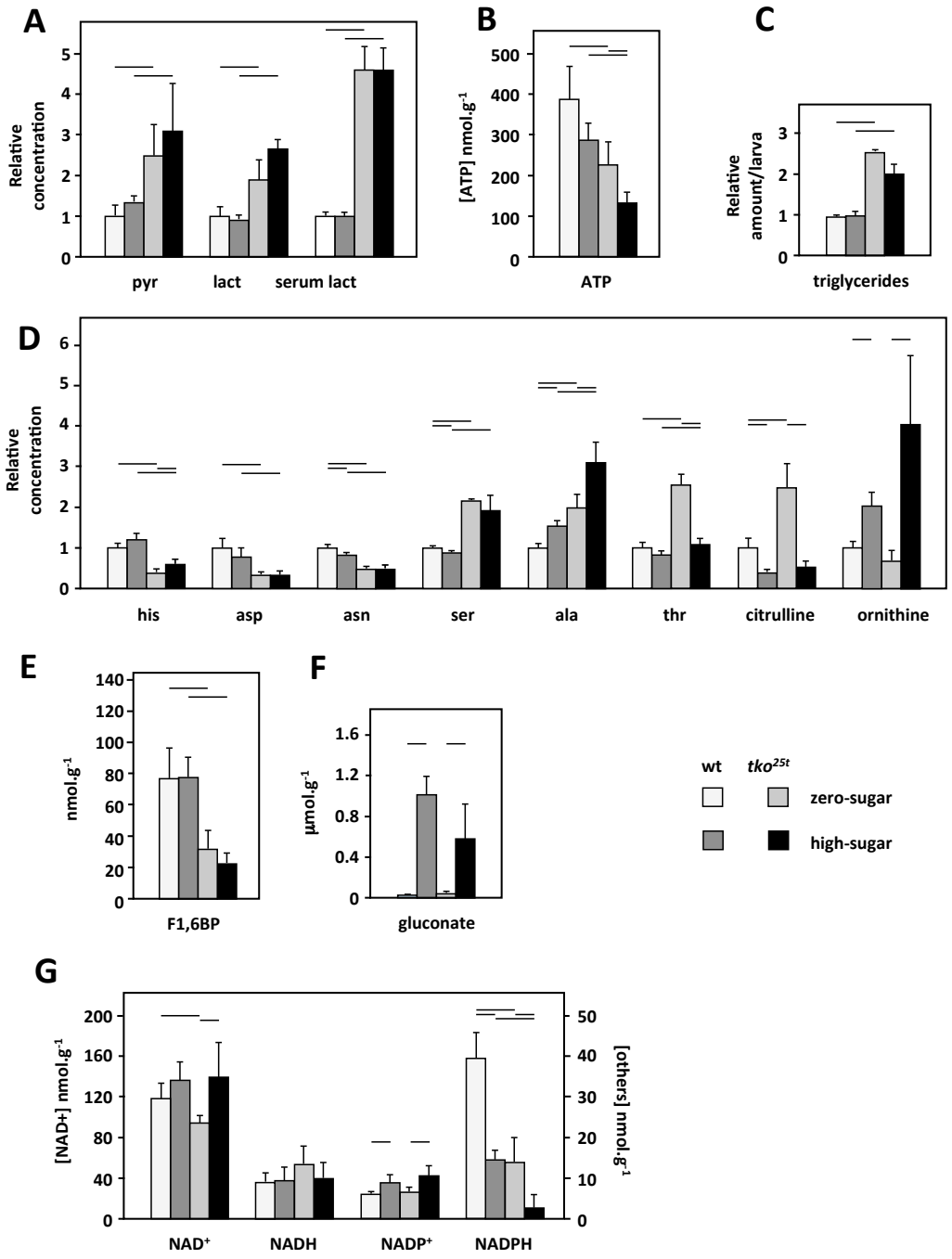

Figure 10. Selected metabolic changes exhibited by *tko*^{25t}. **A**) Pyruvate, lactate and serum lactate concentrations relative to wild-type on HS. **B**) Steady-state ATP levels. **C**) Total body triglycerides relative to wild-type on HS. **D**) Amino acids exhibiting statistically significant changes between to diets or genotypes (relative to wild-type on HS). **E**) Fructose-1,6-bisphosphate levels. **F**) Gluconate levels. **G**) NAD^+/NADH and $NADP^+$/NADPH levels.

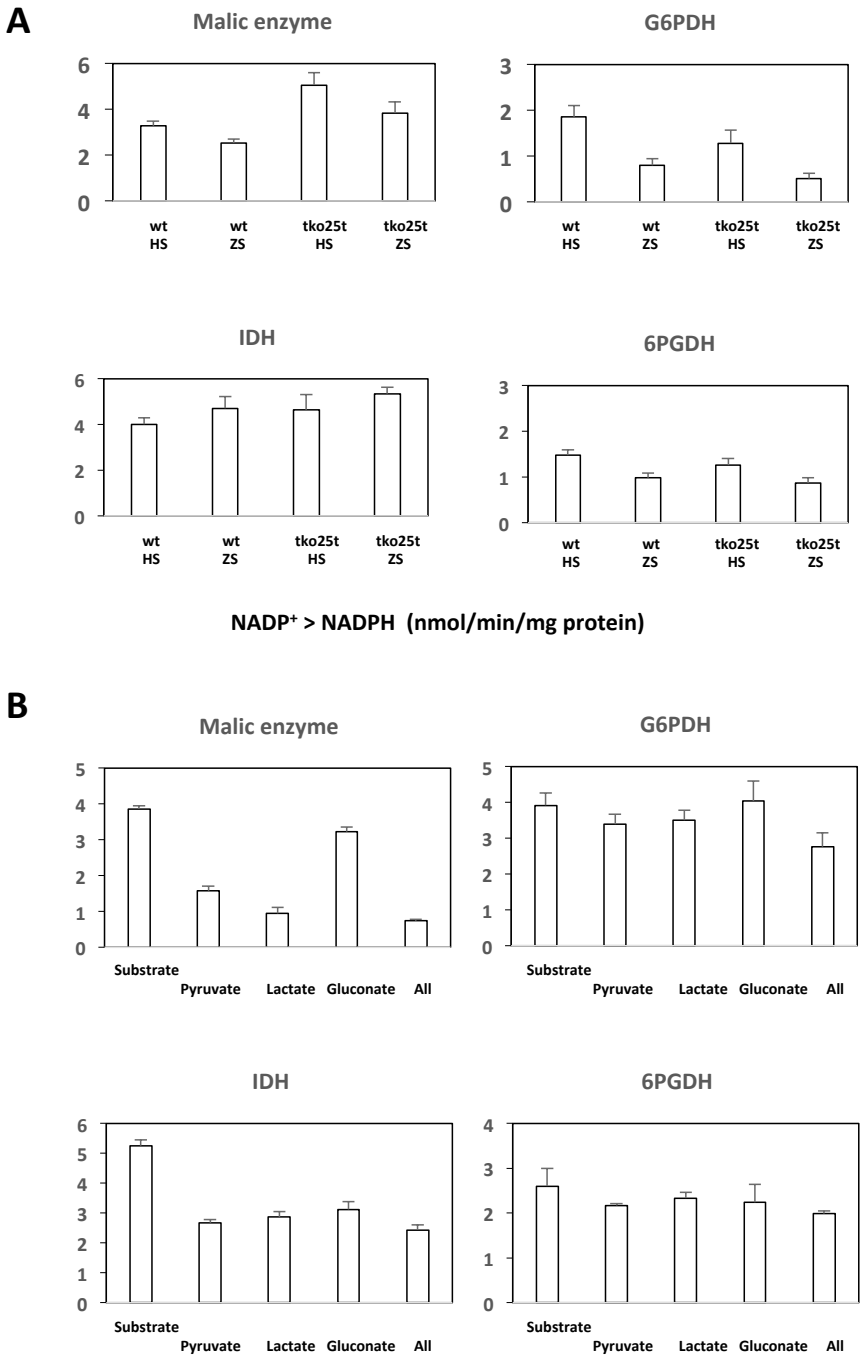

Figure 11. Maximal activities of the primary NADPH-generating enzymes in whole body larval homogenates. **A**) Maximal enzyme activities of malic enzyme, glucose-6-phosphate dehydrogenase (G6PDH), 6-phosphogluconate dehydrogenase (6PGDH) and isocitrate dehydrogenase (IDH). **B**) The effect of enzyme inhibitors in scrambled extracts. Enzyme activities were determined as the rate of $NADP^+$-reduction.

5.3.3 Transcriptional analysis of *tko*^{25t} mutant larvae

Transcriptome-wide analysis of *tko*^{25t} adults identified systematic changes in the expression of genes involved with core nutrient metabolism, namely up-regulation of gut-specific proteases and lipases, with the concomitant down-regulation sugar transporters and glucosidases (Fernández-Ayala et al., 2010). We conducted a similar, global transcriptomic analysis, using RNA sequencing, on feeding mid-to-late wild-type and *tko*^{25t} 3rd instar larvae, reared on either HS or ZS diet. We mapped the sequencing reads to the well-annotated *Drosophila* transcriptome, and performed differential gene expression analysis comparing wild-type and *tko*^{25t} larvae on each diet, and each genotype on the two different diets. In addition, we selected all genes exhibiting at least two-fold up- or down-regulation in a given pairwise comparison and performed a functional annotation enrichment analysis using the DAVID (Database for Annotation, Visualization and Integrated Discovery, http://david.abcc.ncifcrf.gov) gene ontology database tools. These results are summarized and presented in **Appendix II** as KEGG (Kyoto Encyclopedia of Genes and Genomes, http://www.genome.jp/kegg/) enlisted pathways and biological process gene ontologies exhibiting enrichment of pathway components among the up- and down-regulated gene sets. Hundreds of genes showed substantial differential regulation to either direction in each pairwise comparison. Through this analysis, we were able to identify systematic changes with regards to adaptation to the different dietary conditions or to mitochondrial dysfunction during larval growth. Only substantial and coordinate changes in expression patterns are discussed below, while a more detailed analysis of differentially expressed genes can be found in the *Discussion*, and a summary, using a slightly different approach, in (III).

5.3.3.1 Metabolic reprogramming

One of the most noticeable patterns of differential transcriptional regulation involved core nutrient and energy metabolic processes: glycolysis/pentose phosphate pathway, pyruvate metabolism, the TCA cycle and oxidative phosphorylation. These processes/pathways were systematically down-regulated on the zero-sugar diet in wild-type flies, presumably as a part of a natural adaptation to the nutritional environment. Markedly, the same processes were also down-regulated in *tko*^{25t} mutant larvae on both diets, in comparison with wild-type larvae

reared on the high-sugar diet. This suggests that the metabolic changes in mutant larvae mimic those observed in adaptation to low-sugar diet. It is also noteworthy, that the transcriptional regulation of the TCA cycle and oxidative phosphorylation appears to be tightly coupled with that of glycolysis and the pentose phosphate pathway in larvae. Curiously, testis-specific isoforms of enzymes falling into the aforementioned pathways were up-regulated in *tko*^{25t} mutants.

Carbohydrate metabolism was clearly inhibited on zero-sugar diet in wild-type larvae, and on both diets in *tko*^{25t} while gut- and adipose tissue-specific triacylglyceride lipases and phospholipases were consistently and significantly induced under the same conditions. This indicates that the metabolic re-programming is not limited to down-regulation of carbohydrate catabolism, but involves a shift in fuel preference from sugars to lipids.

5.3.3.2 Protein homeostasis and proteotoxic stress responses

Protein synthesis is one of the most ATP-dependent process in cells, accounting for an estimated 30% of total cellular energy consumption (Buttgereit & Brand, 1995). Hence, it is unsurprising that we found numerous genes encoding components of the cytosolic translation machinery to be down-regulated in *tko*^{25t}, particularly on the HS diet, while in wild-type larvae, the high dietary sugar appears to systematically induce the expression of cytoribosome components (III). A similar trend was observed with a large number of genes encoding structural components of muscle, indicating that muscle biosynthesis is closely linked to cytosolic protein synthetic capacity.

We did not observe any global, differential regulation of genes involved in either ER or mitochondrial unfolded protein responses although we had previously identified a mitochondrial stress responsive small heat-shock protein Hsp22, to be significantly up-regulated in *tko*^{25t} (Fernández-Ayala et al., 2010). The transcriptome-wide analysis of larvae did not identify *Hsp22* as being differentially regulated which might have resulted from an *in silico* mapping error in the RNA-sequencing data analysis, since the *Hsp22* coding sequences overlap with the open reading frame of another heat shock protein gene (*Hsp67*). Analysis of *Hsp22* transcript levels using quantitative PCR confirmed it to be significantly up-regulated

in *tko*^{25t} during the larval stages as well (**Fig. 12C**). The induction of a stereotypical mitochondrial chaperone protein (Morrow et al., 2000) was an indication of mitochondrial proteotoxic stress resulting potentially from oxidative damage or aberrant translation of mitochondrial proteins, or an imbalance between cytosolically and mitochondrially translated polypeptides caused by inhibition of mitochondrial protein synthesis. In order to test the latter hypothesis, we performed a developmental time experiment using media containing low levels of cycloheximide (CHX), a well-known inhibitor of eukaryotic cytosolic translation elongation (Schneider-Poetsch et al., 2010). We hypothesized that sublethal concentrations of CHX might alleviate possible proteotoxic stress. Unsurprisingly, both concentrations of CHX tested significantly retarded development in wild-type flies, as well as in phenotypically wild-type *tko*^{25t} heterozygotes (**Fig. 12B**). In a striking contrast to the response in wild-type flies, the homozygous and hemizygous mutant flies were unresponsive to inhibition of cytosolic protein synthesis (**Fig. 12B**).

5.3.4 Growth signaling network responds to mitochondrial dysfunction during development

The core growth-regulatory signaling network is highly conserved from *Drosophila* to mammals. Since the developmental abnormalities in *tko*^{25t} do not appear to impact the gross morphology of the fly, we hypothesized that the growth inhibition is a result of a coordinated signaling process. We thus chose a few key singaling modules as indicators of activation or inactivation of the three core growth regulatory signaling complexes, the AMP-activated kinase (AMPK), TORC1 and TORC2. We used Western blotting and pan- and phospho-specific antibodies to probe for the selected targets in whole 3rd instar larval homogenates. Representative blots are presented in (**Fig. 12A**).

We observed, a modest increase in the phosphorylation of Akt at ser^{505}, an indicator of TORC2 activity and insulin receptor stimulus (Hietakangas & Cohen, 2009), in larvae reared on high-sugar medium. Yet, this putative increase in Akt/TORC2 signaling was not associated with increased growth rate in either genotype. The phosphorylation of thr^{398} of the translational regulator S6K is a widely accepted readout for TORC1 complex activity (Magnuson, Ekim, & Fingar, 2012). This

TORC1-dependent S6K-phosphorylation was more intense in wild-type larvae on both diets, indicating lower TORC1 activity in *tko*^{25t}. Strikingly, also the total S6K protein level was significantly depleted in *tko*^{25t} larvae on HS diet. One of the known inhibitors of the TOR-complex, the AMP-kinase is activated in response to elevated AMP(ADP)/ATP ratio. AMPK activation was analyzed by detecting phosphorylation of thr^{172}, a site which is phosphorylated to activate the kinase in an AMP(ADP) responsive manner (Pan & Hardie, 2002). The AMPK-phosphorylation was substantially increased in *tko*^{25t} larvae, especially when grown on high-sugar medium, consistent with the severe ATP deficiency.

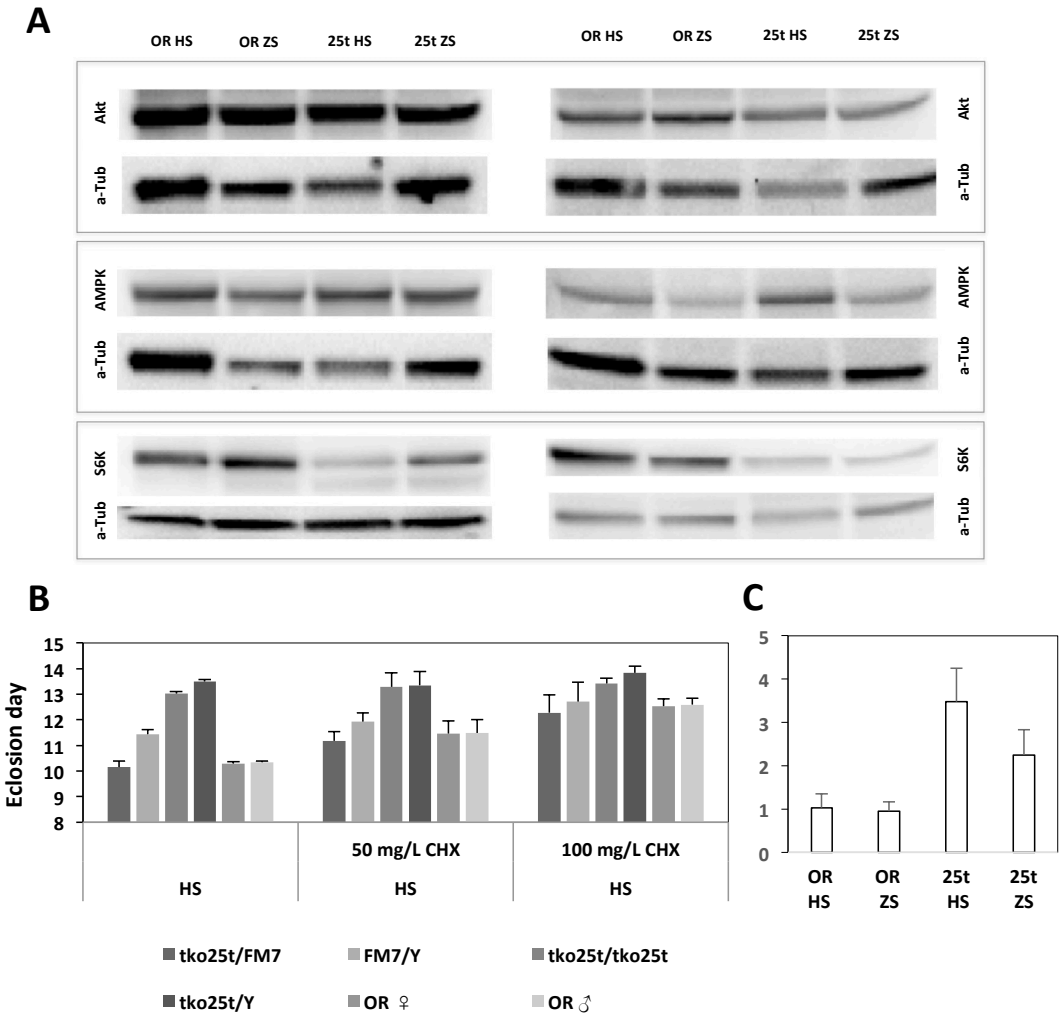

Figure 12. **A**) Representive Western blot illustrating changes in the abundance and phosphorylation status of key signalling molecules. **B**) Mean eclosion day on cycloheximide (CHX) supplemented diets. **C**) Relative transcript levels of *Hsp22* in wild-type (OR, oregon-R) and *tko*^{25t} (25t) larvae.

6. Discussion

The primary aims of this study were to increase our understanding of the molecular and metabolic basis of mitochondrial disease pathogenesis resulting from mild mitochondrial dysfunction. We approached this by first trying to identify genetic factors modifying the disease phenotype. Next, we attempted to understand how the primary molecular defect manifests at the organelle level. Finally, we investigated how multi-cellular organisms can adapt metabolically to often highly deleterious pathological states, and how nutrition modulates these adaptive responses. The *Drosophila tko*^{25t} mutant offered an appropriate tool for these purposes. The molecular defect in this disease model had already been well-characterized (Toivonen et al., 2001; Toivonen et al., 2003). Furthermore, the primary phenotypic features of the mutant flies, developmental delay and bang sensitivity, are quantifiable and correspond to common and relevant clinical manifestations of human mitochondrial disorders. The *tko*^{25t} phenotype is also mild enough to permit genetic and environmental manipulations, which are detrimental to the mutant flies, yet allow for viable flies to develop for analyzing the outcome of such treatments. Although morphologically very different from humans, fruit flies exhibit a high degree of conservation in the composition, structure and function of mitochondria and mitochondrial processes as well as major tissues, organ systems and many developmental processes. At the organismal level, core metabolic pathways and regulatory processes are likewise highly conserved between *Drosophila* and mammals, allowing for clinically relevant research to be conducted using fly mitochondrial disease models, so long as all results and findings are critically assessed.

6.1 Controlled over-expression of the mutant allele completely rescues the *tko*^{25t} phenotype (I)

We had previously observed that inbreeding of homozygous *tko*^{25} females and hemizygous mutant males results in a gradual improvement of the disease

phenotype (Jacobs et al., 2004). This raised two possible explanations: either the expression of the hypomorphic allele was increased, which would compensate for the defective gene product, or the inbreeding and the concomitant selection for fast developing and fertile individuals had resulted in the emergence of phenotype suppressing alleles of one or more other genes. Since the ectopically expressed copies of the mutant allele had previously failed to rescue the phenotype, it appeared likely that the phenotypic recovery is achieved through the action of genetic suppressors. Thus, my aim was to identify such genetic factors, and for this purpose, we imposed inbreeding and a selection regime, starting with a highly heterogenous genetic background, in order to obtain phenotypically rescued tko^{25t} strains. We managed to obtain several such strains, three of which exhibited full recovery of bang sensitivity and developmental delay (**Fig. 3**). In each of the three cases, the rescue resulted from a segmental duplication of an X-chromosomal region containing the tko^{25t} allele (**Fig. 4**). The *Weeble* duplications also carried a second mitoribosomal gene, *mRpL14*. As in the case of the transgenic tko^{25t} alleles, autosomal ectopic expression of extra copies of *mRpL14* under the regulation of its own promoter, did not confer notable phenotypic rescue. Finally, by producing different combinations of the *Weeble* alleles, the *tko* null allele (tko^{3}) and the endogenous tko^{25t}, we were able to demonstrate that over-expressing the tko^{25t} allele alone in its natural chromosomal milieu is sufficient for the rescue (**Fig. 5**). We further verified this by mapping the suppressor allele to the *tko* locus by combining chromosomes carrying deletions flanking the *tko* allele with the *Weeble* suppressor chromosomes (see I for details and results).

Although the genetic evidence strongly implies that the elevated expression of the tko^{25t} allele alone is sufficient for the *Weeble* suppressor effect, we cannot completely exclude the possibility that another gene within the minimal common duplicated interval could at least contribute to the rescue. Yet, we found no reasons to believe this is the case, based on diligent review of the literature with regards to the other duplicated genes (I).

6.1.1 Molecular mechanisms of *tko*^{25t} rescue in the *Weeble* suppressors

Transgenic expression of the wild-type *tko* allele can complement *tko*^{25t} whereas expressing the mutant allele, even at relatively high levels, does not result in significant phenotypic rescue. In this respect, the fact that the *Wb* alleles can fully compensate the *tko*^{25t} mutation despite lower total transcript levels, implies that distal transcriptional enhancers are required to coordinate the increase in expression to a specific developmental stage and/or tissue. Moreover, the substantial recovery of the 12S:16S rRNA ratio in the *Weeble* lines does not bring the ratio close to that observed in wild-type, despite the nearly complete rescue of the phenotype. This further enforces the idea that stringent spatiotemporal regulation is important for *tko* expression, and potentially also for other mitochondrial/mitoribosomal genes. The incomplete rescue of the 12S:16S ratio might, alternatively, indicate that very sharp thresholds operate for tolerance of decreased mitoribosomal RNA levels, or that the ratio is not as reflective of the mitoribosome subunit levels as we've hypothesized. The *tko*^{25t} larvae for instance, exhibit a peculiar pattern of dysregulation of the mitochondrial transcripts: multiple mitochondrial mRNAs, including ATP6, ATP8, ND1 and ND5 are up-regulated while the transcript levels of most mtDNA-encoded genes, including the 12S rRNA, are decreased in *tko*^{25t} compared with wild-type larvae on both diets (III). This suggests that the steady state 12S rRNA level might reflect a more global transcriptional defect or response than just the abundance of the mitoribosomal SSU.

6.2 Alternative respiratory chain enzymes do not rescue *tko*^{25t} (II)

We hypothesized that the mutant phenotype is primarily a consequence of impaired OXPHOS resulting from a limited supply of mitochondrially encoded complex subunits. The obvious potential downstream consequences of the OXPHOS deficiency are shortage of ATP and disturbed redox homeostasis due to a build-up of reduced electron carriers. Under such conditions, the availability of ATP itself could become rate-limiting for the numerous growth-promoting anabolic processes, while the accumulation of NADH, in turn, could signal back to the TCA cycle by inhibiting many of the involved enzymes (Nelson & Cox, 2005). This attenuation of

mitochondrial catabolism is a necessary adaptation to a decreased flux of electrons through the ETC but also disruptive for cellular macromolecule biosynthesis, which the TCA cycle supplies with precursors.

We thus hypothesized that providing a by-pass for a segment of the respiratory chain using the alternative respiratory chain enzymes *Ciona intestinalis* AOX or the *Saccharomyces cerevisiae* Ndi1 would allow for mitochondrial metabolism to proceed, although less efficiently in terms of biological energy conversion, but nonetheless alleviate the disease-like phenotype in tko^{25t}. Furthermore, correlations between changes in phenotype resulting from OXPHOS complex by-pass and those in key physiological parametres, such as ATP levels or ROS-production, could help to dissect the pathogenic processes underlying the mutant phenotype.

Despite the previously demonstrated potency of AOX to compensate for respiratory chain deficiency in flies (Fernandez-Ayala et al., 2009), its ubiquitous expression throughout development, or during adulthood had no obvious phenotypic effects (II) in tko^{25t} flies. Although this did not exclude the possibility that OXPHOS deficiency underlies the organismal phenotype in tko^{25t}, it strongly suggested that the growth limitation might occur at the level of complex I. We therefore performed analogous experiments using Ndi1. Ndi1 had been previously shown to be able to compensate even severe CI deficiency in *Drosophila* (Sanz et al. 2010; Cho et al. 2012), suggesting that the genetic complementation could robustly demonstrate whether CI was the sole underlying cause of the tko^{25t} phenotype. Unlike AOX expression, which had no clear impact on tko^{25t}, Ndi1 expression during development was semi-lethal and highly deleterious selectively to homozygous tko^{25t} mutant flies (**Table 1**). We then finally tested the co-expression of AOX and Ndi1 at 18 °C (as opposed to 25 °C), but again, expressing Ndi1 in the tko^{25t} background proved equally deleterious, with or without the co-expression of AOX (**Table 2**).

To investigate why AOX or Ndi1 expression failed to alleviate the tko^{25t} mutant phenotype, we analyzed two key physiological parameters, ROS-production and steady-state ATP levels, in adult progeny. Our measurements confirmed previous findings of decreased ATP and elevated ROS in the mutant flies (Chen et al., 2012). In accordance with the fact that AOX expression had no effect on the tko^{25t} phenotype, it also had no significant impact on either physiological parameter. Several interpretations of this finding, taken in isolation, are plausible. First, the expression of the mutant phenotype in tko^{25t} might involve only processes not

affected by AOX. Second, the finding is consistent with the possibility that the developmental defect is fully the result of ATP deficiency, resulting from lack of proton-pumping activity at complex III and/or IV since although AOX restores electron flow to oxygen, it does not facilitate proton pumping at the ETC complexes that it bypasses. The expression or co-expression of Ndi1 together with AOX, aggravated the phenotype, despite having only a negligible effect on both ROS production and ATP levels. This suggests that the severity of the mutant phenotype is determined rather by complex metabolic factors, than simply limited ATP supply, although a significant recovery in steady-state ATP-levels was associated with phenotypic rescue in the dietary experiments (III**, Fig. 10A**).

6.3 OXPHOS dysfunction and its impacts on physiology, development and the CNS in *Drosophila* (II,III)

The *tko*^{25t} flies exhibit mild to severe developmental delay depending on the diet and genetic background. The controlled inhibition of growth rate appears to be the only obvious gross developmental abnormality resulting from the rather severe OXPHOS dysfunction in these mutants, with the exception of thin mutant bristles. Interestingly, a *tko*^{25t}-like phenotype is exhibited by several *Drosophila* ATP-deficient mitochondrial mutants, including the mitochondrial adenine nucleotide translocase *sesB*^{1} and citrate synthase (*knock-down*, *kdn*) mutants (Fergestad et al., 2006), implying similar underlying pathological mechanisms. Both of the aforementioned mutants also exhibit the bang-sensitive behavior characteristic of *tko*^{25t}. Despite a wealth of studies on *Drosophila* bang-sensitive mutants, the precise molecular mechanisms behind this phenotype remain unknown and are probably heterogeneous. Insufficient supply of ATP to support normal neuromuscular function has been proposed as one of the possible underlying pathogenic mechanisms in all three mutants since all of them suffer from a variable degree of ATP deficiency (Fergestad et al., 2006). In neurons, ATP is particularly crucial for the maintenance of ionic gradients over cell membranes (Beal et al. 1993; Attwell & Laughlin 2001). This is in agreement with the phenotype of several *Drosophila* ion-channel mutants, such as the Na+/K+ ATPase alpha-subunit (*Atp*α) and the Na(+) channel gain-of-function *para* mutants, which exhibit bang sensitivity as well

(Fergestad et al., 2006; Howlett et al., 2013). Nevertheless, the fact that we found no signs of age-dependent deterioration associated with the bang sensitivity (II), strongly implied that, in *tko*^{25t}, this phenotype is developmentally determined, rather than resulting from an acute ATP deficiency during adulthood.

As we have demonstrated in *Drosophila* and as has been documented in other organisms and context, OXPHOS deficiency can also result in metabolite build-up, most notably of that of pyruvate, lactate and TCA cycle intermediates, resulting from a block in the electron transport chain, which inhibits TCA cycle and the flux of pyruvate into mitochondria. The accumulating cytosolic pyruvate needs to be shunted into lactate in order to regenerate NAD^+ and maintain high glycolytic flux. Fluctuations of pyruvate and lactate homeostasis are thus directly linked to the cellular NAD^+/NADH equilibrium. Surprisingly, despite the elevated pyruvate and lactate in *tko*^{25t} larvae, we did not observe significant disturbance of this balance when comparing with wild-type larvae (**Fig. 10**). Yet, pyruvate and lactate themselves appear to be contribute to the metabolic crisis as both can partially phenocopy both *tko*^{25t} and the effect of high-sugar diet on the mutant larvae (III).

Whilst the NAD^+/NADH homeostasis in *tko*^{25t} remained superficially unaffected, another key redox metabolite, NADPH, was severely depleted in *tko*^{25t} larvae on the high-sugar medium (**Fig. 10**). NADPH is required primarily by biosynthetic reactions, such as fatty acid synthesis and, importantly, for ROS detoxification, providing hints of the processes possibly handicapping development of *tko*^{25t} mutant larvae. While the shortage of ATP, NADPH, other metabolites or macromolecules might underlie the developmental delay in *tko*^{25t}, the growth inhibition must nevertheless be carefully regulated to provide a means of completing development in the presence of elevated levels of toxic compounds, such as pyruvate and lactate, allowing time for excretion or detoxification processes (*e.g.* lactate clearance). The metabolomics analysis also identified other metabolites, the levels of which were elevated in *tko*^{25t} larvae on HS and normalized on the ZS diet. These metabolites included *e.g.* ornithine, which has been shown to inhibit larval growth when administered through diet (Hinton, 1956), although we failed to reproduce these findings (III). Similar approach could naturally be employed to testing most of the metabolites, which showed depletion or accumulation in *tko*^{25t} larvae, particularly on the HS diet, but this was unfortunately not in the scope of this study.

One of the peculiar features of mitochondrial dysfunction is the often highly tissue-specific manner in which symptoms manifest. In the case of mtDNA mutations, this phenomenon is often explained with a drift in heteroplasmy levels and tissue-specific threshold for mitochondrial mutations (DiMauro, 2013). The tendency of muscle and nervous system to be the predominantly affected tissues in mitochondrial disorders, likely stems from the fact that these tissues are highly dependent on mitochondrial ATP synthesis, as well as coordinated fluxes of Ca^{2+} ions, a process in which mitochondria are considered to be involved in (Ylikallio & Suomalainen, 2012). Muscle and nervous system dysfunction is also heavily implicated in *tko*^{25t} as exemplified by the bang sensitivity and the down-regulation of multiple structural genes of the muscle in *tko*^{25t} larvae on HS, suggestive of a decrease in muscle biosynthesis (III). Intriguingly, the temperature sensitive expression of a wild-type copy of the *tko*-allele specifically in the gut, suggested that mitochondrial function in this tissue could also be a crucial determinant of the viability of the entire organism (III).

6.3.1 Protein homeostasis

The role of proteotoxic stress is becoming increasingly well appreciated in the pathogenesis of many metabolic disorders (Hutt, Powers, & Balch, 2009). In the context of mitochondrial dysfunction, particularly when involving defective mitochondrial protein synthesis, toxic accumulation of unfolded or damaged proteins may occur as a result of aberrant translation. Decreased mitochondrial protein synthesis capacity could also create an imbalance between mitochondrially and cytosolically translated proteins.

We did not have direct evidence of the impaired mitochondrial translation resulting in truncated, mutated or misfolded proteins. Neither did the transcriptomics data suggest induction of large-scale mitochondrial or ER unfolded protein response. Nevertheless, the *tko*^{25t} larvae exhibited prominent induction of a mitochondrial chaperone protein Hsp22 (**Fig. 12**). This small heat-shock protein has been shown to be induced *e.g.* by oxidative stress and during aging (Gruenewald et al., 2009; King & Tower, 1999) and we thus decided to test whether the mutant larvae would show differential sensitivity to the cytosolic protein synthesis inhibitor cycloheximide compared to wild-type. We hypothesized that if the defective mitochondrial translation resulted in a cytosolic-mitochondrial protein imbalance, inhibiting

cytosolic protein synthesis might relieve such stress conditions. To our surprise, the mutant larvae appeared to be unresponsive to inhibition of cytosolic protein synthesis, unlike wild-type controls, in which the CHX administration resulted in significant developmental delay (**Fig. 12**). One interpretation of this is that the *tko*^{25t} larvae already exhibit significant developmental delay, irrespective of the cause, which simply masks the effects of the CHX treatment. On the other hand, inhibition of translation initiation (see below) might be epistatic to that of elongation, and thus the effect of CHX to *tko*^{25t} could be minimal. Nevertheless, the phenomenon implies that cytosolic protein synthetic capacity is not growth limiting in larvae.

6.3.2 Growth signaling

OXPHOS dysfunction occurring in specific tissues and cell-types is very likely to have, not only systemic metabolic consequences, but also to affect growth regulation through systemic (endocrine) signaling. Since the developmental delay of the mutant larvae appears to reflect a coordinated inhibition of larval growth rather than a catastrophic failure in development processes in general, we attempted to identify markers of changes in the growth-regulatory signaling network in whole larval homogenates, accounting for the growth inhibition. Unsurprisingly, AMP-activated kinase activity was induced in *tko*^{25t} larvae on HS, as indicated by the increased phosphorylation at Thr172 (**Fig. 12**). AMPK activation accords with the significantly decreased ATP to AMP/ADP ratio resulting from ATP depletion. Besides its direct targets, such as the acetyl-CoA carboxylase, AMPK also interacts with other pathways, such as the TOR-signaling pathway (Hardie, 2014). We therefore tested specific targets of both of the TOR-signaling complexes. The TORC1 target, S6K exhibited decreased activation through phosphorylation in *tko*^{25t} larvae on both diets, consistent with the observed activation of AMPK and the known roles of S6K and TORC1 in promoting growth (**Fig. 12**). Quite remarkably, we also consistently observed a decrease in the total S6-kinase protein levels in HS-grown *tko*^{25t} larvae, suggestive of an additional, previously uncharacterized mechanism regulating its expression in mutant larvae, under the most stressful conditions. Finally, we analyzed the activation of TORC2-dependent regulation of the *Drosophila* Akt kinase. Based on TORC2-sensitive phosphorylation at Ser505, Akt activity was slightly higher in wild-type larvae, again consistent with the higher larval growth rate (**Fig. 12**). Akt phosphorylation at this particular serine is also sensitive to insulin-Pi3K-signaling, at least in *Drosophila* (Parisi et al., 2011),

implying that this growth/metabolic signaling pathway is modestly affected in *tko*^{25t} as well. Consistent with this finding, we found Thor (4E-BP), a transcriptional target of *FoxO*, to be up-regulated in *tko*^{25t} larvae (III). *FoxO* itself is inactivated by Akt signaling, by restricting its subcellular localization to the cytosol (Teleman et al., 2008).

Since the analysis was performed in whole body lysates, we do not know whether growth signaling is differentially affected in the various tissues of the developing larvae. However, it is tempting to hypothesize that mitochondrial dysfunction, specifically in cells in the brain responsible for the secretion of insulin-like peptides, or the neuroendocrine organ, prothoracic gland, could significantly inhibit growth systemically. For example, AMPK activation in the silkworm *Bombyx mori* prothoracic gland has been shown to inhibit the secretion of the molting hormone ecdysone (Gu et al., 2013). Furthermore, developmental delay resulting from nutrient deprivation can be fully compensated by activating TOR solely in the *Drosophila* prothoracic gland (Layalle, Arquier, & Léopold, 2008).

6.4 Excess dietary sugar is selectively developmentally toxic to *tko*^{25t} mutants (III)

Irrespective of the underlying molecular and physiological mechanisms, our findings indicate that, in the *tko*^{25t} model, OXPHOS dysfunction impairs the metabolic plasticity that wild-type flies exhibit with respect to being able to adapt to diets of variable composition. In the dietary experiments, diets with highly variable sugar, fat, protein and calorie content supported normal development of wild-type flies. *tko*^{25t} flies, in contrast, showed dose-dependent sensitivity to increasing concentrations of dietary sugar, while being insensitive to alterations in relative dietary fat and protein content (**Fig. 8**).

Very high concentrations of dietary sugar have been shown to inhibit larval growth in wild-type *Drosophila* larvae as well (Havula et al., 2013; Na et al., 2013). However, it should be noted that the concentrations of dietary sugar used in this study were well tolerated by wild-type flies, resulting in no apparent developmental abnormalities. In this respect. *tko*^{25t} and its aggravated sugar sensitivity provides a paradigm for understanding the underlying genetic and metabolic reasons for sugar

tolerance. OXPHOS deficiency may be just one of many physiological conditions which could subject organisms to such carbohydrate-induced growth retardation. However, the role of mitochondria in nutrient metabolism and growth is undeniably central.

In addition to providing insight into the pathogenic mechanisms of sugar toxicity, the observation that *tko*^{25t} mutants develop faster and exhibit less severe bang sensitivity on low-sugar diet implies that dietary modulation of the disease phenotype provides a means of investigating how the respiratory chain deficiency impacts growth rate. We thus focused on investigating the metabolic and physiological changes occurring with respect to genotype, *i.e.* wild-type versus mutant larvae, but also their different responses to dietary sugar.

Through a mechanism still unclear to us, the ZS diet resulted in a dramatic recovery of steady-state ATP-levels in *tko*^{25t} larvae. We did not identify a single clear explanation for the dramatic rescue of the ATP deficiency, such as induction of mitochondrial biogenesis, from the pattern of transcriptional changes. On the contrary: mitochondrial transcripts were similarly up- and down-regulated in mutant larvae on both diets, while transcripts of respiratory chain complex subunits, TCA cycle and glycolytic enzymes were systematically down-regulated in *tko*^{25t} larvae (**Appendix II**). Thus, a complex network of metabolic changes is more likely to underlie the adaptive advantage of the zero-sugar diet, as discussed below.

Correlating with the rescue of the ATP deficiency of *tko*^{25t} larvae by low dietary sugar, the depleted NADPH-levels were significantly elevated on the ZS diet (**Fig. 10**). Despite the hypothetically reduced flux through the NADPH-regenerating pentose phosphate pathway, indicated by the decreased maximal activity of G6PDH and 6PGDH (**Fig. 11**), the lower concentrations of lactate and pyruvate on the ZS diet might eventually result in a higher total rate of NADPH-production because of decreased inhibition of malic enzyme (**Fig. 11**). Furthermore, the ability to protect cells from the toxic effects of excess sugar, such as spontaneous reactions with the lysine residues of proteins via the Maillard reaction (Grandhee & Monnier, 1991), is likely to be partially dependent on the availability of NADPH. We observed high levels of gluconate, the inert product of glucose dehydrogenase catalyzed glucose oxidation (Gld) (Cavener & MacIntyre, 1983), in larvae reared on the high-sugar

diet (**Fig. 10**). The exact identity of the primary electron acceptor of glucose dehydrogenase is unknown, but its regeneration in the cytosol is likely to depend on the NADPH-consuming cytochrome P450 system (Ferri, Kojima, & Sode, 2011).

6.5 Metabolic reprogramming provides means of adapting to mitochondrial dysfunction (III)

Understanding the metabolic requirements of larval development is pivotal in interpreting the physiological rationale of the metabolic changes exhibited by the *tko*^{25t} larvae. During mid-embryogenesis, developing *Drosophila* initiate the larval metabolic program, which relies heavily on aerobic glycolysis to support the exponential increase in biomass throughout larval development (Tennessen et al., 2014). This shift in metabolism resembles the classic Warburg effect (Vander Heiden, Cantley, & Thompson, 2009) and is accordingly accompanied by the induction of expression of glycolytic enzymes, mediated in *Drosophila* by the estrogen-related receptor (*ERR*) (Diaz-Ruiz, Rigoulet, & Devin, 2011; Tennessen et al., 2011). Compared to early stage embryos, towards the end of embryogenesis, several metabolites, such as glycerol-3-phosphate (G3P), β-alanine, serine, urate and the TCA cycle intermediates citrate, isocitrate, α-ketoglutarate and succinate exhibit significant accumulation, while others, such as glutamate and aspartate, become depleted (III**, Fig. 10**). Many of these metabolic changes, *e.g.* the increase in G3P, urate and citrate, and the decrease in glutamate and aspartate levels, are identical to the metabolic changes observed in *tko*^{25t} larvae compared with wild-type, towards the end of larval development. This implies that the metabolic changes necessary to adapt to mitochondrial dysfunction are at least partially overlapping with those required to meet the metabolic requirements of the developing larva, or growth dependent on aerobic glycolysis, in general. Quite fittingly, Otto Warburg initially interpreted his observations of the increased glycolytic flux in cancer cells as a sign of mitochondrial respiratory impairment (Vander Heiden et al., 2009; Warburg, 1956).

The metabolic switch in mid-embryogenic larvae includes the coordinate up-regulation of glycolytic enzymes and respiratory chain components, suggesting that despite the canonical view of glycolytic metabolism being crucial for ATP production while TCA cycle is largely responsible for producing precursors for fatty

acid and amino acid biosynthesis, the respiratory chain is nevertheless pivotal for this process in highly proliferative cells. This also provides another possible explanation for why the respiratory chain deficiency in *tko*^{25t} might impair development: the mutant larvae may be starving for macromolecules rather than the energy to synthesize them. Under such conditions, low-sugar diet might be beneficial since this condition appears to naturally increase the ingestion of fatty acids (as discussed below), perhaps compensating for the inability to sufficiently produce them *de novo* in *tko*^{25t}. In accordance with this hypothesis, we observed higher steady-state levels of ATP and NADPH (both of which are consumed by biosynthetic processes), in both genotypes on the ZS diet.

In addition to inhibition of carbohydrate metabolism, the transcriptional and metabolic profiling of mutant and wild-type larvae also provides evidence for a switch from glucose metabolism to the use of fatty acids in mutant larvae, particularly on the high-sugar diet. First, lipolytic enzymes were systematically induced in *tko*^{25t} larvae while gut-specific sugar transporters were concomitantly down-regulated (**Appendix II,** III). Secondly, medium chain fatty acids (octanoate, decanoate and dodecanoate) were either detected at very low level, or completely depleted in HS reared *tko*^{25t} larvae, suggesting that either their catabolism is considerably elevated, or that their availability is limited (**Appendix I,** III). Since the ZS diet also appears to induce the expression of lipolytic enzymes, the availability of FAs is likely to be higher on the low-sugar diet, supporting the hypothesis of increased fatty acid catabolism.

In apparent contradiction of this hypothesis, the *tko*^{25t} mutants also exhibit elevated triglyceride levels on both diets (**Fig. 10**). This puzzling finding could be explained by multiple physiological reasons. First and foremost, a block in electron transport chain will inevitably result in increased acetyl-CoA and citrate concentrations, as many TCA cycle enzymes become inhibited by the elevated NADH. Both, the excess citrate and acetyl-CoA are transported into the cytosol, where they are converted to malonyl-CoA, the substrate for *de novo* fatty acid synthesis, but also an inhibitor of CPTI, and subsequently mitochondrial FA catabolism (Foster, 2012). The CPTI inhibition promotes fatty acid esterification and thus prevents the futile oxidation of newly synthesized fatty acids. In agreement with the TCA cycle and ETC inhibition, *tko*^{25t} larvae from both diets, exhibit increased levels of citrate and the acetylated form of carnitine (o-acetylcarnitine), which can act as a acetyl-group sink under such pathological conditions (Lindeboom et al., 2014). All of the

metabolic transformations described above can promote lipogenesis by elevating the cytosolic acetyl-CoA. Furthermore, the significant rise in the glycerol-3-phosphate levels in the mutant larvae can also contribute to the increased lipogenesis, a process, which has been shown to protect *Drosophila* from the deleterious effects of excess dietary sugar (Musselman et al., 2013). G3P is generated through multiple pathways: via phosphorylation of glycerol (catalyzed by glycerol kinase) originating from TAG lipolysis, or via glyceroneogenesis from *e.g.* pyruvate and lactate. G3P also lies in a crucial intersection between different metabolic processes: in addition to the aforementioned reactions, G3P is an intermediate of the α-glycerophosphate cycle, an interconversion between the glycolytic intermediate dihydroxyacetone phosphate (DHAP) and G3P, catalyzed by the mitochondrial and cytosolic glycerol-3-phosphate dehydrogenases. These two dehydrogenases also transport electrons from the cytosolic NADH pool to the mitochondrial ubiquinone. In the case of OXPHOS deficiency, the cytosolic NADH/NAD^+ ratio is often high and the ubiquinone pool overreduced. Under these circumstances, G3P may accumulate since the conversion of G3P to DHAP, is coupled with the reduction of NAD^+ to NADH and would thus be unfavorable.

Finally, despite the fact that changes in levels of amino acids and the expression of proteolytic enzymes appear to be superficially inconsistent, the potential impact of alterations in protein and amino acid metabolism to the tko^{25t} metabolic phenotype cannot be overlooked. We observed a very high increase in urate levels in tko^{25t} larvae reared on both diets. Terrestrial insects such as *Drosophila*, are generally ureotelic organisms*, i.e.* excrete uric acid as the primary nitrogenous waste product (Singer, 2003). The increase in urate would thus imply increased amino acid deamination, and possibly energy production reliant on anaplerotic flux of carbon to the TCA cycle. In addition, urate is the end product of purine metabolism. Purine metabolism, like amino acid catabolism, can provide the TCA cycle with carbon skeletons and, furthermore, the conversion of purines to uric acid can maintain a presumably ancient and quite inefficient form of ATP production, which nonetheless, has been proposed to be of significance in *e.g.* skeletal muscle during exercise (Lowenstein & Goodman, 1978).

What then, is finally the outcome of all of the metabolic transformations for tko^{25t} during development? Stochiometrically, a switch from sugars to fatty acid oxidation results theoretically in proportionally more electrons being transferred to ubiquinone through complex II and the electron transferring flavoprotein dehydrogenase, than

through complex I. This could hypothetically relieve the electron transfer activity of CI, which has been proposed to be the major site of electron leak ROS production in mitochondria (see Review of literature). Complex I also carries the most mitochondrially encoded subunits of all the respiratory chain complexes, and is perhaps the most severely affected respiratory chain complex in *tko*^{25t} larvae (Toivonen et al., 2001). Although we did not assay ROS-production directly *in vitro* in larvae, but elevated methionine sulfoxide (Stadtman, Moskovitz, & Levine, 2003) in *tko*^{25t} larvae indicated increased ROS derived damage. Notably, this oxidative protein damage marker is detected at relatively high levels only in *tko*^{25t} on HS diet, and rescued to wild-type levels by the ZS diet (**Appendix I**). It is also compelling to draw parallels between the growth impairment caused by the OXPHOS deficiency in *tko*^{25t} larvae and the anti-tumorigenic effect of biguanides (such as metformin and phenformin), which is presumably achieved by inhibiting complex I (Evans et al., 2005; Shackelford et al., 2013). Unfortunately, as in the case of *tko*^{25t}, the exact molecular mechanisms of the biguanide-induced growth inhibition are unknown, but are likely not limited to disruption of bioenergetics (Andrzejewski et al., 2014; Wheaton et al., 2014). Nevertheless, the fact that understanding how the delicate balance between the biosynthetic and bioenergetic processes is achieved in proliferating cells, is currently of utmost interest in the field of cancer research, will also inevitably benefit mitochondrial research as it will provide clues on how we could address the numerous metabolic perturbations caused by mitochondrial dysfunction. Our study highlights the potentially critical role of sufficient NADPH regeneration during growth and development, and the fact, that this process could be compromised by OXPHOS deficiency. Maintaining a steady supply of ATP and a stable NADH/NAD^+ ratio, while ensuring the production of biosynthetic precursor molecules and limiting ROS-production are widely accepted as perhaps the most central requirements for cell viability, growth and proliferation, but what tends to get overlooked is the fact that NADPH is the currency at the expense of which many of the relevant processes are operating, and that the shortage of NADPH could constrain growth equally well as *e.g.* that of ATP.

7. CONCLUSIONS

We have previously shown that ectopically expressed copies of the hypomorphic *tko*^{25t} allele fail to rescue the mutant phenotype, but a partial phenotypic suppression can be achieved by successive inbreeding of the mutant flies (Toivonen et al., 2001; Toivonen et al., 2003). In the present work, we successfully reproduced the phenotypic rescue by inbreeding *tko*^{25t} flies, and generated three *Weeble* suppressor lines, all of which exhibited near full reversal of the mutant phenotype. All three *Weeble* lines carried a duplication of a segment of the X-chromosome, which in all cases contained the *tko*^{25t} allele itself. We further validated that the duplication of another mitoribosomal gene (*mRpL14*) within the amplified interval, did not contribute to the phenotypic rescue. It thus seems very likely that the increased copy number of the *tko*^{25t} allele alone is sufficient for the near full rescue of the phenotype, but that the natural chromosomal milieu is required to coordinate the elevated expression to a correct tissue or developmental stage.

We also analyzed the ability of two alternative, single subunit respiratory chain enzymes (AOX and Ndi1), to compensate the OXPHOS deficiency in *tko*^{25t}. AOX expression did not to improve the gross mutant phenotype while ubiquitous expression of Ndi1 in the mutant background proved highly deleterious. The fact that AOX failed to compensate the *tko*^{25t} phenotype, superficially implied that the residual activity of complexes III and IV was sufficient to support adequate respiratory chain activity in the mutant flies. This further suggests that complex I deficiency might largely underlie the phenotype in *tko*^{25t}. Yet, rather than ameliorating the phenotype, Ndi1 expression, alone or in combination with AOX, caused lethality in *tko*^{25t} flies. This strongly implies that the residual proton-pumping activity of the endogenous complex I remained vital for *tko*^{25t}, and Ndi1 as a non-proton translocating enzyme attenuated the NADH-driven generation of the proton gradient. On the other hand, we did not observe a drop in steady-state ATP levels or elevation in ROS production when Ndi1 was expressed in the mutant background, suggesting that rather than a mere OXPHOS deficiency, a more complex metabolic disturbance might underlie the *tko*^{25t} phenotype or that crucial

developmental stage or tissue specific phenomena are being ignored by performing all of the experiments in whole tissue homogenates.

In support of the metabolic crisis hypothesis, the metabolic and transcriptional characterization of *tko*^{25t} larvae revealed significant changes in core cellular metabolism. More precisely, mitochondrial dysfunction triggers a large-scale metabolic reprogramming in *tko*^{25t} larvae, suggestive of intolerance to dietary sugar. This was indicated by the systematic induction of genes involved in dietary lipid metabolism, namely gut-specific triglyceride lipases and phospholipases, and the concomitant down-regulation of sugar metabolism, implying a shift in fuel preference from sugars to fats and fatty acids. But despite the apparent induction of fat catabolism, the mutant larvae still accumulated more triglycerides than wild-type controls. This was potentially due to the impaired mitochondrial substrate oxidation resulting from diminished OXPHOS capacity. Indicative of this, the mutant larvae also exhibited elevated levels of citrate, acetyl-L-carnitine and glycerol-3-phosphate associated with transcriptional down-regulation of the components of the glycerophosphate shuttle, all of which can promote *de novo* lipogenesis by providing it with precursors.

Consistent with the metabolic re-programming, the mutant larvae responded favourably to low dietary sugar content. Low-sugar diet nearly fully suppressed the developmental delay exhibited by *tko*^{25t} larvae, irrespective of the dietary fat and protein content, implying that dietary glucose and sucrose or their metabolism, or the products of their metabolism are developmentally toxic to mutant larvae. Although this study did not reveal the exact cause of this sugar toxicity, the careful analysis of mutant larvae reared on both "favourable and unfavourable" diet (ZS and HS, respectively) provided hints of possible mechanisms. For example, excess production of pyruvate (and concomitantly of that of lactate) by glycolytic breakdown of glucose and fructose might overburden both the maintenance of cellular redox balance (NAD+/NADH ratio) and lactate clearance, under conditions in which both are already operating at, or near maximum capacity due to the OXPHOS dysfunction and the high dependence on aerobic glycolysis during larval growth (Tennessen et al., 2014). Pyruvate or lactate, both of which accumulated in *tko*^{25t} larvae, showed toxicity when administered via diet to either wild-type or mutant larvae. Irrespective of the mechanism, low-sugar diet corrected several crucial physiological parameters in *tko*^{25t} larvae, such as pyruvate overload and severe ATP and NADPH deficiencies.

Altogether, our findings raised the intriguing question why is it necessary for the *tko*^{25t} flies to deploy a large scale metabolic response in order to adapt to the disturbances of mitochondrial homeostasis while a mere increase in mitochondrial translational capacity would appear sufficient to compensate for the underlying molecular defect. One possible explanation is that many of the processes required for the maintenance of mitochondrial function are coordinately regulated, and correcting for distinct imbalances between different aspects of mitochondrial metabolic homeostasis might thus be difficult or impossible. Understanding the reasons underlying this phenomenon is of particular interest with regards to mitochondrial disease treatment since some of the potential novel therapeutic methods are based on inducing large-scale mitochondrial biogenesis (*e.g.* via PGC-1a activation) rather than targeting specific imbalances potentially contributing to the disease pathogenesis. Based on our findings with *tko*^{25t}, such approaches might thus not be universally applicable in mitochondrial disorders. Furthermore, different forms of dietary intervention carry significant potential as exemplified by *tko*^{25t} and other mitochondrial disease models, yet again, understanding the disease etiology remains crucial in order to avoid unexpected complications from drastic changes in diet. Dietary sugar for example, provides an "easily accessible" source of energy, which can be indispensable for some patients suffering from deficient supply of ATP to cells and tissues, but when certain mitochondrial functions are impaired, its metabolism may have toxic effects. This also underlines the need for more research on the interactions between the different dietary components and the various mitochondrial defects.

Acknowledgements

The work presented in this thesis was carried out in the Mitochondrial Gene Expression and Disease group at the Institute of Biosciences and Medical Technology (BioMediTech), University of Tampere. The research was supported by the Academy of Finland, Tampere University Hospital Medical Research Fund, the Sigrid Juselius Foundation and EU. I wish to express my gratitude towards the members of my thesis committee, Professors Anu Wartiovaara and Kevin O'Dell who've known and supported me ever since my undergraduate years. Likewise, I wish to express my deepest gratitude for the external reviewers of my thesis, Dr. Aurelio Teleman and Dr. Orian Shirihai, who both kindly accommodated my very thigh schedule to that of theirs and provided me with valuable comments and criticism on my thesis, and took the time to share their own ideas on many of the topics addressed in this study. I also wish to thank Professor Aleksandra Filipovska for accepting to act as the opponent in the public defense of this dissertation.

I'll be forever grateful for Professor Howy Jacobs, not just for his scientific supervision through my undergraduate and graduate studies, but even more so for being a truly compassionate, supportive and inspirational human being throughout sometimes difficult times. You also manage to bring a fresh breath of openness and idealism to a world where scientific brilliance is too often accompanied by cynicism and self-centeredness. This spirit has also helped to make Howylab such a unique environment, a place where all new ideas and opinions are equally welcome and valuable, irrespective of whether they are presented by an undergraduate student or a senior scientist.

I wish to thank all of my co-authors and our collaborators, with a special thanks to all of the students and civilian servants who've helped me enormously over the past several years. Eric, Alberto, Giuseppe, Janne, Gertjan and Priit – your experience and expertise have been pivotal in overcoming many of the sometimes agonizing challenges of my work and you've truly helped me grow in all aspects of this profession. Outi, Tea and Merja – I owe you my deepest gratitude for your tireless efforts to make life easier for everybody else. You rarely get the acknowledgement you'd truly deserve. Most of all I wish to thank the past and current members of Howylab for creating such a family-like atmosphere, and a place of work which has

always been equally welcoming for a young undergraduate and often times tired and grumpy graduate student (both referring to yours truly). I'm particularly thankful for Janne and Rimmy, the early team *tko*, for taking me under their wings as a first year undergraduate (and introducing me to the O'C's pub quiz), and Jack, my associate in crime the last few years, for never being too busy for my endless rants in the lab.

Above all, I wish to express my gratitude to my family and friends who've been there to support me in every imaginable way throughout this process, particularly my parents Irja and Esa, who've never questioned my choices in life, irrespective of how irrational they might have seemed. You've also taught me the resilience and tenacity to overcome all obstacles and reach any goal imaginable. Mother – I will always cherish the infinite wisdom of the people of Teisko: "It's just life not paradise", and use it as a strength of character. Father – you were always so proud of everything I did, I wish you could have been here to see this one long chapter in my life to come to its end. Antti and Sofia – you often get to see us at our worst, tired and exhausted, but always manage to bring joy to our lives. I will also always remain grateful for my parents-in-law, Seija and Ari, who've become much more than just family to me. I hope I can one day repay the kindness and unconditional support I, and the whole family have received from you.

Finally, I wish to express my most heartfelt gratitude to my wife Kia who has been by my side through every single day of this journey. You mean so much more to me than you could ever possible imagine! Silja and Samuel – you bring so much joy to our lives and help to keep things in perspective. Hopefully, one day you will understand why mom and dad had to go take care of fruit flies all those mornings, evenings and weekends. It wasn't just to get money for diapers.

References

Acín-Pérez, R., Bayona-Bafaluy, M. P., Fernández-Silva, P., Moreno-Loshuertos, R., Pérez-Martos, A., Bruno, C., … Enríquez, J. A. (2004). Respiratory complex III is required to maintain complex I in mammalian mitochondria. *Molecular Cell*, *13*(6), 805–15.

Acín-Pérez, R., Fernández-Silva, P., Peleato, M. L., Pérez-Martos, A., & Enriquez, J. A. (2008). Respiratory active mitochondrial supercomplexes. *Molecular Cell*, *32*(4), 529–39. http://doi.org/10.1016/j.molcel.2008.10.021

Ahola-Erkkilä, S., Carroll, C. J., Peltola-Mjösund, K., Tulkki, V., Mattila, I., Seppänen-Laakso, T., … Suomalainen, A. (2010). Ketogenic diet slows down mitochondrial myopathy progression in mice. *Human Molecular Genetics*, *19*(10), 1974–84. http://doi.org/10.1093/hmg/ddq076

Akabane, S., Ueda, T., Nierhaus, K. H., & Takeuchi, N. (2014). Ribosome rescue and translation termination at non-standard stop codons by ICT1 in mammalian mitochondria. *PLoS Genetics*, *10*(9), e1004616. http://doi.org/10.1371/journal.pgen.1004616

Albert, V., & Hall, M. N. (2014). mTOR signaling in cellular and organismal energetics. *Current Opinion in Cell Biology*, *33C*, 55–66. http://doi.org/10.1016/j.ceb.2014.12.001

Alessi, D. R., James, S. R., Downes, C. P., Holmes, A. B., Gaffney, P. R., Reese, C. B., & Cohen, P. (1997). Characterization of a 3-phosphoinositide-dependent protein kinase which phosphorylates and activates protein kinase Balpha. *Current Biology : CB*, *7*(4), 261–9.

Alexeyev, M., Shokolenko, I., Wilson, G., & LeDoux, S. (2013). The maintenance of mitochondrial DNA integrity--critical analysis and update. *Cold Spring Harbor Perspectives in Biology*, *5*(5), a012641. http://doi.org/10.1101/cshperspect.a012641

Anderson, S., Bankier, A. T., Barrell, B. G., de Bruijn, M. H., Coulson, A. R., Drouin, J., … Young, I. G. (1981). Sequence and organization of the human mitochondrial genome. *Nature*, *290*(5806), 457–65.

Andrzejewski, S., Gravel, S.-P., Pollak, M., & St-Pierre, J. (2014). Metformin directly acts on mitochondria to alter cellular bioenergetics. *Cancer & Metabolism*, *2*, 12. http://doi.org/10.1186/2049-3002-2-12

Antonicka, H., Ostergaard, E., Sasarman, F., Weraarpachai, W., Wibrand, F., Pedersen, A. M. B., … Shoubridge, E. A. (2010). Mutations in C12orf65 in

patients with encephalomyopathy and a mitochondrial translation defect. *American Journal of Human Genetics*, *87*(1), 115–22. http://doi.org/10.1016/j.ajhg.2010.06.004

Antonicka, H., Sasarman, F., Nishimura, T., Paupe, V., & Shoubridge, E. A. (2013). The mitochondrial RNA-binding protein GRSF1 localizes to RNA granules and is required for posttranscriptional mitochondrial gene expression. *Cell Metabolism*, *17*(3), 386–98. http://doi.org/10.1016/j.cmet.2013.02.006

Arruda, A. P., Pers, B. M., Parlakgül, G., Güney, E., Inouye, K., & Hotamisligil, G. S. (2014). Chronic enrichment of hepatic endoplasmic reticulum–mitochondria contact leads to mitochondrial dysfunction in obesity. *Nature Medicine*, *advance on*. http://doi.org/10.1038/nm.3735

Attwell, D., & Laughlin, S. B. (2001). An energy budget for signaling in the grey matter of the brain. *Journal of Cerebral Blood Flow and Metabolism : Official Journal of the International Society of Cerebral Blood Flow and Metabolism*, *21*(10), 1133–45. http://doi.org/10.1097/00004647-200110000-00001

Bai, H., Kang, P., & Tatar, M. (2012). Drosophila insulin-like peptide-6 (dilp6) expression from fat body extends lifespan and represses secretion of Drosophila insulin-like peptide-2 from the brain. *Aging Cell*, *11*(6), 978–85. http://doi.org/10.1111/acel.12000

Bai, Y., Hájek, P., Chomyn, A., Chan, E., Seo, B. B., Matsuno-Yagi, A., … Attardi, G. (2001). Lack of complex I activity in human cells carrying a mutation in MtDNA-encoded ND4 subunit is corrected by the Saccharomyces cerevisiae NADH-quinone oxidoreductase (NDI1) gene. *The Journal of Biological Chemistry*, *276*(42), 38808–13. http://doi.org/10.1074/jbc.M106363200

Balaban, R. S., Nemoto, S., & Finkel, T. (2005). Mitochondria, oxidants, and aging. *Cell*, *120*(4), 483–95. http://doi.org/10.1016/j.cell.2005.02.001

Bassett, A. R., & Liu, J.-L. (2014). CRISPR/Cas9 and genome editing in Drosophila. *Journal of Genetics and Genomics = Yi Chuan Xue Bao*, *41*(1), 7–19. http://doi.org/10.1016/j.jgg.2013.12.004

Beal, M. F., Hyman, B. T., & Koroshetz, W. (1993). Do defects in mitochondrial energy metabolism underlie the pathology of neurodegenerative diseases? *Trends in Neurosciences*, *16*(4), 125–31.

Becker, T., Gebert, M., Pfanner, N., & van der Laan, M. (2009). Biogenesis of mitochondrial membrane proteins. *Current Opinion in Cell Biology*, *21*(4), 484–93. http://doi.org/10.1016/j.ceb.2009.04.002

Bereiter-Hahn, J., & Vöth, M. (1994). Dynamics of mitochondria in living cells: shape changes, dislocations, fusion, and fission of mitochondria. *Microscopy Research and Technique*, *27*(3), 198–219. http://doi.org/10.1002/jemt.1070270303

Bernt, M., Braband, A., Schierwater, B., & Stadler, P. F. (2013). Genetic aspects of mitochondrial genome evolution. *Molecular Phylogenetics and Evolution*, *69*(2), 328–38. http://doi.org/10.1016/j.ympev.2012.10.020

Bianchi, C., Genova, M. L., Parenti Castelli, G., & Lenaz, G. (2004). The mitochondrial respiratory chain is partially organized in a supercomplex assembly: kinetic evidence using flux control analysis. *The Journal of Biological Chemistry*, *279*(35), 36562–9. http://doi.org/10.1074/jbc.M405135200

Bier, E. (2005). Drosophila, the golden bug, emerges as a tool for human genetics. *Nature Reviews. Genetics*, *6*(1), 9–23. http://doi.org/10.1038/nrg1503

Boczonadi, V., & Horvath, R. (2014). Mitochondria: impaired mitochondrial translation in human disease. *The International Journal of Biochemistry & Cell Biology*, *48*, 77–84. http://doi.org/10.1016/j.biocel.2013.12.011

Boelens, R., & Gualerzi, C. O. (2002). Structure and function of bacterial initiation factors. *Current Protein & Peptide Science*, *3*(1), 107–19.

Bogenhagen, D. F. (2009). Biochemical isolation of mtDNA nucleoids from animal cells. *Methods in Molecular Biology (Clifton, N.J.)*, *554*, 3–14. http://doi.org/10.1007/978-1-59745-521-3_1

Bogenhagen, D. F., Martin, D. W., & Koller, A. (2014). Initial steps in RNA processing and ribosome assembly occur at mitochondrial DNA nucleoids. *Cell Metabolism*, *19*(4), 618–29. http://doi.org/10.1016/j.cmet.2014.03.013

Bogenhagen, D. F., Wang, Y., Shen, E. L., & Kobayashi, R. (2003). Protein components of mitochondrial DNA nucleoids in higher eukaryotes. *Molecular & Cellular Proteomics : MCP*, *2*(11), 1205–16. http://doi.org/10.1074/mcp.M300035-MCP200

Bonn, F., Tatsuta, T., Petrungaro, C., Riemer, J., & Langer, T. (2011). Presequence-dependent folding ensures MrpL32 processing by the m-AAA protease in mitochondria. *The EMBO Journal*, *30*(13), 2545–56. http://doi.org/10.1038/emboj.2011.169

Börner, G. V, Zeviani, M., Tiranti, V., Carrara, F., Hoffmann, S., Gerbitz, K. D., … Pääbo, S. (2000). Decreased aminoacylation of mutant tRNAs in MELAS but not in MERRF patients. *Human Molecular Genetics*, *9*(4), 467–75.

Boyer, P. D. (1997). The ATP synthase--a splendid molecular machine. *Annual Review of Biochemistry*, *66*, 717–49. http://doi.org/10.1146/annurev.biochem.66.1.717

Brand, A. H., & Perrimon, N. (1993). Targeted gene expression as a means of altering cell fates and generating dominant phenotypes. *Development (Cambridge, England)*, *118*(2), 401–15.

Brock, S., Szkaradkiewicz, K., & Sprinzl, M. (1998). Initiation factors of protein biosynthesis in bacteria and their structural relationship to elongation and termination factors. *Molecular Microbiology*, *29*(2), 409–17.

Brogiolo, W., Stocker, H., Ikeya, T., Rintelen, F., Fernandez, R., & Hafen, E. (2001). An evolutionarily conserved function of the Drosophila insulin receptor and insulin-like peptides in growth control. *Current Biology : CB*, *11*(4), 213–21.

Brown, G. C., & Borutaite, V. (2012). There is no evidence that mitochondria are the main source of reactive oxygen species in mammalian cells. *Mitochondrion*, *12*(1), 1–4. http://doi.org/10.1016/j.mito.2011.02.001

Brown, T. A., Tkachuk, A. N., Shtengel, G., Kopek, B. G., Bogenhagen, D. F., Hess, H. F., & Clayton, D. A. (2011). Superresolution fluorescence imaging of mitochondrial nucleoids reveals their spatial range, limits, and membrane interaction. *Molecular and Cellular Biology*, *31*(24), 4994–5010. http://doi.org/10.1128/MCB.05694-11

Brunet, A., Bonni, A., Zigmond, M. J., Lin, M. Z., Juo, P., Hu, L. S., … Greenberg, M. E. (1999). Akt promotes cell survival by phosphorylating and inhibiting a Forkhead transcription factor. *Cell*, *96*(6), 857–68.

Brzezniak, L. K., Bijata, M., Szczesny, R. J., & Stepien, P. P. Involvement of human ELAC2 gene product in 3' end processing of mitochondrial tRNAs. *RNA Biology*, *8*(4), 616–26. http://doi.org/10.4161/rna.8.4.15393

Bullerwell, C. E., & Gray, M. W. (2004). Evolution of the mitochondrial genome: protist connections to animals, fungi and plants. *Current Opinion in Microbiology*, *7*(5), 528–34. http://doi.org/10.1016/j.mib.2004.08.008

Burman, J. L., Itsara, L. S., Kayser, E.-B., Suthammarak, W., Wang, A. M., Kaeberlein, M., … Pallanck, L. J. (2014). A Drosophila model of mitochondrial disease caused by a complex I mutation that uncouples proton pumping from electron transfer. *Disease Models & Mechanisms*, *7*(10), 1165–74. http://doi.org/10.1242/dmm.015321

Buttgereit, F., & Brand, M. D. (1995). A hierarchy of ATP-consuming processes in mammalian cells. *The Biochemical Journal*, *312 (Pt 1*, 163–7.

Bykhovskaya, Y., Casas, K., Mengesha, E., Inbal, A., & Fischel-Ghodsian, N. (2004). Missense mutation in pseudouridine synthase 1 (PUS1) causes mitochondrial myopathy and sideroblastic anemia (MLASA). *American Journal of Human Genetics*, *74*(6), 1303–8. http://doi.org/10.1086/421530

Calvo, S., Jain, M., Xie, X., Sheth, S. A., Chang, B., Goldberger, O. A., … Mootha, V. K. (2006). Systematic identification of human mitochondrial disease genes through integrative genomics. *Nature Genetics*, *38*(5), 576–82. http://doi.org/10.1038/ng1776

Carroll, C. J., Isohanni, P., Pöyhönen, R., Euro, L., Richter, U., Brilhante, V., … Suomalainen, A. (2013). Whole-exome sequencing identifies a mutation in the mitochondrial ribosome protein MRPL44 to underlie mitochondrial infantile cardiomyopathy. *Journal of Medical Genetics*, *50*(3), 151–9. http://doi.org/10.1136/jmedgenet-2012-101375

Cavdar Koc, E., Burkhart, W., Blackburn, K., Moseley, A., & Spremulli, L. L. (2001). The small subunit of the mammalian mitochondrial ribosome. Identification of the full complement of ribosomal proteins present. *The Journal of Biological Chemistry*, *276*(22), 19363–74. http://doi.org/10.1074/jbc.M100727200

Cavener, D. R., & MacIntyre, R. J. (1983). Biphasic expression and function of glucose dehydrogenase in Drosophila melanogaster. *Proceedings of the National Academy of Sciences of the United States of America*, *80*(20), 6286–8.

Celniker, S. E., & Rubin, G. M. (2003). The Drosophila melanogaster genome. *Annual Review of Genomics and Human Genetics*, *4*, 89–117. http://doi.org/10.1146/annurev.genom.4.070802.110323

Cerveny, K. L., Tamura, Y., Zhang, Z., Jensen, R. E., & Sesaki, H. (2007). Regulation of mitochondrial fusion and division. *Trends in Cell Biology*, *17*(11), 563–9. http://doi.org/10.1016/j.tcb.2007.08.006

Chandel, N. S. (2014). Mitochondria and cancer. *Cancer & Metabolism*, *2*(1), 8. http://doi.org/10.1186/2049-3002-2-8

Chen, S., Oliveira, M. T., Sanz, A., Kemppainen, E., Fukuoh, A., Schlicht, B., … Jacobs, H. T. (2012). A cytoplasmic suppressor of a nuclear mutation affecting mitochondrial functions in Drosophila. *Genetics*, *192*(2), 483–93. http://doi.org/10.1534/genetics.112.143719

Chen, X., Prosser, R., Simonetti, S., Sadlock, J., Jagiello, G., & Schon, E. A. (1995). Rearranged mitochondrial genomes are present in human oocytes. *American Journal of Human Genetics*, *57*(2), 239–47.

Chinnery, P. F., & Hudson, G. (2013). Mitochondrial genetics. *British Medical Bulletin*, *106*(1), 135–59. http://doi.org/10.1093/bmb/ldt017

Cho, J., Hur, J. H., Graniel, J., Benzer, S., & Walker, D. W. (2012a). Expression of yeast NDI1 rescues a Drosophila complex I assembly defect. *PloS One*, *7*(11), e50644. http://doi.org/10.1371/journal.pone.0050644

Cho, J., Hur, J. H., Graniel, J., Benzer, S., & Walker, D. W. (2012b). Expression of yeast NDI1 rescues a Drosophila complex I assembly defect. *PloS One*, *7*(11), e50644. http://doi.org/10.1371/journal.pone.0050644

Clark, I. E., Dodson, M. W., Jiang, C., Cao, J. H., Huh, J. R., Seol, J. H., … Guo, M. (2006). Drosophila pink1 is required for mitochondrial function and interacts

genetically with parkin. *Nature*, *441*(7097), 1162–6. http://doi.org/10.1038/nature04779

Colombani, J., Andersen, D. S., & Léopold, P. (2012). Secreted peptide Dilp8 coordinates Drosophila tissue growth with developmental timing. *Science (New York, N.Y.)*, *336*(6081), 582–5. http://doi.org/10.1126/science.1216689

Colombani, J., Raisin, S., Pantalacci, S., Radimerski, T., Montagne, J., & Léopold, P. (2003). A Nutrient Sensor Mechanism Controls Drosophila Growth. *Cell*, *114*(6), 739–749. http://doi.org/10.1016/S0092-8674(03)00713-X

Copeland, W. C. Defects in mitochondrial DNA replication and human disease. *Critical Reviews in Biochemistry and Molecular Biology*, *47*(1), 64–74. http://doi.org/10.3109/10409238.2011.632763

Copeland, W. C., & Longley, M. J. (2014). Mitochondrial genome maintenance in health and disease. *DNA Repair*, *19*, 190–8. http://doi.org/10.1016/j.dnarep.2014.03.010

Cotney, J., & Shadel, G. S. (2006). Evidence for an early gene duplication event in the evolution of the mitochondrial transcription factor B family and maintenance of rRNA methyltransferase activity in human mtTFB1 and mtTFB2. *Journal of Molecular Evolution*, *63*(5), 707–17. http://doi.org/10.1007/s00239-006-0075-1

Dassa, E. P., Dufour, E., Gonçalves, S., Paupe, V., Hakkaart, G. A. J., Jacobs, H. T., & Rustin, P. (2009). Expression of the alternative oxidase complements cytochrome c oxidase deficiency in human cells. *EMBO Molecular Medicine*, *1*(1), 30–6. http://doi.org/10.1002/emmm.200900001

Detmer, S. A., & Chan, D. C. (2007). Functions and dysfunctions of mitochondrial dynamics. *Nature Reviews. Molecular Cell Biology*, *8*(11), 870–9. http://doi.org/10.1038/nrm2275

Diaz-Ruiz, R., Rigoulet, M., & Devin, A. (2011). The Warburg and Crabtree effects: On the origin of cancer cell energy metabolism and of yeast glucose repression. *Biochimica et Biophysica Acta*, *1807*(6), 568–76. http://doi.org/10.1016/j.bbabio.2010.08.010

DiMauro, S. (2013). Mitochondrial DNA mutation load: chance or destiny? *JAMA Neurology*, *70*(12), 1484–5. http://doi.org/10.1001/jamaneurol.2013.4401

Dudek, J., Rehling, P., & van der Laan, M. (2013). Mitochondrial protein import: common principles and physiological networks. *Biochimica et Biophysica Acta*, *1833*(2), 274–85. http://doi.org/10.1016/j.bbamcr.2012.05.028

Dudkina, N. V, Kudryashev, M., Stahlberg, H., & Boekema, E. J. (2011). Interaction of complexes I, III, and IV within the bovine respirasome by single particle cryoelectron tomography. *Proceedings of the National Academy of*

Sciences of the United States of America, *108*(37), 15196–200. http://doi.org/10.1073/pnas.1107819108

El-Hattab, A. W., & Scaglia, F. (2013). Mitochondrial DNA depletion syndromes: review and updates of genetic basis, manifestations, and therapeutic options. *Neurotherapeutics : The Journal of the American Society for Experimental NeuroTherapeutics*, *10*(2), 186–98. http://doi.org/10.1007/s13311-013-0177-6

El-Khoury, R., Dufour, E., Rak, M., Ramanantsoa, N., Grandchamp, N., Csaba, Z., … Rustin, P. (2013). Alternative oxidase expression in the mouse enables bypassing cytochrome c oxidase blockade and limits mitochondrial ROS overproduction. *PLoS Genetics*, *9*(1), e1003182. http://doi.org/10.1371/journal.pgen.1003182

Elliott, D. A., & Brand, A. H. (2008). The GAL4 system : a versatile system for the expression of genes. *Methods in Molecular Biology (Clifton, N.J.)*, *420*, 79–95. http://doi.org/10.1007/978-1-59745-583-1_5

Engelman, J. A., Luo, J., & Cantley, L. C. (2006). The evolution of phosphatidylinositol 3-kinases as regulators of growth and metabolism. *Nature Reviews. Genetics*, *7*(8), 606–19. http://doi.org/10.1038/nrg1879

Evans, J. M. M., Donnelly, L. A., Emslie-Smith, A. M., Alessi, D. R., & Morris, A. D. (2005). Metformin and reduced risk of cancer in diabetic patients. *BMJ (Clinical Research Ed.)*, *330*(7503), 1304–5. http://doi.org/10.1136/bmj.38415.708634.F7

Falkenberg, M., Gaspari, M., Rantanen, A., Trifunovic, A., Larsson, N.-G., & Gustafsson, C. M. (2002). Mitochondrial transcription factors B1 and B2 activate transcription of human mtDNA. *Nature Genetics*, *31*(3), 289–94. http://doi.org/10.1038/ng909

Fergestad, T., Bostwick, B., & Ganetzky, B. (2006). Metabolic disruption in Drosophila bang-sensitive seizure mutants. *Genetics*, *173*(3), 1357–64. http://doi.org/10.1534/genetics.106.057463

Fernández-Ayala, D. J. M., Chen, S., Kemppainen, E., O'Dell, K. M. C., & Jacobs, H. T. (2010). Gene expression in a Drosophila model of mitochondrial disease. *PloS One*, *5*(1), e8549. http://doi.org/10.1371/journal.pone.0008549

Fernandez-Ayala, D. J. M., Sanz, A., Vartiainen, S., Kemppainen, K. K., Babusiak, M., Mustalahti, E., … Jacobs, H. T. (2009). Expression of the Ciona intestinalis alternative oxidase (AOX) in Drosophila complements defects in mitochondrial oxidative phosphorylation. *Cell Metabolism*, *9*(5), 449–60. http://doi.org/10.1016/j.cmet.2009.03.004

Ferri, S., Kojima, K., & Sode, K. (2011). Review of glucose oxidases and glucose dehydrogenases: a bird's eye view of glucose sensing enzymes. *Journal of Diabetes Science and Technology*, *5*(5), 1068–76.

Foster, D. W. (2012). Malonyl-CoA: the regulator of fatty acid synthesis and oxidation. *Journal of Clinical Investigation*, *122*(6), 1958–1959. http://doi.org/10.1172/JCI63967

Freyer, C., Cree, L. M., Mourier, A., Stewart, J. B., Koolmeister, C., Milenkovic, D., … Chinnery, P. F. (2012). Variation in germline mtDNA heteroplasmy is determined prenatally but modified during subsequent transmission. *Nature Genetics*, *44*(11), 1282–5. http://doi.org/10.1038/ng.2427

Galluzzi, L., Kepp, O., & Kroemer, G. (2012). Mitochondria: master regulators of danger signalling. *Nature Reviews. Molecular Cell Biology*, *13*(12), 780–8. http://doi.org/10.1038/nrm3479

Galmiche, L., Serre, V., Beinat, M., Assouline, Z., Lebre, A.-S., Chretien, D., … Rötig, A. (2011). Exome sequencing identifies MRPL3 mutation in mitochondrial cardiomyopathy. *Human Mutation*, *32*(11), 1225–31. http://doi.org/10.1002/humu.21562

Garelli, A., Gontijo, A. M., Miguela, V., Caparros, E., & Dominguez, M. (2012). Imaginal discs secrete insulin-like peptide 8 to mediate plasticity of growth and maturation. *Science (New York, N.Y.)*, *336*(6081), 579–82. http://doi.org/10.1126/science.1216735

Garrido, N., Griparic, L., Jokitalo, E., Wartiovaara, J., van der Bliek, A. M., & Spelbrink, J. N. (2003). Composition and dynamics of human mitochondrial nucleoids. *Molecular Biology of the Cell*, *14*(4), 1583–96. http://doi.org/10.1091/mbc.E02-07-0399

Geisler, S., Holmström, K. M., Skujat, D., Fiesel, F. C., Rothfuss, O. C., Kahle, P. J., & Springer, W. (2010). PINK1/Parkin-mediated mitophagy is dependent on VDAC1 and p62/SQSTM1. *Nature Cell Biology*, *12*(2), 119–31. http://doi.org/10.1038/ncb2012

Géminard, C., Rulifson, E. J., & Léopold, P. (2009). Remote control of insulin secretion by fat cells in Drosophila. *Cell Metabolism*, *10*(3), 199–207. http://doi.org/10.1016/j.cmet.2009.08.002

Gilbert, L. I., & Warren, J. T. (2005). A molecular genetic approach to the biosynthesis of the insect steroid molting hormone. *Vitamins and Hormones*, *73*, 31–57. http://doi.org/10.1016/S0083-6729(05)73002-8

Goard, C. A., & Schimmer, A. D. (2014). Mitochondrial matrix proteases as novel therapeutic targets in malignancy. *Oncogene*, *33*(21), 2690–9. http://doi.org/10.1038/onc.2013.228

González-Cabo, P., & Palau, F. (2013). Mitochondrial pathophysiology in Friedreich's ataxia. *Journal of Neurochemistry*, *126 Suppl* , 53–64. http://doi.org/10.1111/jnc.12303

Goto, Y., Nonaka, I., & Horai, S. (1990a). A mutation in the tRNA(Leu)(UUR) gene associated with the MELAS subgroup of mitochondrial encephalomyopathies. *Nature*, *348*(6302), 651–3. http://doi.org/10.1038/348651a0

Goto, Y., Nonaka, I., & Horai, S. (1990b). A mutation in the tRNA(Leu)(UUR) gene associated with the MELAS subgroup of mitochondrial encephalomyopathies. *Nature*, *348*(6302), 651–3. http://doi.org/10.1038/348651a0

Graham, B. H., Li, Z., Alesii, E. P., Versteken, P., Lee, C., Wang, J., & Craigen, W. J. (2010). Neurologic dysfunction and male infertility in Drosophila porin mutants: a new model for mitochondrial dysfunction and disease. *The Journal of Biological Chemistry*, *285*(15), 11143–53. http://doi.org/10.1074/jbc.M109.080317

Grandhee, S. K., & Monnier, V. M. (1991). Mechanism of formation of the Maillard protein cross-link pentosidine. Glucose, fructose, and ascorbate as pentosidine precursors. *The Journal of Biological Chemistry*, *266*(18), 11649–53.

Gray, L. R., Tompkins, S. C., & Taylor, E. B. (2014). Regulation of pyruvate metabolism and human disease. *Cellular and Molecular Life Sciences : CMLS*, *71*(14), 2577–604. http://doi.org/10.1007/s00018-013-1539-2

Gray, M. W. (2012). Mitochondrial evolution. *Cold Spring Harbor Perspectives in Biology*, *4*(9), a011403. http://doi.org/10.1101/cshperspect.a011403

Greaves, L. C., Reeve, A. K., Taylor, R. W., & Turnbull, D. M. (2012). Mitochondrial DNA and disease. *The Journal of Pathology*, *226*(2), 274–86. http://doi.org/10.1002/path.3028

Greene, J. C., Whitworth, A. J., Kuo, I., Andrews, L. A., Feany, M. B., & Pallanck, L. J. (2003). Mitochondrial pathology and apoptotic muscle degeneration in Drosophila parkin mutants. *Proceedings of the National Academy of Sciences of the United States of America*, *100*(7), 4078–83. http://doi.org/10.1073/pnas.0737556100

Grönke, S., Clarke, D.-F., Broughton, S., Andrews, T. D., & Partridge, L. (2010). Molecular evolution and functional characterization of Drosophila insulin-like peptides. *PLoS Genetics*, *6*(2), e1000857. http://doi.org/10.1371/journal.pgen.1000857

Gruenewald, C., Botella, J. A., Bayersdorfer, F., Navarro, J. A., & Schneuwly, S. (2009). Hyperoxia-induced neurodegeneration as a tool to identify neuroprotective genes in Drosophila melanogaster. *Free Radical Biology & Medicine*, *46*(12), 1668–76. http://doi.org/10.1016/j.freeradbiomed.2009.03.025

Gu, S.-H., Hsieh, Y.-C., Young, S.-C., & Lin, P.-L. (2013). Involvement of phosphorylation of adenosine 5'-monophosphate-activated protein kinase in

PTTH-stimulated ecdysteroidogenesis in prothoracic glands of the silkworm, Bombyx mori. *PloS One*, *8*(5), e63102. http://doi.org/10.1371/journal.pone.0063102

Gunter, T. E., Yule, D. I., Gunter, K. K., Eliseev, R. A., & Salter, J. D. (2004). Calcium and mitochondria. *FEBS Letters*, *567*(1), 96–102. http://doi.org/10.1016/j.febslet.2004.03.071

Gwinn, D. M., Shackelford, D. B., Egan, D. F., Mihaylova, M. M., Mery, A., Vasquez, D. S., … Shaw, R. J. (2008). AMPK phosphorylation of raptor mediates a metabolic checkpoint. *Molecular Cell*, *30*(2), 214–26. http://doi.org/10.1016/j.molcel.2008.03.003

Hakkaart, G. A. J., Dassa, E. P., Jacobs, H. T., & Rustin, P. (2006). Allotopic expression of a mitochondrial alternative oxidase confers cyanide resistance to human cell respiration. *EMBO Reports*, *7*(3), 341–5. http://doi.org/10.1038/sj.embor.7400601

Hällberg, B. M., & Larsson, N.-G. (2014a). Making Proteins in the Powerhouse. *Cell Metabolism*, *20*(2), 226–40. http://doi.org/10.1016/j.cmet.2014.07.001

Hällberg, B. M., & Larsson, N.-G. (2014b). Making Proteins in the Powerhouse. *Cell Metabolism*, *20*(2), 226–240. http://doi.org/10.1016/j.cmet.2014.07.001

Hardie, D. G. (2011). AMP-activated protein kinase: an energy sensor that regulates all aspects of cell function. *Genes & Development*, *25*(18), 1895–908. http://doi.org/10.1101/gad.17420111

Hardie, D. G. (2014). AMPK—Sensing Energy while Talking to Other Signaling Pathways. *Cell Metabolism*, *20*(6), 939–952. http://doi.org/10.1016/j.cmet.2014.09.013

Havula, E., Teesalu, M., Hyötyläinen, T., Seppälä, H., Hasygar, K., Auvinen, P., … Hietakangas, V. (2013). Mondo/ChREBP-Mlx-regulated transcriptional network is essential for dietary sugar tolerance in Drosophila. *PLoS Genetics*, *9*(4), e1003438. http://doi.org/10.1371/journal.pgen.1003438

Haynes, C. M., & Ron, D. (2010). The mitochondrial UPR - protecting organelle protein homeostasis. *Journal of Cell Science*, *123*(Pt 22), 3849–55. http://doi.org/10.1242/jcs.075119

Hengartner, M. O., & Horvitz, H. R. (1994). C. elegans cell survival gene ced-9 encodes a functional homolog of the mammalian proto-oncogene bcl-2. *Cell*, *76*(4), 665–676. http://doi.org/10.1016/0092-8674(94)90506-1

Hietakangas, V., & Cohen, S. M. (2009). Regulation of tissue growth through nutrient sensing. *Annual Review of Genetics*, *43*, 389–410. http://doi.org/10.1146/annurev-genet-102108-134815

Hinton, T. (1956). The effects of arginine, ornithine and citrulline on the growth of Drosophila. *Archives of Biochemistry and Biophysics*, *62*(1), 78–85. http://doi.org/10.1016/0003-9861(56)90089-3

Hirst, J. (2011). Why does mitochondrial complex I have so many subunits? *The Biochemical Journal*, *437*(2), e1–3. http://doi.org/10.1042/BJ20110918

Holmström, K. M., & Finkel, T. (2014). Cellular mechanisms and physiological consequences of redox-dependent signalling. *Nature Reviews. Molecular Cell Biology*, *15*(6), 411–21. http://doi.org/10.1038/nrm3801

Holt, I. J., Harding, A. E., & Morgan-Hughes, J. A. (1988). Deletions of muscle mitochondrial DNA in patients with mitochondrial myopathies. *Nature*, *331*(6158), 717–9. http://doi.org/10.1038/331717a0

Holt, I. J., He, J., Mao, C.-C., Boyd-Kirkup, J. D., Martinsson, P., Sembongi, H., … Spelbrink, J. N. (2007). Mammalian mitochondrial nucleoids: organizing an independently minded genome. *Mitochondrion*, *7*(5), 311–21. http://doi.org/10.1016/j.mito.2007.06.004

Holz, M. K., Ballif, B. A., Gygi, S. P., & Blenis, J. (2005). mTOR and S6K1 mediate assembly of the translation preinitiation complex through dynamic protein interchange and ordered phosphorylation events. *Cell*, *123*(4), 569–80. http://doi.org/10.1016/j.cell.2005.10.024

Holzmann, J., Frank, P., Löffler, E., Bennett, K. L., Gerner, C., & Rossmanith, W. (2008). RNase P without RNA: identification and functional reconstitution of the human mitochondrial tRNA processing enzyme. *Cell*, *135*(3), 462–74. http://doi.org/10.1016/j.cell.2008.09.013

Hoppins, S., & Nunnari, J. (2009). The molecular mechanism of mitochondrial fusion. *Biochimica et Biophysica Acta*, *1793*(1), 20–6. http://doi.org/10.1016/j.bbamcr.2008.07.005

Horvath, R. (2012). Update on clinical aspects and treatment of selected vitamin-responsive disorders II (riboflavin and CoQ 10). *Journal of Inherited Metabolic Disease*, *35*(4), 679–87. http://doi.org/10.1007/s10545-011-9434-1

Howlett, I. C., Rusan, Z. M., Parker, L., & Tanouye, M. A. (2013). Drosophila as a model for intractable epilepsy: gilgamesh suppresses seizures in para(bss1) heterozygote flies. *G3 (Bethesda, Md.)*, *3*(8), 1399–407. http://doi.org/10.1534/g3.113.006130

Huang, X., Warren, J. T., & Gilbert, L. I. (2008). New players in the regulation of ecdysone biosynthesis. *Journal of Genetics and Genomics = Yi Chuan Xue Bao*, *35*(1), 1–10. http://doi.org/10.1016/S1673-8527(08)60001-6

Hutt, D. M., Powers, E. T., & Balch, W. E. (2009). The proteostasis boundary in misfolding diseases of membrane traffic. *FEBS Letters*, *583*(16), 2639–46.

Ikeya, T., Galic, M., Belawat, P., Nairz, K., & Hafen, E. (2002). Nutrient-dependent expression of insulin-like peptides from neuroendocrine cells in the CNS contributes to growth regulation in Drosophila. *Current Biology : CB*, *12*(15), 1293–300.

Inoki, K., Li, Y., Zhu, T., Wu, J., & Guan, K.-L. (2002). TSC2 is phosphorylated and inhibited by Akt and suppresses mTOR signalling. *Nature Cell Biology*, *4*(9), 648–57. http://doi.org/10.1038/ncb839

Inoki, K., Zhu, T., & Guan, K.-L. (2003). TSC2 mediates cellular energy response to control cell growth and survival. *Cell*, *115*(5), 577–90.

Jacobs, H. T., Fernández-Ayala, D. J. M., Manjiry, S., Kemppainen, E., Toivonen, J. M., & O'Dell, K. M. C. (2004). Mitochondrial disease in flies. *Biochimica et Biophysica Acta*, *1659*(2-3), 190–6. http://doi.org/10.1016/j.bbabio.2004.07.004

Jewell, J. L., Russell, R. C., & Guan, K.-L. (2013). Amino acid signalling upstream of mTOR. *Nature Reviews. Molecular Cell Biology*, *14*(3), 133–9. http://doi.org/10.1038/nrm3522

Jourdain, A. A., Koppen, M., Wydro, M., Rodley, C. D., Lightowlers, R. N., Chrzanowska-Lightowlers, Z. M., & Martinou, J.-C. (2013). GRSF1 regulates RNA processing in mitochondrial RNA granules. *Cell Metabolism*, *17*(3), 399–410. http://doi.org/10.1016/j.cmet.2013.02.005

Jünger, M. A., Rintelen, F., Stocker, H., Wasserman, J. D., Végh, M., Radimerski, T., … Hafen, E. (2003). The Drosophila forkhead transcription factor FOXO mediates the reduction in cell number associated with reduced insulin signaling. *Journal of Biology*, *2*(3), 20. http://doi.org/10.1186/1475-4924-2-20

Juszczuk, I. M., & Rychter, A. M. (2003). Alternative oxidase in higher plants. *Acta Biochimica Polonica*, *50*(4), 1257–71. http://doi.org/0350041257

Kapahi, P., Chen, D., Rogers, A. N., Katewa, S. D., Li, P. W.-L., Thomas, E. L., & Kockel, L. (2010). With TOR, less is more: a key role for the conserved nutrient-sensing TOR pathway in aging. *Cell Metabolism*, *11*(6), 453–65. http://doi.org/10.1016/j.cmet.2010.05.001

Kazak, L., Reyes, A., & Holt, I. J. (2012). Minimizing the damage: repair pathways keep mitochondrial DNA intact. *Nature Reviews Molecular Cell Biology*, *13*(11), 726–726. http://doi.org/10.1038/nrm3458

Kemppainen, K. K., Rinne, J., Sriram, A., Lakanmaa, M., Zeb, A., Tuomela, T., … Jacobs, H. T. (2014). Expression of alternative oxidase in Drosophila ameliorates diverse phenotypes due to cytochrome oxidase deficiency. *Human Molecular Genetics*, *23*(8), 2078–93. http://doi.org/10.1093/hmg/ddt601

Kerr, D. S. (2010). Treatment of mitochondrial electron transport chain disorders: a review of clinical trials over the past decade. *Molecular Genetics and Metabolism*, *99*(3), 246–55. http://doi.org/10.1016/j.ymgme.2009.11.005

King, V., & Tower, J. (1999). Aging-specific expression of Drosophila hsp22. *Developmental Biology*, *207*(1), 107–18. http://doi.org/10.1006/dbio.1998.9147

Kirkman, H. N., Rolfo, M., Ferraris, A. M., & Gaetani, G. F. (1999). Mechanisms of Protection of Catalase by NADPH: KINETICS AND STOICHIOMETRY. *Journal of Biological Chemistry*, *274*(20), 13908–13914. http://doi.org/10.1074/jbc.274.20.13908

Kmita, K., & Zickermann, V. (2013). Accessory subunits of mitochondrial complex I. *Biochemical Society Transactions*, *41*(5), 1272–9. http://doi.org/10.1042/BST20130091

Koc, E. C., Burkhart, W., Blackburn, K., Moseley, A., Koc, H., & Spremulli, L. L. (2000). A proteomics approach to the identification of mammalian mitochondrial small subunit ribosomal proteins. *The Journal of Biological Chemistry*, *275*(42), 32585–91. http://doi.org/10.1074/jbc.M003596200

Koc, E. C., Burkhart, W., Blackburn, K., Moyer, M. B., Schlatzer, D. M., Moseley, A., & Spremulli, L. L. (2001). The large subunit of the mammalian mitochondrial ribosome. Analysis of the complement of ribosomal proteins present. *The Journal of Biological Chemistry*, *276*(47), 43958–69. http://doi.org/10.1074/jbc.M106510200

Koc, E. C., & Spremulli, L. L. (2002). Identification of mammalian mitochondrial translational initiation factor 3 and examination of its role in initiation complex formation with natural mRNAs. *The Journal of Biological Chemistry*, *277*(38), 35541–9. http://doi.org/10.1074/jbc.M202498200

Korhonen, J. A., Pham, X. H., Pellegrini, M., & Falkenberg, M. (2004). Reconstitution of a minimal mtDNA replisome in vitro. *The EMBO Journal*, *23*(12), 2423–9. http://doi.org/10.1038/sj.emboj.7600257

Kruse, B., Narasimhan, N., & Attardi, G. (1989). Termination of transcription in human mitochondria: Identification and purification of a DNA binding protein factor that promotes termination. *Cell*, *58*(2), 391–397. http://doi.org/10.1016/0092-8674(89)90853-2

Kukat, C., Wurm, C. A., Spåhr, H., Falkenberg, M., Larsson, N.-G., & Jakobs, S. (2011). Super-resolution microscopy reveals that mammalian mitochondrial nucleoids have a uniform size and frequently contain a single copy of mtDNA. *Proceedings of the National Academy of Sciences of the United States of America*, *108*(33), 13534–9. http://doi.org/10.1073/pnas.1109263108

Layalle, S., Arquier, N., & Léopold, P. (2008). The TOR pathway couples nutrition and developmental timing in Drosophila. *Developmental Cell*, *15*(4), 568–77. http://doi.org/10.1016/j.devcel.2008.08.003

Ledesma, A., de Lacoba, M., & Rial, E. (2002). The mitochondrial uncoupling proteins. *Genome Biology*, *3*(12), reviews3015.1–reviews3015.9. http://doi.org/10.1186/gb-2002-3-12-reviews3015

Lee, K.-W., Okot-Kotber, C., LaComb, J. F., & Bogenhagen, D. F. (2013). Mitochondrial ribosomal RNA (rRNA) methyltransferase family members are positioned to modify nascent rRNA in foci near the mitochondrial DNA nucleoid. *The Journal of Biological Chemistry*, *288*(43), 31386–99. http://doi.org/10.1074/jbc.M113.515692

Lee, Y., Jeong, S.-Y., Karbowski, M., Smith, C. L., & Youle, R. J. (2004). Roles of the mammalian mitochondrial fission and fusion mediators Fis1, Drp1, and Opa1 in apoptosis. *Molecular Biology of the Cell*, *15*(11), 5001–11. http://doi.org/10.1091/mbc.E04-04-0294

Lehninger principles of biochemistry - NLM Catalog - NCBI. (2005). Retrieved March 11, 2015, from http://www.ncbi.nlm.nih.gov/nlmcatalog/101303262

Lemasters, J. J., Qian, T., Bradham, C. A., Brenner, D. A., Cascio, W. E., Trost, L. C., … Herman, B. (1999). Mitochondrial dysfunction in the pathogenesis of necrotic and apoptotic cell death. *Journal of Bioenergetics and Biomembranes*, *31*(4), 305–19.

Leonhard, K., Guiard, B., Pellecchia, G., Tzagoloff, A., Neupert, W., & Langer, T. (2000). Membrane protein degradation by AAA proteases in mitochondria: extraction of substrates from either membrane surface. *Molecular Cell*, *5*(4), 629–38.

Lewis, M. R., & Lewis, W. H. (1914). MITOCHONDRIA IN TISSUE CULTURE. *Science (New York, N.Y.)*, *39*(1000), 330–3. http://doi.org/10.1126/science.39.1000.330

Liao, H. X., & Spremulli, L. L. (1991). Initiation of protein synthesis in animal mitochondria. Purification and characterization of translational initiation factor 2. *The Journal of Biological Chemistry*, *266*(31), 20714–9.

Lind, C., Sund, J., & Aqvist, J. (2013). Codon-reading specificities of mitochondrial release factors and translation termination at non-standard stop codons. *Nature Communications*, *4*, 2940. http://doi.org/10.1038/ncomms3940

Lindeboom, L., Nabuurs, C. I., Hoeks, J., Brouwers, B., Phielix, E., Kooi, M. E., … Schrauwen-Hinderling, V. B. (2014). Long-echo time MR spectroscopy for skeletal muscle acetylcarnitine detection. *The Journal of Clinical Investigation*, *124*(11), 4915–25. http://doi.org/10.1172/JCI74830

Loewith, R., Jacinto, E., Wullschleger, S., Lorberg, A., Crespo, J. L., Bonenfant, D., … Hall, M. N. (2002). Two TOR complexes, only one of which is rapamycin sensitive, have distinct roles in cell growth control. *Molecular Cell*, *10*(3), 457–68.

Lowenstein, J. M., & Goodman, M. N. (1978). The purine nucleotide cycle in skeletal muscle. *Federation Proceedings*, *37*(9), 2308–12.

Lu, J., & Holmgren, A. (2014). The thioredoxin antioxidant system. *Free Radical Biology & Medicine*, *66*, 75–87. http://doi.org/10.1016/j.freeradbiomed.2013.07.036

Luft, R., Ikkos, D., Palmieri, G., Ernster, l., & Afzelius, B. (1962). A case of severe hypermetabolism of nonthyroid origin with a defect in the maintenance of mitochondrial respiratory control: a correlated clinical, biochemical, and morphological study. *The Journal of Clinical Investigation*, *41*, 1776–804. http://doi.org/10.1172/JCI104637

Maggert, K. A., Gong, W. J., & Golic, K. G. (2008). Methods for homologous recombination in Drosophila. *Methods in Molecular Biology (Clifton, N.J.)*, *420*, 155–74. http://doi.org/10.1007/978-1-59745-583-1_9

Magnuson, B., Ekim, B., & Fingar, D. C. (2012). Regulation and function of ribosomal protein S6 kinase (S6K) within mTOR signalling networks. *The Biochemical Journal*, *441*(1), 1–21. http://doi.org/10.1042/BJ20110892

Maiuri, M. C., Zalckvar, E., Kimchi, A., & Kroemer, G. (2007). Self-eating and self-killing: crosstalk between autophagy and apoptosis. *Nature Reviews. Molecular Cell Biology*, *8*(9), 741–52. http://doi.org/10.1038/nrm2239

Maranzana, E., Barbero, G., Falasca, A. I., Lenaz, G., & Genova, M. L. (2013). Mitochondrial respiratory supercomplex association limits production of reactive oxygen species from complex I. *Antioxidants & Redox Signaling*, *19*(13), 1469–80. http://doi.org/10.1089/ars.2012.4845

Marella, M., Seo, B. B., Thomas, B. B., Matsuno-Yagi, A., & Yagi, T. (2010). Successful amelioration of mitochondrial optic neuropathy using the yeast NDI1 gene in a rat animal model. *PloS One*, *5*(7), e11472. http://doi.org/10.1371/journal.pone.0011472

Martin, M., Cho, J., Cesare, A. J., Griffith, J. D., & Attardi, G. (2005). Termination Factor-Mediated DNA Loop between Termination and Initiation Sites Drives Mitochondrial rRNA Synthesis. *Cell*, *123*(7), 1227–1240. http://doi.org/10.1016/j.cell.2005.09.040

Martinus, R. D., Garth, G. P., Webster, T. L., Cartwright, P., Naylor, D. J., Høj, P. B., & Hoogenraad, N. J. (1996). Selective induction of mitochondrial chaperones in response to loss of the mitochondrial genome. *European Journal of Biochemistry / FEBS*, *240*(1), 98–103.

Matsuda, N., Sato, S., Shiba, K., Okatsu, K., Saisho, K., Gautier, C. A., … Tanaka, K. (2010). PINK1 stabilized by mitochondrial depolarization recruits Parkin to damaged mitochondria and activates latent Parkin for mitophagy. *The Journal of Cell Biology*, *189*(2), 211–21. http://doi.org/10.1083/jcb.200910140

Matsushima, Y., Goto, Y., & Kaguni, L. S. (2010). Mitochondrial Lon protease regulates mitochondrial DNA copy number and transcription by selective degradation of mitochondrial transcription factor A (TFAM). *Proceedings of the National Academy of Sciences of the United States of America*, *107*(43), 18410–5. http://doi.org/10.1073/pnas.1008924107

McInerney, J. O., O'Connell, M. J., & Pisani, D. (2014). The hybrid nature of the Eukaryota and a consilient view of life on Earth. *Nature Reviews. Microbiology*, *12*(6), 449–55. http://doi.org/10.1038/nrmicro3271

McLelland, G.-L., Soubannier, V., Chen, C. X., McBride, H. M., & Fon, E. A. (2014). Parkin and PINK1 function in a vesicular trafficking pathway regulating mitochondrial quality control. *The EMBO Journal*, *33*(4), 282–95. http://doi.org/10.1002/embj.201385902

Mears, J. A., Sharma, M. R., Gutell, R. R., McCook, A. S., Richardson, P. E., Caulfield, T. R., … Harvey, S. C. (2006). A structural model for the large subunit of the mammalian mitochondrial ribosome. *Journal of Molecular Biology*, *358*(1), 193–212. http://doi.org/10.1016/j.jmb.2006.01.094

Meinnel, T., Sacerdot, C., Graffe, M., Blanquet, S., & Springer, M. (1999). Discrimination by Escherichia coli initiation factor IF3 against initiation on non-canonical codons relies on complementarity rules. *Journal of Molecular Biology*, *290*(4), 825–37. http://doi.org/10.1006/jmbi.1999.2881

Metodiev, M. D., Lesko, N., Park, C. B., Cámara, Y., Shi, Y., Wibom, R., … Larsson, N.-G. (2009). Methylation of 12S rRNA is necessary for in vivo stability of the small subunit of the mammalian mitochondrial ribosome. *Cell Metabolism*, *9*(4), 386–97. http://doi.org/10.1016/j.cmet.2009.03.001

Miller, C., Saada, A., Shaul, N., Shabtai, N., Ben-Shalom, E., Shaag, A., … Elpeleg, O. (2004). Defective mitochondrial translation caused by a ribosomal protein (MRPS16) mutation. *Annals of Neurology*, *56*(5), 734–8. http://doi.org/10.1002/ana.20282

Miller, F. J. (2003). Precise determination of mitochondrial DNA copy number in human skeletal and cardiac muscle by a PCR-based assay: lack of change of copy number with age. *Nucleic Acids Research*, *31*(11), 61e–61. http://doi.org/10.1093/nar/gng060

Minczuk, M., He, J., Duch, A. M., Ettema, T. J., Chlebowski, A., Dzionek, K., … Holt, I. J. (2011). TEFM (c17orf42) is necessary for transcription of human mtDNA. *Nucleic Acids Research*, *39*(10), 4284–99. http://doi.org/10.1093/nar/gkq1224

Miron, M., Lasko, P., & Sonenberg, N. (2003). Signaling from Akt to FRAP/TOR targets both 4E-BP and S6K in Drosophila melanogaster. *Molecular and Cellular Biology*, *23*(24), 9117–26.

Mirth, C. K., & Riddiford, L. M. (2007). Size assessment and growth control: how adult size is determined in insects. *BioEssays : News and Reviews in Molecular, Cellular and Developmental Biology*, *29*(4), 344–55. http://doi.org/10.1002/bies.20552

Mirth, C., Truman, J. W., & Riddiford, L. M. (2005). The role of the prothoracic gland in determining critical weight for metamorphosis in Drosophila melanogaster. *Current Biology : CB*, *15*(20), 1796–807. http://doi.org/10.1016/j.cub.2005.09.017

Montagne, J., Stewart, M. J., Stocker, H., Hafen, E., Kozma, S. C., & Thomas, G. (1999). Drosophila S6 kinase: a regulator of cell size. *Science (New York, N.Y.)*, *285*(5436), 2126–9.

Montgomery, M. K., & Turner, N. (2014). Mitochondrial dysfunction and insulin resistance: an update. *Endocrine Connections*. http://doi.org/10.1530/EC-14-0092

Montoya, J., Christianson, T., Levens, D., Rabinowitz, M., & Attardi, G. (1982). Identification of initiation sites for heavy-strand and light-strand transcription in human mitochondrial DNA. *Proceedings of the National Academy of Sciences of the United States of America*, *79*(23), 7195–9.

Montoya, J., Ojala, D., & Attardi, G. (1981). Distinctive features of the 5′-terminal sequences of the human mitochondrial mRNAs. *Nature*, *290*(5806), 465–470. http://doi.org/10.1038/290465a0

Morrow, G., Inaguma, Y., Kato, K., & Tanguay, R. M. (2000). The small heat shock protein Hsp22 of Drosophila melanogaster is a mitochondrial protein displaying oligomeric organization. *The Journal of Biological Chemistry*, *275*(40), 31204–10. http://doi.org/10.1074/jbc.M002960200

Mossmann, D., Meisinger, C., & Vögtle, F.-N. Processing of mitochondrial presequences. *Biochimica et Biophysica Acta*, *1819*(9-10), 1098–106. http://doi.org/10.1016/j.bbagrm.2011.11.007

Muller, H. J. (1964). The relation of recombination to mutational advance. *Mutation Research/Fundamental and Molecular Mechanisms of Mutagenesis*, *1*(1), 2–9. http://doi.org/10.1016/0027-5107(64)90047-8

Murphy, M. P. (2009). How mitochondria produce reactive oxygen species. *The Biochemical Journal*, *417*(1), 1–13. http://doi.org/10.1042/BJ20081386

Musselman, L. P., Fink, J. L., Ramachandran, P. V., Patterson, B. W., Okunade, A. L., Maier, E., … Baranski, T. J. (2013). Role of fat body lipogenesis in protection against the effects of caloric overload in Drosophila. *The Journal of*

Biological Chemistry, *288*(12), 8028–42. http://doi.org/10.1074/jbc.M112.371047

Na, J., Musselman, L. P., Pendse, J., Baranski, T. J., Bodmer, R., Ocorr, K., & Cagan, R. (2013). A Drosophila model of high sugar diet-induced cardiomyopathy. *PLoS Genetics*, *9*(1), e1003175. http://doi.org/10.1371/journal.pgen.1003175

Nagaike, T., Suzuki, T., Katoh, T., & Ueda, T. (2005). Human mitochondrial mRNAs are stabilized with polyadenylation regulated by mitochondria-specific poly(A) polymerase and polynucleotide phosphorylase. *The Journal of Biological Chemistry*, *280*(20), 19721–7. http://doi.org/10.1074/jbc.M500804200

Nagaike, T., Suzuki, T., Tomari, Y., Takemoto-Hori, C., Negayama, F., Watanabe, K., & Ueda, T. (2001). Identification and characterization of mammalian mitochondrial tRNA nucleotidyltransferases. *The Journal of Biological Chemistry*, *276*(43), 40041–9. http://doi.org/10.1074/jbc.M106202200

Naon, D., & Scorrano, L. (2014). At the right distance: ER-mitochondria juxtaposition in cell life and death. *Biochimica et Biophysica Acta*, *1843*(10), 2184–94. http://doi.org/10.1016/j.bbamcr.2014.05.011

Narendra, D., Tanaka, A., Suen, D.-F., & Youle, R. J. (2008). Parkin is recruited selectively to impaired mitochondria and promotes their autophagy. *The Journal of Cell Biology*, *183*(5), 795–803. http://doi.org/10.1083/jcb.200809125

Nargund, A. M., Pellegrino, M. W., Fiorese, C. J., Baker, B. M., & Haynes, C. M. (2012). Mitochondrial import efficiency of ATFS-1 regulates mitochondrial UPR activation. *Science (New York, N.Y.)*, *337*(6094), 587–90. http://doi.org/10.1126/science.1223560

Nasrallah, C. M., & Horvath, T. L. (2014). Mitochondrial dynamics in the central regulation of metabolism. *Nature Reviews. Endocrinology*, *10*(11), 650–658. http://doi.org/10.1038/nrendo.2014.160

Ngo, H. B., Kaiser, J. T., & Chan, D. C. (2011). The mitochondrial transcription and packaging factor Tfam imposes a U-turn on mitochondrial DNA. *Nature Structural & Molecular Biology*, *18*(11), 1290–6. http://doi.org/10.1038/nsmb.2159

Noguchi, K., & Yoshida, K. (2008). Interaction between photosynthesis and respiration in illuminated leaves. *Mitochondrion*, *8*(1), 87–99. http://doi.org/10.1016/j.mito.2007.09.003

Nolden, M., Ehses, S., Koppen, M., Bernacchia, A., Rugarli, E. I., & Langer, T. (2005). The m-AAA protease defective in hereditary spastic paraplegia controls ribosome assembly in mitochondria. *Cell*, *123*(2), 277–89. http://doi.org/10.1016/j.cell.2005.08.003

Nozaki, Y., Matsunaga, N., Ishizawa, T., Ueda, T., & Takeuchi, N. (2008). HMRF1L is a human mitochondrial translation release factor involved in the decoding of the termination codons UAA and UAG. *Genes to Cells : Devoted to Molecular & Cellular Mechanisms*, *13*(5), 429–38. http://doi.org/10.1111/j.1365-2443.2008.01181.x

Nunnari, J., & Suomalainen, A. (2012). Mitochondria: in sickness and in health. *Cell*, *148*(6), 1145–59. http://doi.org/10.1016/j.cell.2012.02.035

Ogasahara, S., Engel, A. G., Frens, D., & Mack, D. (1989). Muscle coenzyme Q deficiency in familial mitochondrial encephalomyopathy. *Proceedings of the National Academy of Sciences of the United States of America*, *86*(7), 2379–82.

Oldham, S., Montagne, J., Radimerski, T., Thomas, G., & Hafen, E. (2000). Genetic and biochemical characterization of dTOR, the Drosophila homolog of the target of rapamycin. *Genes & Development*, *14*(21), 2689–94.

Osman, C., Voelker, D. R., & Langer, T. (2011). Making heads or tails of phospholipids in mitochondria. *The Journal of Cell Biology*, *192*(1), 7–16. http://doi.org/10.1083/jcb.201006159

Pagliarini, D. J., Calvo, S. E., Chang, B., Sheth, S. A., Vafai, S. B., Ong, S.-E., … Mootha, V. K. (2008). A mitochondrial protein compendium elucidates complex I disease biology. *Cell*, *134*(1), 112–23. http://doi.org/10.1016/j.cell.2008.06.016

Pakendorf, B., & Stoneking, M. (2005). Mitochondrial DNA and human evolution. *Annual Review of Genomics and Human Genetics*, *6*, 165–83. http://doi.org/10.1146/annurev.genom.6.080604.162249

Palmer, J. D. (1997). Organelle Genomes--Going, Going, Gone! *Science*, *275*(5301), 790–790. http://doi.org/10.1126/science.275.5301.790

Pan, D. A., & Hardie, D. G. (2002). A homologue of AMP-activated protein kinase in Drosophila melanogaster is sensitive to AMP and is activated by ATP depletion. *The Biochemical Journal*, *367*(Pt 1), 179–86. http://doi.org/10.1042/BJ20020703

Panini, S. R. (2013). *Medical Biochemistry - An Illustrated Review*. Thieme.

Parisi, F., Riccardo, S., Daniel, M., Saqcena, M., Kundu, N., Pession, A., … Bellosta, P. (2011). Drosophila insulin and target of rapamycin (TOR) pathways regulate GSK3 beta activity to control Myc stability and determine Myc expression in vivo. *BMC Biology*, *9*(1), 65. http://doi.org/10.1186/1741-7007-9-65

Park, C. B., Asin-Cayuela, J., Cámara, Y., Shi, Y., Pellegrini, M., Gaspari, M., … Larsson, N.-G. (2007). MTERF3 is a negative regulator of mammalian mtDNA transcription. *Cell*, *130*(2), 273–85. http://doi.org/10.1016/j.cell.2007.05.046

Park, J. S., Li, Y.-F., & Bai, Y. (2007). Yeast NDI1 improves oxidative phosphorylation capacity and increases protection against oxidative stress and cell death in cells carrying a Leber's hereditary optic neuropathy mutation. *Biochimica et Biophysica Acta*, *1772*(5), 533–42. http://doi.org/10.1016/j.bbadis.2007.01.009

Pasquale, M. G. Di. (2007). *Amino Acids and Proteins for the Athlete: The Anabolic Edge, Second Edition* (Vol. 30). CRC Press.

Pellegrino, M. W., Nargund, A. M., & Haynes, C. M. (2013). Signaling the mitochondrial unfolded protein response. *Biochimica et Biophysica Acta*, *1833*(2), 410–6. http://doi.org/10.1016/j.bbamcr.2012.02.019

Peralta, S., Torraco, A., Iommarini, L., & Diaz, F. (2015). Mitochondrial diseases Part III: Therapeutic interventions in mouse models of oxphos deficiencies. *Mitochondrion*. http://doi.org/10.1016/j.mito.2015.01.007

Pfeffer, G., Horvath, R., Klopstock, T., Mootha, V. K., Suomalainen, A., Koene, S., … Chinnery, P. F. (2013). New treatments for mitochondrial disease-no time to drop our standards. *Nature Reviews. Neurology*, *9*(8), 474–81. http://doi.org/10.1038/nrneurol.2013.129

Piechota, J., Tomecki, R., Gewartowski, K., Szczesny, R., Dmochowska, A., Kudła, M., … Bartnik, E. (2006). Differential stability of mitochondrial mRNA in HeLa cells. *Acta Biochimica Polonica*, *53*(1), 157–68.

Ponka, P. (1997). Tissue-specific regulation of iron metabolism and heme synthesis: distinct control mechanisms in erythroid cells. *Blood*, *89*(1), 1–25.

Potter, C. J., Pedraza, L. G., & Xu, T. (2002). Akt regulates growth by directly phosphorylating Tsc2. *Nature Cell Biology*, *4*(9), 658–65. http://doi.org/10.1038/ncb840

Poulton, J., Morten, K. J., Marchington, D., Weber, K., Brown, G. K., Rötig, A., & Bindoff, L. (1995). Duplications of mitochondrial DNA in Kearns-Sayre syndrome. *Muscle & Nerve. Supplement*, *3*, S154–8.

Prezant, T. R., Agapian, J. V, Bohlman, M. C., Bu, X., Oztas, S., Qiu, W. Q., … Rotter, J. I. (1993). Mitochondrial ribosomal RNA mutation associated with both antibiotic-induced and non-syndromic deafness. *Nature Genetics*, *4*(3), 289–94. http://doi.org/10.1038/ng0793-289

Rajan, A., & Perrimon, N. (2012). Drosophila cytokine unpaired 2 regulates physiological homeostasis by remotely controlling insulin secretion. *Cell*, *151*(1), 123–37. http://doi.org/10.1016/j.cell.2012.08.019

Rasmusson, A. G., Soole, K. L., & Elthon, T. E. (2004). Alternative NAD(P)H dehydrogenases of plant mitochondria. *Annual Review of Plant Biology*, *55*, 23–39. http://doi.org/10.1146/annurev.arplant.55.031903.141720

Reinders, J., Zahedi, R. P., Pfanner, N., Meisinger, C., & Sickmann, A. (2006). Toward the complete yeast mitochondrial proteome: multidimensional separation techniques for mitochondrial proteomics. *Journal of Proteome Research*, *5*(7), 1543–54. http://doi.org/10.1021/pr050477f

Richter, R., Rorbach, J., Pajak, A., Smith, P. M., Wessels, H. J., Huynen, M. A., … Chrzanowska-Lightowlers, Z. M. (2010). A functional peptidyl-tRNA hydrolase, ICT1, has been recruited into the human mitochondrial ribosome. *The EMBO Journal*, *29*(6), 1116–25. http://doi.org/10.1038/emboj.2010.14

Riddiford, L. M., Cherbas, P., & Truman, J. W. (2000). Ecdysone receptors and their biological actions. *Vitamins and Hormones*, *60*, 1–73.

Rio, D. C., Laski, F. A., & Rubin, G. M. (1986). Identification and immunochemical analysis of biologically active Drosophila P element transposase. *Cell*, *44*(1), 21–32.

Roman, G., Endo, K., Zong, L., & Davis, R. L. (2001). P[Switch], a system for spatial and temporal control of gene expression in Drosophila melanogaster. *Proceedings of the National Academy of Sciences of the United States of America*, *98*(22), 12602–7. http://doi.org/10.1073/pnas.221303998

Rorbach, J., Soleimanpour-Lichaei, R., Lightowlers, R. N., & Chrzanowska-Lightowlers, Z. M. A. (2007). How do mammalian mitochondria synthesize proteins? *Biochemical Society Transactions*, *35*(Pt 5), 1290–1. http://doi.org/10.1042/BST0351290

Ross, J. M., Stewart, J. B., Hagström, E., Brené, S., Mourier, A., Coppotelli, G., … Larsson, N.-G. (2013). Germline mitochondrial DNA mutations aggravate ageing and can impair brain development. *Nature*, *501*(7467), 412–5. http://doi.org/10.1038/nature12474

Rötig, A. (2011). Human diseases with impaired mitochondrial protein synthesis. *Biochimica et Biophysica Acta*, *1807*(9), 1198–205. http://doi.org/10.1016/j.bbabio.2011.06.010

Rötig, A., & Poulton, J. (2009). Genetic causes of mitochondrial DNA depletion in humans. *Biochimica et Biophysica Acta*, *1792*(12), 1103–8. http://doi.org/10.1016/j.bbadis.2009.06.009

Rouault, T. A., & Tong, W.-H. (2005). Iron-sulphur cluster biogenesis and mitochondrial iron homeostasis. *Nature Reviews. Molecular Cell Biology*, *6*(4), 345–51. http://doi.org/10.1038/nrm1620

Royden, C. S., Pirrotta, V., & Jan, L. Y. (1987). The tko locus, site of a behavioral mutation in D. melanogaster, codes for a protein homologous to prokaryotic ribosomal protein S12. *Cell*, *51*(2), 165–73.

Rubin, G. M. (2000). Comparative Genomics of the Eukaryotes. *Science*, *287*(5461), 2204–2215. http://doi.org/10.1126/science.287.5461.2204

Rubio-Cosials, A., Sidow, J. F., Jiménez-Menéndez, N., Fernández-Millán, P., Montoya, J., Jacobs, H. T., … Solà, M. (2011). Human mitochondrial transcription factor A induces a U-turn structure in the light strand promoter. *Nature Structural & Molecular Biology*, *18*(11), 1281–9. http://doi.org/10.1038/nsmb.2160

Rustin, P., & Lance, C. (1986). Malate Metabolism in Leaf Mitochondria from the Crassulacean Acid Metabolism Plant Kalanchoë blossfeldiana Poelln. *Plant Physiology*, *81*(4), 1039–43.

Saada, A., Shaag, A., Arnon, S., Dolfin, T., Miller, C., Fuchs-Telem, D., … Elpeleg, O. (2007). Antenatal mitochondrial disease caused by mitochondrial ribosomal protein (MRPS22) mutation. *Journal of Medical Genetics*, *44*(12), 784–6. http://doi.org/10.1136/jmg.2007.053116

Sajid, W., Kulahin, N., Schluckebier, G., Ribel, U., Henderson, H. R., Tatar, M., … De Meyts, P. (2011). Structural and biological properties of the Drosophila insulin-like peptide 5 show evolutionary conservation. *The Journal of Biological Chemistry*, *286*(1), 661–73. http://doi.org/10.1074/jbc.M110.156018

Sancak, Y., Thoreen, C. C., Peterson, T. R., Lindquist, R. A., Kang, S. A., Spooner, E., … Sabatini, D. M. (2007). PRAS40 is an insulin-regulated inhibitor of the mTORC1 protein kinase. *Molecular Cell*, *25*(6), 903–15. http://doi.org/10.1016/j.molcel.2007.03.003

Sanchez, M. I. G. L., Mercer, T. R., Davies, S. M. K., Shearwood, A.-M. J., Nygård, K. K. A., Richman, T. R., … Filipovska, A. (2011). RNA processing in human mitochondria. *Cell Cycle (Georgetown, Tex.)*, *10*(17), 2904–16.

Sanz, A., Soikkeli, M., Portero-Otín, M., Wilson, A., Kemppainen, E., McIlroy, G., … Jacobs, H. T. (2010). Expression of the yeast NADH dehydrogenase Ndi1 in Drosophila confers increased lifespan independently of dietary restriction. *Proceedings of the National Academy of Sciences of the United States of America*, *107*(20), 9105–10. http://doi.org/10.1073/pnas.0911539107

Sasarman, F., Antonicka, H., & Shoubridge, E. A. (2008). The A3243G tRNALeu(UUR) MELAS mutation causes amino acid misincorporation and a combined respiratory chain assembly defect partially suppressed by overexpression of EFTu and EFG2. *Human Molecular Genetics*, *17*(23), 3697–707. http://doi.org/10.1093/hmg/ddn265

Schägger, H., de Coo, R., Bauer, M. F., Hofmann, S., Godinot, C., & Brandt, U. (2004). Significance of respirasomes for the assembly/stability of human respiratory chain complex I. *The Journal of Biological Chemistry*, *279*(35), 36349–53. http://doi.org/10.1074/jbc.M404033200

Schneider-Poetsch, T., Ju, J., Eyler, D. E., Dang, Y., Bhat, S., Merrick, W. C., … Liu, J. O. (2010). Inhibition of eukaryotic translation elongation by cycloheximide and lactimidomycin. *Nature Chemical Biology*, *6*(3), 209–217. http://doi.org/10.1038/nchembio.304

Schon, E. A., DiMauro, S., & Hirano, M. (2012). Human mitochondrial DNA: roles of inherited and somatic mutations. *Nature Reviews. Genetics*, *13*(12), 878–90. http://doi.org/10.1038/nrg3275

Scorrano, L. (2013). Keeping mitochondria in shape: a matter of life and death. *European Journal of Clinical Investigation*, *43*(8), 886–93. http://doi.org/10.1111/eci.12135

Seidel-Rogol, B. L., McCulloch, V., & Shadel, G. S. (2003). Human mitochondrial transcription factor B1 methylates ribosomal RNA at a conserved stem-loop. *Nature Genetics*, *33*(1), 23–4. http://doi.org/10.1038/ng1064

Shackelford, D. B., Abt, E., Gerken, L., Vasquez, D. S., Seki, A., Leblanc, M., … Shaw, R. J. (2013). LKB1 inactivation dictates therapeutic response of non-small cell lung cancer to the metabolism drug phenformin. *Cancer Cell*, *23*(2), 143–58. http://doi.org/10.1016/j.ccr.2012.12.008

Sharma, M. R., Koc, E. C., Datta, P. P., Booth, T. M., Spremulli, L. L., & Agrawal, R. K. (2003). Structure of the mammalian mitochondrial ribosome reveals an expanded functional role for its component proteins. *Cell*, *115*(1), 97–108.

Shoffner, J. M., Lott, M. T., Lezza, A. M., Seibel, P., Ballinger, S. W., & Wallace, D. C. (1990a). Myoclonic epilepsy and ragged-red fiber disease (MERRF) is associated with a mitochondrial DNA tRNA(Lys) mutation. *Cell*, *61*(6), 931–7.

Shoffner, J. M., Lott, M. T., Lezza, A. M., Seibel, P., Ballinger, S. W., & Wallace, D. C. (1990b). Myoclonic epilepsy and ragged-red fiber disease (MERRF) is associated with a mitochondrial DNA tRNA(Lys) mutation. *Cell*, *61*(6), 931–7.

Shoubridge, E. A., & Wai, T. (2007). Mitochondrial DNA and the mammalian oocyte. *Current Topics in Developmental Biology*, *77*, 87–111. http://doi.org/10.1016/S0070-2153(06)77004-1

Sickmann, A., Reinders, J., Wagner, Y., Joppich, C., Zahedi, R., Meyer, H. E., … Meisinger, C. (2003). The proteome of Saccharomyces cerevisiae mitochondria. *Proceedings of the National Academy of Sciences of the United States of America*, *100*(23), 13207–12. http://doi.org/10.1073/pnas.2135385100

Siedow, J. N., & Umbach, A. L. (2000). The mitochondrial cyanide-resistant oxidase: structural conservation amid regulatory diversity. *Biochimica et Biophysica Acta*, *1459*(2-3), 432–9.

Sims, R. J., Belotserkovskaya, R., & Reinberg, D. (2004). Elongation by RNA polymerase II: the short and long of it. *Genes & Development*, *18*(20), 2437–68. http://doi.org/10.1101/gad.1235904

Singer, M. A. (2003). Dietary protein-induced changes in excretory function: a general animal design feature. *Comparative Biochemistry and Physiology Part B: Biochemistry and Molecular Biology*, *136*(4), 785–801. http://doi.org/10.1016/j.cbpc.2003.08.012

Skladal, D., Halliday, J., & Thorburn, D. R. (2003). Minimum birth prevalence of mitochondrial respiratory chain disorders in children. *Brain : A Journal of Neurology*, *126*(Pt 8), 1905–12. http://doi.org/10.1093/brain/awg170

Smith, D. M. (1931). The ontogenetic history of the mitochondria of the hepatic cell of the white rat. *Journal of Morphology*, *52*(2), 485–511. http://doi.org/10.1002/jmor.1050520206

Smits, P., Saada, A., Wortmann, S. B., Heister, A. J., Brink, M., Pfundt, R., … van den Heuvel, L. P. (2011). Mutation in mitochondrial ribosomal protein MRPS22 leads to Cornelia de Lange-like phenotype, brain abnormalities and hypertrophic cardiomyopathy. *European Journal of Human Genetics : EJHG*, *19*(4), 394–9. http://doi.org/10.1038/ejhg.2010.214

Soleimanpour-Lichaei, H. R., Kühl, I., Gaisne, M., Passos, J. F., Wydro, M., Rorbach, J., … Chrzanowska-Lightowlers, Z. (2007). mtRF1a is a human mitochondrial translation release factor decoding the major termination codons UAA and UAG. *Molecular Cell*, *27*(5), 745–57. http://doi.org/10.1016/j.molcel.2007.06.031

Spencer, A. C., & Spremulli, L. L. (2004). Interaction of mitochondrial initiation factor 2 with mitochondrial fMet-tRNA. *Nucleic Acids Research*, *32*(18), 5464–70. http://doi.org/10.1093/nar/gkh886

Spremulli, L. L., Coursey, A., Navratil, T., & Hunter, S. E. (2004). Initiation and elongation factors in mammalian mitochondrial protein biosynthesis. *Progress in Nucleic Acid Research and Molecular Biology*, *77*, 211–61. http://doi.org/10.1016/S0079-6603(04)77006-3

Stadtman, E. R., Moskovitz, J., & Levine, R. L. (2003). Oxidation of methionine residues of proteins: biological consequences. *Antioxidants & Redox Signaling*, *5*(5), 577–82. http://doi.org/10.1089/152308603770310239

Starkov, A. A. (2008). The role of mitochondria in reactive oxygen species metabolism and signaling. *Annals of the New York Academy of Sciences*, *1147*, 37–52. http://doi.org/10.1196/annals.1427.015

Stewart, J. B., Freyer, C., Elson, J. L., & Larsson, N.-G. (2008). Purifying selection of mtDNA and its implications for understanding evolution and mitochondrial disease. *Nature Reviews. Genetics*, *9*(9), 657–62. http://doi.org/10.1038/nrg2396

Stewart, J. B., Freyer, C., Elson, J. L., Wredenberg, A., Cansu, Z., Trifunovic, A., & Larsson, N.-G. (2008). Strong purifying selection in transmission of mammalian mitochondrial DNA. *PLoS Biology*, *6*(1), e10. http://doi.org/10.1371/journal.pbio.0060010

Suzuki, T., Nagao, A., & Suzuki, T. (2011). Human mitochondrial tRNAs: biogenesis, function, structural aspects, and diseases. *Annual Review of Genetics*, *45*, 299–329. http://doi.org/10.1146/annurev-genet-110410-132531

Suzuki, T., Terasaki, M., Takemoto-Hori, C., Hanada, T., Ueda, T., Wada, A., & Watanabe, K. (2001). Proteomic analysis of the mammalian mitochondrial ribosome. Identification of protein components in the 28 S small subunit. *The Journal of Biological Chemistry*, *276*(35), 33181–95. http://doi.org/10.1074/jbc.M103236200

Tanaka, A., Cleland, M. M., Xu, S., Narendra, D. P., Suen, D.-F., Karbowski, M., & Youle, R. J. (2010a). Proteasome and p97 mediate mitophagy and degradation of mitofusins induced by Parkin. *The Journal of Cell Biology*, *191*(7), 1367–80. http://doi.org/10.1083/jcb.201007013

Tanaka, A., Cleland, M. M., Xu, S., Narendra, D. P., Suen, D.-F., Karbowski, M., & Youle, R. J. (2010b). Proteasome and p97 mediate mitophagy and degradation of mitofusins induced by Parkin. *The Journal of Cell Biology*, *191*(7), 1367–80. http://doi.org/10.1083/jcb.201007013

Tatsuta, T., & Langer, T. (2008). Quality control of mitochondria: protection against neurodegeneration and ageing. *The EMBO Journal*, *27*(2), 306–14. http://doi.org/10.1038/sj.emboj.7601972

Teleman, A. A., Chen, Y.-W., & Cohen, S. M. (2005). 4E-BP functions as a metabolic brake used under stress conditions but not during normal growth. *Genes & Development*, *19*(16), 1844–8. http://doi.org/10.1101/gad.341505

Teleman, A. A., Hietakangas, V., Sayadian, A. C., & Cohen, S. M. (2008). Nutritional control of protein biosynthetic capacity by insulin via Myc in Drosophila. *Cell Metabolism*, *7*(1), 21–32. http://doi.org/10.1016/j.cmet.2007.11.010

Temperley, R., Richter, R., Dennerlein, S., Lightowlers, R. N., & Chrzanowska-Lightowlers, Z. M. (2010). Hungry codons promote frameshifting in human mitochondrial ribosomes. *Science (New York, N.Y.)*, *327*(5963), 301. http://doi.org/10.1126/science.1180674

Tennessen, J. M., Baker, K. D., Lam, G., Evans, J., & Thummel, C. S. (2011). The Drosophila estrogen-related receptor directs a metabolic switch that supports developmental growth. *Cell Metabolism*, *13*(2), 139–48. http://doi.org/10.1016/j.cmet.2011.01.005

Tennessen, J. M., Bertagnolli, N. M., Evans, J., Sieber, M. H., Cox, J., & Thummel, C. S. (2014). Coordinated metabolic transitions during Drosophila embryogenesis and the onset of aerobic glycolysis. *G3 (Bethesda, Md.)*, *4*(5), 839–50. http://doi.org/10.1534/g3.114.010652

Tennessen, J. M., & Thummel, C. S. (2011). Coordinating growth and maturation - insights from Drosophila. *Current Biology : CB*, *21*(18), R750–7. http://doi.org/10.1016/j.cub.2011.06.033

Terzioglu, M., Ruzzenente, B., Harmel, J., Mourier, A., Jemt, E., López, M. D., … Larsson, N.-G. (2013). MTERF1 Binds mtDNA to Prevent Transcriptional

Interference at the Light-Strand Promoter but Is Dispensable for rRNA Gene Transcription Regulation. *Cell Metabolism*, *17*(4), 618–626. http://doi.org/10.1016/j.cmet.2013.03.006

Tettweiler, G., Miron, M., Jenkins, M., Sonenberg, N., & Lasko, P. F. (2005). Starvation and oxidative stress resistance in Drosophila are mediated through the eIF4E-binding protein, d4E-BP. *Genes & Development*, *19*(16), 1840–3. http://doi.org/10.1101/gad.1311805

Thummel, C. S. (2001). Molecular Mechanisms of Developmental Timing in C. elegans and Drosophila. *Developmental Cell*, *1*(4), 453–465. http://doi.org/10.1016/S1534-5807(01)00060-0

Tischner, C., Hofer, A., Wulff, V., Stepek, J., Dumitru, I., Becker, L., … Wenz, T. (2014). MTO1 mediates tissue-specificity of OXPHOS defects via tRNA modification and translation optimization, which can be bypassed by dietary intervention. *Human Molecular Genetics*. http://doi.org/10.1093/hmg/ddu743

Toivonen, J. M., Boocock, M. R., & Jacobs, H. T. (1999). Modelling in Escherichia coli of mutations in mitoribosomal protein S12: novel mutant phenotypes of rpsL. *Molecular Microbiology*, *31*(6), 1735–46.

Toivonen, J. M., Manjiry, S., Touraille, S., Alziari, S., O'Dell, K. M. C., & Jacobs, H. T. (2003). Gene dosage and selective expression modify phenotype in a Drosophila model of human mitochondrial disease. *Mitochondrion*, *3*(2), 83–96. http://doi.org/10.1016/S1567-7249(03)00077-1

Toivonen, J. M., O'Dell, K. M., Petit, N., Irvine, S. C., Knight, G. K., Lehtonen, M., … Jacobs, H. T. (2001). Technical knockout, a Drosophila model of mitochondrial deafness. *Genetics*, *159*(1), 241–54.

Tsuboi, M., Morita, H., Nozaki, Y., Akama, K., Ueda, T., Ito, K., … Takeuchi, N. (2009). EF-G2mt is an exclusive recycling factor in mammalian mitochondrial protein synthesis. *Molecular Cell*, *35*(4), 502–10. http://doi.org/10.1016/j.molcel.2009.06.028

Vafai, S. B., & Mootha, V. K. (2012). Mitochondrial disorders as windows into an ancient organelle. *Nature*, *491*(7424), 374–83. http://doi.org/10.1038/nature11707

Valero, T. (2014). Mitochondrial biogenesis: pharmacological approaches. *Current Pharmaceutical Design*, *20*(35), 5507–9.

Vander Haar, E., Lee, S.-I., Bandhakavi, S., Griffin, T. J., & Kim, D.-H. (2007). Insulin signalling to mTOR mediated by the Akt/PKB substrate PRAS40. *Nature Cell Biology*, *9*(3), 316–23. http://doi.org/10.1038/ncb1547

Vander Heiden, M. G., Cantley, L. C., & Thompson, C. B. (2009). Understanding the Warburg effect: the metabolic requirements of cell proliferation. *Science (New York, N.Y.)*, *324*(5930), 1029–33. http://doi.org/10.1126/science.1160809

Verstreken, P., Ly, C. V, Venken, K. J. T., Koh, T.-W., Zhou, Y., & Bellen, H. J. (2005). Synaptic mitochondria are critical for mobilization of reserve pool vesicles at Drosophila neuromuscular junctions. *Neuron*, *47*(3), 365–78. http://doi.org/10.1016/j.neuron.2005.06.018

Vögtle, F.-N., Wortelkamp, S., Zahedi, R. P., Becker, D., Leidhold, C., Gevaert, K., … Meisinger, C. (2009). Global analysis of the mitochondrial N-proteome identifies a processing peptidase critical for protein stability. *Cell*, *139*(2), 428–39. http://doi.org/10.1016/j.cell.2009.07.045

Wallace, D. C., Fan, W., & Procaccio, V. (2010). Mitochondrial energetics and therapeutics. *Annual Review of Pathology*, *5*, 297–348. http://doi.org/10.1146/annurev.pathol.4.110807.092314

Wallace, D. C., Singh, G., Lott, M. T., Hodge, J. A., Schurr, T. G., Lezza, A. M., … Nikoskelainen, E. K. (1988). Mitochondrial DNA mutation associated with Leber's hereditary optic neuropathy. *Science (New York, N.Y.)*, *242*(4884), 1427–30.

Warburg, O. (1956). On the origin of cancer cells. *Science (New York, N.Y.)*, *123*(3191), 309–14.

Wenz, T., Luca, C., Torraco, A., & Moraes, C. T. (2009). mTERF2 regulates oxidative phosphorylation by modulating mtDNA transcription. *Cell Metabolism*, *9*(6), 499–511. http://doi.org/10.1016/j.cmet.2009.04.010

Wheaton, W. W., Weinberg, S. E., Hamanaka, R. B., Soberanes, S., Sullivan, L. B., Anso, E., … Chandel, N. S. (2014). Metformin inhibits mitochondrial complex I of cancer cells to reduce tumorigenesis. *eLife*, *3*, e02242.

Williams, G. S. B., Boyman, L., Chikando, A. C., Khairallah, R. J., & Lederer, W. J. (2013). Mitochondrial calcium uptake. *Proceedings of the National Academy of Sciences of the United States of America*, *110*(26), 10479–86. http://doi.org/10.1073/pnas.1300410110

Winterbourn, C. C. (2013). The biological chemistry of hydrogen peroxide. *Methods in Enzymology*, *528*, 3–25. http://doi.org/10.1016/B978-0-12-405881-1.00001-X

Wu, G., Fang, Y.-Z., Yang, S., Lupton, J. R., & Turner, N. D. (2004). Glutathione Metabolism and Its Implications for Health. *J. Nutr.*, *134*(3), 489–492.

Xu, F., Ackerley, C., Maj, M. C., Addis, J. B. L., Levandovskiy, V., Lee, J., … Robinson, B. H. (2008). Disruption of a mitochondrial RNA-binding protein gene results in decreased cytochrome b expression and a marked reduction in ubiquinol-cytochrome c reductase activity in mouse heart mitochondria. *The Biochemical Journal*, *416*(1), 15–26. http://doi.org/10.1042/BJ20080847

Yagi, T., Seo, B. B., Di Bernardo, S., Nakamaru-Ogiso, E., Kao, M. C., & Matsuno-Yagi, A. (2001). NADH dehydrogenases: from basic science to biomedicine. *Journal of Bioenergetics and Biomembranes*, *33*(3), 233–42.

Yang, Q., Inoki, K., Kim, E., & Guan, K.-L. (2006). TSC1/TSC2 and Rheb have different effects on TORC1 and TORC2 activity. *Proceedings of the National Academy of Sciences of the United States of America*, *103*(18), 6811–6. http://doi.org/10.1073/pnas.0602282103

Ylikallio, E., & Suomalainen, A. (2012). Mechanisms of mitochondrial diseases. *Annals of Medicine*, *44*(1), 41–59. http://doi.org/10.3109/07853890.2011.598547

Yoshida, K., Shibata, M., Terashima, I., & Noguchi, K. (2010). Simultaneous determination of in vivo plastoquinone and ubiquinone redox states by HPLC-based analysis. *Plant & Cell Physiology*, *51*(5), 836–41. http://doi.org/10.1093/pcp/pcq044

Zhang, H., Stallock, J. P., Ng, J. C., Reinhard, C., & Neufeld, T. P. (2000). Regulation of cellular growth by the Drosophila target of rapamycin dTOR. *Genes & Development*, *14*(21), 2712–24.

Zhang, Y. Q., Roote, J., Brogna, S., Davis, A. W., Barbash, D. A., Nash, D., & Ashburner, M. (1999). stress sensitive B encodes an adenine nucleotide translocase in Drosophila melanogaster. *Genetics*, *153*(2), 891–903.

Zhang, Y., & Spremulli, L. L. (1998). Identification and cloning of human mitochondrial translational release factor 1 and the ribosome recycling factor. *Biochimica et Biophysica Acta*, *1443*(1-2), 245–50.

Zhao, Q., Wang, J., Levichkin, I. V, Stasinopoulos, S., Ryan, M. T., & Hoogenraad, N. J. (2002). A mitochondrial specific stress response in mammalian cells. *The EMBO Journal*, *21*(17), 4411–9.

Zhu, P.-P., Patterson, A., Stadler, J., Seeburg, D. P., Sheng, M., & Blackstone, C. (2004). Intra- and intermolecular domain interactions of the C-terminal GTPase effector domain of the multimeric dynamin-like GTPase Drp1. *The Journal of Biological Chemistry*, *279*(34), 35967–74. http://doi.org/10.1074/jbc.M404105200

Appendix I

Metabolites decreased in tko25t on both diets								[nmol g-1]	
Anions/Cations	KEGG	Average wt HS	STDEV	Average wt ZS	STDEV	Average tko25t HS	STDEV	Average tko25t ZS	STDEV
F1,6P	C00354	78.4	12.7	77.8	19.6	22.7	6.4	32.2	11.8
S7P	C05382	130.8	24.7	77.1	10.1	73.0	13.3	52.8	3.8
Glutarate	C00489	18.0	0.3	18.6	4.1	9.0	3.8	12.5	2.1
Threonate	C01620	29.9	3.7	21.4	2.0	16.3	1.7	17.2	1.7
Glucuronate	C00191	11.9	0.8	14.8	0.4	7.6	1.6	10.2	0.6
N-Acetylglucosamine 1-phosphate	C04501	20.9	0.7	20.0	0.7	12.7	3.2	13.4	1.1
N-Acetylglucosamine 6-phosphate	C00357	52.3	2.3	53.1	2.1	32.3	5.1	28.7	2.3
NADPH	C00005	14.6	2.3	30.8	6.3	2.6	3.2	14.0	6.0
UDP	C00015	16.7	0.9	18.9	3.5	10.8	1.5	11.7	2.1
GDP	C00035	40.6	2.5	37.0	4.6	22.7	2.6	24.4	3.6
UTP	C00075	8.7	2.4	15.5	5.9	3.9	1.7	5.6	2.7
ATP	C00002	289.3	42.1	389.6	81.5	133.1	25.9	228.1	56.7
Putrescine(1,4-Butanediamine)	C00134	36.5	2.3	20.5	3.2	17.5	3.7	14.7	2.2
beta-Ala	C00099	1526.4	127.6	1835.2	219.7	1082.7	217.2	554.8	84.5
GABA	C00334	85.6	10.8	68.0	7.3	63.8	8.4	44.3	4.7
Histamine	C00388	121.5	23.3	92.7	16.0	20.6	7.1	1.1	0.8
Betaine	C00719	283.5	59.1	286.3	19.5	102.9	39.3	29.3	5.5
Pipecolate	C00408	16.5	1.0	33.9	4.6	8.0	2.8	9.5	1.6
Asn	C00152	2152.1	130.3	2597.2	202.9	1229.9	198.3	1253.8	127.5
Asp	C00049	495.0	142.5	641.4	137.4	210.8	58.6	203.1	43.8
gamma-Butyrobetaine	C01181	13.7	2.4	9.5	1.6	8.4	2.4	5.9	1.4
Lys	C00047	5685.2	551.7	6070.2	924.7	4524.5	514.3	3318.3	282.8
His	C00135	2417.8	276.7	2004.3	219.0	1161.8	231.3	746.4	156.0
3-Hydroxykynurenine	C02794	1019.8	74.2	805.8	9.6	618.8	74.6	415.5	49.5

Metabolites increased in tko25t on both diets								[nmol g-1]	
Anions/Cations	KEGG	Average wt HS	STDEV	Average wt ZS	STDEV	Average tko25t HS	STDEV	Average tko25t ZS	STDEV
Pyruvate	C00022	187.4	67.3	107.0	14.9	481.0	156.4	486.7	46.9
2-Oxoisopentanoate	C00141	9.0	1.7	8.4	1.2	12.9	0.8	18.2	3.1
4-Hydroxy-3-methoxybenzoate + Urate	C06672	278.8	136.6	361.5	124.6	1189.3	536.8	1519.9	675.8
Ala	C00041	7140.5	674.4	4627.7	471.2	14438.6	2337.1	9212.6	1481.4
Ser	C00065	784.5	32.5	894.8	29.1	1717.5	334.6	1927.4	177.4
Thr	C00188	2325.1	292.4	2821.6	359.1	3056.0	428.2	7177.5	740.2
Spermidine	C00315	33.9	4.9	25.6	3.1	53.0	5.1	53.9	8.3
Phosphorylcholine	C00588	769.9	76.8	964.6	36.4	1477.0	135.5	1405.3	169.4
N6,N6,N6-Trimethyllysine	C03793	5.2	0.7	5.0	0.1	7.5	1.2	10.6	1.5
SAM+	C00019	13.8	2.8	11.1	1.6	24.4	4.1	19.8	2.3
o-Acetylcarnitine	C02571	151.6	23.4	120.7	20.4	246.6	58.0	213.2	46.9

Metabolites increased on HS in both genotypes								[nmol g-1]	
		Average	STDEV	Average	STDEV	Average	STDEV	Average	STDEV
Anions/Cations	KEGG	wt HS		wt ZS		tko25t HS		tko25t ZS	
Ala	C00041	7140.5	674.4	4627.7	471.2	14438.6	2337.1	9212.6	1481.4
GABA	C00334	85.6	10.8	68.0	7.3	63.8	8.4	44.3	4.7
Ornithine	C00077	285.2	46.8	140.5	22.4	567.5	238.5	93.9	34.6
3-Hydroxykynurenine	C02794	1019.8	74.2	805.8	9.6	618.8	74.6	415.5	49.5

Metabolites decreased on HS in both genotypes								[nmol g-1]	
		Average	STDEV	Average	STDEV	Average	STDEV	Average	STDEV
Anions/Cations	KEGG	wt HS		wt ZS		tko25t HS		tko25t ZS	
Isocitrate	C00311	43.9	6.5	59.9	10.5	49.1	10.9	67.8	9.1
Glucuronate	C00191	11.9	0.8	14.8	0.4	7.6	1.6	10.2	0.6
Carnitine	C00318	34.1	7.4	49.1	3.4	29.8	5.8	41.3	3.8
Citrulline	C00327	14.4	2.5	38.7	8.8	19.8	5.6	95.8	23.0
N-epsilon-Acetyllysine	C02727	2.5	2.9	7.2	1.1	7.1	2.3	19.5	4.3

Metabolites increased in tko25t on HS but "rescued" by ZS								[nmol g-1]	
		Average	STDEV	Average	STDEV	Average	STDEV	Average	STDEV
Anions/Cations	KEGG	wt HS		wt ZS		tko25t HS		tko25t ZS	
Ala	C00041	7140.5	674.4	4627.7	471.2	14438.6	2337.1	9212.6	1481.4
Methionine sulfoxide	C02989	266.3	64.5	426.9	69.5	646.5	164.9	303.9	142.0
Saccharopine	C00449	20.6	3.1	17.2	1.8	31.1	3.1	15.5	2.8

Metabolites decreased in tko25t on HS but "rescued" by ZS								[nmol g-1]	
		Average	STDEV	Average	STDEV	Average	STDEV	Average	STDEV
Anions/Cations	KEGG	wt HS		wt ZS		tko25t HS		tko25t ZS	
Glucuronate	C00191	11.9	0.8	14.8	0.4	7.6	1.6	10.2	0.6
Adenylosuccinate	C03794	24.0	4.9	31.1	3.1	9.2	1.1	27.2	9.9
ATP	C00002	289.3	42.1	389.6	81.5	133.1	25.9	228.1	56.7
UDP-N-acetylglucosamine	C00043	173.5	19.4	175.4	17.4	128.2	11.4	154.4	12.5
Glu	C00025	3884.2	363.4	4406.1	282.8	3209.2	254.5	3902.0	362.3
Arg	C00062	3121.3	388.9	3206.0	165.9	2380.0	219.9	2870.7	296.6
DOPA	C00355	20.6	4.3	18.5	2.4	12.1	1.6	17.6	3.5

Up-regulated on ZS vs. HS in wild-type

KEGG term	Count	Biological process term	Count
00903:Limonene and pinene degradation	27	GO:0042742~defense response to bacterium	23
04142:Lysosome	25	GO:0006022~aminoglycan metabolic process	33
00511:Other glycan degradation	11	GO:0006508~proteolysis	89
00600:Sphingolipid metabolism	10	GO:0019731~antibacterial humoral response	13
00980:Metabolism of xenobiotics by cytochrome P450	16	GO:0006030~chitin metabolic process	26
00982:Drug metabolism	16	GO:0006026~aminoglycan catabolic process	11
00830:Retinol metabolism	9	GO:0000272~polysaccharide catabolic process	11
00564:Glycerophospholipid metabolism	12	GO:0006643~membrane lipid metabolic process	9
00983:Drug metabolism	11	GO:0007559~histolysis	15
00500:Starch and sucrose metabolism	11	GO:0006027~glycosaminoglycan catabolic process	7

Up-regulated on ZS vs. HS in *tko*^{25t}

KEGG term	Count	Biological process term	Count
00350:Tyrosine metabolism	12	GO:0009072~aromatic amino acid family metabolic process	11
00980:Metabolism of xenobiotics by cytochrome P450	13	GO:0019752~carboxylic acid metabolic process	27
00982:Drug metabolism	13	GO:0006520~cellular amino acid metabolic process	19
00903:Limonene and pinene degradation	14	GO:0006508~proteolysis	46
00511:Other glycan degradation	6	GO:0006570~tyrosine metabolic process	6
00260:Glycine, serine and threonine metabolism	6	GO:0044106~cellular amine metabolic process	19
00480:Glutathione metabolism	9	GO:0006026~aminoglycan catabolic process	6
00380:Tryptophan metabolism	4	GO:0000272~polysaccharide catabolic process	6
00830:Retinol metabolism	5	GO:0006022~aminoglycan metabolic process	12
00360:Phenylalanine metabolism	4	GO:0046653~tetrahydrofolate metabolic process	3

Down-regulated on ZS vs. HS in OR

KEGG term	Count	Biological process term	Count
00010:Glycolysis / Gluconeogenesis	15	GO:0045333~cellular respiration	25
00190:Oxidative phosphorylation	25	GO:0019752~carboxylic acid metabolic process	40
00020:Citrate cycle (TCA cycle)	12	GO:0006006~glucose metabolic process	17
00620:Pyruvate metabolism	12	GO:0006030~chitin metabolic process	23
00903:Limonene and pinene degradation	16	GO:0006022~aminoglycan metabolic process	26
00564:Glycerophospholipid metabolism	13	GO:0044275~cellular carbohydrate catabolic process	15
00350:Tyrosine metabolism	9	GO:0019320~hexose catabolic process	13
00360:Phenylalanine metabolism	6	GO:0022904~respiratory electron transport chain	17
00030:Pentose phosphate pathway	6	GO:0046365~monosaccharide catabolic process	13
			27

Down-regulated on ZS vs. HS in *tko*^{25t}

KEGG term	Count	Biological process term	Count
04080:Neuroactive ligand-receptor interaction	6	GO:0006508~proteolysis	59
00480:Glutathione metabolism	6	GO:0006030~chitin metabolic process	23
00903:Limonene and pinene degradation	7	GO:0006022~aminoglycan metabolic process	24
00982:Drug metabolism	6	GO:0006820~anion transport	8
00010:Glycolysis / Gluconeogenesis	5	GO:0046942~carboxylic acid transport	8
		GO:0015711~organic anion transport	5
		GO:0006865~amino acid transport	6
		GO:0007594~puparial adhesion	4
		GO:0015672~monovalent inorganic cation transport	12
		GO:0015698~inorganic anion transport	4

Up-regulated in *tko*^{25t} vs. OR on HS

KEGG term	Count	Biological process term	Count
00230:Purine metabolism	24	GO:0009124~nucleoside monophosphate biosynthetic process	16
00500:Starch and sucrose metabolism	12	GO:0006022~aminoglycan metabolic process	28
00010:Glycolysis / Gluconeogenesis	11	GO:0019731~antibacterial humoral response	10
00030:Pentose phosphate pathway	7	GO:0042742~defense response to bacterium	16
00051:Fructose and mannose metabolism	7	GO:0006030~chitin metabolic process	22
00511:Other glycan degradation	5	GO:0034654~nucleobase, nucleoside, nucleotide and NA biosynthesis	27
00980:Metabolism of xenobiotics by cytochrome P450	10	GO:0034404~nucleobase, nucleoside and nucleotide biosynthesis	27
00620:Pyruvate metabolism	8	GO:0006508~proteolysis	86
00982:Drug metabolism	10	GO:0019320~hexose catabolic process	11
00790:Folate biosynthesis	5	GO:0044275~cellular carbohydrate catabolic process	12

Up-regulated in *tko*^{25t} vs. OR on ZS

KEGG term	Count	Biological process term	Count
00350:Tyrosine metabolism	10	GO:0006508~proteolysis	87
00561:Glycerolipid metabolism	10	GO:0019752~carboxylic acid metabolic process	38
00903:Limonene and pinene degradation	14	GO:0009063~cellular amino acid catabolic process	10
00620:Pyruvate metabolism	9	GO:0009309~amine biosynthetic process	12
00051:Fructose and mannose metabolism	7	GO:0006022~aminoglycan metabolic process	23
00980:Metabolism of xenobiotics by cytochrome P450	10	GO:0046394~carboxylic acid biosynthetic process	14
00982:Drug metabolism	10	GO:0009310~amine catabolic process	10
00010:Glycolysis / Gluconeogenesis	8	GO:0046395~carboxylic acid catabolic process	11
00360:Phenylalanine metabolism	5	GO:0006030~chitin metabolic process	19
00910:Nitrogen metabolism	5	GO:0044106~cellular amine metabolic process	24

Down-regulated in *tko*^{25t} vs. OR on HS

KEGG term	Count	Biological process term	Count
00190:Oxidative phosphorylation	56	GO:0006119~oxidative phosphorylation	54
00260:Glycine, serine and threonine metabolism	15	GO:0043436~oxoacid metabolic process	78
00903:Limonene and pinene degradation	33	GO:0022900~electron transport chain	39
00350:Tyrosine metabolism	18	GO:0022904~respiratory electron transport chain	33
00280:Valine, leucine and isoleucine degradation	17	GO:0015980~energy derivation by oxidation of organic compounds	41
00980:Metabolism of xenobiotics by cytochrome P450	26	GO:0006520~cellular amino acid metabolic process	42
00071:Fatty acid metabolism	18	GO:0044106~cellular amine metabolic process	45
00360:Phenylalanine metabolism	13	GO:0006022~aminoglycan metabolic process	39
00982:Drug metabolism	26	GO:0055086~nucleobase, nucleoside and nucleotide metabolic process	49
00010:Glycolysis / Gluconeogenesis	21	GO:0006732~coenzyme metabolic process	29

Down-regulated in *tko*^{25t} vs. OR on ZS

KEGG term	Count	Biological process term	Count
00903:Limonene and pinene degradation	36	GO:0006508~proteolysis	144
00980:Metabolism of xenobiotics by cytochrome P450	28	GO:0006022~aminoglycan metabolic process	35
00982:Drug metabolism	28	GO:0006030~chitin metabolic process	30
00830:Retinol metabolism	17	GO:0019752~carboxylic acid metabolic process	46
00983:Drug metabolism	22	GO:0042742~defense response to bacterium	18
00511:Other glycan degradation	11	GO:0044242~cellular lipid catabolic process	10
04080:Neuroactive ligand-receptor interaction	15	GO:0006026~aminoglycan catabolic process	11
00053:Ascorbate and aldarate metabolism	14	GO:0000272~polysaccharide catabolic process	11
04142:Lysosome	25	GO:0006631~fatty acid metabolic process	14
00150:Androgen and estrogen metabolism	13	GO:0034754~cellular hormone metabolic process	7

Original communications

Mitochondrion 9 (2009) 353–363

Contents lists available at ScienceDirect

Mitochondrion

journal homepage: www.elsevier.com/locate/mito

Phenotypic suppression of the *Drosophila* mitochondrial disease-like mutant *tko*^{25t} by duplication of the mutant gene in its natural chromosomal context

Esko Kemppainen [a], Daniel Jose Moreno Fernández-Ayala [a,1], Laura C.A. Galbraith [b], Kevin M.C. O'Dell [b], Howard T. Jacobs [a,b,*]

[a] *Institute of Medical Technology and Tampere University Hospital, FI-33014 University of Tampere, Finland*
[b] *Molecular Genetics, Faculty of Biomedical and Life Sciences, University of Glasgow, Glasgow G12 8QQ, Scotland, UK*

ARTICLE INFO

Article history:
Received 20 March 2009
Received in revised form 24 June 2009
Accepted 13 July 2009
Available online 17 July 2009

Keywords:
Drosophila
Mitochondrial disease
technical knockout
Ribosome

ABSTRACT

A mutation in the *Drosophila* gene *technical knockout* (*tko*^{25t}), encoding mitoribosomal protein S12, phenocopies human mitochondrial disease. We isolated three spontaneous X-dominant suppressors of *tko*^{25t} (designated *Weeble*), exhibiting almost wild-type phenotype and containing overlapping segmental duplications including the mutant allele, plus a second mitoribosomal protein gene, *mRpL14*. Ectopic, expressed copies of *tko*^{25t} and *mRpL14* conferred no phenotypic suppression. When placed over a null allele of *tko*, *Weeble* retained the mutant phenotype, even in the presence of additional transgenic copies of *tko*^{25t}. Increased mutant gene dosage can thus compensate the mutant phenotype, but only when located in its normal chromosomal context.

1. Introduction

Human mitochondrial diseases affecting the oxidative phosphorylation (OXPHOS) system can result from a large number of different mutations, both in the nuclear genome or in the maternally inherited mitochondrial DNA (mtDNA) (Schon, 2000; Smeitink, 2003). Many such pathological mutations impact the apparatus of intramitochondrial protein synthesis (Jacobs and Turnbull, 2005; Scheper et al., 2007), including mtDNA-encoded rRNAs and tRNAs, as well as nuclear DNA-encoded mitoribosomal proteins, translation elongation factors, RNA modification enzymes and aminoacyl-tRNA ligases. Although the tissues most obviously dependent on bioenergy are commonly affected in mitochondrial disease, the specific phenotypes, as well as the full range of tissues involved, are not well understood. In particular, the severity of disease can vary greatly between individuals bearing the identical pathological mutation. Although in part explicable by variable patterns of heteroplasmy in the case of mtDNA mutations, the causes of such phenotypic heterogeneity remain largely unknown.

We have been studying a mutant of *Drosophila melanogaster* (*tko*^{25t}) that constitutes a model for mitochondrial diseases, especially those affecting intramitochondrial protein synthesis. The mutant carries a mis-sense mutation (L85H) in the X-linked nuclear gene for mitoribosomal protein S12 (*technical knockout*, *tko*), resulting in a phenotype of developmental delay, bang-sensitivity (temporarily paralysis induced by mechanical shock), impaired responsiveness to sound and defective male courtship. Compared with wild-type strains, *tko*^{25t} exhibits decreased activities of the OXPHOS enzymes dependent on intramitochondrial translation products and a relative deficiency of mitoribosomal small subunit rRNA relative to large subunit rRNA (Toivonen et al., 2001). The gross organismal phenotype is shared with other mutants impaired in mitochondrial bioenergy metabolism, such as *sesB*, encoding the adenine nucleotide translocase (Zhang et al., 1999), or *knockdown*, encoding citrate synthase (Fergestad et al., 2006). Null alleles of *tko*, such as *tko*^{3}, are homozygous lethal at the larval stage, confirming that *tko* is an essential gene; in fact, *tko*^{25t} is the only viable *tko* mutant allele yet isolated.

Flies transgenic for a *tko*^{25t} allele which has been reverted to leucine at amino-acid 85, still in the *tko*^{25t} background, display a fully wild-type phenotype (Toivonen et al., 2001), whereas flies with an unreverted transgenic copy of *tko*^{25t} retain a fully mutant phenotype (Toivonen et al., 2001, 2003), even when the ectopic *tko*^{25t} transgene is expressed in adult flies at levels comparable with, or even in excess of, that of the endogenous gene (Toivonen et al., 2003). In earlier studies we also noticed that, when maintained as an inbred stock over many generations, the phenotype of *tko*^{25t} flies became attenuated (Toivonen et al., 2001). To investigate this further, we backcrossed *tko*^{25t} into two different wild-type backgrounds (Canton S and Oregon R), then mated *tko*^{25t}

* Corresponding author. Address: Institute of Medical Technology, FI-33014 University of Tampere, Finland. Tel.: +358 3 3551 7731; fax: +358 3 3551 7710.
E-mail address: howard.t.jacobs@uta.fi (H.T. Jacobs).
[1] Present address: Centro Andaluz de Biología del Desarrollo (CABD-CSIC/UPO), Universidad Pablo Olavide, Carretera de Utrera, Km. 1, 41013 Seville, Spain.

1567-7249/$ - see front matter © 2009 Elsevier B.V. and Mitochondria Research Society. All rights reserved.
doi:10.1016/j.mito.2009.07.002

Canton S females to *tko*^{25t} Oregon R males, creating an F1 hybrid that exhibited a much more pronounced mutant phenotype (Jacobs et al., 2004), characterized by so-called semi-lethality (i.e. the failure of most progeny to complete development and eclose as adult flies). Inbred lines were then established from individual mating pairs from this cross and maintained under selection for accelerated development over at least 12 generations (see Section 2). Six such inbred lines were analysed phenotypically, and found to eclose at a time intermediate between that of the original F1 hybrid and wild-type flies (Jacobs et al., 2004). Two of the lines showed a particularly pronounced suppression of the mutant phenotype and were selected for more detailed study.

In the present work we present the phenotypic analysis of these lines, plus one additional suppressor line obtained from the reciprocal cross, and establish the molecular nature of the suppressor. Surprisingly, we found that all three suppressors contain local duplications of overlapping regions of the X-chromosome, including the (still mutant) *tko*^{25t} allele, as well as one other mitoribosomal protein gene, *mRpL14*. Genetic analysis of the suppressors, in combination with deletion and point mutants of the *tko* region, as well as of transgenic lines containing expressed, ectopic copies of either the mutant *tko*^{25t} allele, *mRpL14* or both, lead to the conclusion that suppression requires an additional copy of the *tko*^{25t} allele, but that it must be in its natural chromosomal context on the X-chromosome. Increased gene dosage of *mRpL14* appears not to be required for suppression. The findings provide insight into genetic factors which may underlie phenotypic differences in mitochondrial disease, and suggest possible ways to intervene therapeutically.

2. Materials and methods

2.1. Drosophila stocks and maintenance

Wild-type (Canton S and Oregon R), *w*^{1118}, *FM7a*, *CyO* and *TM3Sb* balancer, *tko*^{3} mutant and deficiency stocks were obtained from stock centres. Bloomington deficiency stocks 733, 6892 and 935 have, respectively, the following genotypes: Df(1)w258-42;*y*^{1}/FM1;*lz*$^{+}$, Df(1)JC19/FM7c and Df(1)TEM7,*y*^{2}*w*^{i}*ct*^{6}*f*^{1}/FM7c. *tko*^{25t} mutant flies were originally supplied by Dr. C.-F. Wu. *tko*^{3} was maintained over the *FM7a* balancer. Transgenic lines A1 and A3, containing *P*{*tko*^{25t}} transgenes, respectively on chromosomes 3 and 2, were described previously (Toivonen et al., 2003). Flies were maintained at 25 °C on a 12 h light/dark cycle in standard medium containing 1.5% (w/v) sucrose (Merck), 3% glucose (Sigma), 3.5% Instant Dry Baker's Yeast (European), 1.5% maize flour (Oriola), 1% wheat germ (Oriola), 1% soya flour (Oriola), 1% agar (Oriola) and 3% Lyle's black treacle (Tate & Lyle, UK), to which was added 0.1% methyl 4-hydroxybenzoate (Sigma) and 0.5% (v/v) propionic acid (JT Baker).

2.2. Selection of *tko*^{25t} suppressor lines

tko^{25t} was backcrossed over >12 generations into wild-type strains Canton S and Oregon R, which were then mated to create an F1 generation with a fully penetrant mutant phenotype. Inbred suppressor lines were initiated from single mating pairs, whose progeny were then maintained under selection for >12 generations by selecting the first eclosing six females and three males from the progeny in each generation to create the next.

2.3. Eclosion timing

Mean developmental time to eclosion at 25 °C was measured by setting up 10 parallel crosses of 10 females and 5 males for each experiment, which was itself repeated at least three times. In each cross, flies were allowed to copulate for one day, then transferred to fresh food vials at a fixed time, after which the first set of vials was discarded. The flies were transferred to a fresh set of vials twice more, allowing the flies to lay eggs for exactly 24 h each time. After having laid eggs for 24 h in the third and last set of vials, the mated flies were discarded. The number of eclosing offspring was counted every day at noon.

2.4. Bang-sensitivity

Bang-sensitivity was measured essentially as previously (Toivonen et al., 2001). Freshly eclosed flies were anaesthetized using CO_2 and separated into empty food vials (one fly per vial). Sexed and separated flies were transferred to 25 °C for 2–3 h to recover from anesthesia. Individual flies were vortexed for 15 s, and time to recovery recorded (defined as the time taken for the flies to be standing upright with apparently normal locomotor activity).

2.5. RNA extraction

Total RNA was extracted from aliquots of 100 mg of flies (30 females or 40 males) anaesthetized on ice and immediately frozen at 80 °C. Frozen flies were ground using a plastic homogenizer in 200 μl of Trizol reagent (Invitrogen). An additional 800 μl of Trizol was added, and the extract was thoroughly mixed. The homogenate was incubated at room temperature for 5 min, after which 200 μl of chloroform was added and the mix incubated for an additional 3 min before centrifugation for 15 min at 12,000 g_{max} at 4 °C. The upper, aqueous phase was transferred to a fresh vial and RNA precipitated by adding 500 μl of isopropanol and incubating at room temperature for 10 min. The precipitate was pelleted by centrifugation for 10 min at 12,000 g_{max} at 4 °C, washed with 75% ethanol, air-dried, resuspended in 89 μl DEPC-treated water, to which was added 1 μl (10 units) DNaseI (Amersham Biosciences) and 10 μl of 10× DNase I buffer (60 mM $MgCl_2$, 400 mM Tris–HCl, pH 7.5), and incubated for 1 h at 37 °C. The RNA was recovered by phenol/chloroform extraction and ethanol precipitation and finally resuspended in 50 μl of DEPC-treated water.

2.6. Quantitative RT-PCR

Complementary DNAs were synthesized from 2 μg aliquots of RNA denatured at 90 °C for 3 min in reaction volumes of 11 μl containing 1 μl of 10 mM dNTP mix (Finnzymes) and 1 μl of 0.0125 U/μl random hexamers (Amersham Biosciences). The reactions were transferred to ice and 4 μl of 5× reaction buffer (250 mM Tris–HCl, 250 mM KCl, 20 mM $MgCl_2$, 50 mM DTT, pH 8.3) plus 0.5 μl of 40 U/μl RNase inhibitor (Fermentas) and 2.5 μl of DEPC-treated water were added. After incubation at 25 °C for 10 min, 2 μl of 20 U/μl MMuLV reverse transcriptase (Fermentas) were added and the reactions incubated further at 25 °C for 10 min then at 37 °C for 1 h. Reactions were stopped by heating at 70 °C for 10 min. The levels of mitochondrial 12S and 16S rRNA, as well as *tko* and *mRpL14* mRNA, were measured relative to an internal standard (*RpL32*) using custom-designed (TibMolBiol) hybridization probes on a Roche LightCycler 1.5 instrument (see Supplementary data for full details). All RNA extractions were performed in triplicate, and each of these extractions was treated as an individual experiment. Each total RNA extract was used as a template for three separate cDNA synthesis reactions, which were then pooled and analysed in triplicate, producing a total of 9 data points per fly line or developmental stage.

2.7. Genomic DNA extraction

Genomic DNA was extracted from aliquots of 100 mg of flies (30 females or 40 males) anaesthetized on ice and ground for 1 min using a plastic homogenizer in 200 μl of lysis buffer (100 mM Tris–HCl, 100 mM EDTA, 100 mM NaCl, 0.5% SDS, pH 7.5). An additional 300 μl of lysis buffer was added and the mixture was homogenized for a further 1 min, or until only cuticles visibly remained. For DNA to be used in Southern blots, the homogenates were incubated at 37 °C for 1 h. Nucleic acids were isolated by gentle phenol–chloroform extraction, followed by centrifugation at 5000 g_{max} for 5 min at room temperature, and precipitation of 400 μl of the upper, aqueous phase by the addition of 200 μl 5 M potassium acetate (pH 5.6) and 400 μl of isopropanol. The vial was inverted with care to mix all solutions and DNA was recovered by centrifugation at 12,000 g_{max} for 15 min at room temperature, washed with 70% ethanol, air-dried and resuspended without pipetting in 150 μl of Tris–HCl (pH 7.5) for one day at 4 °C. For DNA to be used in PCR-based methods, homogenates were incubated at 65 °C for 30 min, after which 800 μl of collection buffer (1.4 M potassium acetate, 4.3 M LiCl) was added to each sample prior to incubation on ice for 30 min. Homogenates were centrifuged for 15 min at 12,000 g_{max}, and 1 ml of each resulting supernatant was transferred to a fresh microcentrifuge tube and mixed with 600 μl of isopropanol to precipitate nucleic acids. The centrifugation was repeated and the supernatants discarded. DNA pellets were washed with 70% ethanol, air-dried and resuspended in TE (10 mM Tris–HCl, 1 mM EDTA, pH 8.0).

2.8. Gene dosage analysis by Southern blots

Twenty micrograms of DNA was digested with *Nde*I (manufacturer's buffer and recommended conditions; NEB) and fractionated on a 0.75% agarose gel. Depurination, capillary blotting to nylon membrane and UV-crosslinking were performed as described previously (Toivonen et al., 2001). Blots were prehybridized for 30 min at 65 °C in hybridization solution (250 mM sodium phosphate, 1 mM EDTA, 7% SDS, pH 7.2) and hybridized overnight in the same solution with PCR-derived probes as indicated in Supplementary data. After hybridization, the blot was washed at 65 °C twice for 15 min with 5× SSC plus 0.1% SDS, once for 15 min with 1× SSC plus 0.1% SDS, and finally for 15 min in 0.1× SSC plus 0.1% SDS. Finally, the blot was exposed to autoradiography films (Kodak Biomax MS). Images were digitized and analysed using Scion Densiometry Software (NIH, USA).

2.9. Gene dosage analysis by quantitative PCR

Two DNA extracts from both males and virgin females of a given genotype were pooled and used as a template, diluted to a final concentration of approximately 100 ng/μl. Amplification reactions were performed in 20 μl final volume consisting of 5 μl of template DNA, 10 μl of QuantiTect SYBR Green PCR Master Mix (Qiagen) and 1 μl of 10 μM forward and reverse primers (see Supplementary data for primer sequences and full details).

2.10. Construction of transgenic lines

The *mRpL14* gene region was amplified from genomic DNA using customized primers (see Supplementary data for primer information and full cloning details), producing a 1.8 kb product containing the gene itself, plus 750 bp upstream and 430 bp downstream of the transcription unit (see Supplementary Fig. 1). The product was cloned using Zero Blunt TOPO PCR Cloning Kit (Invitrogen) under manufacturer's recommended conditions. After sequence verification, the *mRpL14*insert was liberated by digestion with *Xba*I (Fermentas) and *Spe*I (Fermentas) and introduced into a modified version of the vector pGREEN-H-Pelican (Barolo et al., 2000), obtained from Drosophila Genomics Resource Center, Bloomington, IN, USA (see Supplementary Fig. 1 for details). The construct leaves transgenic *mRpL14* under the control of its own promoter, but protected from readthrough transcription by flanking *gypsy* insulator elements. The final plasmid, following sequence and restriction-map verification, was purified by standard phenol/chloroform extraction and ethanol precipitation and sent to Vanedis Drosophila Injection Service (Oslo, Norway) for microinjection. Transgenic progeny were identified by the w^+ eye colour marker in the w^{1118} background, then sib-crossed to establish stable homozygous transgenic lines, from which males were crossed to white-eyed double-balancer females (w^{1118}/w^{1118}; +/CyO; +/Tm3Sb), to identify insertions on chromosomes 2 or 3.

2.11. Insertion site mapping by inverse PCR

Genomic DNA (3.5 μg) from homozygous transgenic flies of each line was digested with 10 units of *Scr*FI (Fermentas) in manufacturer's buffer for 3 h at 37 °C, in a total volume of 25 μl. The enzyme cuts in the *foot* segment of the Pelican vector, between the P-element 3′ end and the upstream insulator, and at a high frequency in genomic DNA. After heat inactivation of the restriction enzyme, the digested DNA was circularized by self-ligation overnight at 4 °C in a total volume of 400 μl, using four Weiss units of T4 DNA ligase (Fermentas) in the manufacturer's buffer. Ligated DNA was ethanol precipitated and resuspended in 100 μl of 10 mM Tris–HCl (pH 8.0). Ten microliters of this was used for PCR amplification using the *foot*-segment specific primer set (see Supplementary data), and products were sequenced using the same primers to identify transgene insertion sites by comparison with the genomic DNA reference sequence.

2.12. Analysis of gene expression by Affymetrix microarrays

RNA extraction and purification, and cRNA probe synthesis was performed using Affymetrix® protocols and kits provided by Qiagen, from three independent groups of 40 males of wild-type, tko^{25t}, $Weeb^1$ and $Weeb^2$ strains. Each of the three replicates of cRNA was hybridized to independent GeneChip® Drosophila Genome 2.0 Arrays (Affymetrix). Data extraction, cell intensity calculation and computational analysis were performed using GeneChip® Operating Software and Expression Console Release Software from Affymetrix. For each pair-wise comparative analysis, the signal value (MAS5 and RMA algorithms, at linear scale) of each probe was compared as follows: wild-type to tko^{25t}, $Weeb^1$ and $Weeb^2$, and tko^{25t} to $Weeb^1$ and $Weeb^2$. Statistics were performed with Microsoft® Office Excel 2003. Firstly, the data were prefiltered according to their detection p-value, selecting those with p-value <0.05. Secondly, SAM (Significance Analysis of Microarrays, Stanford Tools) was performed as described (http://www-stat.stanford.edu/~tibs/SAM/sam.pdf) using $s_0 = 20$ and minimum fold change (R) = 1.5 as fixed parameters, and Δ-value so that False Discovery Rate (FDR) <2.5%. Finally, probes showing significantly altered expression in both $Weeb^1$–wild-type and $Weeb^1$–tko^{25t} comparisons were selected for further analysis. Probes showing significantly altered expression in both $Weeb^2$–wild type and $Weeb^2$–tko^{25t} comparisons were similarly selected.

3. Results

3.1. Isolation of tko^{25t} suppressors under selection

As described in Section 2, inbred lines of *Drosophila* carrying the tko^{25t} mutation were established by crossing tko^{25t} homozygous fe-

males and *tko*^{25t} hemizygous males outbred into different wild-type backgrounds (Canton S and Oregon R, respectively), then establishing lines from individual mating pairs. These were then placed under selection for accelerated development over >12 generations, developmental delay being one of the cardinal phenotypes of *tko*^{25t}. This procedure generated sets of inbred lines which showed stable and characteristically different degrees of phenotypic rescue (Jacobs et al., 2004). Two lines, denoted *Weeble*^{1} (*Weeb*^{1}) and *Weeble*^{2} (*Weeb*^{2}) showed an especially pronounced phenotypic rescue (Fig. 1) and were selected for further study. We initially confirmed by sequencing that both retained the original *tko*^{25t} mutation, with no wild-type copy of the *tko* gene (Supplementary Fig. 2A), and no other mutations within the *tko* transcription unit or its immediate flanking sequences. Both lines exhibited an almost wild-type developmental timing (Fig. 1A) and were no longer bang-sensitive (Fig. 1B). Note that flies of both sexes were studied in all experiments, since *tko* is located on the X-chromosome, and differential expression in males and females would be one potential complication of any suppressor effect. In crosses to *tko*^{25t}, *Weeb*^{1} behaved as a (semi-) dominant X-linked suppressor (Supplementary Fig. 2B), regardless of the parent of origin (Supplementary Fig. 2C). In both of the *Weeble* lines the ratio of 12S:16S mitochondrial rRNAs, which represents a marker for the relative amount of small and large mitoribosomal subunits, and is diagnostic for the mutant phenotype, was found to be intermediate (Fig. 1C) between that seen in outbred *tko*^{25t} flies (between 0.3 and 0.4) and in wild-type flies (approximately 1.0). The improvement was mainly due to a recovery in 12S rRNA levels (Supplementary Fig. 2D). A third line, designated *Weeb*^{3}, showing a similar degree of phenotypic recovery (Fig. 1), was obtained from a similar selection procedure using the reciprocal cross (Oregon R *tko*^{25t} females, Canton S *tko*^{25t} males).

3.2. Weeble suppressors contain overlapping X-chromosomal duplications

To map *Weeb*^{1} more precisely, having established that it was X-linked, we crossed *Weeb*^{1} males to *tko*^{25t} females homozygous also for the *w*$^{-}$ (*white*$^{-}$) mutation, located on the X-chromosome close to *tko*, and conferring white eye colour. This approach allowed us to determine the location of *Weeb*^{1} with respect to *white*, using a standard recombination mapping approach. Female progeny from the cross were crossed to wild-type males. The resulting male progeny carry either parental or recombinant X-chromosomes, which can be distinguished on the basis of the combined eye colour and eclosion day phenotypes. Our reasoning was that, if *w*

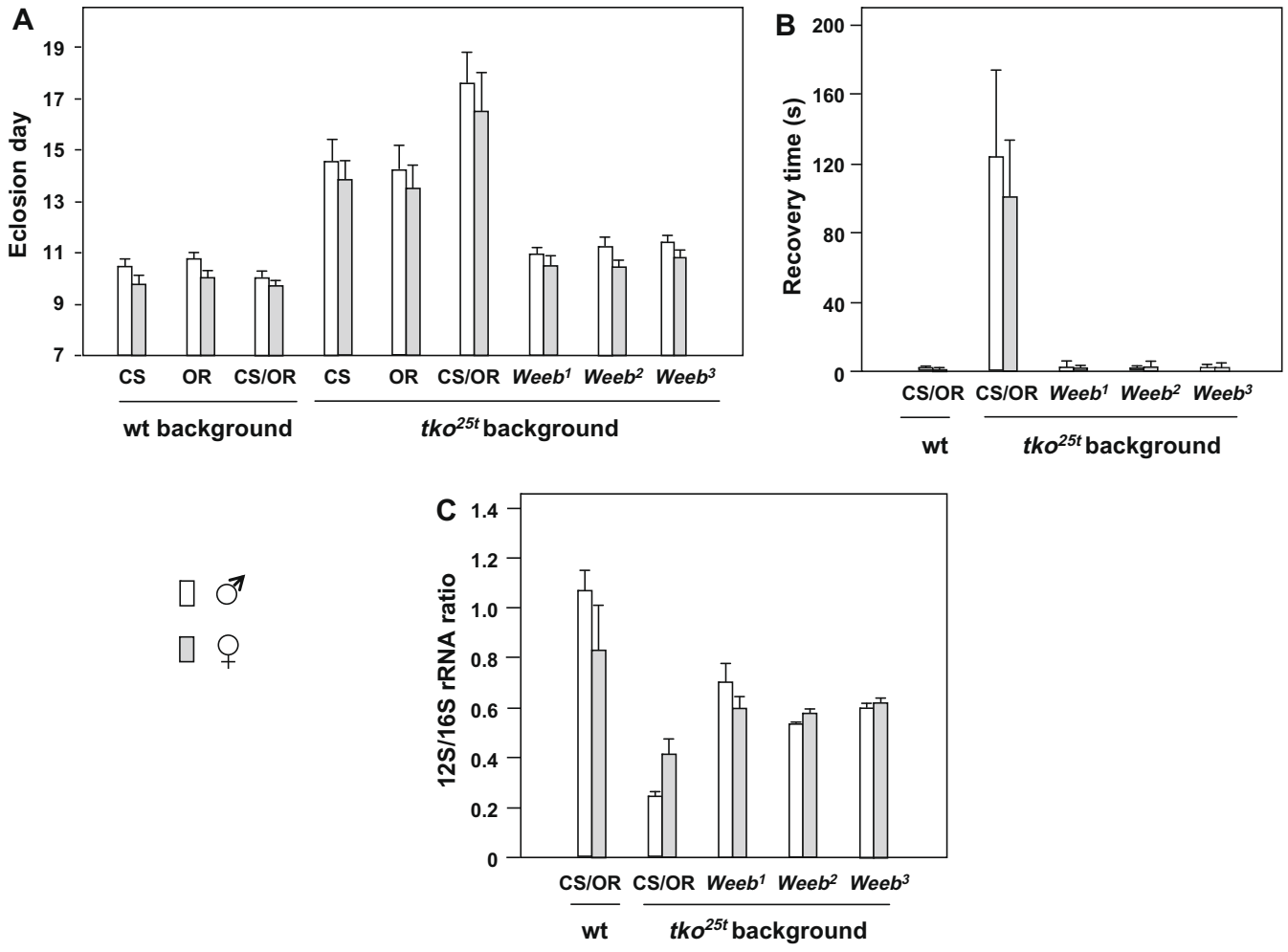

Fig. 1. *Phenotypic suppression of tko*^{25t} *by Weeble*. (A) Mean eclosion day + SD of flies of the strains, sex and genotypes indicated, at 25 °C. CS – Canton S, OR – Oregon R, CS/OR – F1 hybrid of Canton S females and Oregon R males. Where indicated as *tko*^{25t} background, *tko*^{25t} was backcrossed into each of the wild-type strains over >12 generations, and the F1 hybrid was thus between Canton S females homozygous for *tko*^{25t} and Oregon R males hemizygous for *tko*^{25t}, which is located on the X-chromosome. The suppressors *Weeb*^{1}, *Weeb*^{2} and *Weeb*^{3} were obtained as described in the text. (B) Bang-sensitivity (mean recovery time from paralysis induced by vortexing, ±SD) of newly eclosed adult flies of the strains, sex and genotypes indicated. (C) Ratio of 12S to 16S rRNA in adult flies of the strains, sex and genotypes indicated, means + SD, based on Q-RT-PCR.

and *Weeb* are closely linked, then most red-eyed males should eclose before their white-eyed male sibs. From the results (Fig. 2A), it is clear that *Weeb*^{1} does indeed map close to *w*. A conservative estimate, considering all red-eyed progeny eclosing after day 13 as recombinants, would place *Weeb*^{1} within six map-units of *w*, an interval including *tko* itself.

A transcriptomic analysis revealed independently that *Weeb*^{1} and *Weeb*^{2} adult males each showed approximately 2-fold elevated expression of most members of a contiguous set of genes in overlapping segments of the X-chromosome, including *tko* (Fig. 2B), suggesting gene duplication as the mechanism of suppression. An increased copy number of the mutant *tko* gene in both *Weeb*^{1} and *Weeb*^{2} males was confirmed by Southern blotting (Fig. 2C). The gene *CG8636*, some 167 kb to the right of *tko*, and located amongst a group of genes showing 2-fold elevated expression in *Weeb*^{2} but not in *Weeb*^{1}, was found by Southern blotting to have elevated copy number in *Weeb*^{2} but not *Weeb*^{1}. A gene outside of the region which had shown elevated expression, *CG12498*, was at normal copy number in both *Weeb*^{1} and *Weeb*^{2}. To investigate the issue further, Q-PCR was carried out on genomic DNA of males from the *Weeble* lines, using primer pairs specific for *tko* and for each of a number of genes or non-coding DNA elements from the surrounding region of the X-chromosome. This confirmed the duplication of *tko* in both *Weeb*^{1} and *Weeb*^{2}, as well as in *Weeb*^{3} (Fig. 2D). In all cases, the duplication was inferred to span a region of the X-chromosome in which *tko* was positioned approximately centrally. The left break-point of the duplication in all three *Weeble* lines was mapped to a non-coding region between the right end of the transposable element Tirant 24, and the gene *CG14050*. The right-hand duplication break-point of *Weeb*^{1} was mapped to the region between the genes *trol* and *CG13758*, implying a duplication of approximately 228 kb, whereas the right-hand beak-point of both *Weeb*^{2} and *Weeb*^{3} was located a further 60–65 kb along the chromosome, between the genes *CG8636* and *Tsp3A*.

3.3. Autosomal *tko*^{25t} and mRpL14 transgenes do not suppress the *tko*^{25t} mutant phenotype

Previous data indicated clearly that additional, ectopic copies of the mutant *tko* gene in the *tko*^{25t} background did not confer any significant phenotypic rescue, even where these transgenes were expressed in adult flies at up to several times the expression level of the endogenous *tko* gene (Toivonen et al., 2003). We noted that the duplicated interval in the three *Weeble* suppressors of *tko*^{25t} also included the gene for a second mitoribosomal protein *mRpL14*. We reasoned that phenotypic suppression of *tko*^{25t} might require additional copies of both *mRpL14* and *tko*^{25t}. To test this we established transgenic lines carrying additional, ectopic copies of *mRpL14* and crossed them into the *tko*^{25t} background with or without additional transgenic copies of *tko*^{25t}, then tested for any rescue of the *tko*^{25t} mutant phenotype. To minimize any transgene-specific, chromosome-specific or other background effects, we conducted all experiments in the same Canton S/Oregon R *tko*^{25t} F1 hybrid background as used to profile the effects of *tko*^{25t} and the suppression by *Weeble*. The presence of an *mRpL14* transgene failed to rescue developmental delay (Fig. 3A and B). Ectopic copies of the mutant allele *tko*^{25t} produced, as previously, no rescue of bang-sensitivity (Fig. 3C) and only a minimal rescue of developmental delay (Fig. 3A and B), even in the case of flies carrying the *tko*^{25t} transgene *P*{*tko*^{25t}(A3)} on chromosome 2, which were found to express *tko*^{25t} in males at approximately 5-fold higher levels than the original mutant (Fig. 3D). The combination of an *mRpL14* and a *tko*^{25t} transgene produced no further improvement in phenotype (Fig. 3A–C), even though both transgenes were expressed in such adults at levels comparable with their expression in *Weeb*^{1} adults (Fig. 3D). The ratio of 12S to 16S rRNA in adult females carrying the *P*{*tko*^{25t}(A3)} transgene was the same as in adult *tko*^{25t} females (Fig. 3E), although there was a partial rescue towards a more wild-type ratio in males. However, the ratio remained lower than in *Weeb*^{1} adults. The additional presence of the *mRpL14* transgene did not affect the 12S:16S rRNA ratio.

3.4. Increased dosage of *tko*^{25t} in its normal chromosomal context is necessary and sufficient for action of the Weeble suppression

Extra copies of both *mRpL14* and *tko*^{25t}, producing 2-fold elevated expression of each of these genes in adults, thus gave only a minimal phenotypic rescue, whereas local duplication of the region of the X-chromosome containing these genes gave substantial rescue even in females containing the duplication on only one X-chromosome (Supplementary Figs. 2B and C; Fig. 3). Since the transgenic constructs used for both *mRpL14* and *tko*^{25t} contained all intronic and flanking DNA, including regions overlapping the upstream transcription unit and extending at least a further 0.5 kb downstream, this finding implies that some other, more distant sequence element within the duplication must be involved in the phenotypic rescue, and that doubled expression of both genes in adult flies is insufficient to bring about suppression of the *tko*^{25t} mutant phenotype. To confirm and investigate this issue further, we set up crosses to combine *Weeble* X-chromosomes with test chromosomes containing deletions or point mutations of the *tko* region. All three *Weeble* chromosomes in combination with the null allele *tko*^{3} gave a female phenotype that was still completely mutant, both for developmental delay (Fig. 4A) and bang-sensitivity (Fig. 4B). Consistent with this, the *tko*^{25t} mutant phenotype was regenerated by combining any of the *Weeble* chromosomes with an X-chromosomal deletion including the *tko* gene, but not with X-chromosomal deletions affecting flanking regions that do not include *tko* (Fig. 4C and D). Finally, the combination of *Weeb*^{1} *and tko*^{3} on the X-chromosome retained the mutant phenotype even when an expressed, ectopic copy of *tko*^{25t} was also present (Fig. 4E). Thus, although increased gene dosage of *tko*^{25t} is required for suppression, it must be in its natural chromosomal context to be effective.

4. Discussion

Previously we found that ectopic, expressed copies of the mutant *tko*^{25t} gene failed to complement the *tko*^{25t} mutation (Toivonen et al., 2001, 2003). In the present study, we isolated three suppressors of *tko*^{25t}, carrying overlapping duplications of a portion of the X-chromosome including the (mutant) *tko*^{25t} allele (Fig. 2). These *Weeble* suppressors showed almost complete rescue of the *tko*^{25t} mutant phenotype, with restoration of the ratio of 12S to 16S rRNA to an intermediate level (Fig. 1). The *Weeble* duplications include a second mitoribosomal protein gene, *mRpL14* (Fig. 2), but ectopic, expressed copies of it had no effect on phenotype, even when combined with ectopic *tko*^{25t} (Fig. 3). Finally, combining *Weeble* and other chromosomes in various combinations (Fig. 4) led to the conclusion that suppression requires additional copies of *tko*^{25t} in their correct chromosomal milieu.

4.1. Molecular mechanism of suppression

Ectopic expression of wild-type *tko* results in complementation of the *tko*^{25t} mutant phenotype (Toivonen et al., 2001, 2003; Jacobs et al., 2004), whereas similar expression of the mutant allele does not (Toivonen et al., 2001, 2003; Fig. 3). The fact that the 12:16S rRNA ratio was only restored to an intermediate level, even when the organismal phenotype was virtually wild-type, implies the operation of rather sharp threshold effects. If mitoribosome biogenesis falls below such a threshold, we posit that mitochondrial

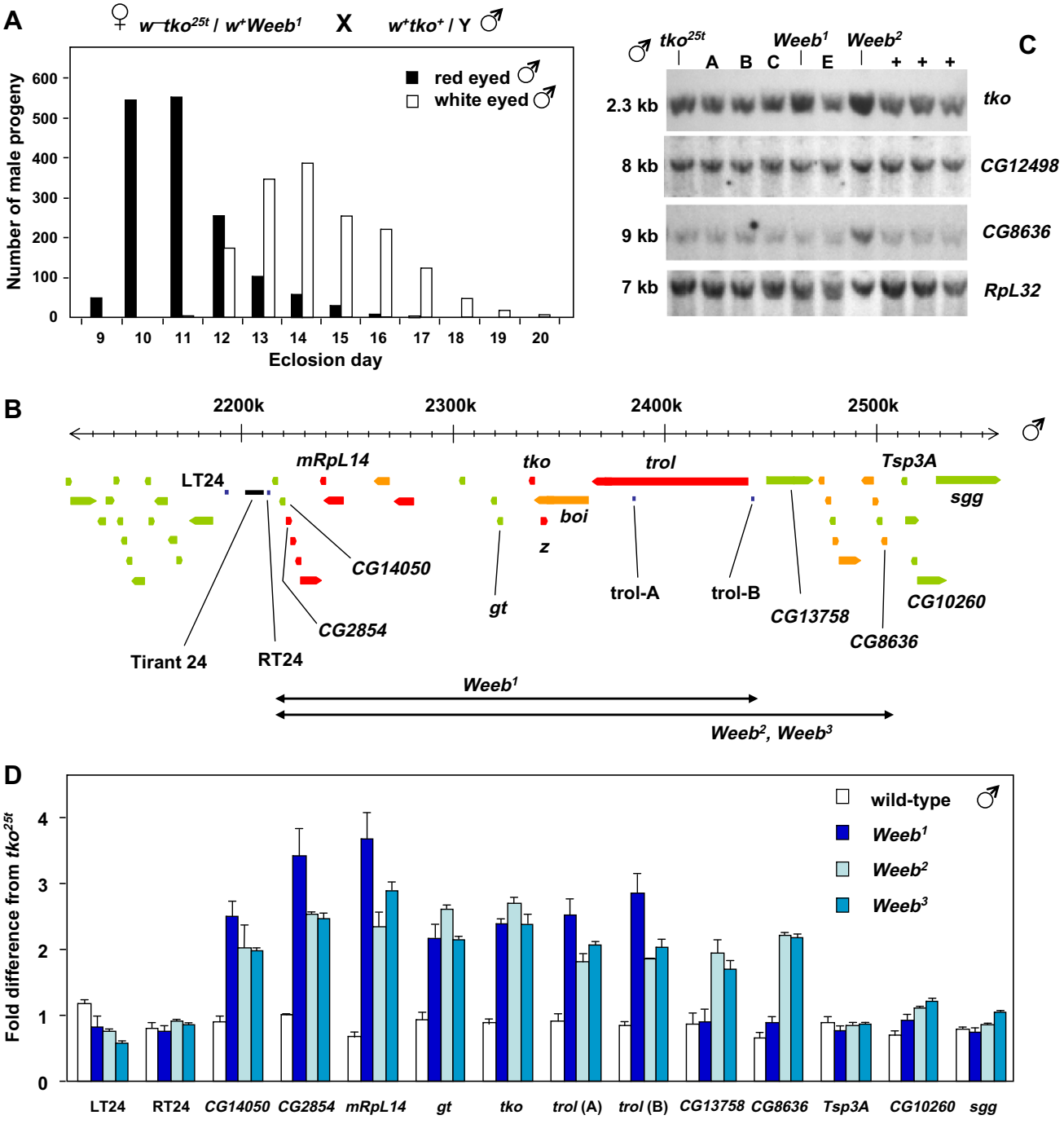

Fig. 2. *Mapping of Weeble suppressors of tko^{25t}.* (A) Eclosion-day profiles of red- and white-eyed male progeny in test cross of w^{-} tko^{25t}/w^{+} Weeb^{1} females to wild-type males (w^{+}/Y) at 25 °C. (B) Summary of transcriptomic analysis of the tko^{25t} region of the X-chromosome, bar-scale showing physical map position. Genes indicated in red showed 2-fold elevated expression in both Weeb^{1} and Weeb^{2} males compared with both wild-type and tko^{25t} males. Genes indicated in orange showed 2-fold elevated expression in Weeb^{2} only, other genes shown in green. Expression of the gene *sgg*, shown in green, was elevated in both Weeb^{1} and Weeb^{2}, but also in tko^{25t}, hence is shown in green. Black bar indicates position of transposable element Tirant 24, with blue bars showing the positions of non-coding region probes LT24 and RT24 and the *trol* probes trol-A and trol-B. The regions denoted by arrows were inferred to be duplicated in Weeb^{1}, Weeb^{2} and Weeb^{3}, based on the data of part (D). (C) Southern blot of genomic DNAs from males of genotypes indicated (A, B, C, and E – partial suppressors of tko^{25t} (Jacobs et al., 2004)), probed for the genes indicated. (D) Q-PCR copy number analysis of genes from the tko^{25t} region of the X-chromosome, in wild-type, Weeb^{1}, Weeb^{2} and Weeb^{3} males, fold-change relative to tko^{25t} males. Data shown are means + SD from at least three replicates from three independently isolated DNA samples. Based on these data alone, a region including the genes *CG2854* and *mRpL14* might be triplicated in Weeb^{1}, although Southern blot and expression data were more consistent with duplication. For positions of genes and probes see panel (B). Similar analysis of genomic DNAs from females gave qualitatively indistinguishable results.

protein synthesis is no longer sufficient for maintaining physiological homeostasis, resulting in a pathological phenotype, as inferred also in humans (Miller et al., 2004; Saada et al., 2007).

Increased expression of tko^{25t} directed by ectopic tko^{25t} transgenes is associated with a modestly improved 12S:16S rRNA ratio (Fig. 3D and E). However, the expression level of the tko^{25t} mutant allele in adults of these lines is comparable with, or even exceeds that seen in Weeb^{1}, where the 12S:16S rRNA ratio is improved further, and the organismal mutant phenotype is suppressed. The expression level of tko^{25t} in adult flies thus does not correlate

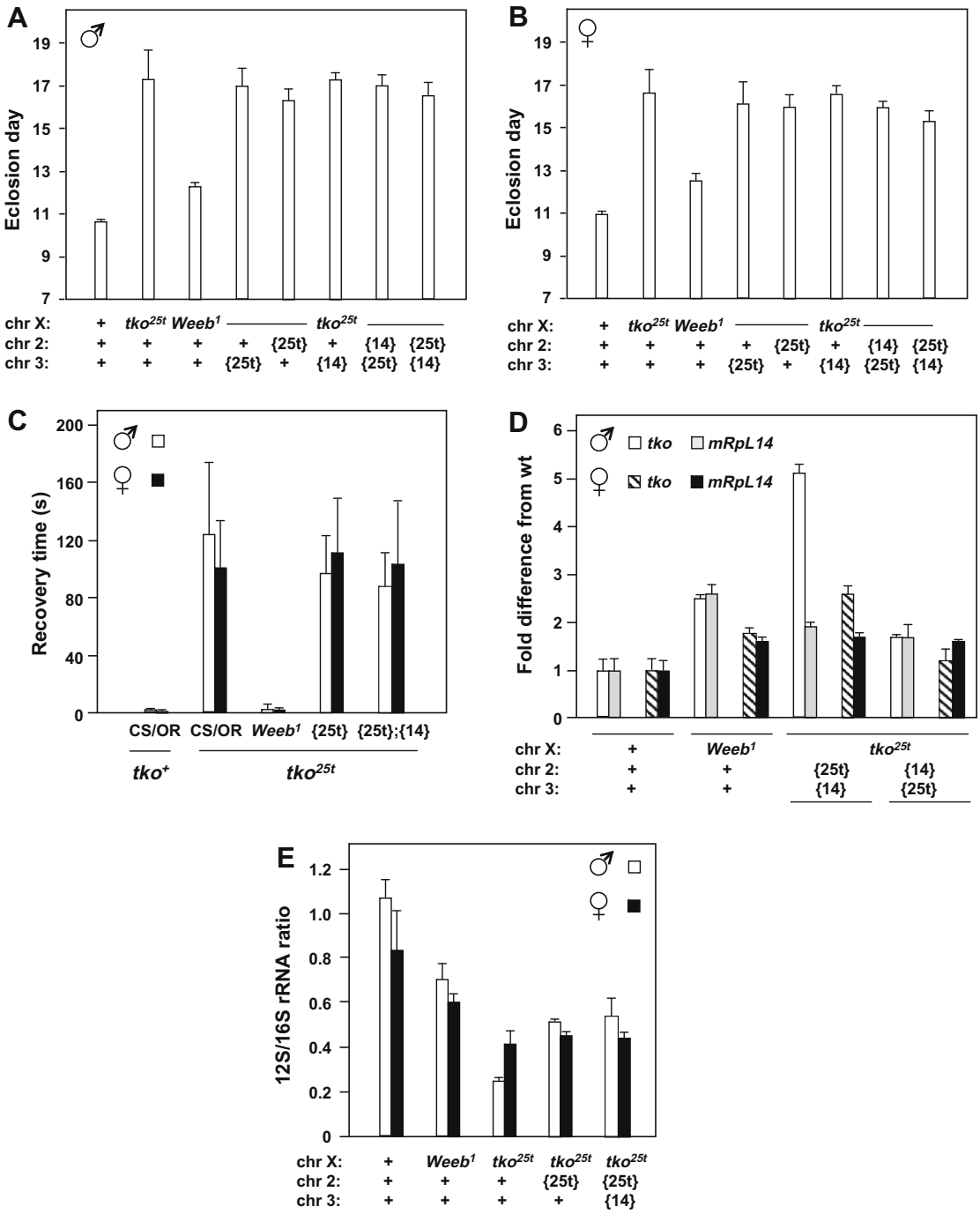

Fig. 3. *Expressed, ectopic copies of tko^{25t} and mRpL14 fail to suppress the tko^{25t} mutant phenotype.* (A) and (B) Mean eclosion day + SD of flies of the sex and genotypes indicated, at 25 °C. {25t} denotes presence of a *tko^{25t}* transgene on the indicated chromosome, i.e. *P*{*tko^{25t}*(A3)}, derived from the original line A3 (Toivonen et al., 2001), on chromosome 2, or *P*{*tko^{25t}*(A1)}, derived from the original line A1 (Toivonen et al., 2001), on chromosome 3. {14} denotes presence of the *P*{*mRpL14*} transgene on the indicated chromosome. (C) Bang-sensitivity (mean recovery time from paralysis induced by vortexing, ±SD) of newly eclosed adult flies of the strains, sex and genotypes indicated. {25t} denotes transgene *P*{*tko^{25t}*(A3)} on chromosome 2, {14} denotes transgene *P*{*mRpL14*} on chromosome 3. (D) Levels of *tko* and *mRpL14* mRNAs in adult flies of the sex and genotypes indicated, fold-change relative to the level of the same mRNA in wild-type flies of the same sex. Transgene nomenclature as in panel (A). (E) Ratio of 12S to 16S rRNA in adult flies of the strains, sex and genotypes indicated, means + SD. Transgene nomenclature as in panel (A). CS/OR denotes F1 hybrids as in Fig. 1. Data for bang-sensitivity and 12S/16S ratio of wild-type, *tko^{25t}* and *Weeb^{1}* are reproduced from panels (B) and (C) of Fig. 1, but were determined in parallel with data from the other strains. Throughout the figure all indicated genotypes were homozygous, except *tko^{25t}* and *Weeb^{1}*, which were hemizygous in males, and *Weeb^{1}* which was heterozygous in females, combined with *tko^{25t}*.

strictly with phenotypic suppression, even though increased gene dosage appears to be necessary for it. One simple way to reconcile these findings is to postulate that the phenotype is determined by the *tko* expression level at an earlier, perhaps specific time in development, or in a restricted set of cells, for which the RNA level in whole adult flies is not a good marker. Alternatively, the *tko* mRNA level may not correlate with synthesis of the *tko* protein, which could depend on expression of another function supplied in *cis*. Some other genes in the duplicated region, with undiscovered roles in mitoribosome biogenesis, may contribute to the phenotypic rescue. However, there are no good candidates, and the experiments shown in Fig. 4 imply that their role, if any, must be minor.

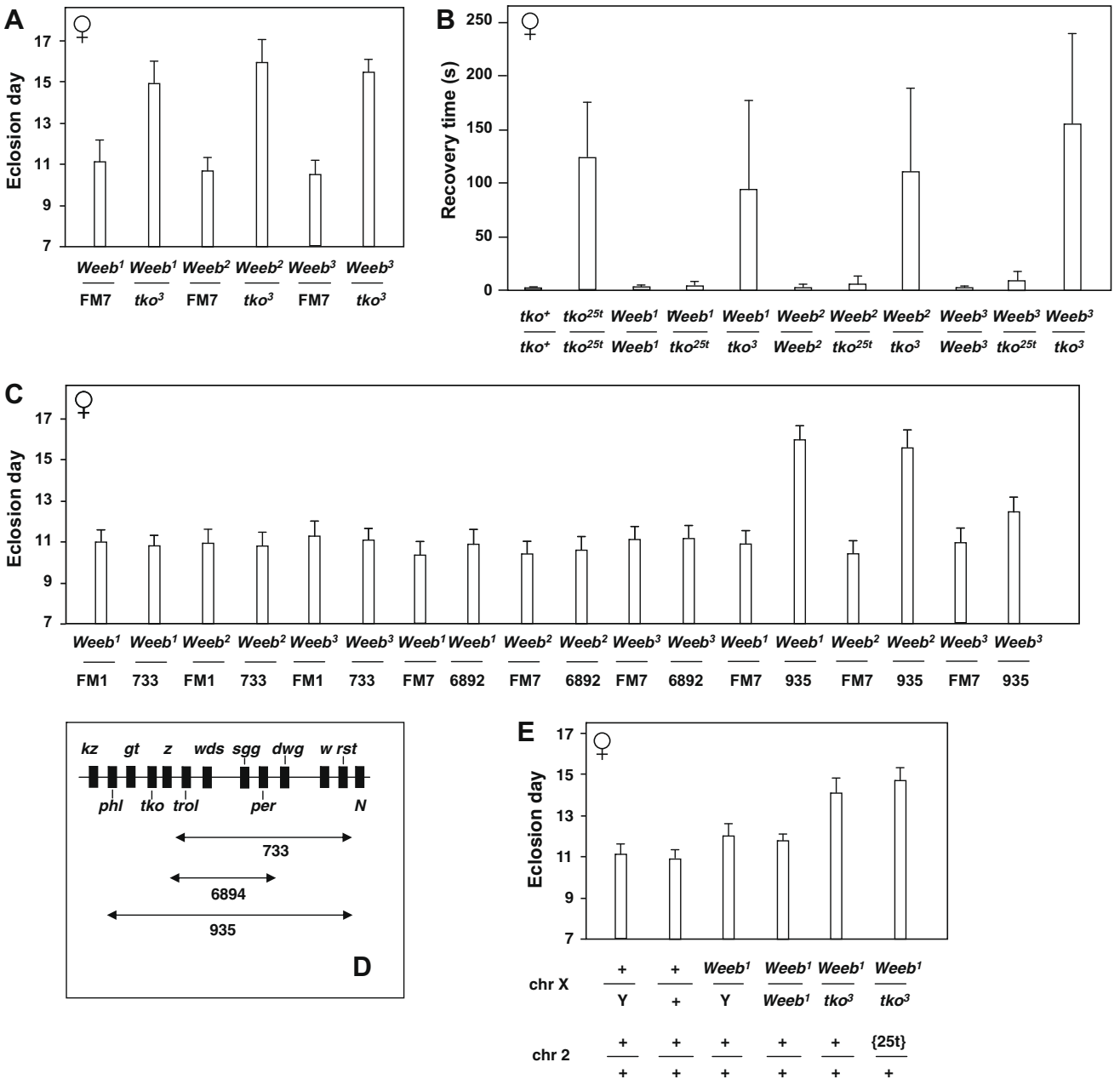

Fig. 4. *Weeble suppression requires increased gene dosage of tko^{25t}.* (A), (C), and (E) Mean eclosion day and (B) bang-sensitivity (±SD) of adult female flies of the indicated X-chromosomal and second chromosomal genotypes. {25t} denotes the *P*{*tko^{25t}*(A3)} transgene on chromosome 2. FM1 and FM7 are balancer chromosomes wild-type for *tko*. *tko^{3}* is a null point mutant of *tko*; 733, 6894 and 935 are Bloomington stock numbers of deletion mutants, as shown in (D), a schematic map of the *tko* region of the X-chromosome (see Section 2 for full genotypes). Genes indicated by standard symbols, not to scale.

4.2. Cis-regulation of tko expression

An additional copy of the mutant gene on the X-chromosome complements the *tko^{25t}* mutant phenotype, whereas an ectopic copy does not. The transgenic construct used to create the ectopic lines contains a 3.2 kb insert of genomic DNA from the *tko^{25t}* mutant strain (Fig. 5). This includes the entire *tko* coding sequence, the single intron, the full 5′ and 3′ untranslated (utr) sequences of *tko* mRNA, plus 1027 bp of 5′ flanking and 539 bp of 3′ flanking DNA. The 5′ flanking DNA includes 677 bp of overlap with the 3′ utr of the mRNA of the upstream gene, *boi* (*brother of iHog*). We infer that this transgenic construct must lack more distant regulatory information directing expression at a critical developmental stage or cell-type, or else responding directly to mitochondrial stress.

Enhancers and other regulatory elements of *Drosophila* genes are generally located in the kilobase of 5′ flanking DNA, plus the first intron and occasionally the 3′ flanking region, although many exceptions are known, including some genes finely regulated during development. The Hox genes, for example, are governed by compartment-specific enhancers located sometimes tens of kilobases from the transcription start site, often inside very long introns (Zhou and Levine, 1999; Akbari et al., 2008). A recent study showed that even where *cis*-regulatory information such as an enhancer is located close to the gene, distant secondary enhancers, often embedded within other genes, can play an important accessory role in regulation (Hong et al., 2008). Moreover, specific enhancers are able to skip over intervening regulatory elements, including insulators, to activate target genes (Zhou and Levine,

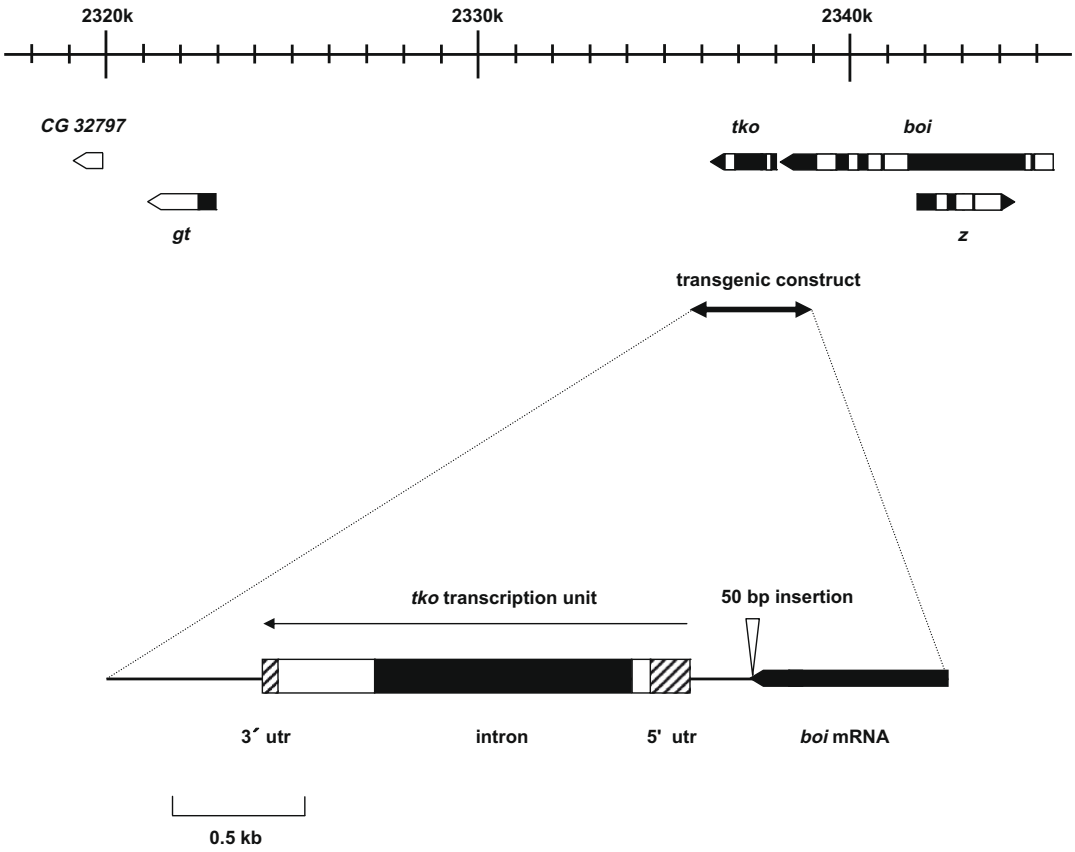

Fig. 5. *Schematic map of tko^{25t} transgenic construct and tko region of X-chromosome.* Bar-scale (top) indicated physical map position. Introns denoted in black, exons in white, untranslated segments of *tko* mRNA cross-hatched.

1999). Another factor influencing the behaviour of *cis*-regulatory sequences is the local chromosomal context, which can determine whether a specific element functions as an activator or insulator (Soshnev et al., 2008). Major chromosomal rearrangements, such as the *Weeble* duplications, may disturb or modify the action of such context-dependent elements. Regulation by very distant elements is also seen in mammalian genomes (Kleinjan and van Heyningen, 2005). Based on these precedents, we propose that *tko* expression is regulated in a developmentally specific manner by distant X-chromosomal elements, whose action might depend on signalling of OXPHOS insufficiency, as we have shown recently for the promoter of the mammalian *tko* homologue *Mrps12* (Zanotto et al., 2008).

The location of such response elements need not be within the region duplicated in the *Weeble* strains. However, an obvious candidate location would be within the 13 kb non-coding region immediately downstream of *tko* (Fig. 5), although such expanses are relatively common in the *Drosophila* genome (nine more are found within 500 kb of *tko*, for example). The segment downstream of *tko* contains no transposable elements or any other type of repetitive DNA. However, it does contain two non protein-coding transcribed regions, one of which has a short region conserved in *Drosophila erecta*.

The region upstream of the *tko* transcription unit comprises only 200 bp before the 3′ end of *boi*, but includes also a 50 bp insertion found in *tko*^{25t} but not in wild-type genomic DNA. Regulatory elements influencing *tko* may also lie within the *boi* transcription unit, which extends a further 26 kb upstream and overlaps that of *zeste* (*z*) on the opposite strand. To identify such element(s) by conventional transgenesis would be a major undertaking. Defining the critical cell-types and developmental stages for rescue, using the GAL4 system, may facilitate an approach using suitable reporter constructs.

Whatever the nature of regulation by distant elements, it is clearly unnecessary for phenotypic complementation by the wild-type allele, which brought about complete rescue and even full dosage compensation in males, using the equivalent construct (Toivonen et al., 2003). The hypothesized distant element is thus required only to boost expression of the hypomorphic *tko*^{25t} allele.

4.3. Mitochondrial disease relevance

As far as we are aware, segmental duplication of a chromosome region is unprecedented as a mechanism of suppression of a missense mutation. However, there are many cases where such a lesion is associated with pathology, attributable to abnormal gene dosage (Lupski, 1998). For example, Charcot–Marie Tooth Disease Type 1A is most commonly associated with a 1.5 Mb duplication on human chromosome 17 (Lupski et al., 1991; Valentijn et al., 1992), which includes the gene for peripheral myelin protein 22 (*PMP-22*). Many cases of Pelizaeus–Merzbacher syndrome result from a contiguous gene duplication on the X-chromosome (Ellis and Malcolm, 1994; Woodward et al., 2005) which can vary in size from 0.1–4.6 Mb. Germline duplications have been reported to cause autism (Ullmann et al., 2007) and early-onset Alzheimer dementia (Rovelet-Lecrux et al., 2006), and somatic duplications are commonly associated with the development and progression of many types of cancer (Redon et al., 2006). Examples are also known where segmental duplications provide protection against pathological insults. The copy number of the *CCL3L1* chemokine receptor gene influences both HIV susceptibility (Gonzalez et al., 2005) and the risk of developing the auto-immune disease sys-

temic lupus erythaematosus (Mamtani et al., 2008), which is also affected by *FCGR3* gene copy number (Aitman et al., 2006).

Segmental duplications with no obvious phenotype are common in humans and other species (see http://www.projects.tcag.ca/variation). The human genome contains a surprisingly large number, covering approximately 6% of the genome in 'wild-type' individuals (Bailey and Eichler, 2006), and these have been postulated to provide an important reservoir of genetic variation (Redon et al., 2006; Bailey and Eichler, 2006; Jakobsson et al., 2008; Shen et al., 2008; Symmons et al., 2008). Our findings may thus have a more general relevance in mitochondrial disease. Copy number variation (CNV) and single-nucleotide polymorphisms (SNPs) both contribute to inter-individual differences in gene expression, and both may play roles in the expression of mitochondrial disease phenotypes. In mitochondrial diseases, especially those caused by mutations in genes for the protein synthetic apparatus such as tRNAs, there is a wide range of phenotypic variation, both in severity and tissue-specificity (Zeviani and Di Donato, 2004; Wong, 2007; Haas et al., 2007). Whilst some of this is explicable by heteroplasmy, variable expression of many genes involved in mitochondrial protein synthesis is likely to play a ley role. Finding ways to enhance their expression might therefore be a useful approach therapeutically.

The *tko*^{25t} mutation results in a deficiency of mitoribosomal small subunits, causes by their defective assembly or instability (Toivonen et al., 1999, 2001). In bacterial ribosomes S12 is one of the second group of polypeptides to be assembled (Culver, 2003), but is also an essential component of the small subunit. Increased expression of the mutant *tko* protein may thus compensate partially for the inefficiency of its incorporation into assembled subunits. However, pathological mutants in *MRPS16* and *MRPS22* have a similar mitoribosome assembly phenotype (Miller et al., 2004; Saada et al., 2007; Emdadul Haque et al., 2008), therefore increased expression of *MRPS12* alone may be insufficient to alleviate defects in mitochondrial translation. Further studies of mitoribosome assembly may reveal a limiting step that could provide a useful pharmacological target. Another type of target might be transacting factors governing the machinery of mitochondrial biosynthesis more globally, such as nuclear respiratory factors NRF-1 and NRF-2 (Scarpulla, 2008), NF-Y (Fontanesi et al., 2008; Zanotto et al., 2008) or co-activators of the PGC-1 family (Lin et al., 2005; Scarpulla, 2008).

Acknowledgements

We thank Academy of Finland, Juselius Foundation, Tampere University Hospital Medical Research Fund and the EU (EUMITOCOMBAT project) for financial support. We are indebted to Tea Tuomela, Tuomas Brock and Rami Kurimo for technical assistance. We thanks also Johanna Schleutker and John Armour for useful discussions on segmental duplications.

Appendix A. Supplementary material

Supplementary data associated with this article can be found, in the online version, at doi:10.1016/j.mito.2009.07.002.

References

Aitman, T.J., Dong, R., Vyse, T.J., Norsworthy, P.J., Johnson, M.D., Smith, J., Mangion, J., Roberton-Lowe, C., Marshall, A.J., Petretto, E., Hodges, M.D., Bhangal, G., Patel, S.G., Sheehan-Rooney, K., Duda, M., Cook, P.R., Evans, D.J., Domin, J., Flint, J., Boyle, J.J., Pusey, C.D., Cook, H.T., 2006. Copy number polymorphism in Fcgr3 predisposes to glomerulonephritis in rats and humans. Nature 439, 851–855.

Akbari, O.S., Bae, E., Johnsen, H., Villaluz, A., Wong, D., Drewell, R.A., 2008. A novel promoter-tethering element regulates enhancer-driven gene expression at the bithorax complex in the drosophila embryo. Development 135, 123–131.

Bailey, J.A., Eichler, E.E., 2006. Primate segmental duplications: crucibles of evolution, diversity and disease. Nat. Rev. Genet. 7, 552–564.

Barolo, S., Carver, L.A., Posakony, J.W., 2000. GFP and beta-galactosidase transformation vectors for promoter/enhancer analysis in drosophila. BioTechniques 29, 726–732.

Culver, G.M., 2003. Assembly of the 30S ribosomal subunit. Biopolymers 68, 234–249.

Ellis, D., Malcolm, S., 1994. Proteolipid protein gene dosage effect in Pelizaeus–Merzbacher disease. Nat. Genet. 6, 333–334.

Emdadul Haque, M., Grasso, D., Miller, C., Spremulli, L.L., Saada, A., 2008. The effect of mutated mitochondrial ribosomal proteins S16 and S22 on the assembly of the small and large ribosomal subunits in human mitochondria. Mitochondrion 8, 254–261.

Fergestad, T., Bostwick, B., Ganetzky, B., 2006. Metabolic disruption in drosophila bang-sensitive seizure mutants. Genetics 173, 1357–1364.

Fontanesi, F., Jin, C., Tzagoloff, A., Barrientos, A., 2008. Transcriptional activators HAP/NF-Y rescue a cytochrome c oxidase defect in yeast and human cells. Hum. Mol. Genet. 17, 775–788.

Gonzalez, E., Kulkarni, H., Bolivar, H., Mangano, A., Sanchez, R., Catano, G., Nibbs, R.J., Freedman, B.I., Quinones, M.P., Bamshad, M.J., Murthy, K.K., Rovin, B.H., Bradley, W., Clark, R.A., Anderson, S.A., O'Connell, R.J., Agan, B.K., Ahuja, S.S., Bologna, R., Sen, L., Dolan, M.J., Ahuja, S.K., 2005. The influence of CCL3L1 gene-containing segmental duplications on HIV-1/AIDS susceptibility. Science 307, 1434–1440.

Haas, R.H., Parikh, S., Falk, M.J., Saneto, R.P., Wolf, N.I., Darin, N., Cohen, B.H., 2007. Mitochondrial disease: a practical approach for primary care physicians. Pediatrics 120, 1326–1333.

Hong, J.W., Hendrix, D.A., Levine, M.S., 2008. Shadow enhancers as a source of evolutionary novelty. Science 321, 1314.

Jacobs, H.T., Fernandez-Ayala, D.J.M., Manjiry, S., Kemppainen, E., Toivonen, J.M., O'Dell, K.M.C., 2004. Mitochondrial disease in flies. Biochim. Biophys. Acta 1659, 190–196.

Jacobs, H.T., Turnbull, D.M., 2005. Nuclear genes and mitochondrial translation, a new class of genetic disease. Trends Genet. 21, 312–314.

Jakobsson, M., Scholz, S.W., Scheet, P., Gibbs, J.R., VanLiere, J.M., Fung, H.C., Szpiech, Z.A., Degnan, J.H., Wang, K., Guerreiro, R., Bras, J.M., Schymick, J.C., Hernandez, D.G., Traynor, B.J., Simon-Sanchez, J., Matarin, M., Britton, A., van de Leemput, J., Rafferty, I., Bucan, M., Cann, H.M., Hardy, J.A., Rosenberg, N.A., Singleton, A.B., 2008. Genotype, haplotype and copy-number variation in worldwide human populations. Nature 451, 998–1003.

Kleinjan, D.A., van Heyningen, V., 2005. Long-range control of gene expression: emerging mechanisms and disruption in disease. Am. J. Hum. Genet. 76, 8–32.

Lin, J.D., Handschin, C., Spiegelman, B.M., 2005. Metabolic control through the PGC-1 family of transcription coactivators. Cell Metab. 1, 361–370.

Lupski, J.R., 1998. Genomic disorders: structural features of the genome can lead to DNA rearrangements and human disease traits. Trends Genet. 14, 417–422.

Lupski, J.R., de Oca-Luna, R.M., Slaugenhaupt, S., Pentao, L., Guzzetta, V., Trask, B.J., Saucedo-Cardenas, O., Barker, D.F., Killian, J.M., Garcia, C.A., Chakravarti, A., Patel, P.I., 1991. DNA duplication associated with Charcot–Marie-Tooth disease type 1A. Cell. 66, 219–232.

Mamtani, M., Rovin, B., Brey, R., Camargo, J.F., Kulkarni, H., Herrera, M., Correa, P., Holliday, S., Anaya, J.M., Ahuja, S.K., 2008. CCL3L1 gene-containing segmental duplications and polymorphisms in CCR5 affect risk of systemic lupus erythaematosus. Ann. Rheum. Dis. 67, 1076–1083.

Miller, C., Saada, A., Shaul, N., Shabtai, N., Ben-Shalom, E., Shaag, A., Hershkovitz, E., Elpeleg, O., 2004. Defective mitochondrial translation caused by a ribosomal protein (MRPS16) mutation. Ann. Neurol. 56, 734–738.

Redon, R., Ishikawa, S., Fitch, K.R., Feuk, L., Perry, G.H., Andrews, T.D., Fiegler, H., Shapero, M.H., Carson, A.R., Chen, W., Cho, E.K., Dallaire, S., Freeman, J.L., González, J.R., Gratacòs, M., Huang, J., Kalaitzopoulos, D., Komura, D., MacDonald, J.R., Marshall, C.R., Mei, R., Montgomery, L., Nishimura, K., Okamura, K., Shen, F., Somerville, M.J., Tchinda, J., Valsesia, A., Woodwark, C., Yang, F., Zhang, J., Zerjal, T., Zhang, J., Armengol, L., Conrad, D.F., Estivill, X., Tyler-Smith, C., Carter, N.P., Aburatani, H., Lee, C., Jones, K.W., Scherer, S.W., Hurles, M.E., 2006. Global variation in copy number in the human genome. Nature 444, 444–454.

Rovelet-Lecrux, A., Hannequin, D., Raux, G., Le Meur, N., Laquerrière, A., Vital, A., Dumanchin, C., Feuillette, S., Brice, A., Vercelletto, M., Dubas, F., Frebourg, T., Campion, D., 2006. APP locus duplication causes autosomal dominant early-onset Alzheimer disease with cerebral amyloid angiopathy. Nat. Genet. 38, 24–26.

Saada, A., Shaag, A., Arnon, S., Dolfin, T., Miller, C., Fuchs-Telem, D., Lombes, A., Elpeleg, O., 2007. Antenatal mitochondrial disease caused by mitochondrial ribosomal protein (MRPS22) mutation. J. Med. Genet. 44, 784–786.

Scarpulla, R.C., 2008. Transcriptional paradigms in mammalian mitochondrial biogenesis and function. Physiol. Rev. 88, 611–638.

Scheper, G.C., van der Knaap, M.S., Proud, C.G., 2007. Translation matters: protein synthesis defects in inherited disease. Nat. Rev. Genet. 8, 711–723.

Schon, E.A., 2000. Mitochondrial genetics and disease. Trends Biochem. Sci. 25, 555–560.

Shen, F., Huang, J., Fitch, K.R., Truong, V.B., Kirby, A., Chen, W., Zhang, J., Liu, G., McCarroll, S.A., Jones, K.W., Shapero, M.H., 2008. Improved detection of global copy number variation using high density, non-polymorphic oligonucleotide probes. BMC Genet. 28, 9–27.

Smeitink, J.A., 2003. Mitochondrial disorders: clinical presentation and diagnostic dilemmas. J. Inherit. Metab. Dis. 26, 199–207.

Soshnev, A.A., Li, X., Wehling, M.D., Geyer, P.K., 2008. Context differences reveal insulator and activator functions of a Su (Hw) binding region. PLoS Genet. 4, e1000159.

Symmons, O., Váradi, A., Arányi, T., 2008. How segmental duplications shape our genome: recent evolution of ABCC6 and PKD1 Mendelian disease genes. Mol. Biol. Evol. 25, 2601–2613.

Toivonen, J.M., Boocock, M.R., Jacobs, H.T., 1999. Modeling in Escherichia coli of mutations in mitoribosomal protein S12: novel mutant phenotypes of rpsL. Mol. Microbiol. 31, 1735–1746.

Toivonen, J.M., Manjiry, S., Touraille, S., Alziari, S., O'Dell, K.M.C., Jacobs, H.T., 2003. Gene dosage and selective expression modify phenotype in a Drosophila model of human mitochondrial disease. Mitochondrion 3, 83–96.

Toivonen, J.M., O'Dell, K.M., Petit, N., Irvine, S.C., Knight, G.K., Lehtonen, M., Longmuir, M., Luoto, K., Touraille, S., Wang, Z., Alziari, S., Shah, Z.H., Jacobs, H.T., 2001. *technical knockout*, a drosophila model of mitochondrial deafness. Genetics 159, 241–254.

Ullmann, R., Turner, G., Kirchhoff, M., Chen, W., Tonge, B., Rosenberg, C., Field, M., Vianna-Morgante, A.M., Christie, L., Krepischi-Santos, A.C., Banna, L., Brereton, A.V., Hill, A., Bisgaard, A.M., Müller, I., Hultschig, C., Erdogan, F., Wieczorek, G., Ropers, H.H., 2007. Array CGH identifies reciprocal 16p13.1 duplications and deletions that predispose to autism and/or mental retardation. Hum. Mut. 28, 674–682.

Valentijn, L.J., Bolhuis, P.A., Zorn, I., Hoogendijk, J.E., van den Bosch, N., Hensels, G.W., Stanton Jr., V.P., Housman, D.E., Fischbeck, K.H., Ross, D.A., Nicholson, G.A., Meershoek, E.J., Dauwerse, H.G., van Ommen, G.J., Baas, F., 1992. The peripheral myelin gene PMP-22/GAS-3 is duplicated in Charcot-Marie-Tooth disease type 1A. Nat. Genet. 1, 166–170.

Wong, L.J., 2007. Diagnostic challenges of mitochondrial DNA disorders. Mitochondrion 7, 45–52.

Woodward, K.J., Cundall, M., Sperle, K., Sistermans, E.A., Ross, M., Howell, G., Gribble, S.M., Burford, D.C., Carter, N.P., Hobson, D.L., Garbern, J.Y., Kamholz, J., Heng, H., Hodes, M.E., Malcolm, S., Hobson, G.M., 2005. Heterogeneous duplications in patients with Pelizaeus–Merzbacher disease suggest a mechanism of coupled homologous and nonhomologous recombination. Am. J. Hum. Genet. 77, 966–987.

Zanotto, E., Lehtonen, V., Jacobs, H.T., 2008. Modulation of Mrps12/Sarsm promoter activity in response to mitochondrial stress. Biochim. Biophys. Acta 1783, 2352–2362.

Zeviani, M., Di Donato, S.S., 2004. Mitochondrial disorders. Brain 127, 2153–2172.

Zhang, Y.Q., Roote, J., Brogna, S., Davis, A.W., Barbash, D.A., Nash, D., Ashburner, M., 1999. Stress sensitive B encodes an adenine nucleotide translocase in *Drosophila melanogaster*. Genetics 153, 891–903.

Zhou, J., Levine, M., 1999. A novel cis-regulatory element, the PTS, mediates an anti-insulator activity in the drosophila embryo. Cell 99, 567–575.

The Alternative Oxidase AOX Does Not Rescue the Phenotype of *tko*^{25t} Mutant Flies

Kia K. Kemppainen,*,[1] Esko Kemppainen,*,[1] and Howard T. Jacobs*,†,[2]
*BioMediTech and Tampere University Hospital, FI-33014 University of Tampere, Tampere, Finland and †Research Program of Molecular Neurology, FI-00014 University of Helsinki, Finland

ABSTRACT A point mutation [*technical knockout*^{25t} (*tko*^{25t})] in the *Drosophila* gene coding for mitoribosomal protein S12 generates a phenotype of developmental delay and bang sensitivity. *tko*^{25t} has been intensively studied as an animal model for human mitochondrial diseases associated with deficiency of mitochondrial protein synthesis and consequent multiple respiratory chain defects. Transgenic expression in *Drosophila* of the alternative oxidase (AOX) derived from *Ciona intestinalis* has previously been shown to mitigate the toxicity of respiratory chain inhibitors and to rescue mutant and knockdown phenotypes associated with cytochrome oxidase deficiency. We therefore tested whether AOX expression could compensate the mutant phenotype of *tko*^{25t} using the GeneSwitch system to activate expression at different times in development. The developmental delay of *tko*^{25t} was not mitigated by expression of AOX throughout development. AOX expression for 1 d after eclosion, or continuously throughout development, had no effect on the bang sensitivity of *tko*^{25t} adults, and continued expression in adults older than 30 d also produced no amelioration of the phenotype. In contrast, transgenic expression of the yeast alternative NADH dehydrogenase Ndi1 was synthetically semi-lethal with *tko*^{25t} and was lethal when combined with both AOX and *tko*^{25t}. We conclude that AOX does not rescue *tko*^{25t} and that the mutant phenotype is not solely due to limitations on electron flow in the respiratory chain, but rather to a more complex metabolic defect. The future therapeutic use of AOX in disorders of mitochondrial translation may thus be of limited value.

KEYWORDS
mitochondrial disease
oxidative phosphorylation
gene therapy
seizures
developmental delay

Drosophila provides a useful animal model for human genetic diseases (Lloyd and Taylor 2010; Lu and Vogel 2009), including those associated with mitochondrial dysfunction (Sánchez-Martinez *et al.* 2006, Palladino 2010). Prominent among the latter are the many diseases caused by deficiency or malfunction of components of the machinery of mitochondrial protein synthesis (Pearce *et al.* 2013). These can be caused by point mutations of mitochondrial DNA (mtDNA), by large mtDNA deletions, or by nuclear gene lesions, and can involve interactions with environmental factors, including some antibiotics. Although their clinical phenotypes vary, a common thread is deficiency of multiple respiratory chain complexes, including ATP synthase, which include mtDNA-encoded subunits. The resulting metabolic crisis then produces a developmental and physiological disease condition, which can be widespread, severe, and often fatal.

We have previously investigated a *Drosophila* model of such diseases; *tko*^{25t} carries a (recessive) point mutation in the gene for mitoribosomal protein S12 (Royden *et al.* 1987; Shah *et al.* 1997). *tko*^{25t} flies exhibit developmental delay, sensitivity to seizures induced by mechanical stress ("bang sensitivity"), and a set of linked phenotypes that share features with human mitochondrial disease, including hearing impairment and sensitivity to antibiotics that impair mitochondrial protein synthesis (Toivonen *et al.* 2001). At the molecular level, *tko*^{25t} shows decreased abundance of mitoribosomal small subunits, multiple respiratory chain and ATP synthase deficiency (Toivonen *et al.* 2001), and altered gene expression indicative of a metabolic shift toward glycolytic lactate production and anaplerotic pathways (Fernández-Ayala *et al.* 2010).

The phenotype of *tko*^{25t} flies can be partially suppressed by segmental duplication of the mutant gene in its natural chromosomal milieu (Kemppainen *et al.* 2009), by cybridization to specific suppressor

doi: 10.1534/g3.114.013946
Manuscript received May 1, 2014; accepted for publication August 19, 2014; published Early Online August 21, 2014.

[1]These authors contributed equally to this work.
[2]Corresponding author: BioMediTech, FI-33014 University of Tampere, Finland. E-mail: howard.t.jacobs@uta.fi

cytoplasmic (mtDNA) backgrounds (Chen *et al.* 2012), or by overexpression of *spargel* (Chen *et al.* 2012), the *Drosophila* homolog of PGC1-α, proposed to function as a master regulator of mitochondrial biogenesis (Scarpulla 2011). In other studies, we found that toxic inhibition of complex III (cIII) by antimycin or cIV by cyanide, or phenotypes resulting from mutations or knockdown of cIV subunits or the cIV assembly factor *Surf1* in *Drosophila*, could be mitigated by concomitant expression of the mitochondrial alternative oxidase (AOX) from *Ciona* intestinalis (Fernández-Ayala *et al.* 2009; Kemppainen *et al.* 2014).

AOX is widespread in eukaryotes, being found in plants, fungi, and many animal phyla, although not in arthropods or vertebrates (McDonald *et al.* 2009). It provides a nonproton-translocating bypass of the cytochrome segment of the mitochondrial respiratory chain, maintaining electron flow under conditions in which it would be inhibited by high membrane potential, toxic inhibition, or insufficient capacity of cIII and/or cIV. tko^{25t} flies exhibit multiple respiratory chain deficiency, including profoundly decreased activity of both cIII and cIV (Toivonen *et al.* 2001). However, whereas lactate dehydrogenase can theoretically compensate, at least in part, for the lack of cI (Fernández-Ayala *et al.* 2010), ubiquinone-linked dehydrogenases, such as succinate dehydrogenase (complex II, cII), require the cytochrome chain for onward electron transfer to oxygen to reoxidize ubiquinol. Thus, even though it cannot directly support ATP production, AOX expression in tko^{25t} should facilitate intermediary metabolism, leading to an amelioration of the mutant phenotype if that phenotype is due to limitations on electron flow through cIII and cIV.

We therefore set out to test whether expression of *Ciona* AOX in *Drosophila* at different times in the life-cycle could correct the major organismal phenotypes of tko^{25t}, namely bang sensitivity and developmental delay.

MATERIALS AND METHODS

Flies, maintenance, and behavioral assays

Drosophila lines were as described previously (Toivonen *et al.* 2001; Fernández-Ayala *et al.* 2009; Sanz *et al.* 2010a). Flies were maintained at 25° on standard medium with supplements, as previously described (Fernández-Ayala *et al.* 2009), including RU486 (Mifepristone), with indicated time to eclosion and bang sensitivity at 25° measured as previously described (Toivonen *et al.* 2001).

RNA isolation and analysis

RNA extraction and QRTPCR were performed as previously described (Fernández-Ayala *et al.* 2009). RNA isolations were performed in triplicate from batches of 40 males or 30 virgin females. For QRTPCR, cDNA was synthesized using High-Capacity cDNA Reverse-Transcription kit (Life Technologies, Carlsbad, CA). Analysis used a StepOnePlus instrument (Life Technologies) with the manufacturer's SYBR Green PCR reagents and customized AOX primers and normalization to *RpL32* RNA as previously described (Fernández-Ayala *et al.* 2009).

Metabolic assays

ATP levels in adult female flies were measured as previously described (Chen *et al.*, 2012), along with ATP standards. Mitochondrial reactive oxygen species (ROS) production was measured essentially according to Ballard *et al.* (2007) as hydrogen peroxide produced in whole-body mitochondrial extracts from 2- to 5-d-old females using a substrate mix of 5 mM pyruvate, 5 mM proline, 20 mM sn-glycerol-3-phosphate, and 1 mM ADP.

RESULTS

Transgenic expression of AOX in *Drosophila* using an inducible driver

We previously documented the amount of expression of AOX at the RNA level in transgenic flies containing single and double copies of the UAS-AOX transgene activated by different ubiquitously acting drivers (Fernandez-Ayala *et al.* 2009). In the same study, using the drug-inducible tubulin-GeneSwitch driver (tub-GS), we determined the minimal level of the inducing drug RU486 (10 μM) that would sustain maximal AOX expression throughout development when flies were cultured in drug-containing food. To be able to induce and sustain AOX expression at different times during adult life, we first conducted further tests using the tub-GS driver (Figure 1). Expression of AOX was induced in 1-d-old adults using different concentrations of RU486 and was measured 24 hr later using UAS-AOX–bearing flies with no driver or with the highly active da-GAL4 driver as controls (Figure 1A). Even without drug, the tub-GS driver supported AOX expression at a three-fold to 10-fold higher level than in the absence of any driver. As observed previously using various drivers (Fernandez-Ayala *et al.* 2009), expression in males was always approximately three-fold higher than in females, which is probably a feature of the standard UAS transgenic construct and/or dosage compensation elements associated with the linked mini-white marker gene. RU486 even at low doses increased expression at least 10-fold further, and expression reached a plateau at a drug concentration of 100 μM. To be sure of fully activating expression, we thereafter routinely used 200 μM RU486 as the activating condition.

Next, we determined the kinetics of induced expression and the effects of sustained drug exposure or its withdrawal (Figure 1, B and C). AOX expression already reached a plateau level after 1 d of drug exposure in females (Figure 1B) and males (Figure 1C); thereafter, it remained constant if flies were maintained on drug-containing food. If drug was withdrawn by switching to drug-free food at day five, then expression decreased to a new plateau level by 1 d later. However, this level was two-fold to three-fold higher than that of flies never exposed to drug. Flies endowed with UAS-AOX and tub-GS were cultured continuously on RU486-containing food for many weeks and remained phenotypically indistinguishable from flies grown on drug-free food.

Adult-specific induction of AOX does not rescue bang sensitivity of tko^{25t}

Bang sensitivity is generally considered to arise from a functional defect of nerve conduction during high-frequency stimulation in the giant fiber pathway (Pavlidis and Tanouye 1995; Lee and Wu 2002; Fergestad *et al.* 2006; Ueda *et al.* 2008). Bang-sensitive mutants with an underlying mitochondrial defect, including *kdn* (citrate synthase) and $sesB^{1}$ (adenine nucleotide translocase) as well as tko^{25t} display a characteristic seizure pattern (Fergestad *et al.* 2006). We therefore decided to test whether expression of AOX in tko^{25t} mutant flies could compensate for the mitochondrial defect and thus alleviate bang sensitivity. We crossed tub-GS into the tko^{25t} background using a balancer chromosome strategy to analyze progeny from a single experimental cross that generated flies carrying tko^{25t}, tub-GS, and/or UAS-AOX in all eight possible combinations. Bang sensitivity was tested in 2-d-old males and females of each class, either with or without transfer 24 hr earlier to food containing 200 μM RU486 (Figure 2). Unambiguously, the results indicate that AOX is unable to modify the bang-sensitive phenotype of tko^{25t} adults, and it does not induce any detectable bang sensitivity in control flies. In fact, applying Student's *t* test with Bonferroni correction confirmed that there were no significant

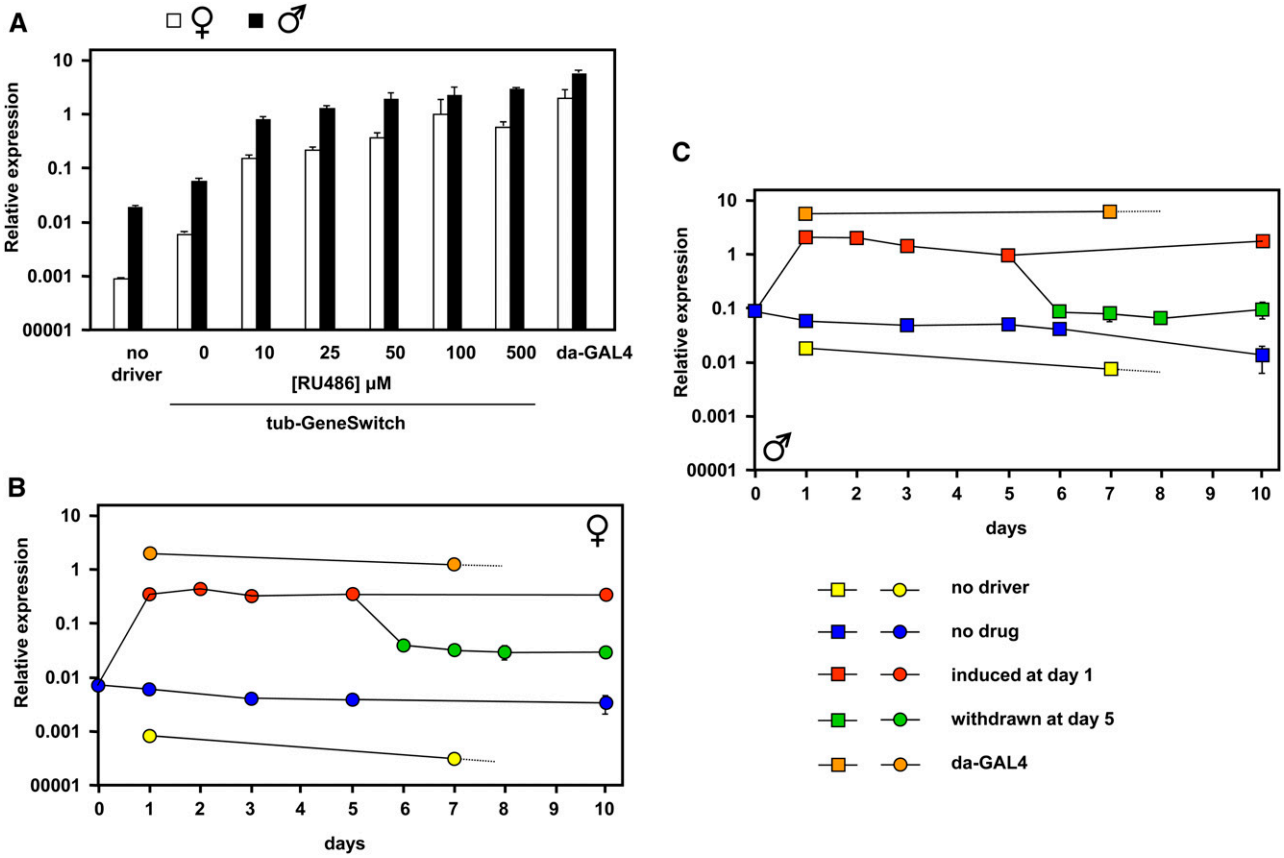

Figure 1 AOX expression in adult flies driven by tubulin-GeneSwitch. (A) Relative AOX expression, determined by QRTPCR normalized to *RpL32* control RNA, in 2-d-old UAS-AOX flies bearing the drivers indicated exposed to different concentrations of RU486 for 24 hr. Means ± SD of three biological replicates. Note the logarithmic scale. (B and C) Relative AOX expression in adult UAS-AOX flies bearing the indicated drivers and exposed to 200 μM RU486 as shown. Means ± SD of three biological replicates.

differences between any of the classes that were mutant for *tko*^{25t}, irrespective of sex, transgene, driver, or RU486 induction. Similarly, there were no significant differences between any of the classes that were wild-type for the *tko* gene, irrespective of these other parameters. As expected, the difference between *tko*^{25t} mutant flies of each class and the corresponding class without *tko*^{25t} was significant ($P < 0.01$) in every case.

Continuous induction of AOX throughout development does not rescue *tko*^{25t}

Considering an alternative hypothesis, that the bang-sensitive phenotype of *tko*^{25t} is established during development, we conducted similar crosses but used fly food containing RU486. In our previous study (Fernandez-Ayala *et al.* 2009), we established that 10 μM RU486 was sufficient to induce maximal transgene expression during the larval stages, so we

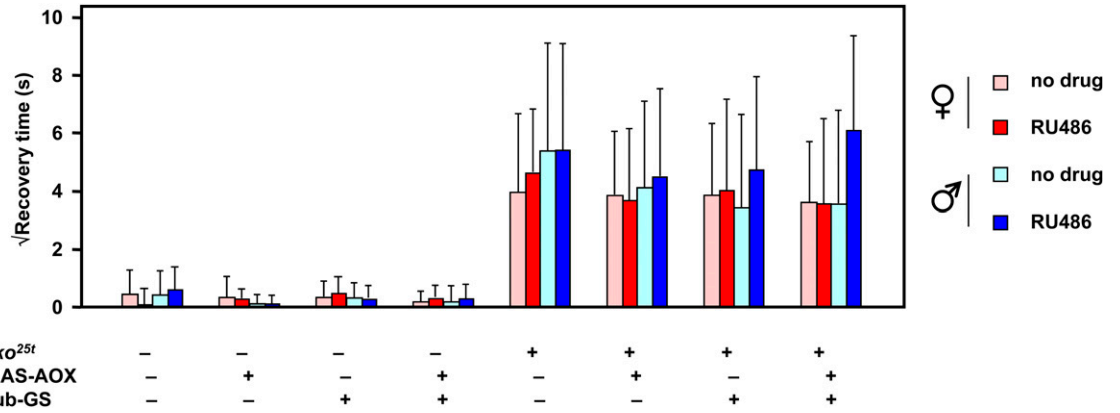

Figure 2 Bang sensitivity is unaffected by AOX induction in adult flies. Bang sensitivity (square-root of recovery time from vortexing) of 2-d-old flies of the sex and genotype indicated, with or without 24 hr of prior treatment with 200 μM RU486. Means ± SD for groups of 30 individually analyzed flies.

used this concentration of the drug along with drug-free control vials. This procedure allowed us also to analyze effects on the second canonical phenotype of *tko*^{25t}, developmental delay, which was previously found to occur uniquely during the larval (growth) stages (Toivonen *et al.* 2001).

Once again, we observed no rescue of the mutant phenotype that was attributable to AOX expression (Figure 3). The developmental delay of *tko*^{25t} mutant flies (Figure 3A) was slightly greater in males than in females, as observed previously (Kemppainen *et al.* 2009), and an additional delay of approximately 1 d was produced in flies of all genotypes and both sexes by the presence of RU486 in the food. The UAS-AOX transgene, the tub-GS driver, and the two in combination did not produce any significant change in developmental timing of *tko*^{25t} mutant flies, although there was a slight delay produced by AOX expression in wild-type flies, as reported previously using the da-GAL4 driver. The bang sensitivity of the progeny flies showed no significant change according to any of the parameters tested, except for the presence of the *tko*^{25t} mutation itself (Figure 3B).

Prolonged adult induction of AOX does not rescue bang sensitivity of *tko*^{25t}

To test whether correction of the *tko*^{25t} phenotype in adult flies requires long-term expression of AOX, we cultured *tko*^{25t} flies generated in the previous crosses continuously for a period of 30 d on food either with or without RU486 at the inducing concentration of 200 μM, noting the previous result that sustained expression requires continuous exposure to the drug. This also enabled us to check the stability of the phenotype during adult life, which, to our knowledge, has not previously been studied systematically.

Bang sensitivity was unaffected by any of the parameters tested in this experiment (Figure 4). There was no rescue (or worsening) of the phenotype either by basal or by induced AOX expression, no effect of age, no difference between the sexes, and no effect of tub-GS.

Ndi1 expression during development is lethal to *tko*^{25t}

Because AOX expression at any stage of the fly life-cycle had no effect on the major phenotypic features of *tko*^{25t} mutants, we considered the hypothesis that the steps in mitochondrial electron flow that AOX bypasses may not be crucial determinants of the phenotype. The *tko*^{25t} mutation impacts all four of the enzymatic complexes of the oxidative phosphorylation (OXPHOS) system that contain mitochondrial translation components (Toivonen *et al.* 2001), but it is unclear which is limiting for respiration or ATP synthesis. Because complex I (cI) activity is severely affected by the mutation, we considered the alternative hypothesis that a decreased capacity for electron flow through cI alone underlies the *tko*^{25t} mutant phenotype, and that decreased capacity of complexes III and/or IV is immaterial, thus accounting for a failure of AOX expression to modify the phenotype.

To test this idea, we set-up a genetic cross (Figure 5A) to investigate whether an analogous bypass of cI using the nonproton-pumping NADH dehydrogenase from yeast (Ndi1) could rescue the phenotype. Ndi1 expression was shown previously to be benign in *Drosophila* and to rescue the lethality of severe knockdown of cI subunits (Sanz *et al.* 2010b). We introduced the ubiquitously acting da-GAL4 driver and a UAS-Ndi1 transgene separately into the *tko*^{25t} mutant strain and then crossed females heterozygous both for *tko*^{25t} and UAS-Ndi1 with *tko*^{25t} males carrying da-GAL4 (Figure 5A). The cross repeatedly gave

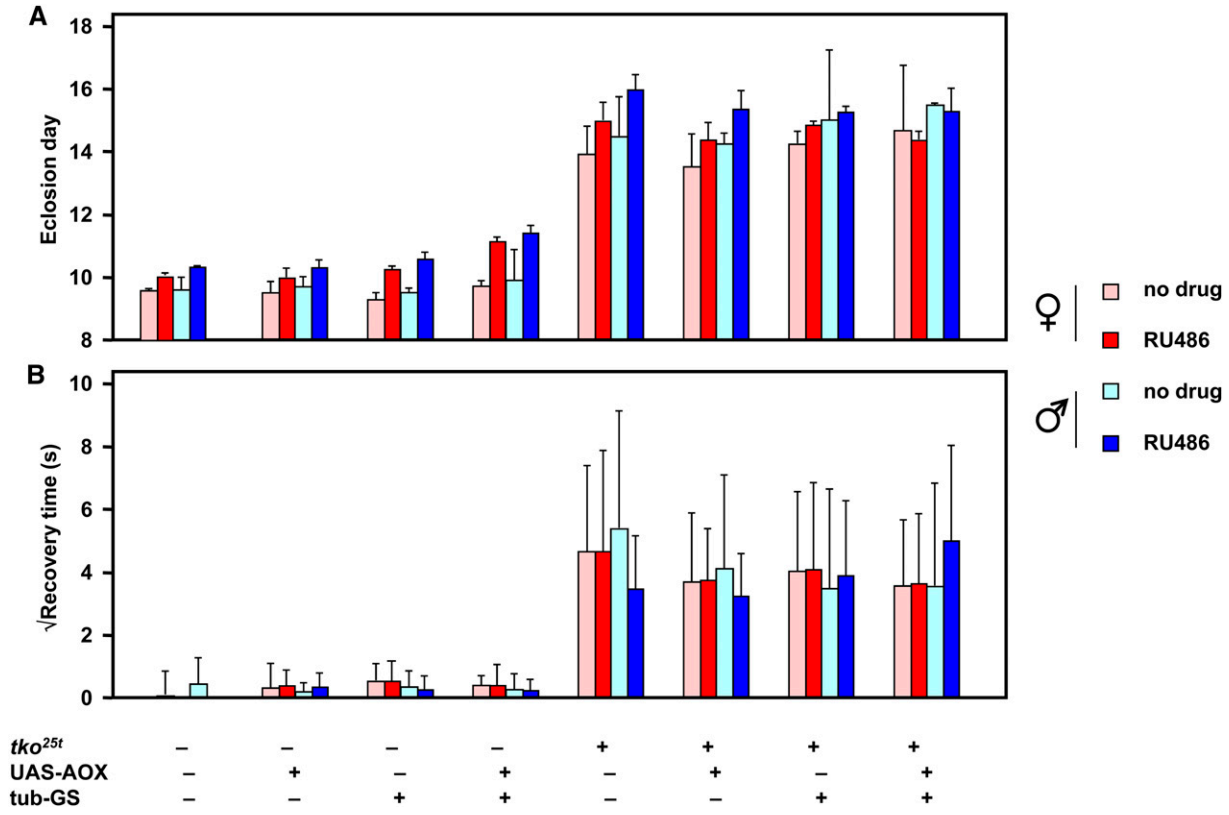

Figure 3 Phenotype of *tko*^{25t} is unaffected by AOX expression throughout development. (A) Eclosion day and (B) bang sensitivity of 1-d-old flies of the sex and genotype indicated, cultured throughout development on medium with or without 10 μM RU486. Means ± SD based on eclosion data from three replicate experiments and bang sensitivity of groups of 50 individually analyzed flies.

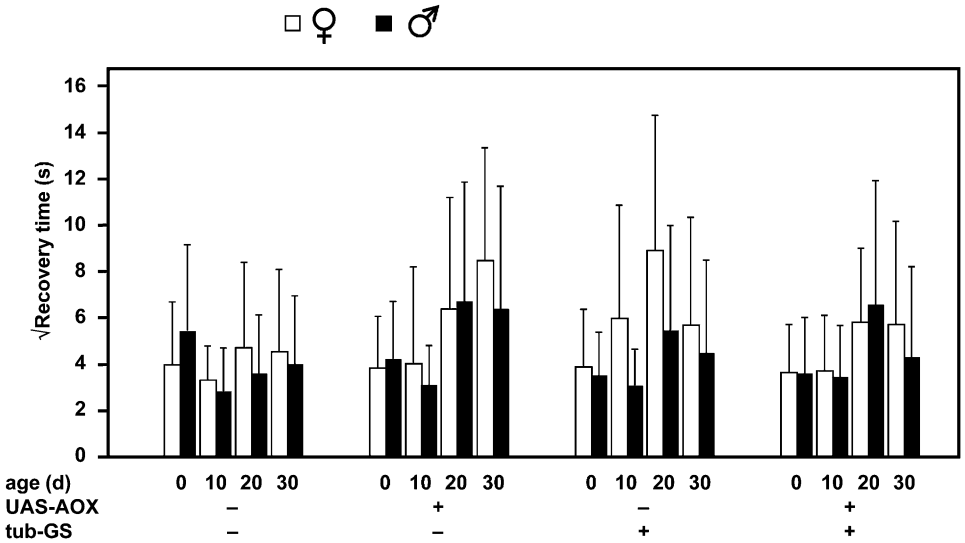

Figure 4 Bang sensitivity is unaffected by continuous AOX expression over 30 d. Bang sensitivity of flies of the sex, genotype, and age indicated, with or without continuous growth as adults on media containing 200 μM RU486. Means ± SD for groups of 50 individually analyzed flies.

a low number of *tko*^{25t} progeny (Table 1). However, almost all of them carried the balancer marker in place of UAS-Ndi1, indicating that the combination of da-GAL4, *tko*^{25t} and UAS-Ndi1 is semi-lethal. Expression of Ndi1 in *tko*^{25t} heterozygotes had a far less dramatic effect. We conclude that, far from rescuing *tko*^{25t}, expression of Ndi1 is selectively deleterious to *tko*^{25t} mutant flies.

This result raises the possibility that although neither Ndi1 nor AOX can individually rescue *tko*^{25t}, the co-expression of both transgenes might do so. This would be the case, for example, if the *tko*^{25t} phenotype were due to a combined limitation on electron flow at both cI and at cIII+cIV of similar magnitude. Although co-expression of Ndi1 and AOX at 25° was previously shown to be synthetically lethal even in wild-type flies (Sanz *et al.* 2010b), in trial experiments we were able to obtain co-expressing flies when cultured at 18°. We therefore implemented the experimental cross illustrated in Figure 5B to determine whether Ndi1 and AOX co-expression can rescue *tko*^{25t}. As shown in Table 2, although control flies were now obtained, and again there were only a few Ndi1-expressing flies in the *tko*^{25t} mutant background, no doubly expressing *tko*^{25t} flies eclosed. We conclude that, far from rescuing *tko*^{25t}, combined expression of the two transgenes is more deleterious than of either alone.

Effects on ATP or ROS do not correlate with modulation of *tko*^{25t} phenotype

In previous studies we found decreased steady-state ATP levels in extracts from *tko*^{25t} mutant flies, as well as elevated production of ROS in isolated *tko*^{25t} mitochondria (Chen *et al.* 2012). However, the relevance of these observations to the organismal phenotype remains to be conclusively demonstrated. The effects of AOX and Ndi1 expression on the *tko*^{25t} phenotype provided an opportunity to test this relationship further. To obtain a sufficient number of *tko*^{25t} flies expressing Ndi1 to conduct this experiment, flies were reared at 18° instead of 25° (see previous section).

We confirmed the previous observation of decreased ATP levels in *tko*^{25t} homozygotes compared with heterozygous controls (Figure 6A) but found no significant alteration thereof when either AOX or Ndi1 was expressed. Mitochondrial ROS production in *tko*^{25t} homozygotes was also elevated in every case compared with heterozygous controls (Figure 6B). This was unaffected by expression of AOX but modestly alleviated by Ndi1 expression, despite the fact that the effect of Ndi1 on the overall organismal phenotype was deleterious. This, plus the wide variation in ROS production according to genetic background (reflecting different balancer chromosomes), implies that the *tko*^{25t} organismal phenotype is also not directly determined by ROS.

DISCUSSION

In this work we set out to determine whether AOX from *Ciona intestinalis* can ameliorate the mutant phenotype of *tko*^{25t}, which carries a mutation in mitoribosomal protein S12, resulting in globally decreased OXPHOS capacity. We found that induced AOX expression, whether during development, in freshly eclosed adults, or maintained in adults over a period of 30 d, has no effect on *tko*^{25t}, nor does it produce a phenocopy of *tko*^{25t} in wild-type flies. In contrast, ubiquitous expression of Ndi1, the alternative NADH dehydrogenase from yeast, was highly deleterious to *tko*^{25t} during development and was lethal when combined with both *tko*^{25t} and AOX.

Failure of AOX rescue suggests that a complex metabolic defect underlies the *tko*^{25t} phenotype

tko^{25t} exhibits a functional deficiency of all four OXPHOS complexes containing mitochondrial translation products (Toivonen *et al.* 2001), but it is unclear which of these is limiting for electron transfer. Because AOX provides a functional bypass of complexes III and IV, its failure to rescue the organismal phenotype can be interpreted in one of several ways. The first would be that the residual activity of cIII/cIV is not limiting for mitochondrial electron transport in *tko*^{25t}, and that the phenotype is entirely due to cI dysfunction. The second postulates that AOX is unable to rescue *tko*^{25t} because, as a nonproton-motive enzyme, it does not support the synthesis of ATP, and ATP deficiency is what underlies the mutant phenotype. A third possibility is that the phenotype is a consequence of one or more processes on which AOX does not impinge, such as elevated ROS production, or proteotoxicity due to the protein synthesis defect. Although none of these can be entirely eliminated, the fact that Ndi1 expression worsens the phenotype, either alone or in combination with AOX, and that changes in ATP level or mitochondrial ROS production do not correlate with it, suggest that the mutant phenotype is determined either by a complex interplay of factors or by other metabolic effects that are as yet unknown. Disrupted redox homeostasis resulting from a cI defect should be rescuable by Ndi1. A combined limitation on electron flow at cI and cIII and/or cIV should be alleviated by combined expression of Ndi1 and AOX. Manifestly, these predictions are inconsistent with our findings.

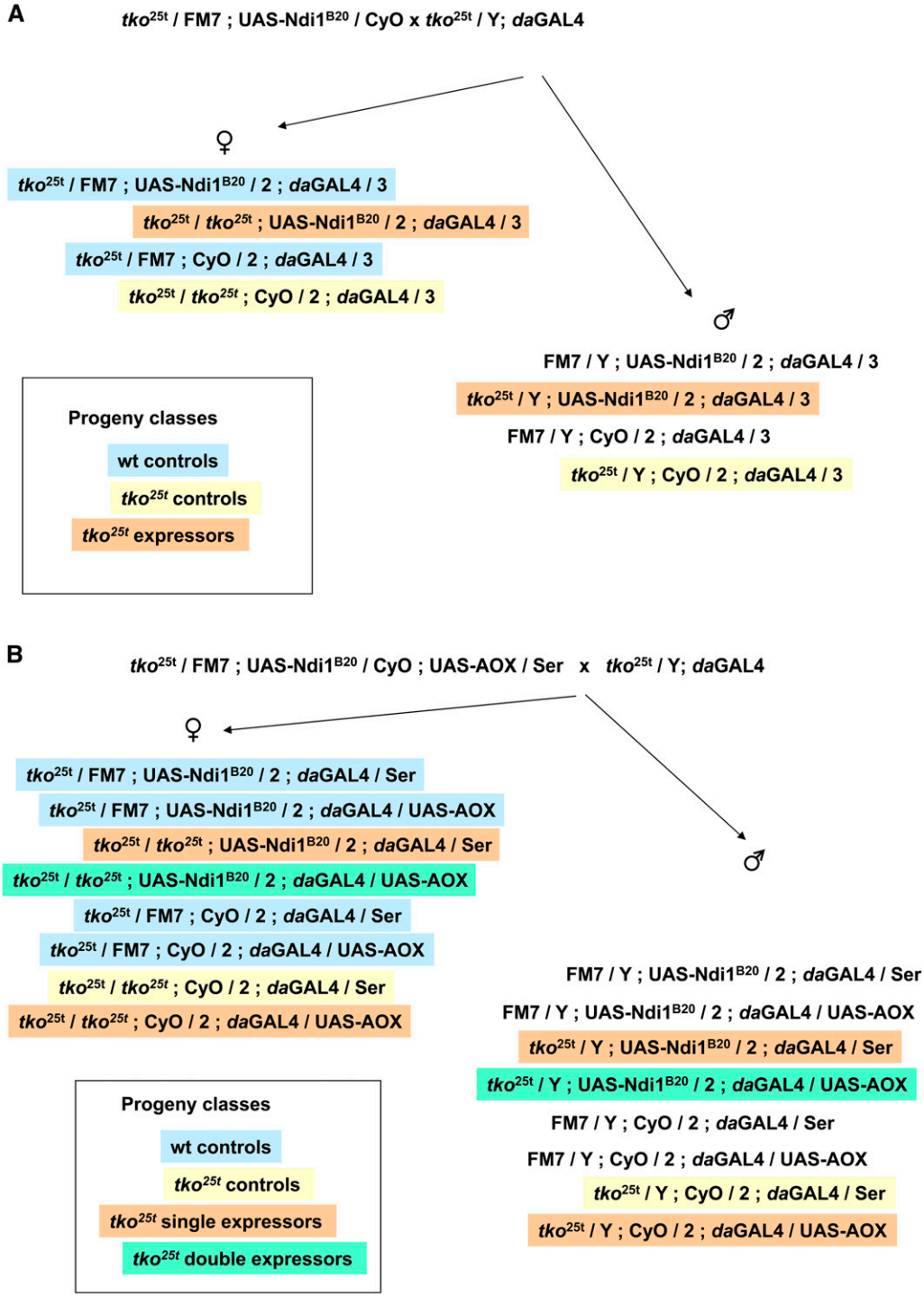

Figure 5 Genetic crosses used to test rescue of *tko*^{25t}. Crosses used to test rescue by (A) Ndi1 or (B) Ndi1 plus AOX combined. Progeny classes are color-coded as indicated to denote their meaning in the experiment. The results of the cross are shown in Table 1. Note that FM7 / Y males do not contain an unmanipulated X-chromosome, so they are not strictly a wild-type control.

Ndi1 is constitutively active (Sanz *et al.* 2010b), consistent with the fact that in its natural setting (in budding yeast) cI is absent. By diverting electrons away from cI, it may act to decrease net ATP production still further, but this seems unlikely to be the explanation for its effect on *tko*^{25t} because the apparent additional decrease in ATP level (Figure 6A) was modest and not statistically significant. However, the low number of successfully eclosing flies may represent the tail of a distribution, with those individuals suffering further ATP depletion simply unable to complete development. Effects on mitochondrial ROS production also did not correlate with the organismal phenotype. Although we confirmed elevated ROS production in *tko*^{25t} flies (Figure 6B), it was more affected by genetic background than by the expression of the alternative respiratory chain enzymes, and the effect of Ndi1 was again paradoxical. Note, however, that all metabolic assays were conducted on materials from flies reared at 18°, whereas for most of the phenotypic experiments reported here flies were cultured at 25°. This may have some bearing on the findings.

Proteotoxicity due to imbalance between cytosolic and mitochondrial protein synthesis has been implicated as a longevity mechanism, acting hormetically via the induction of the mitochondrial unfolded

Table 1 Test of ability of Ndi1 expression to rescue *tko*^{25t}

Genotype[a]	Sex	Number of Progeny[b]
tko^{25t} / FM7 ; CyO / 2 ; *da*GAL4 / 3	Female	152
tko^{25t} / FM7 ; UAS-Ndi1^{B20} / 2 ; *da*GAL4 / 3	Female	72
tko^{25t} / *tko*^{25t} ; CyO / 2 ; *da*GAL4 / 3	Female	57
tko^{25t} / *tko*^{25t} ; UAS-Ndi1^{B20} / 2 ; *da*GAL4 / 3	Female	1
FM7 / Y ; CyO / 2 ; *da*GAL4 / 3	Male	65
FM7 / Y ; UAS-Ndi1^{B20} / 2 ; *da*GAL4 / 3	Male	25
tko^{25t} / Y ; CyO / 2 ; *da*GAL4 / 3	Male	20
tko^{25t} / Y ; UAS-Ndi1^{B20} / 2 ; *da*GAL4 / 3	Male	1

[a] Output from cross shown in Fig. 5A.
[b] A repeat experiment gave similar results.

protein response (Houtkooper *et al.* 2013; Arnsburg and Kirstein-Miles 2014). However, decreased levels of NAD+ are associated with a failure of this mechanism (Mouchiroud *et al.* 2013). The deleterious effect produced by Ndi1 expression is again not consistent with this being the primary mechanism underlying the *tko*^{25t} phenotype.

The failure of AOX to rescue bang sensitivity and developmental delay in *tko*^{25t} reflects a similar finding for a second mutant affecting mitochondrial ATP production, *sesB*^{1} (Vartiainen *et al.* 2014). *sesB*^{1} carries a mutation in the gene encoding the major adult isoform of the adenine nucleotide translocase (Zhang *et al.* 1999) and, like *tko*^{25t}, *sesB*^{1} mutant flies show decreased steady-state ATP levels as well as bang sensitivity and developmental delay (Vartiainen *et al.* 2014). For these reasons, as well as the arguments stated above, we feel the "ATP hypothesis" cannot be entirely discounted, although other metabolic effects need to be further investigated as well.

Bang sensitivity of *tko*^{25t} is a developmental rather than a degenerative phenotype

Bang sensitivity is a commonly observed mutant phenotype in *Drosophila* and is due to lesions affecting a variety of cellular or physiological pathways, including, in addition to mitochondrial protein synthesis, adenine nucleotide transport and the TCA cycle (Fergestad *et al.* 2006), phospholipid metabolism (Pavlidis *et al.* 1994), ion pumps and channels (Schubiger *et al.* 1994; Kane *et al.* 2000; Iovchev *et al.* 2002; Parker *et al.* 2011), and proteolysis (Zhang *et al.* 2002). Although they manifest some similarities in their electrophysiological defects (Engel and Wu 1994), they fall into two classes depending on whether motor neurons are directly affected (Fergestad *et al.* 2006). Some of them show a clear degenerative phenotype with drastically shortened lifespan, whereas others, including *tko*^{25t}, show only a modestly decreased lifespan and associated neuropathology (Fergestad *et al.* 2008). In the current study, we found no significant change in the bang sensitivity of *tko*^{25t} over 30 d of adult life, in contrast to the synergistic and progressive effects on bang sensitivity seen when *tko*^{25t} is combined with other bang-sensitive mutants (Fergestad *et al.* 2008). We conclude that the bang sensitivity of *tko*^{25t} is a developmentally determined phenotype, at least in an otherwise wild-type genetic background

Therapeutic implications for AOX in mitochondrial disease

AOX has been proposed as a therapeutic tool relevant to a wide variety of mitochondrial disorders (El-Khoury *et al.* 2014). The present work indicates important limitations of this concept, whatever the precise link between mitochondrial translational dysfunction and the organismal phenotype in *tko*^{25t}. Despite profound effects on flies exposed to toxins or mutations directly or indirectly affecting cytochrome oxidase (Fernandez-Ayala *et al.* 2009; Kemppainen *et al.* 2014), or even the pleiotropic phenotypes caused by partial knockdown of DNA polymerase γ (Humphrey *et al.* 2012), AOX expression produced no detectable modification to the *tko*^{25t} phenotype.

Table 2 Test of ability of Ndi1 and AOX co-expression to rescue *tko*^{25t}

Genotype[a]	Sex	Number of Progeny[b]
tko^{25t} / FM7 ; CyO / 2 ; *da*GAL4 / Ser	Female	54
tko^{25t} / FM7 ; CyO / 2 ; *da*GAL4 / UAS-AOX	Female	48
tko^{25t} / FM7 ; UAS-Ndi1^{B20} / 2 ; *da*GAL4 / Ser	Female	34
tko^{25t} / FM7 ; UAS-Ndi1^{B20} / 2 ; *da*GAL4 / UAS-AOX	Female	35
tko^{25t} / *tko*^{25t} ; CyO / 2 ; *da*GAL4 / Ser	Female	23
tko^{25t} / *tko*^{25t} ; CyO / 2 ; *da*GAL4 / UAS-AOX	Female	17
tko^{25t} / *tko*^{25t} ; UAS-Ndi1^{B20} / 2 ; *da*GAL4 / Ser	Female	5
tko^{25t} / *tko*^{25t} ; UAS-Ndi1^{B20} / 2 ; *da*GAL4 / UAS-AOX	Female	0
FM7 / Y ; CyO / 2 ; *da*GAL4 / Ser	Male	26
FM7 / Y ; CyO / 2 ; *da*GAL4 / UAS-AOX	Male	27
FM7 / Y ; UAS-Ndi1^{B20} / 2 ; *da*GAL4 / Ser	Male	8
FM7 / Y ; UAS-Ndi1^{B20} / 2 ; *da*GAL4 / UAS-AOX	Male	7
tko^{25t} / Y ; CyO / 2 ; *da*GAL4 / Ser	Male	19
tko^{25t} / Y ; CyO / 2 ; *da*GAL4 / UAS-AOX	Male	14
tko^{25t} / Y ; UAS-Ndi1^{B20} / 2 ; *da*GAL4 / Ser	Male	6
tko^{25t} / Y ; UAS-Ndi1^{B20} / 2 ; *da*GAL4 / UAS-AOX	Male	0

[a] Output from cross shown in Fig. 5B.
[b] A repeat experiment gave similar results.

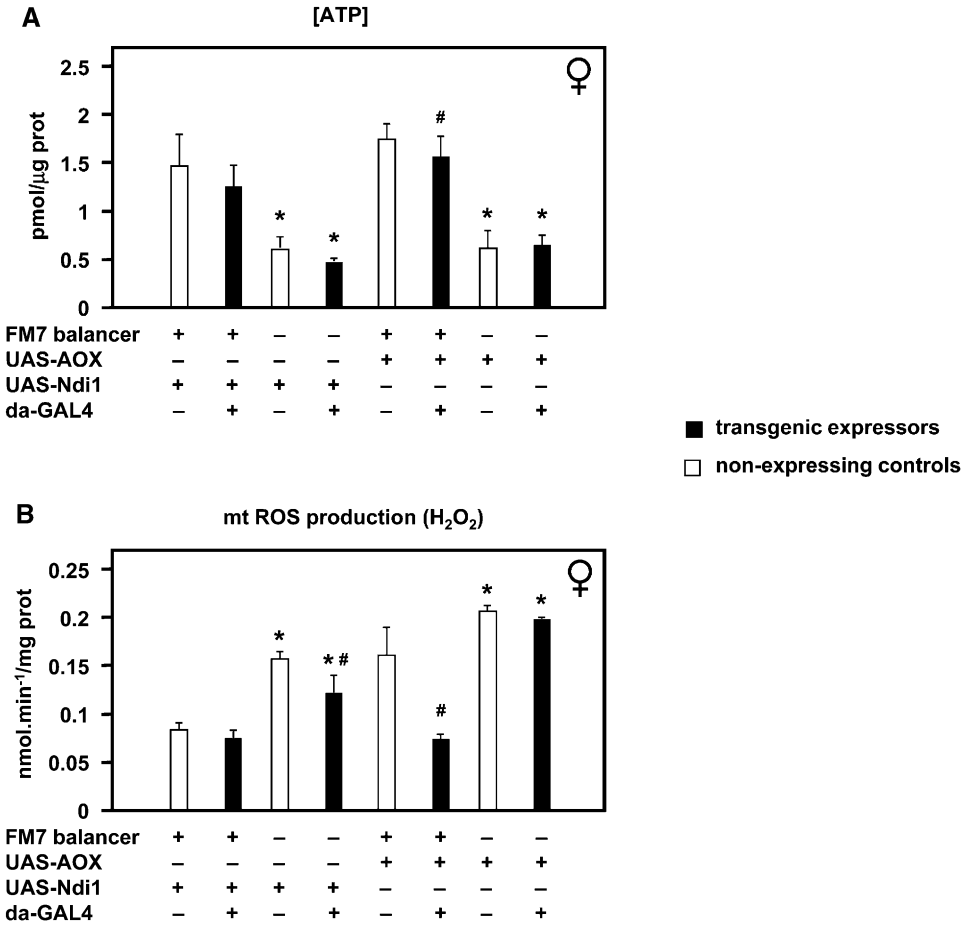

Figure 6 Altered ATP and ROS levels do not account for phenotypic effects of AOX or Ndi1. Effects of Ndi1 and AOX expression on (A) ATP levels and (B) mitochondrial ROS production of female *tko*^{25t} flies of the indicated genotypes, reared at 18°. Flies were homozygous for *tko*^{25t}, except those carrying the FM7 balancer, which are phenotypically wild-type. Means ± SD for three or more biological replicates of each genotype.*Significant differences between *tko*^{25t} homozygotes and heterozygotes of otherwise identical genotypes, $P < 0.01$, Student's *t* test, two-tailed. #Significant differences between Ndi1 or AOX expressors and nonexpressors of otherwise identical genotypes, $P < 0.05$, Student's *t* test, two-tailed.

tko^{25t} has been considered as a model for mitochondrial diseases, exhibiting not only seizures and developmental delay but also hearing impairment (Toivonen *et al.* 2001). It is of particular relevance to those disorders where the primary defect is in the mitochondrial translation system, which applies to many of the commonest pathological mtDNA mutations such as the 3243G > A MELAS mutation, as well as an increasingly recognized subset of nuclear gene mitochondrial disorders exhibiting multiple OXPHOS deficiencies (Pearce *et al.* 2013). The implementation of respiratory chain bypasses such as AOX or Ndi1 should, in theory, alleviate pathological phenotypes associated with restrictions on electron transport, depending on which segments of the respiratory chain are affected. In cases where multiple OXPHOS complexes are affected, both bypasses in combination might be needed to restore electron flow. *tko*^{25t} constitutes a model for such diseases, yet neither AOX nor Ndi1 ameliorated the phenotype, and Ndi1 was even deleterious. As already indicated, Ndi1 and AOX do not restore proton pumping at the respiratory chain segments that they bypass, nor can they alleviate, *a priori*, all other aspects of mitochondrial dysfunction. Their uses in eventual therapy for disorders of mitochondrial translation therefore may be limited and clearly requires a fuller understanding of the pathophysiological mechanism case by case.

ACKNOWLEDGMENTS

We thank Tea Tuomela, Eveliina Kaulio, and Outi Kurronen for technical assistance, and Pierre Rustin, Eric Dufour, Alberto Sanz, and Rhoda Stefanatos for many useful discussions. Funding was provided by Academy of Finland (FinMIT Centre of Excellence, Academy Professorship to H.T.J.), Sigrid Juselius Foundation, and Tampere University Hospital Medical Research Fund. The authors declare no competing interests. H.T.J., K.K.K., and E.K. together conceived and designed the experiments, which K.K.K. and E.K. executed. All authors contributed to data analysis. H.T.J. compiled the figures and drafted the manuscript.

LITERATURE CITED

Arnsburg, K., and J. Kirstein-Miles, 2014 Interrelation between protein synthesis, proteostasis and life span. Curr. Genomics 15: 66–75.

Ballard, J. W., R. G. Melvin, J. T. Muller, and S. D. Katewa, 2007 Sex differences in survival and mitochondrial bioenergetics during aging in *Drosophila*. Aging Cell 6: 699–708.

Chen, S., M. T. Oliveira, A. Sanz, E. Kemppainen, A. Fukuoh *et al.*, 2012 A cytoplasmic suppressor of a nuclear mutation affecting mitochondrial functions in *Drosophila*. Genetics 192: 483–493.

El-Khoury, R., K. K. Kemppainen, E. Dufour, M. Szibor, H. T. Jacobs *et al.*, 2014 Engineering the alternative oxidase gene to better understand and counteract mitochondrial defects: State of the art and perspectives. Br. J. Pharmacol. 171: 2243–2249.

Engel, J. E., and C. F. Wu, 1994 Altered mechanoreceptor response in *Drosophila* bang-sensitive mutants. J. Comp. Physiol. A. 175: 267–78.

Fergestad, T., B. Bostwick, and B. Ganetzky, 2006 Metabolic disruption in *Drosophila* bang-sensitive seizure mutants. Genetics 173: 1357–1364.

Fergestad, T., L. Olson, K. P. Patel, R. Miller, M. J. Palladino *et al.*, 2008 Neuropathology in *Drosophila* mutants with increased seizure susceptibility. Genetics 178: 947–956.

Fernández-Ayala, D. J., A. Sanz, S. Vartiainen, K. K. Kemppainen, M. Babusiak *et al.*, 2009 Expression of the *Ciona intestinalis* alternative oxidase (AOX) in *Drosophila* complements defects in mitochondrial oxidative phosphorylation. Cell Metab. 9: 449–460.

Fernández-Ayala, D. J., S. Chen, E. Kemppainen, K. M. C. O'Dell, and H. T. Jacobs, 2010 Gene expression in a *Drosophila* model of mitochondrial disease. PLoS ONE 5: e8549.

Houtkooper, R. H., L. Mouchiroud, D. Ryu, N. Moullan, E. Katsyuba *et al.*, 2013 Mitonuclear protein imbalance as a conserved longevity mechanism. Nature 497: 451–457.

Humphrey, D. M., R. B. Parsons, Z. N. Ludlow, T. Riemensperger, G. Esposito *et al.*, 2012 Alternative oxidase rescues mitochondria-mediated dopaminergic cell loss in *Drosophila*. Hum. Mol. Genet. 21: 2698–2712.

Iovchev, M., P. Kodrov, A. J. Wolstenholme, W. L. Pak, and E. P. Semenov, 2002 Altered drug resistance and recovery from paralysis in *Drosophila* melanogaster with a deficient histamine-gated chloride channel. J. Neurogenet. 16: 249–261.

Kane, N. S., B. Hirschberg, S. Qian, D. Hunt, B. Thomas *et al.*, 2000 Drug-resistant *Drosophila* indicate glutamate-gated chloride channels are targets for the antiparasitics nodulisporic acid and ivermectin. Proc. Natl. Acad. Sci. USA 97: 13949–13954.

Kemppainen, E, D. J. Fernández-Ayala, L. C. Galbraith, and K. M. C. O'Dell, and H. T. Jacobs, 2009 Phenotypic suppression of the *Drosophila* mitochondrial disease-like mutant *tko*^{25t} by duplication of the mutant gene in its natural chromosomal context. Mitochondrion 9: 353–363.

Kemppainen, K. K., J. Rinne, A. Sriram, M. Lakanmaa, A. Zeb *et al.*, 2014 Expression of alternative oxidase in *Drosophila* ameliorates diverse phenotypes due to cytochrome oxidase deficiency. Hum. Mol. Genet. 23: 2078–2093.

Lee, J., and C. F. Wu, 2002 Electroconvulsive seizure behavior in *Drosophila*: analysis of the physiological repertoire underlying a stereotyped action pattern in bang-sensitive mutants. J. Neurosci. 22: 11065–11079.

Lloyd, T. E., and J. P. Taylor, 2010 Flightless flies: *Drosophila* models of neuromuscular disease. Ann. N. Y. Acad. Sci. 1184: e1–e20.

Lu, B., and H. Vogel, 2009 *Drosophila* models of neurodegenerative diseases. Annu. Rev. Pathol. 4: 315–342.

McDonald, A. E., G. C. Vanlerberghe, and J. F. Staples, 2009 Alternative oxidase in animals: unique characteristics and taxonomic distribution. J. Exp. Biol. 212: 2627–2634.

Mouchiroud, L., R. H. Houtkooper, N. Moullan, E. Katsyuba, D. Ryu *et al.*, 2013 The NAD(+)/sirtuin pathway modulates longevity through activation of mitochondrial UPR and FOXO signaling. Cell 154: 430–441.

Palladino, M. J., 2010 Modeling mitochondrial encephalomyopathy in *Drosophila*. Neurobiol. Dis. 40: 40–45.

Parker, L., M. Padilla, Y. Du, K. Dong, and M. A. Tanouye, 2011 *Drosophila* as a model for epilepsy: bss is a gain-of-function mutation in the *para* sodium channel gene that leads to seizures. Genetics 187: 523–534.

Pavlidis, P., and M. A. Tanouye, 1995 Seizures and failures in the giant fiber pathway of *Drosophila* bang-sensitive paralytic mutants. J. Neurosci. 15: 5810–5819.

Pavlidis, P., M. Ramaswami, and M. A. Tanouye, 1994 The *Drosophila easily shocked* gene: a mutation in a phospholipid synthetic pathway causes seizure, neuronal failure, and paralysis. Cell 79: 23–33.

Pearce, S., C. L. Nezich, and A. Spinazzola, 2013 Mitochondrial diseases: translation matters. Mol. Cell. Neurosci. 55: 1–12.

Royden, C. S., V. Pirrotta, and L. Y. Jan, 1987 The *tko* locus, site of a behavioral mutation in *D. melanogaster*, codes for a protein homologous to prokaryotic ribosomal protein S12. Cell 51: 165–173.

Sánchez-Martínez, A., N. Luo, P. Clemente, C. Adán, R. Hernández-Sierra *et al.*, 2006 Modeling human mitochondrial diseases in flies. Biochim. Biophys. Acta 1757: 1190–1198.

Sanz, A., D. J. Fernández-Ayala, R. K. Stefanatos, and H. T. Jacobs, 2010a Mitochondrial ROS production correlates with, but does not directly regulate lifespan in *Drosophila*. Aging 2: 200–223.

Sanz, A., M. Soikkeli, M. Portero-Otín, A. Wilson, E. Kemppainen *et al.*, 2010b Expression of the yeast NADH dehydrogenase Ndi1 in *Drosophila* confers increased lifespan independently of dietary restriction. Proc. Natl. Acad. Sci. USA 107: 9105–9110.

Scarpulla, R. C., 2011 Metabolic control of mitochondrial biogenesis through the PGC-1 family regulatory network. Biochim. Biophys. Acta 1813: 1269–1278.

Schubiger, M., Y. Feng, D. M. Fambrough, and J. Palka, 1994 A mutation of the *Drosophila* sodium pump alpha subunit gene results in bang-sensitive paralysis. Neuron 12: 373–381.

Shah, Z. H., K. M. C. O'Dell, S. C. Miller, X. An, and H. T. Jacobs, 1997 Metazoan nuclear genes for mitoribosomal protein S12. Gene 204: 55–62.

Toivonen, J. M., K. M. O'Dell, N. Petit, S. C. Irvine, G. K. Knight *et al.*, 2001 *technical knockout*, a *Drosophila* model of mitochondrial deafness. Genetics 159: 241–254.

Ueda, A., C. Grabbe, J. Lee, J. Lee, R. H. Palmer *et al.*, 2008 Mutation of *Drosophila* focal adhesion kinase induces bang-sensitive behavior and disrupts glial function, axonal conduction and synaptic transmission. Eur. J. Neurosci. 27: 2860–2870.

Vartiainen, S., S. Chen, J. George, T. Tuomela, K. R. Luoto *et al.*, 2014 Phenotypic rescue of a *Drosophila* model of mitochondrial ANT1 disease. Dis. Model. Mech. 7: 635–648.

Zhang, H., J. Tan, E. Reynolds, D. Kuebler, S. Faulhaber *et al.*, 2002 The *Drosophila* slamdance gene: a mutation in an aminopeptidase can cause seizure, paralysis and neuronal failure. Genetics 162: 1283–1299.

Zhang, Y. Q., J. Roote, S. Brogna, A. W. Davis, D. A. Barbash *et al.*, 1999 *stress sensitive B* encodes an Adenine Nucleotide Translocase in *Drosophila* melanogaster. Genetics 153: 891–903.

Communicating editor: H. D. Lipshitz